Electron crystallography: imaging and diffraction

E. Mugnaioli (*enrico.mugnaioli@iit.it*)

Istituto Italiano di Tecnologia

Center for Nanotechnology Innovation@NEST – Pisa (Italy)

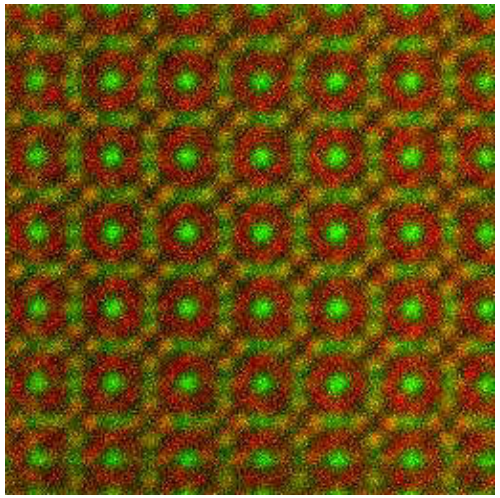

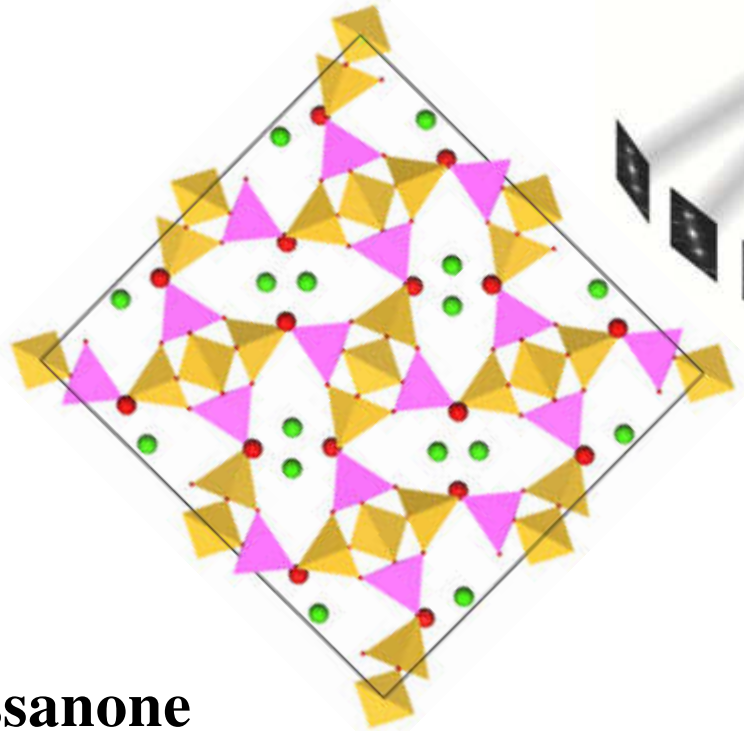

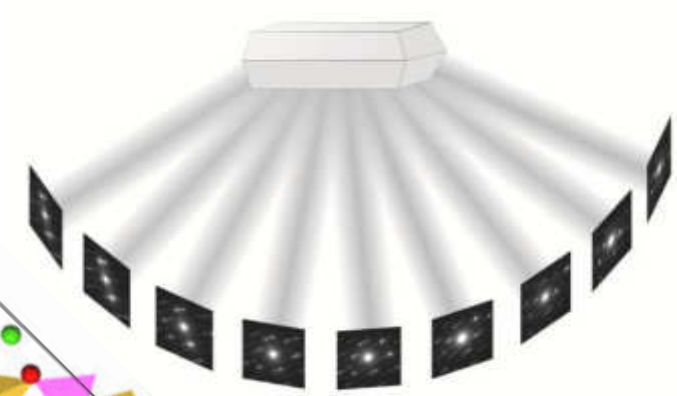

GNM School – Bressanone **February 2018**

Outline

- **Electron crystallography: why and when**
- **Transmission electron microscopy (TEM)**
- **Electron diffraction from oriented zones**
- **Electron diffraction tomography (EDT)**
- **An example of EDT analysis**
- **Three applications to mineralogy and petrography**
- **Strengths and limits of EDT**
- **Some perspectives (very beam sensitive samples)**

Enrico Mugnaioli

2007 PhD in Electron Crystallography at the University of Siena (***geology***)

2007-2014 Post-Doc at the University of Mainz (***physical-chemistry***)

2014-2017 PI for the National Project "Exploring the Nanoworld" at the University of Siena (***geology***)

2017-ongoing senior researcher at IIT@NEST – Pisa (***nanotechnology***)

Crystallography

UN proclaimed **2014** as the **International Year of Crystallography**, celebrating the **centenary** of **Max von Laue's Nobel Prize in Physics** for the discovery of **X-ray scattering**

Crystallography is the science that studies the **atom arrangement** in (crystalline) **solids,** i.e. how solid materials are essentially made

Macroscopic properties of materials largely depend on the atomic structure at the sub-nanometric scale

Visible light has a wavelength of **4000-7000 Å**, **atomic radius and bonds** are about **1-3 Å**

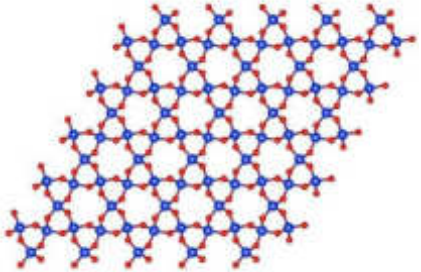

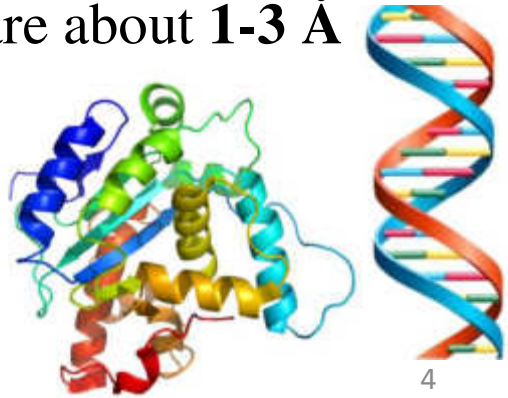

Nano-crystalline materials

Calcite ($CaCO_3$)

Aragonite ($CaCO_3$)

Single-crystal X-ray diffraction

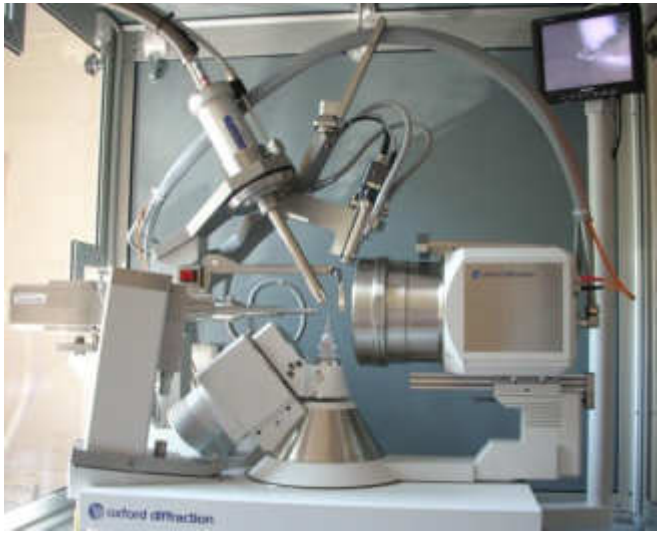

Nano-crystalline materials

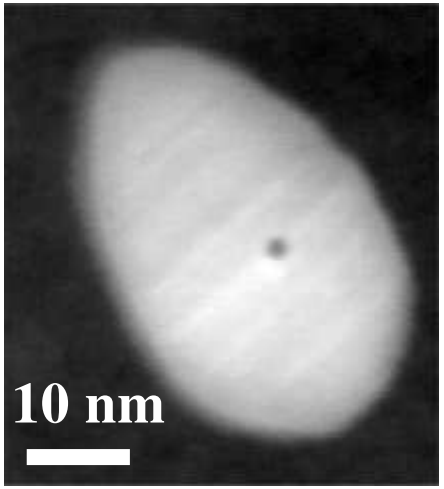

Vaterite ($CaCO_3$)

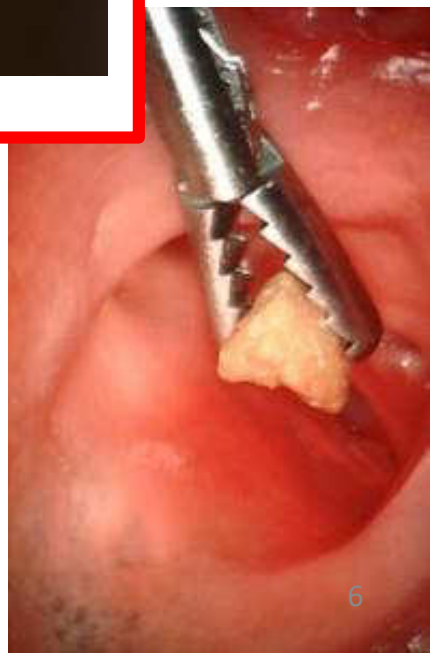

X-ray powder diffraction (XRPD)

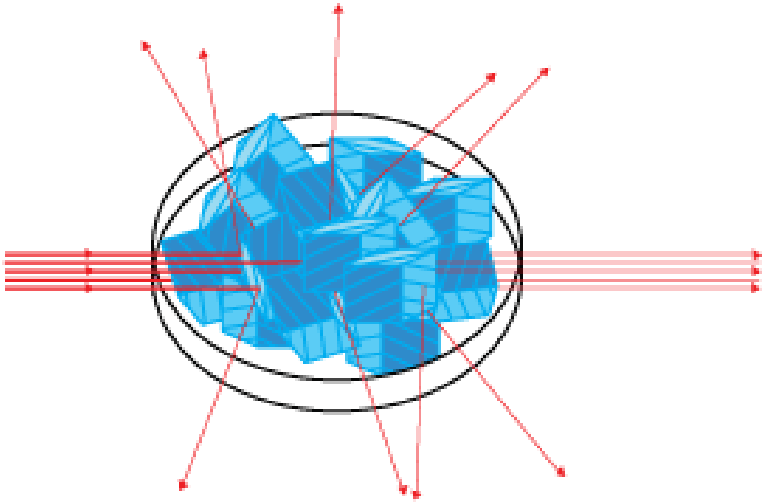

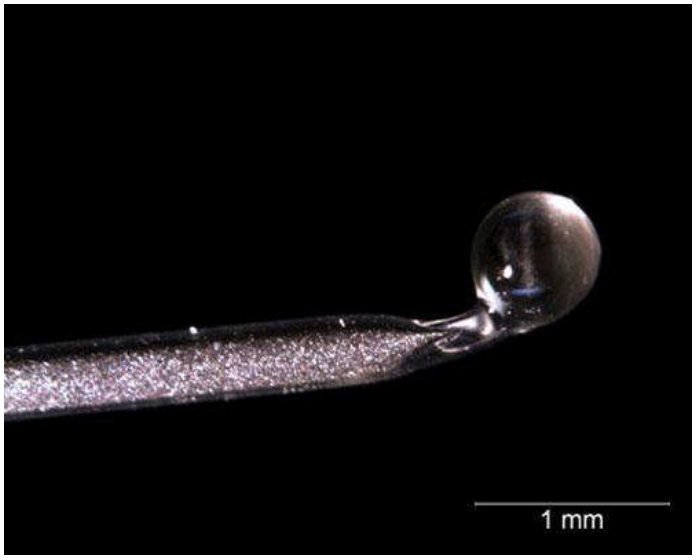

X-ray powder diffraction (XRPD)

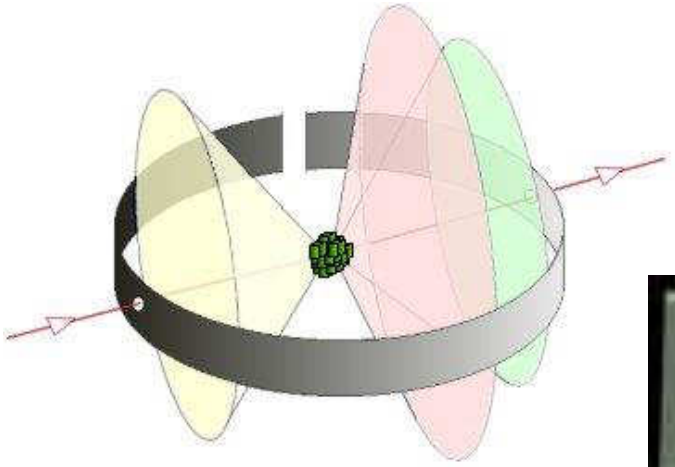

$$d = \frac{n\lambda}{2\sin\theta}$$

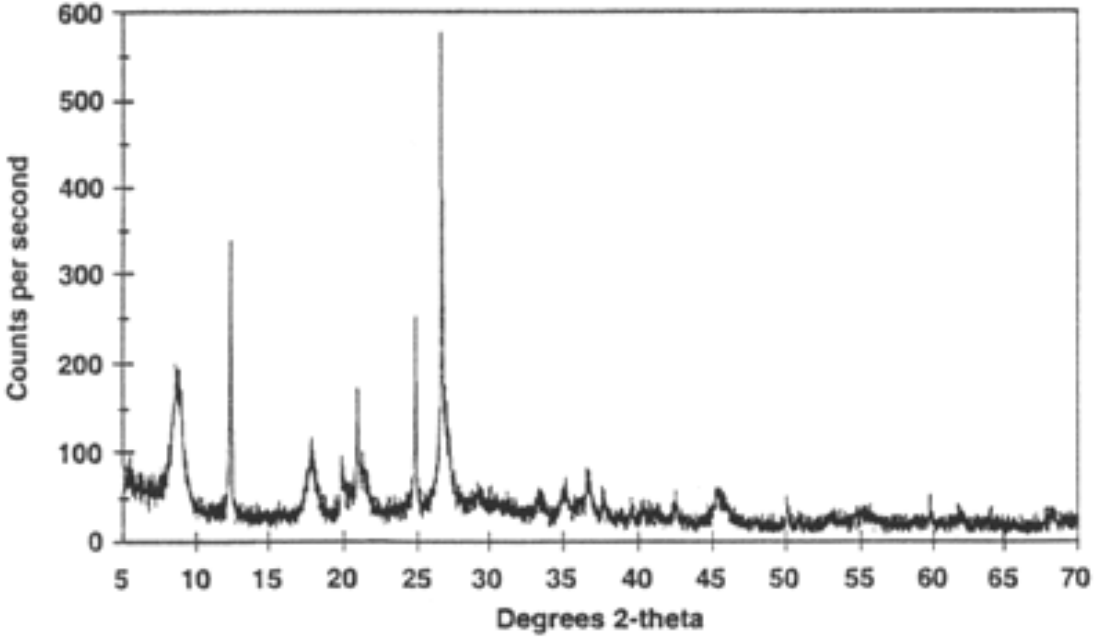

X-ray Powder Diffraction

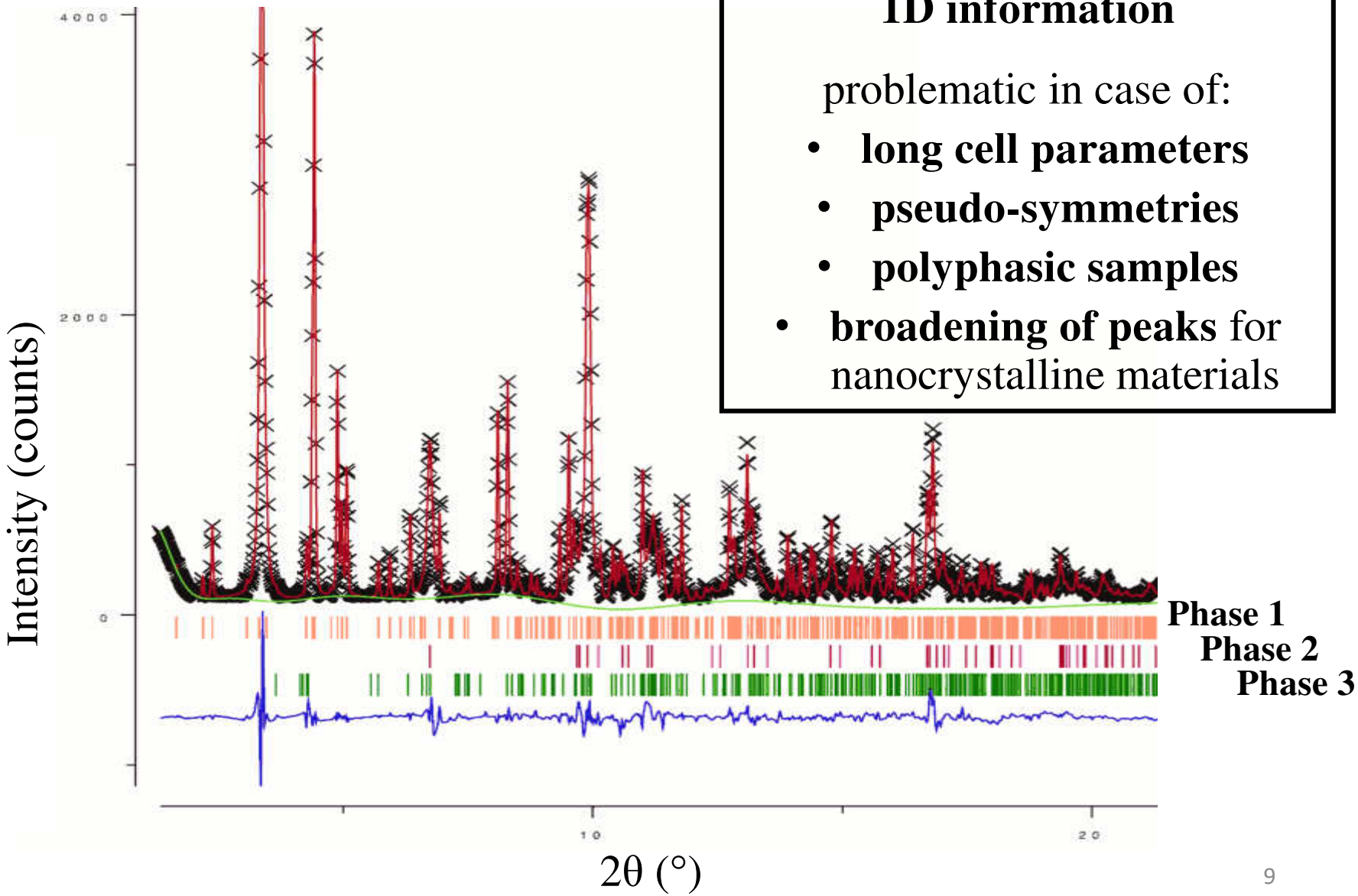

1D information

problematic in case of:

- **long cell parameters**
- **pseudo-symmetries**
- **polyphasic samples**
- **broadening of peaks** for nanocrystalline materials

One single nano-crystal

Polyphasic materials

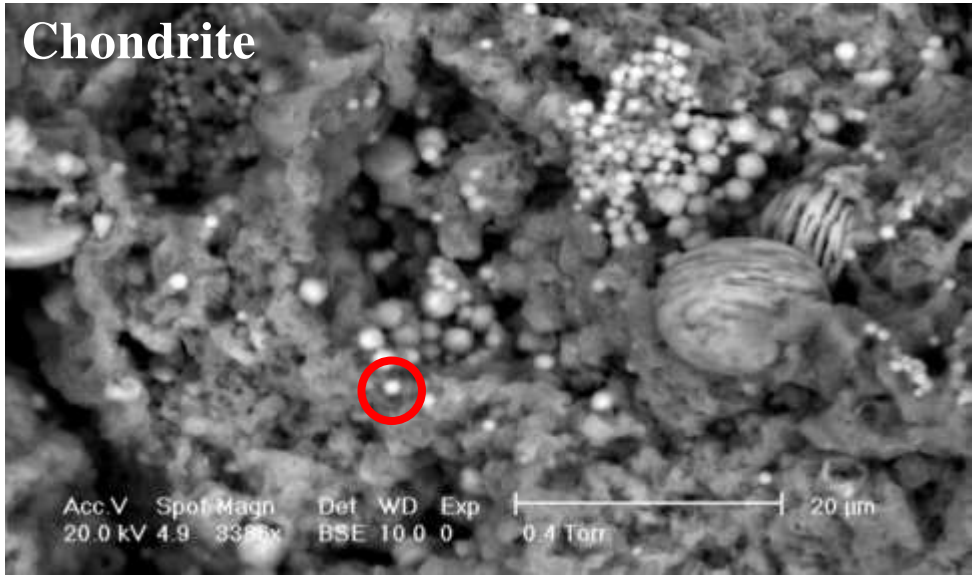

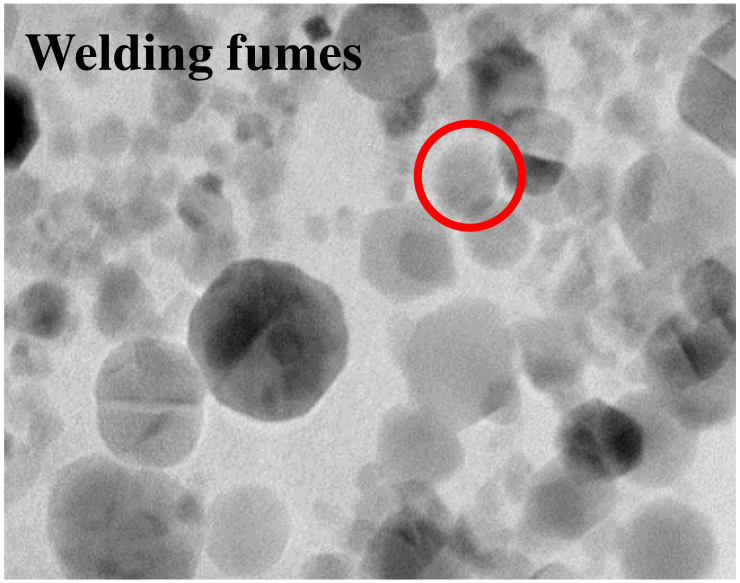

Isolated crystals

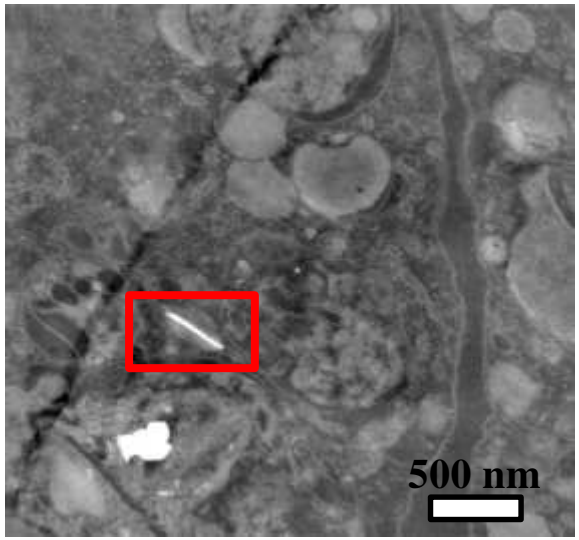

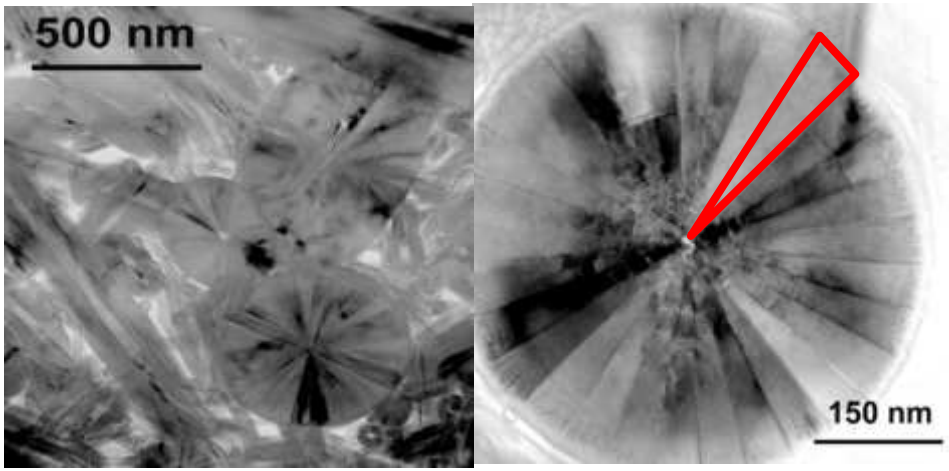

Single sectors of an assemble

SEM & TEM

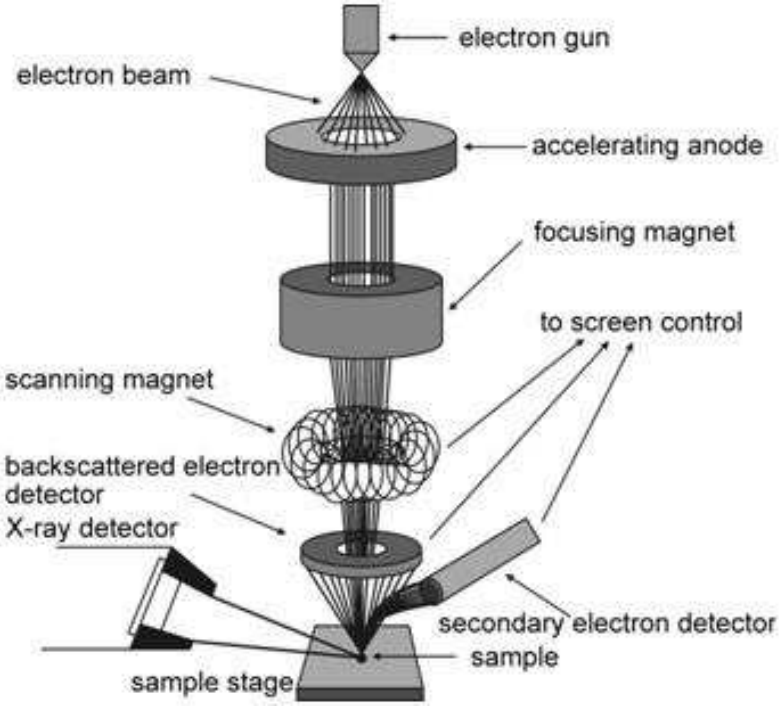

Scanning electron microscope

(SEM)

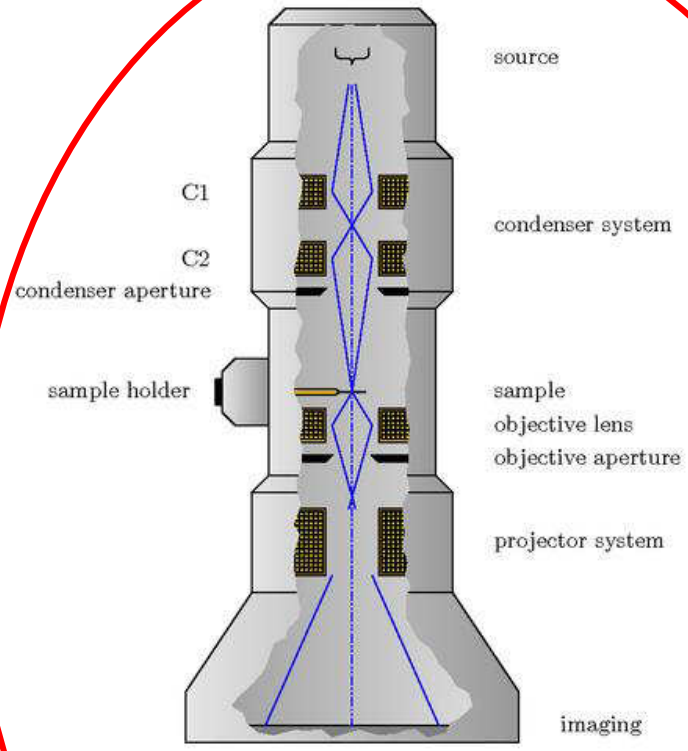

Transmission electron microscope

(TEM)

Scanning-transmission electron microscopy

(STEM)

Transmission Electron Microscope (TEM)

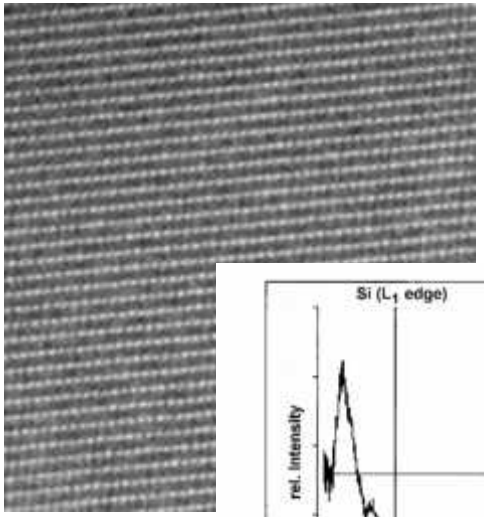

Images

Spectral analysis

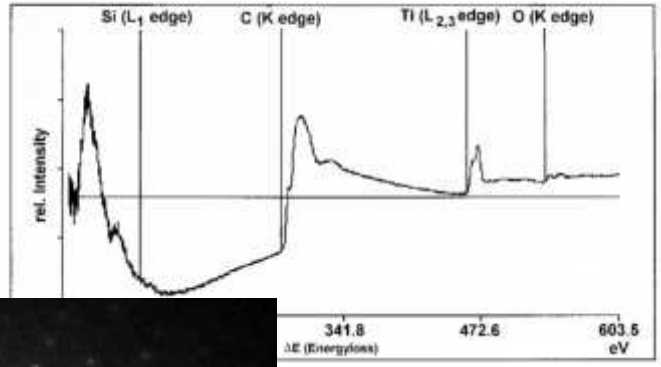

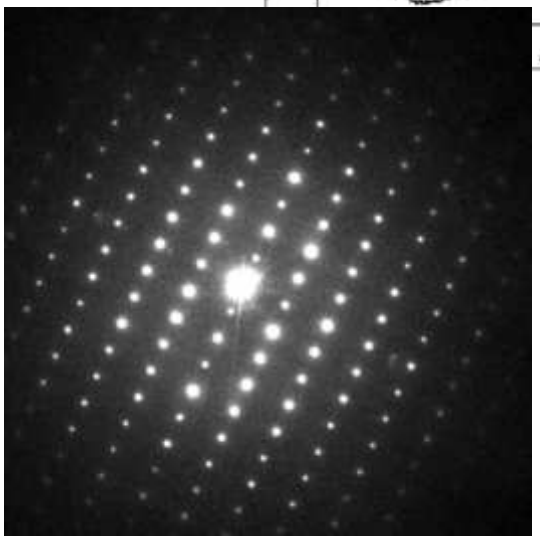

Diffractions

Accelerated electrons

TEM

- Short wavelength (~ 0.01-0.1 Å)
  - **small scattering angle**
  - **almost flat Ewald sphere**
  - **many reflections excited contemporarily**
- Strong (Coulomb) interaction with matter
  - **10^3-10^4 stronger interaction than X-rays**
  - **good signal/noise from nanovolumes**
  - **dynamical scattering**
- Charged (e^-)
  - **easy to deflect and focus in a nanoprobe**
  - **scattered information can be recombined in images**

X-rays *vs.* Electrons

X-rays

Incoming radiation

Sample

Scattering

Diffraction

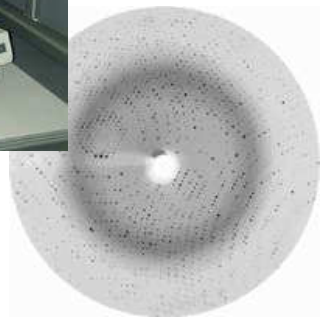

Electrons

Incoming radiation

Sample

Scattering

Lens

Image

Ruska & Knoll, 1932

TEM imaging

HRTEM on nanomaterials: local structure

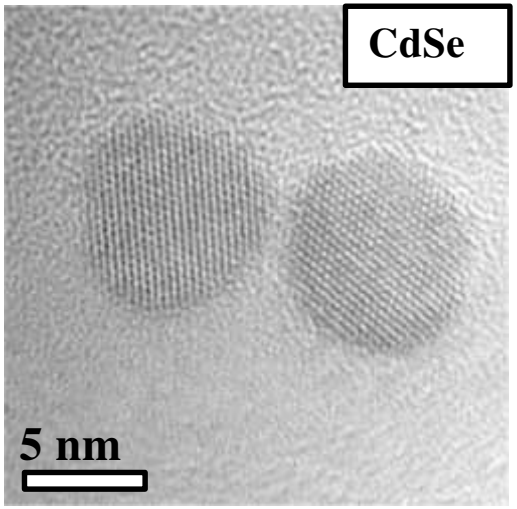

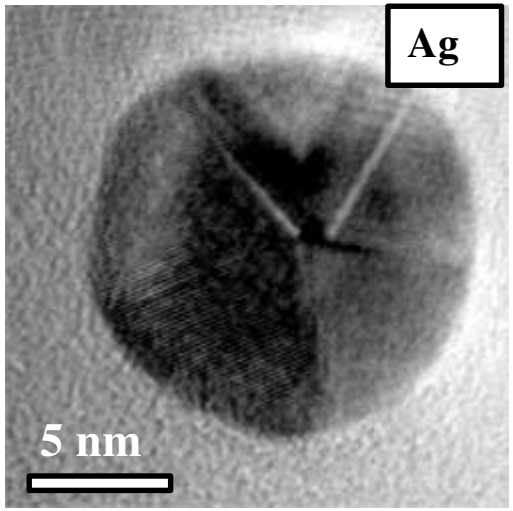

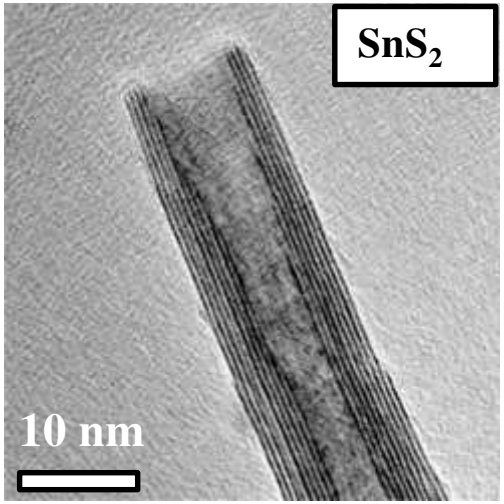

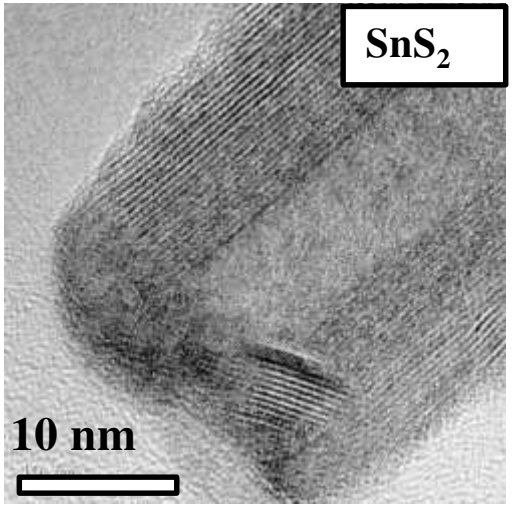

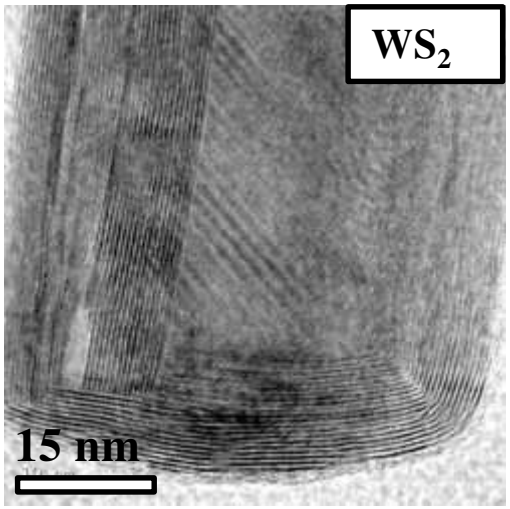

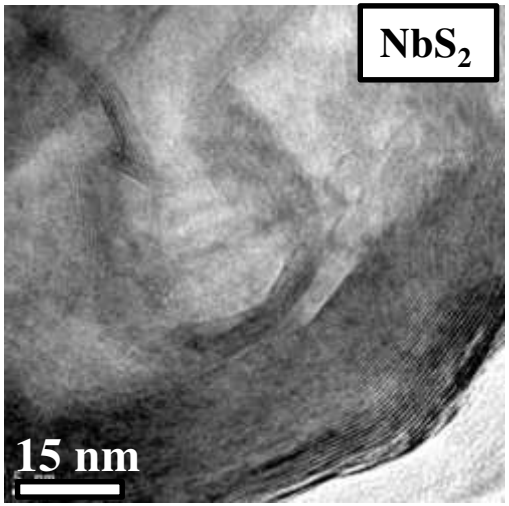

HRTEM on crystal boundaries

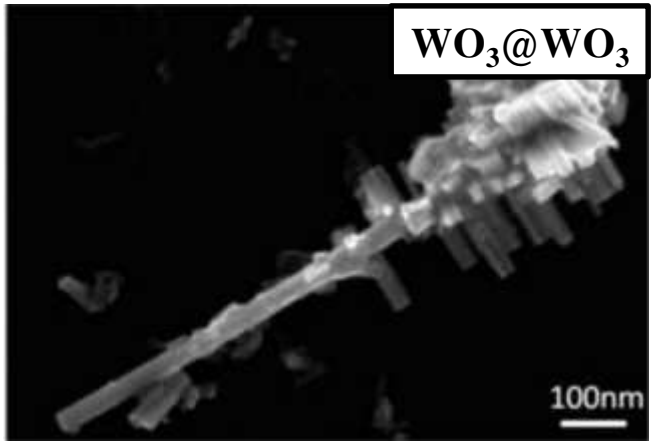

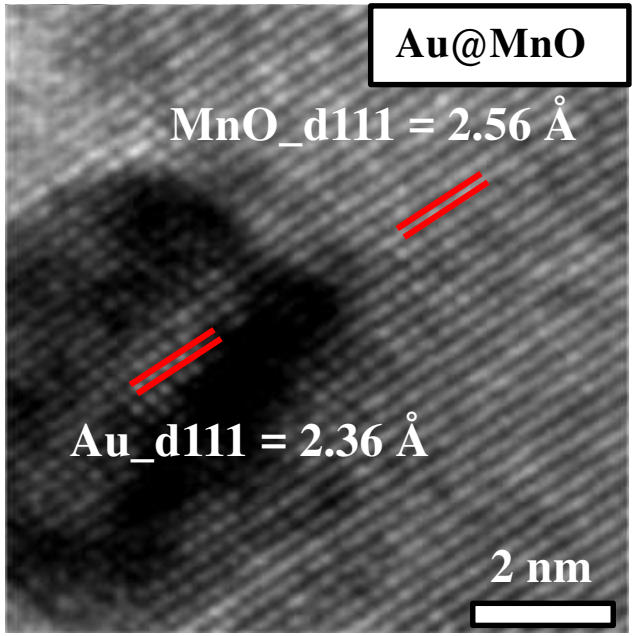

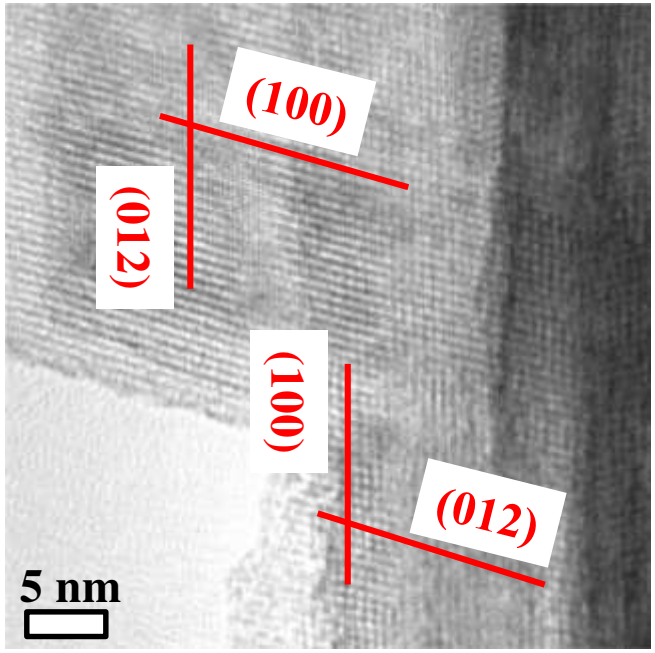

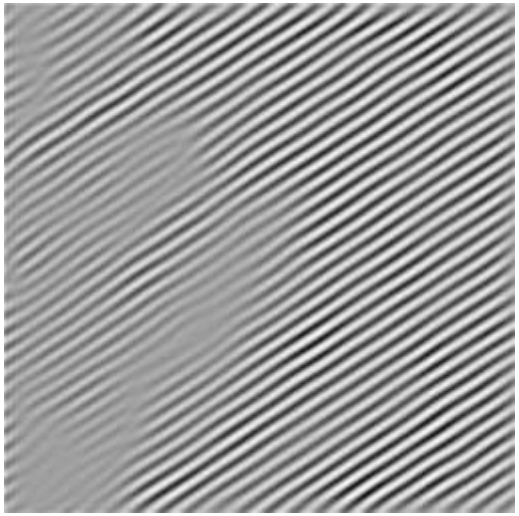

TEM imaging

HRTEM on defects of polytypes

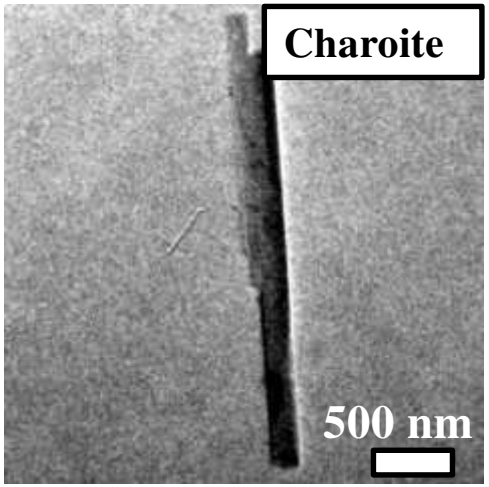

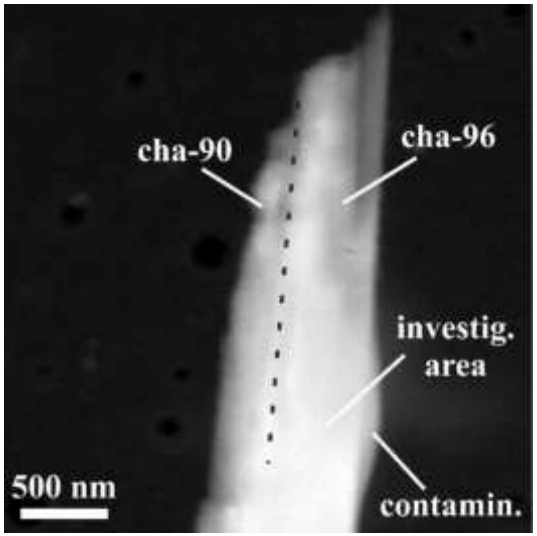

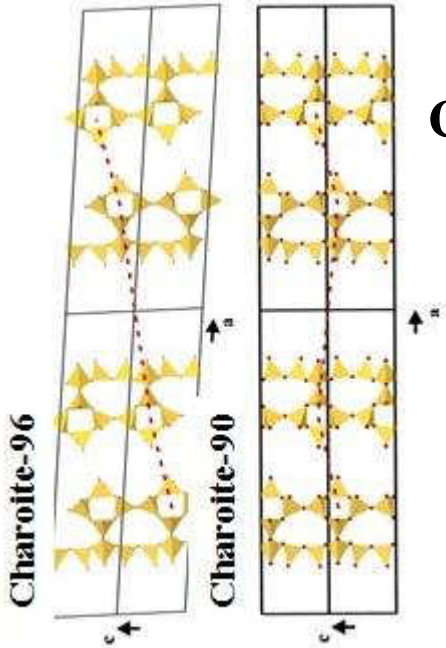

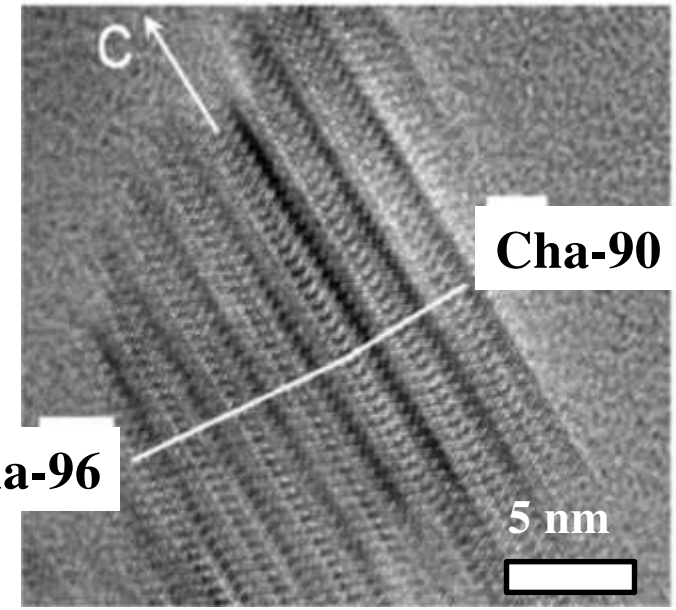

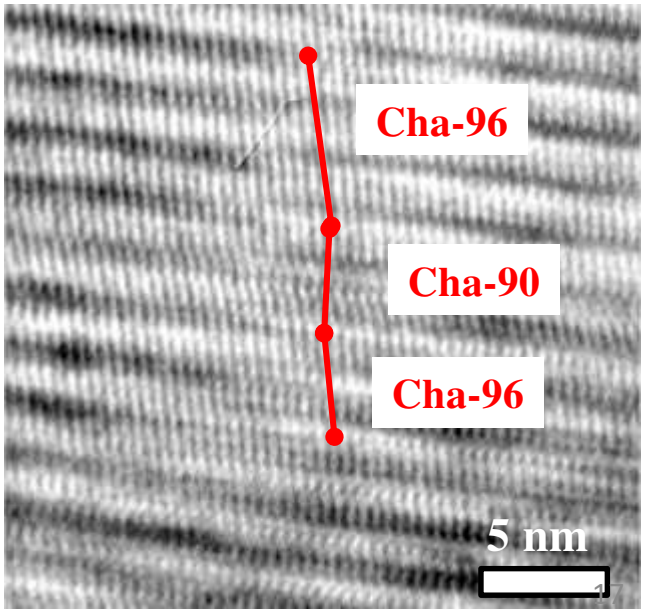

TEM imaging

Polygonal Serpentine

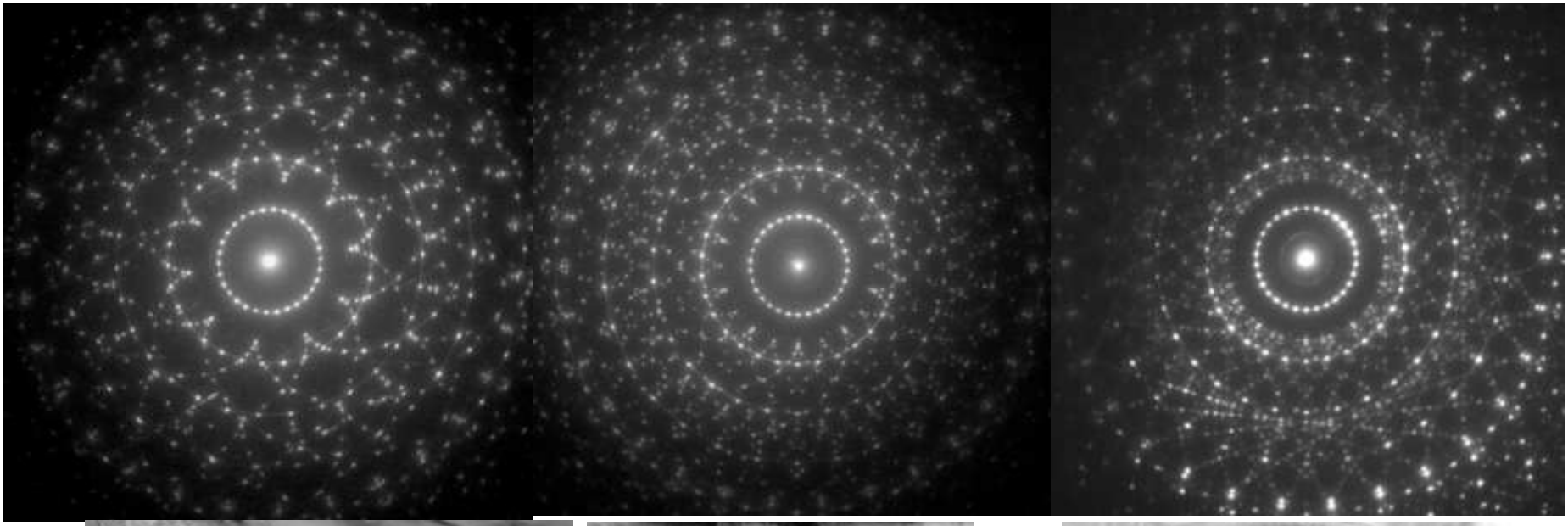

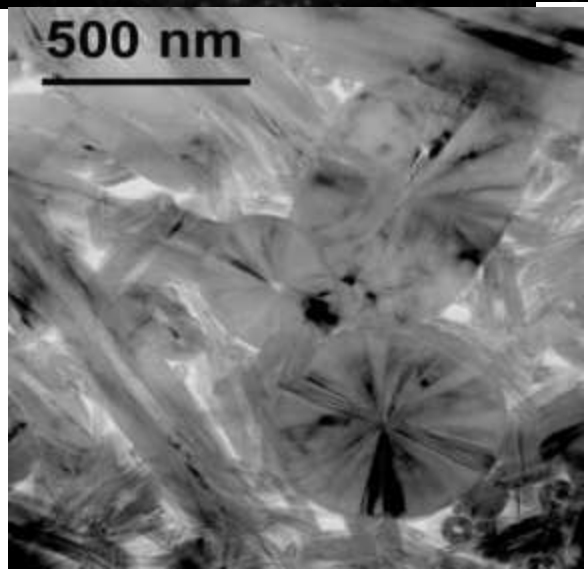

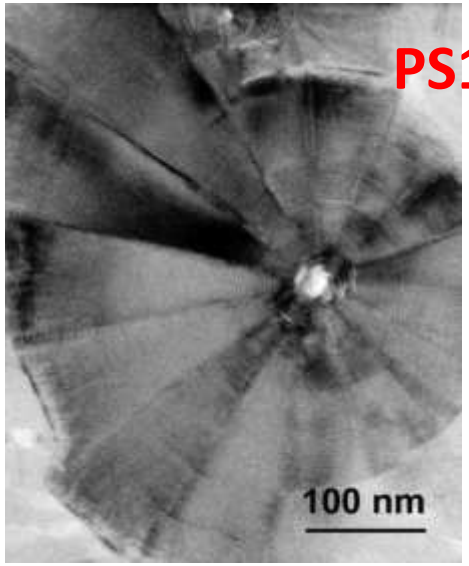

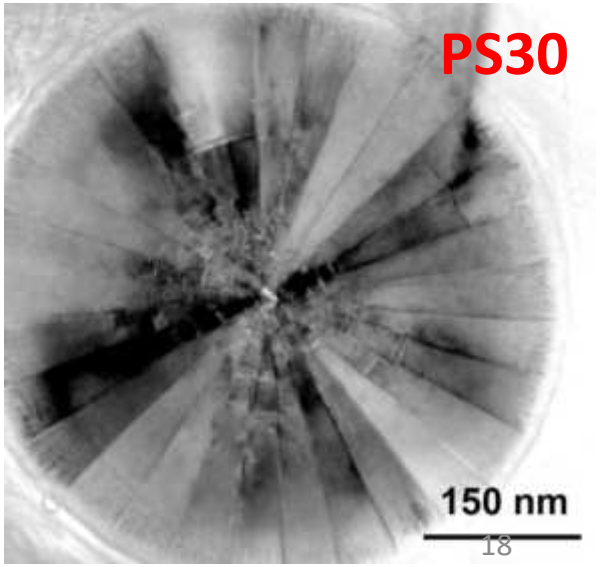

TEM imaging

Polygonal Serpentine

[100]

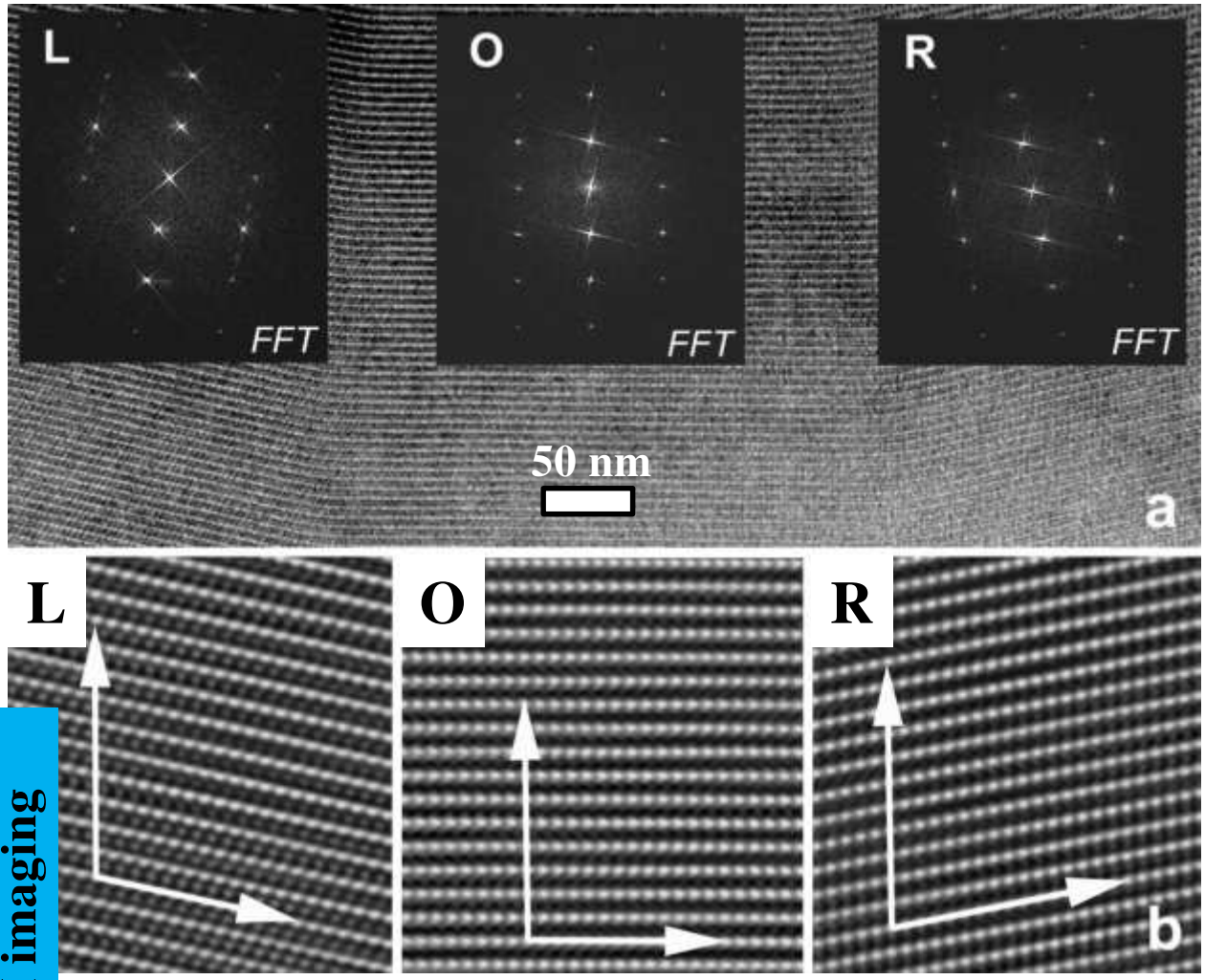

c = 7.3 Å (**O**), 7.5 Å (**R**, **L**)

α = 90° (**O**), 78° (**R**), 102° (**L**), i.e. **± b/6**.

TEM imaging

Polygonal Serpentine

[100]

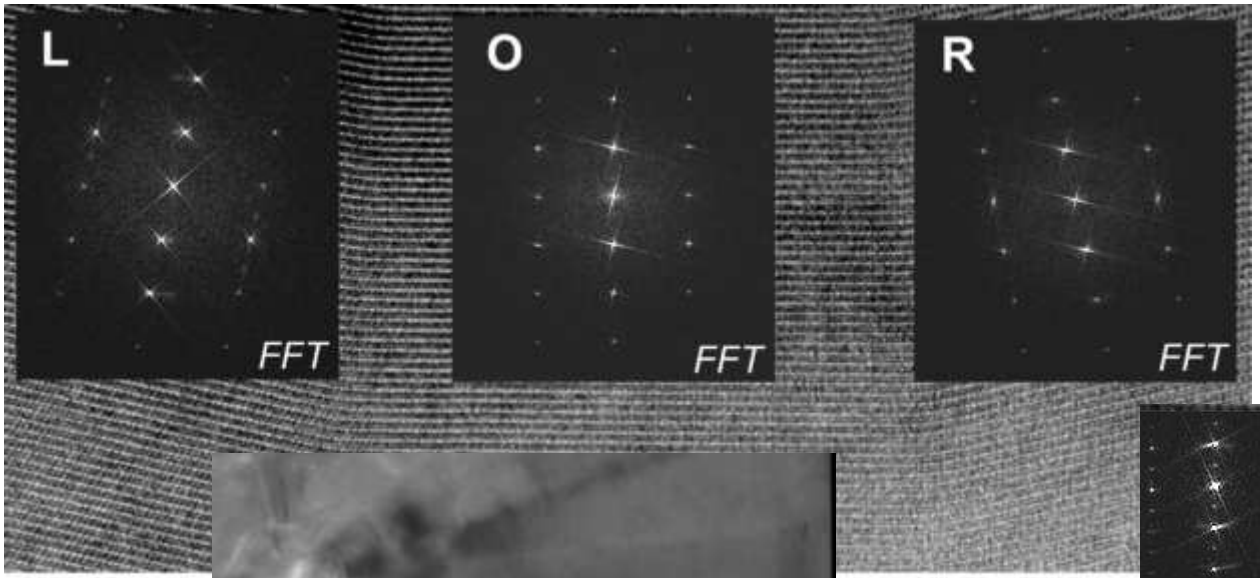

c = 7.3 Å (**O**), 7.5 Å (**R**, **L**)

α = 90° (**O**), 78° (**R**), 102° (**L**), i.e. **± b/6**.

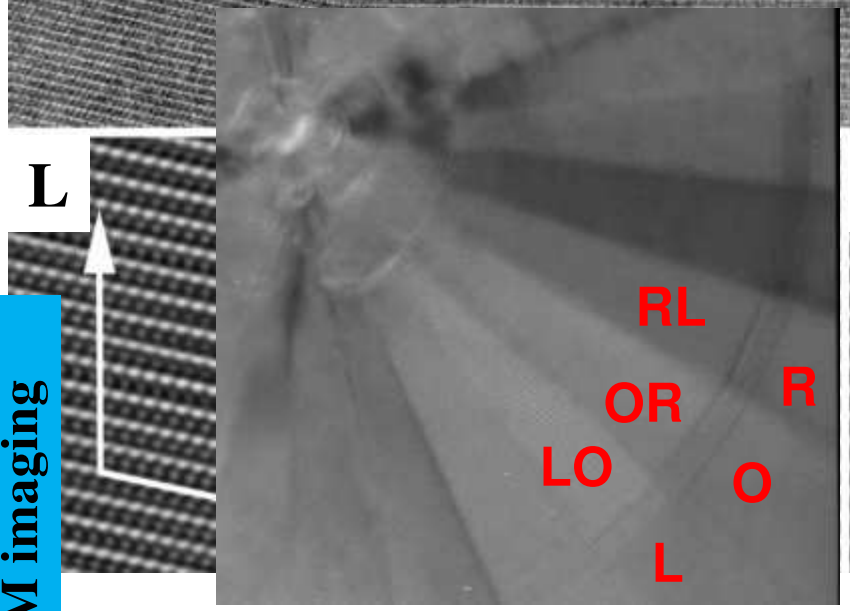

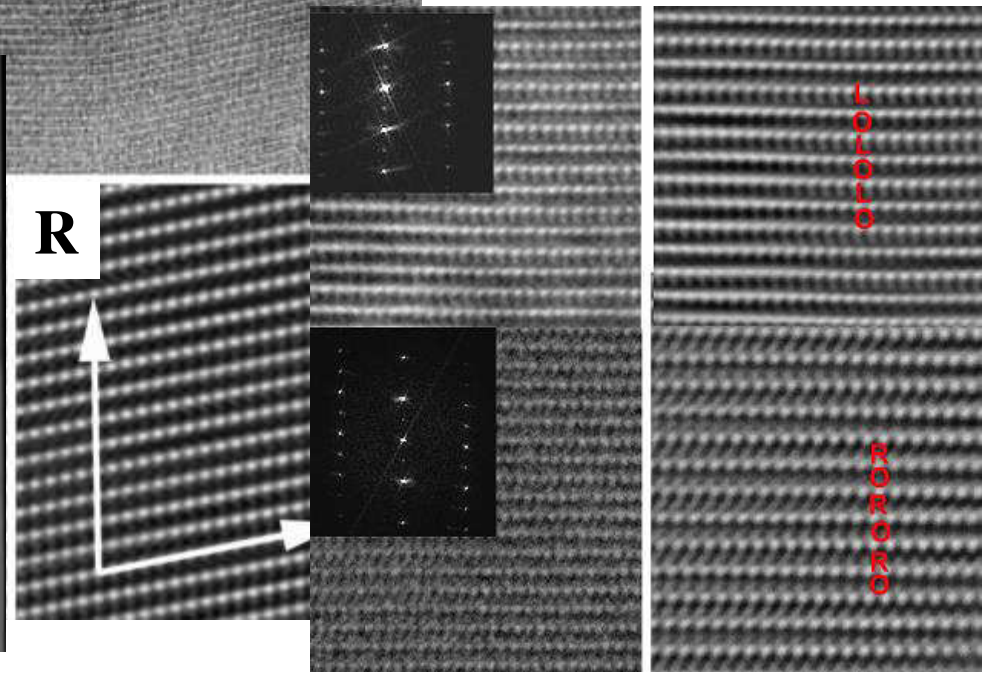

TEM imaging

Polygonal Serpentine

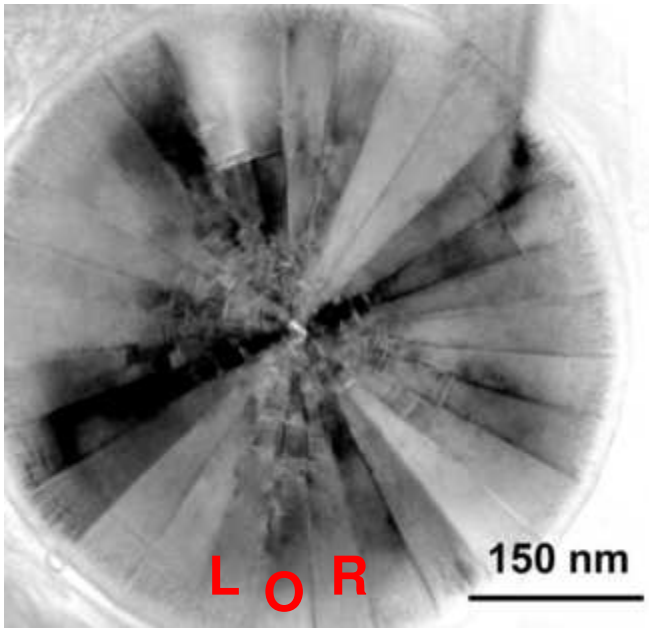

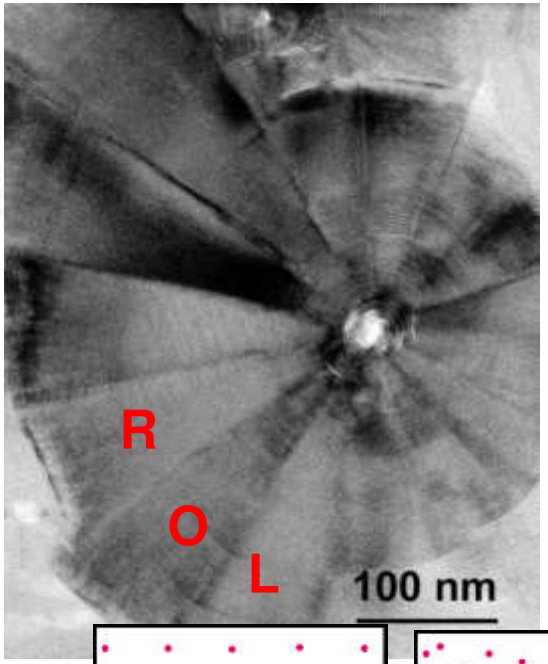

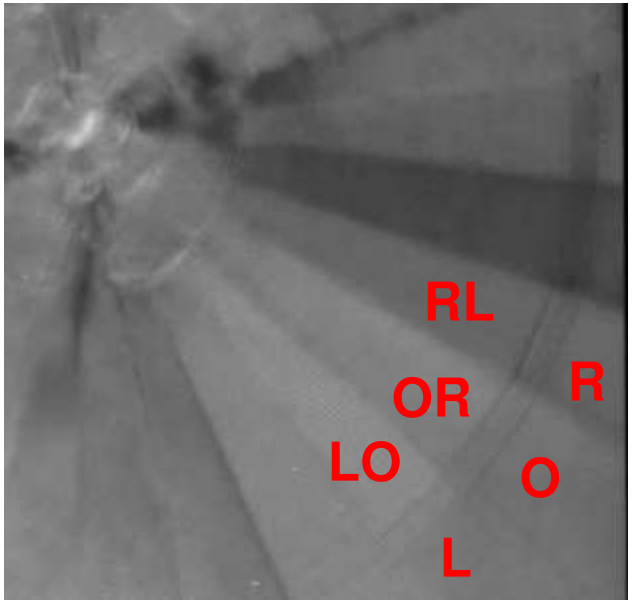

Single layer:

PS15: R-O-L

PS30: L-O-R

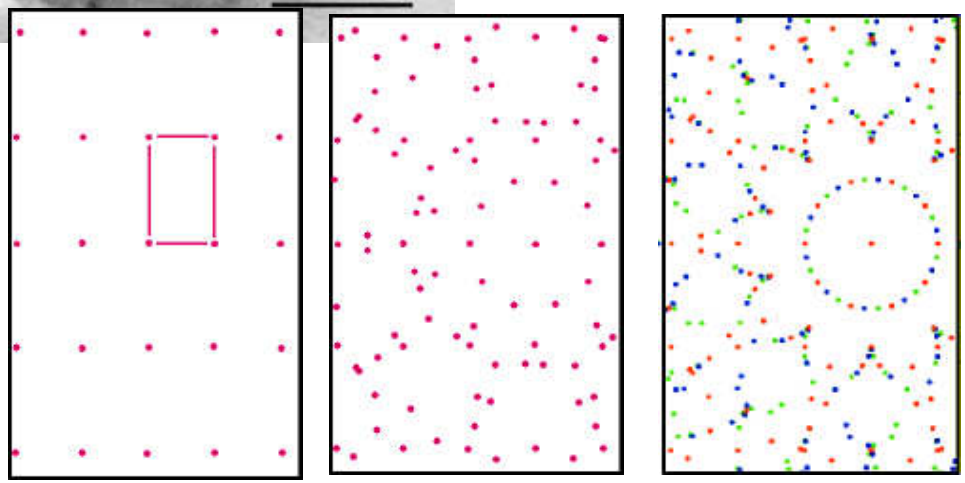

O O · 5 O + R + L

TEM imaging

Polygonal Serpentine

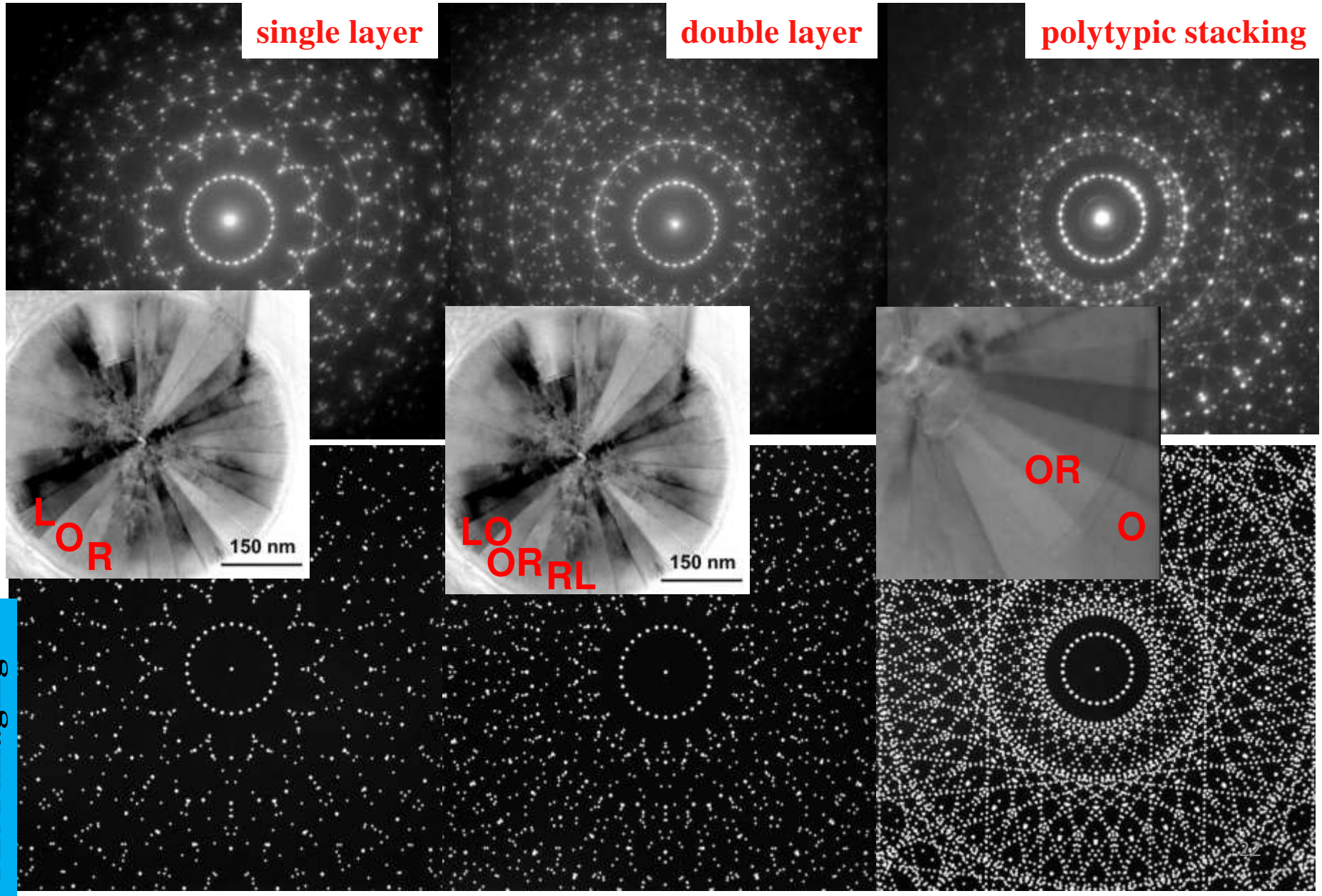

Polygonal Serpentine

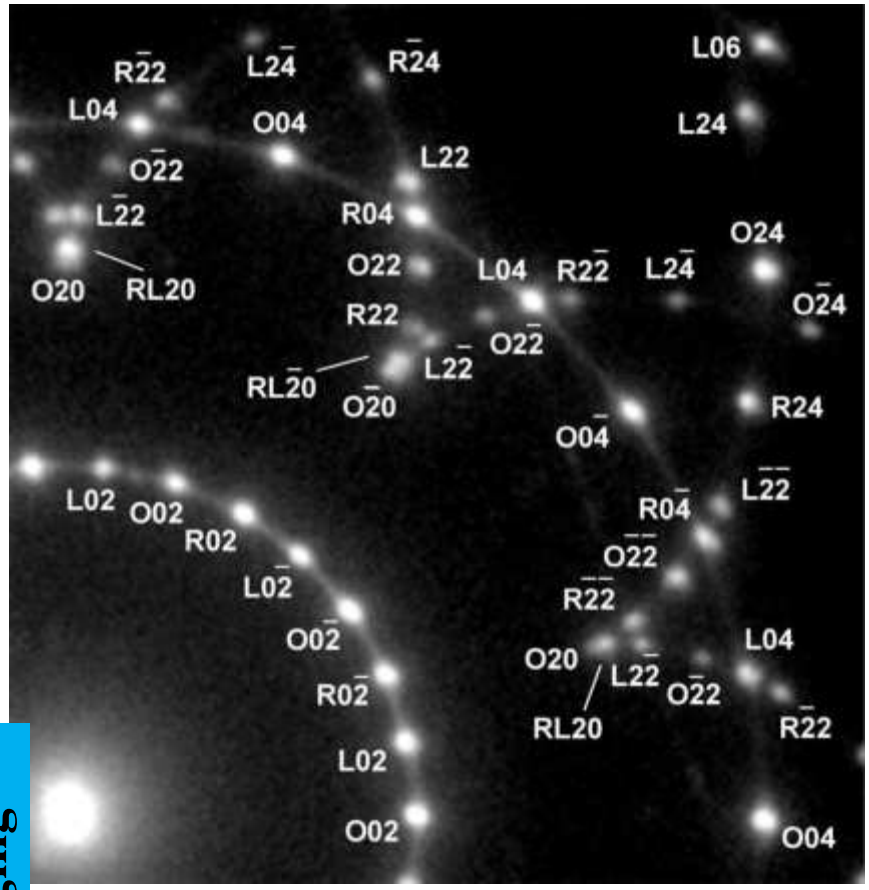

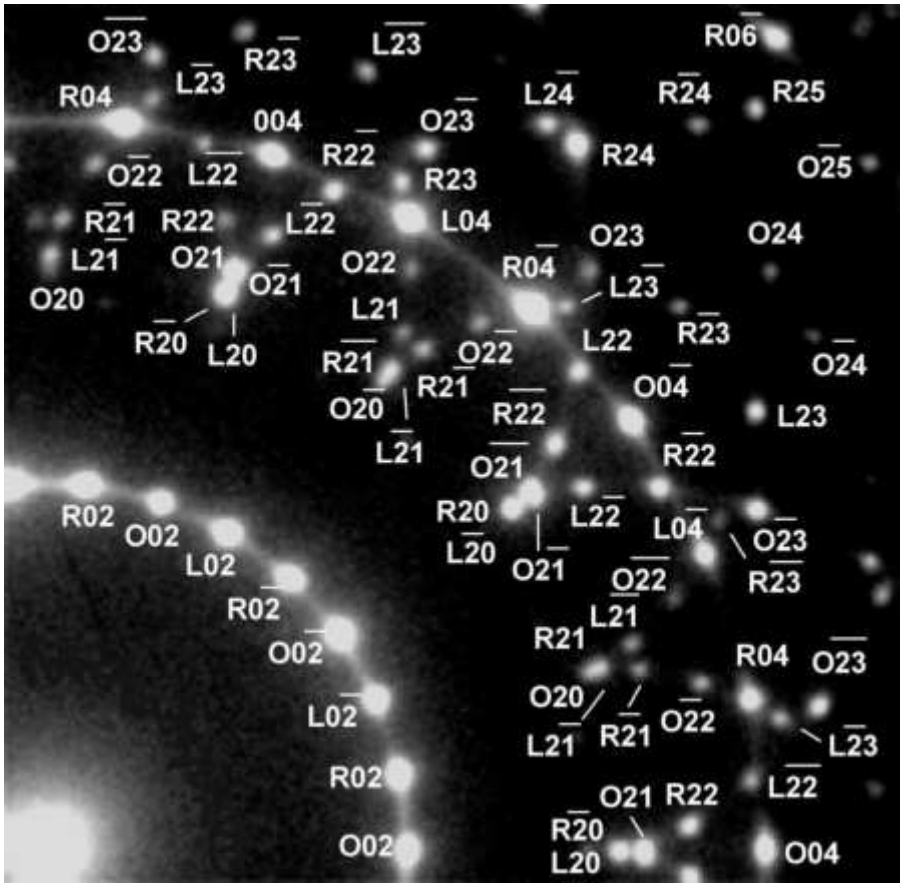

single layer

O, L, R

double layer

O = RL, L = OL, R = OR

TEM imaging

Polygonal Serpentine

[010]

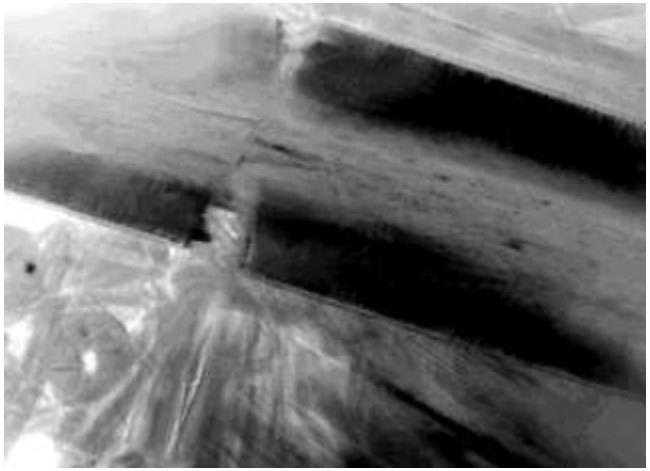

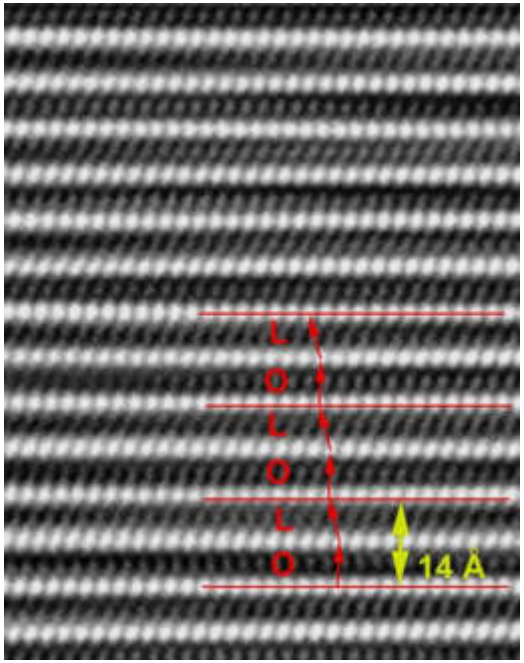

Cell parameters of different polytypes

	a	b	c	α	β	γ	sciv. a	sciv. b
O	5.3	9.2	14.7	90	97	90	no +a/3	no
L	5.3	9.2	15.0	102	97	90	no +a/3	-b/6
R	5.3	9.2	15.0	78	97	90	no +a/3	+b/6
RL	5.3	9.2	14.7	90	97	90	no +a/3	+b/6 -b/6
LO	5.3	9.2	14.8	96	97	90	no +a/3	-b/6 no
OR	5.3	9.2	14.8	84	97	90	no +a/3	no +b/6

Polygonal Serpentine

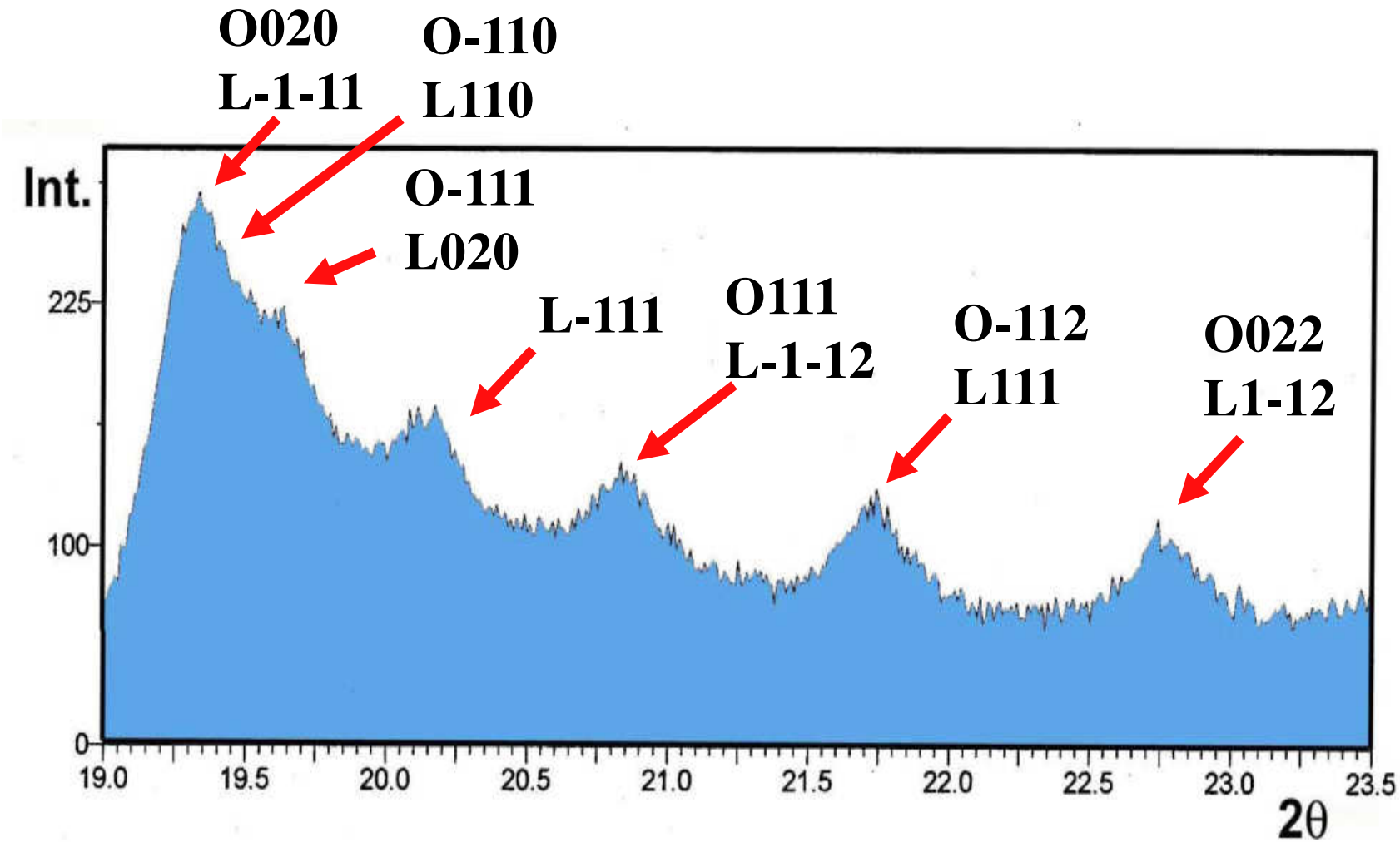

Complexity in 15- and 30-sectors polygonal serpentine: Longitudinal sections, intrasector stacking faults and XRPD satellites. E. Mugnaioli, M. Logar, M. Mellini, C. Viti, *Am Mineral* **92**, 603 (2007).

TEM imaging

Simulated HRTEM

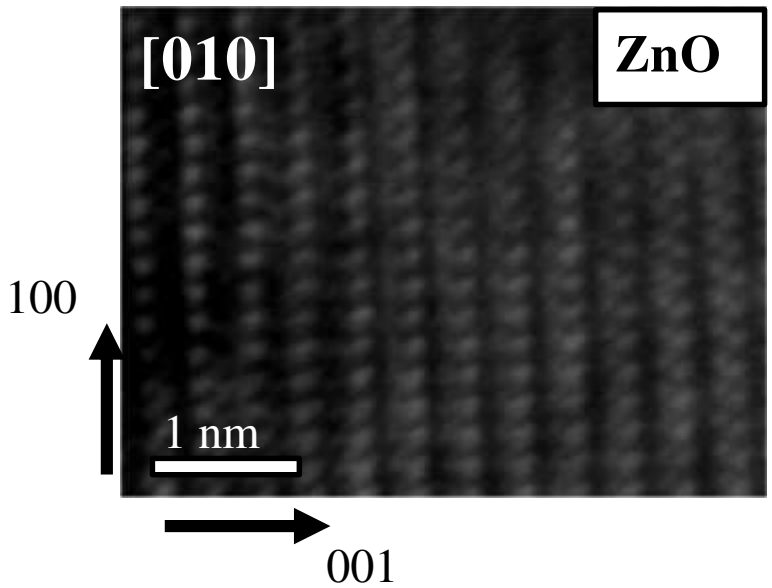

Programs for HRTEM simulation

NCEMSS	free, not easy do handle
JEMS	commercial
CALIDRIS	commercial
CERIUS	commercial

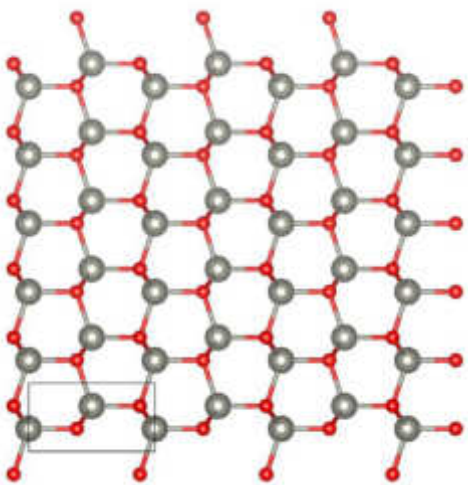

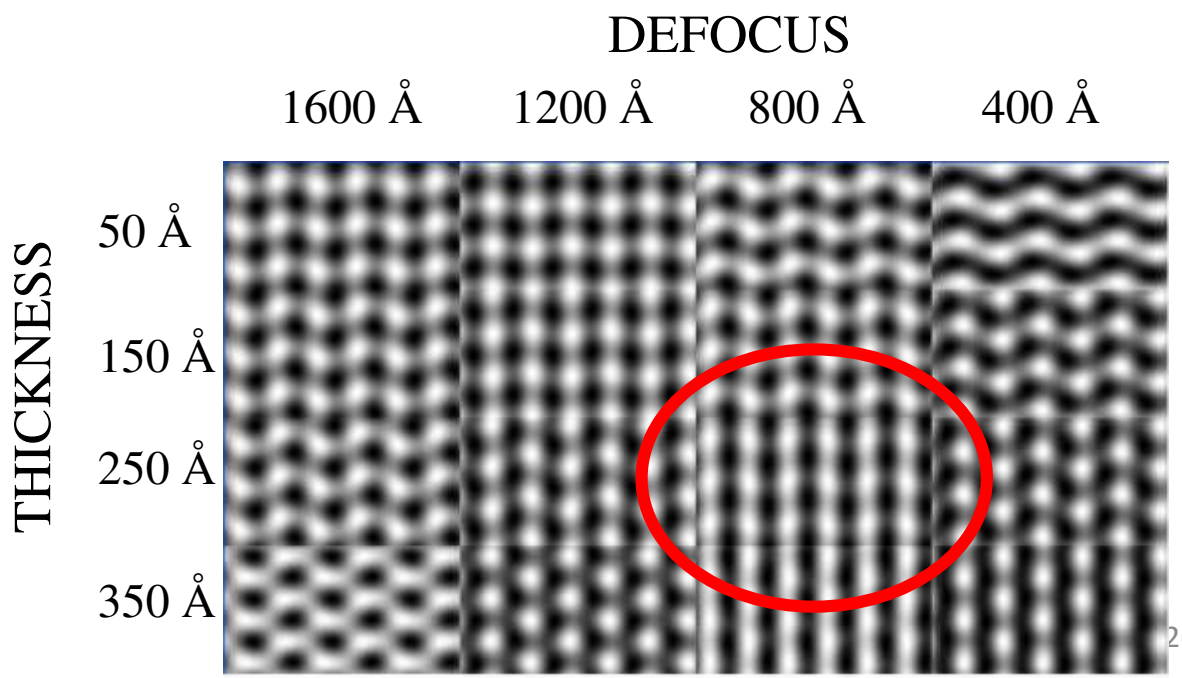

TEM imaging

Simulated HRTEM

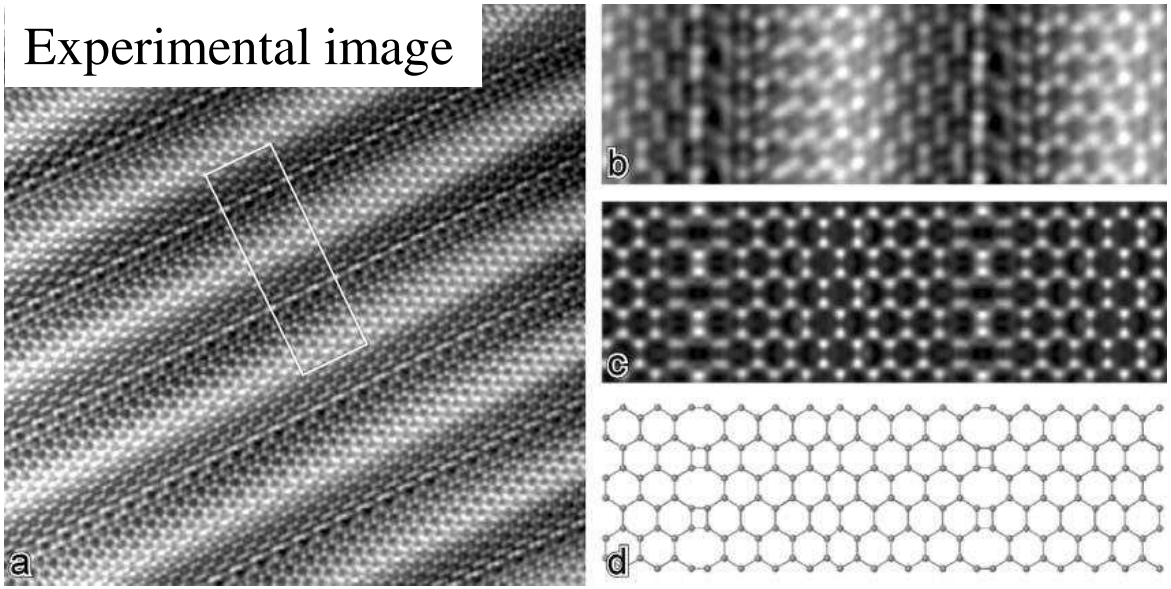

Filtered image

Simulated image

Projected structure

Antigorite
*m*17 [001]

Antigorite
*m*16 [010]

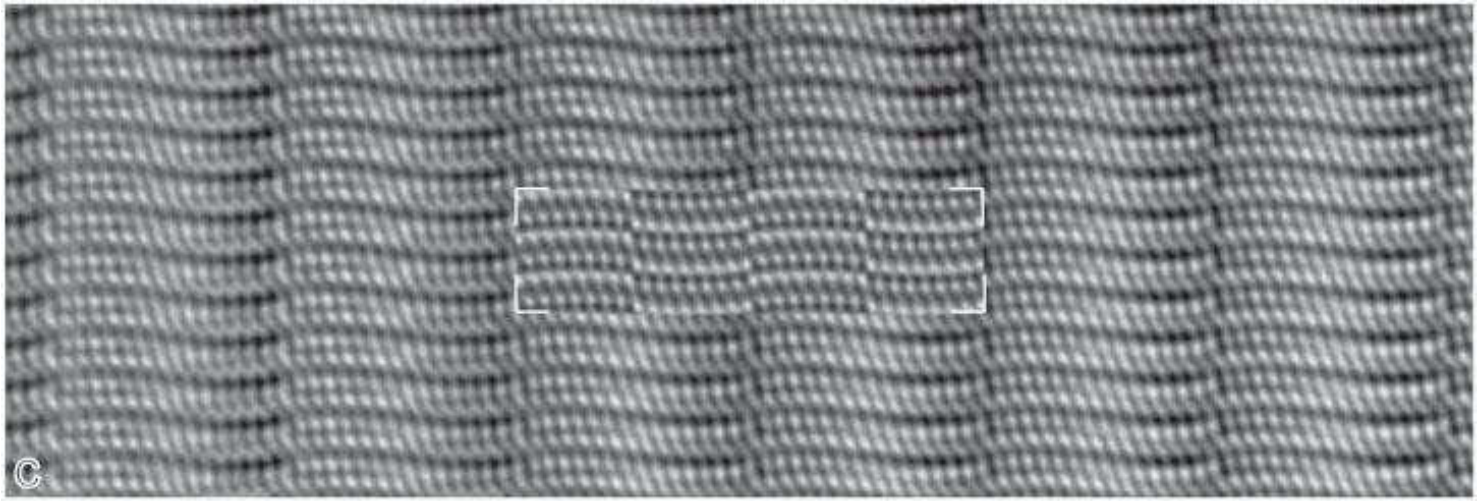

HRTEM evidence for 8-reversals in the *m* = 17 antigorite polysome.
G.C. Capitani, M. Mellini, *Am Mineral* **90**, 991 (2005).

Corrected STEM imaging

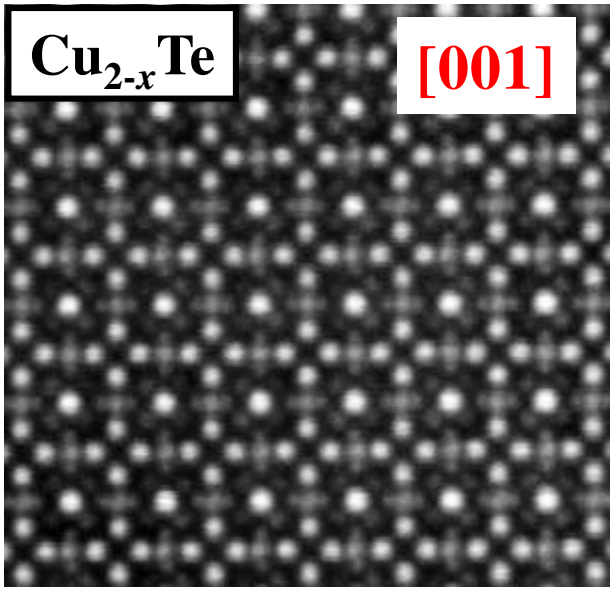

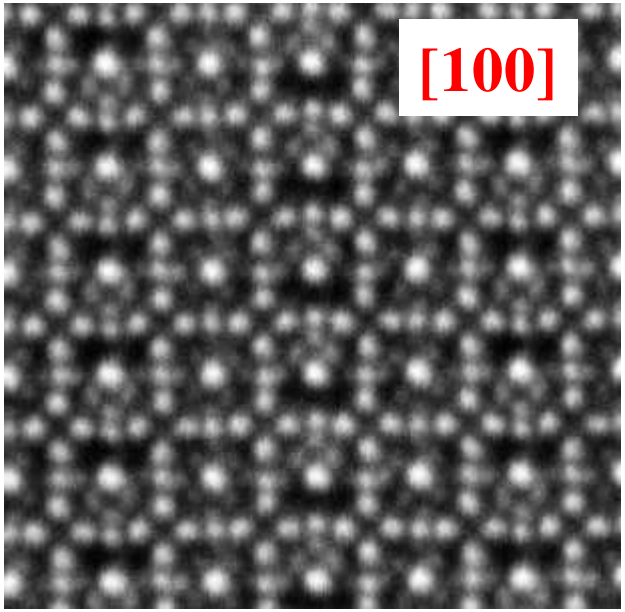

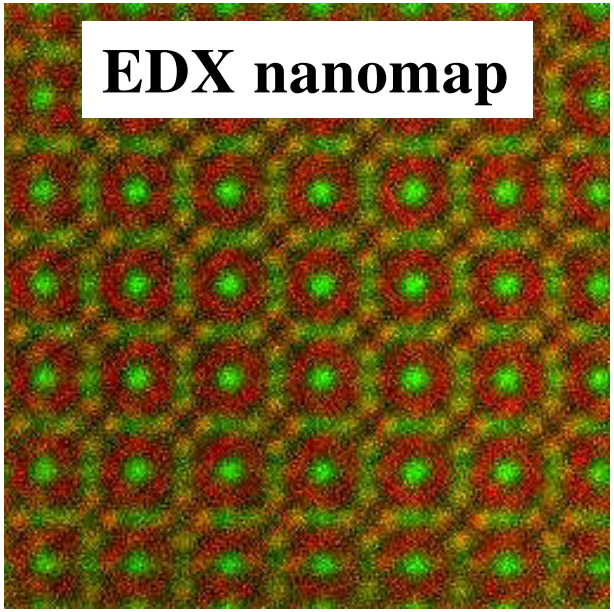

Cu

Te

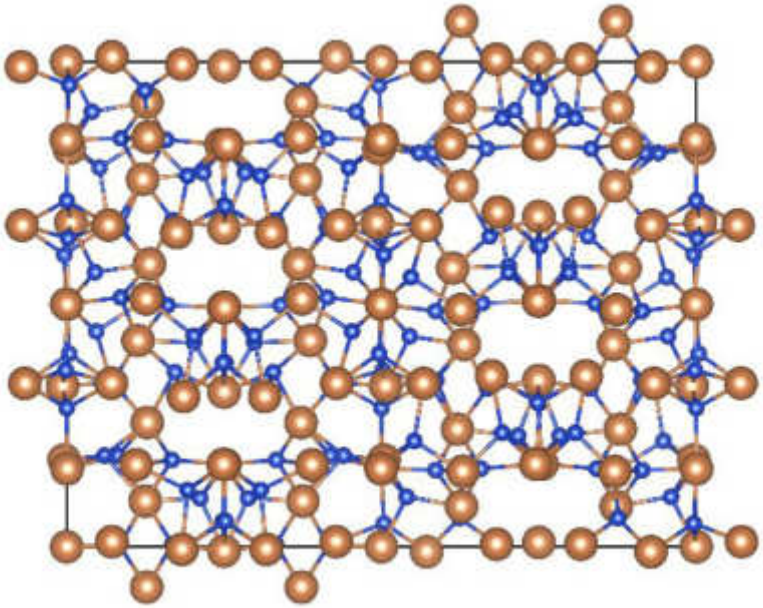

HRTEM for solving structures

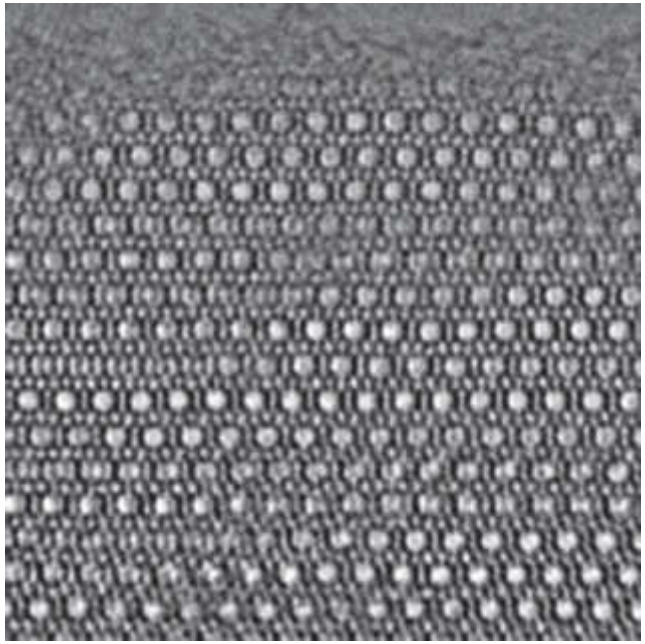

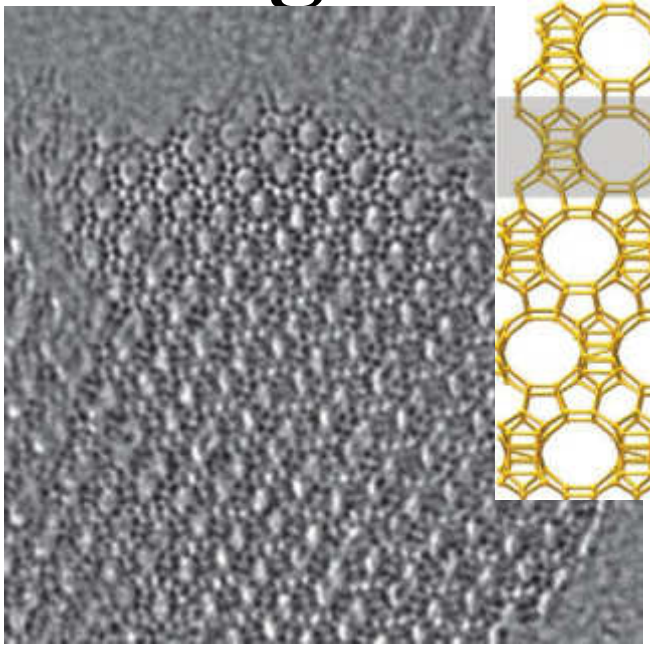

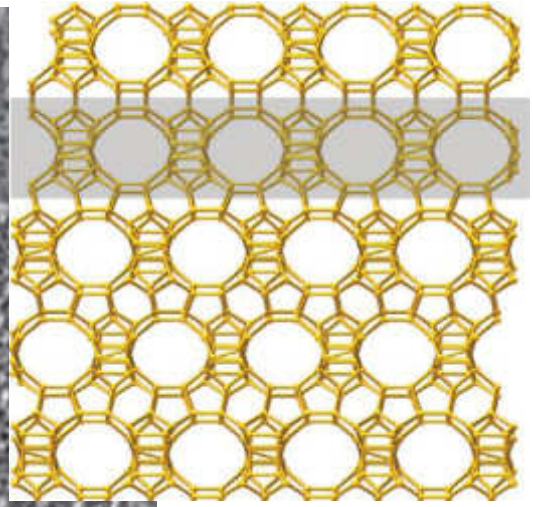

ITQ-39

Resolution limit of about 2.0-1.5 Å for conventional TEM

Necessity of an **optimal orientation**

Very complicate for structure with **long cell parameters**

2D projections - Hard to build a 3D data set

Beam damage

M

ions)

Structure and catalytic properties of the most complex intergrown zeolite ITQ-39 determined by electron crystallography. T. Willhammar, J. Sun, W. Wan, P. Oleynikov, D. Zhang, X. Zou, M. Moliner, J. Gonzalez, C. Martínez, F. Rey, A. Corma, *Nat Chem* **4**, 188 (2012).

Beam damage

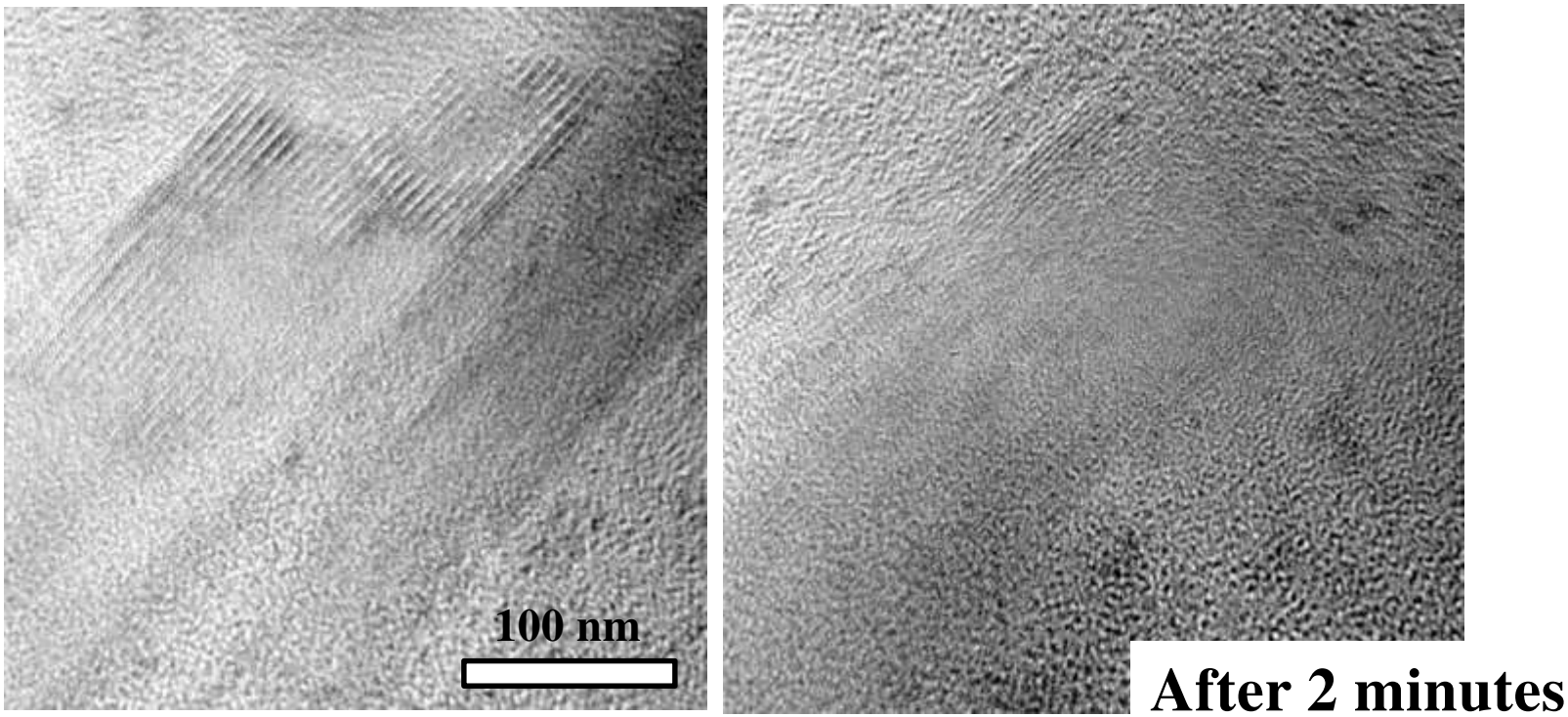

Who is beam sensitive?

All organics, porous materials, water-containing materials, many layered compounds…

at a certain level everything but very conductive materials

Electron imaging vs. Diffraction

X-rays

Incoming radiation

Sample

Scattering

Diffraction

Electrons

Incoming radiation

Sample

Scattering

Diffraction

In diffraction we miss the **crystallographic phases**, but we need a much **milder illumination,** we achieve a **better resolution** and it is more easy to get **3D data**

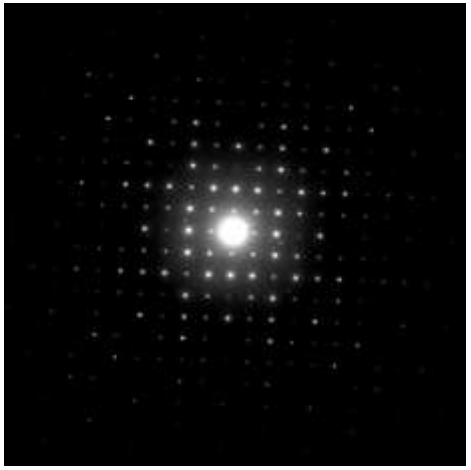

Accelerated electrons

TEM

- Short wavelength (~ 0.01-0.1 Å)
  - **small scattering angle**
  - **almost flat Ewald sphere**
  - **many reflections excited contemporarily**
- Strong (Coulomb) interaction with matter
  - **10^3-10^4 stronger interaction than X-rays**
  - **good signal/noise from nanovolumes**
  - **dynamical scattering**
- Charged (e^-)
  - **easy to deflect and focus in a nanoprobe**
  - **scattered information can be recombined in images**

In-zone electron diffraction

Phase and orientation maps

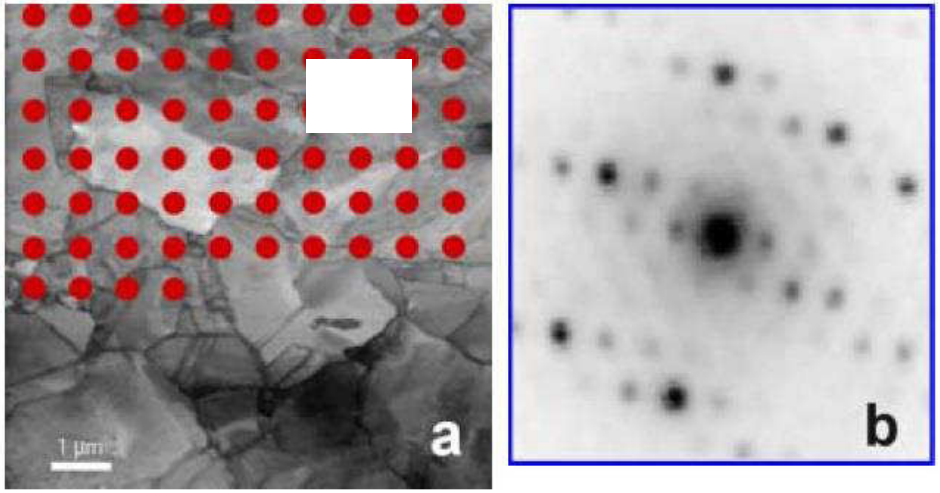

Phase and orientation map through diffraction scanning and template matching

… similar to **EBSD** but a smaller scale

In-zone electron diffraction

Al_2O_3

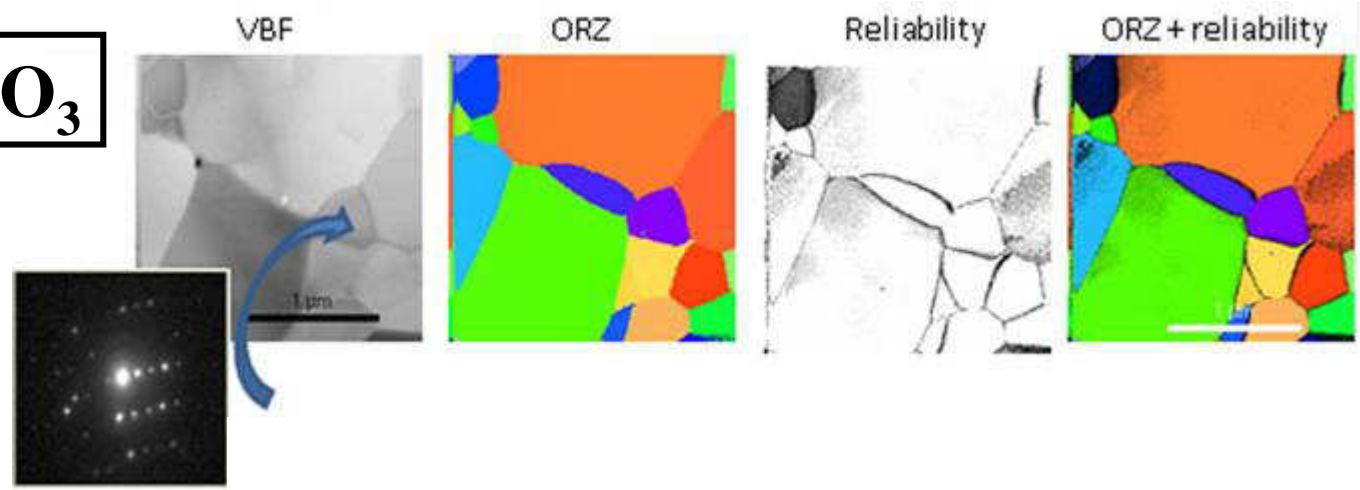

Automated nanocrystal orientation and phase mapping in the transmission electron microscope on the basis of precession electron diffraction. E.F. Rauch, J. Portillo, S. Nicolopoulos, D. Bultreys, S. Rouvimov, P. Moeck, *Z. Kristallogr.* **225**, 103 (2010).

Convergent beam electron diffraction

CBED

Parallel beam

Convergent beam

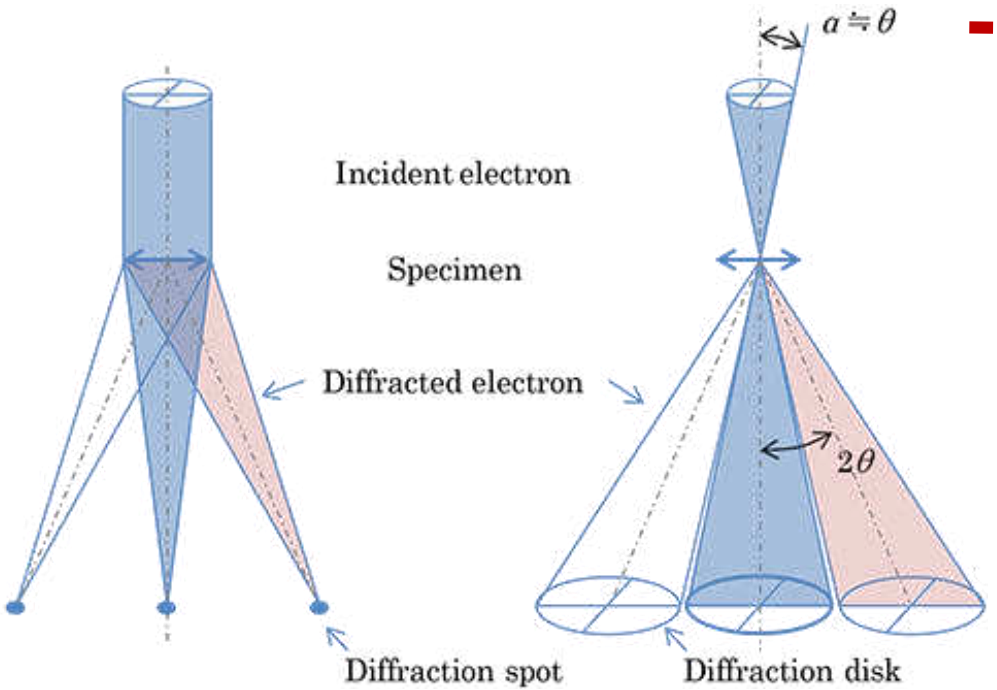

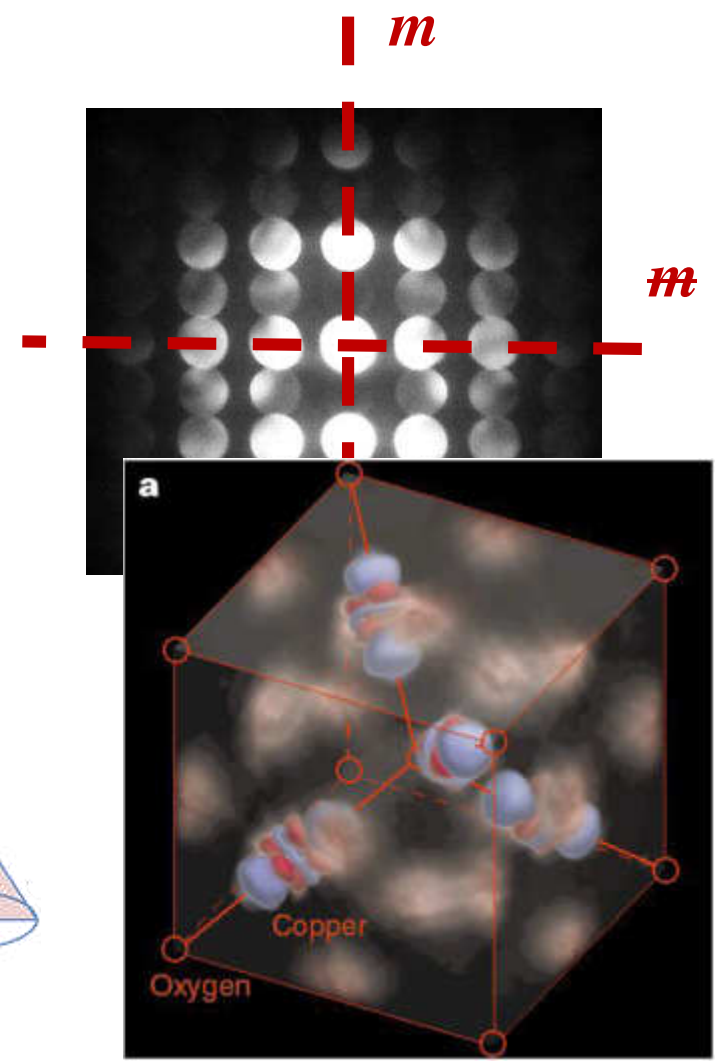

Direct observation of *d*-orbital holes and Cu-Cu bonding in Cu_2O.
J. M. Zuo, M. Kim, M. O'Keeffe, J. C. H. Spence, *Nature* **401**, 49 (199).

In-zone electron diffraction

Double-tilt acquisition of in-zone ED

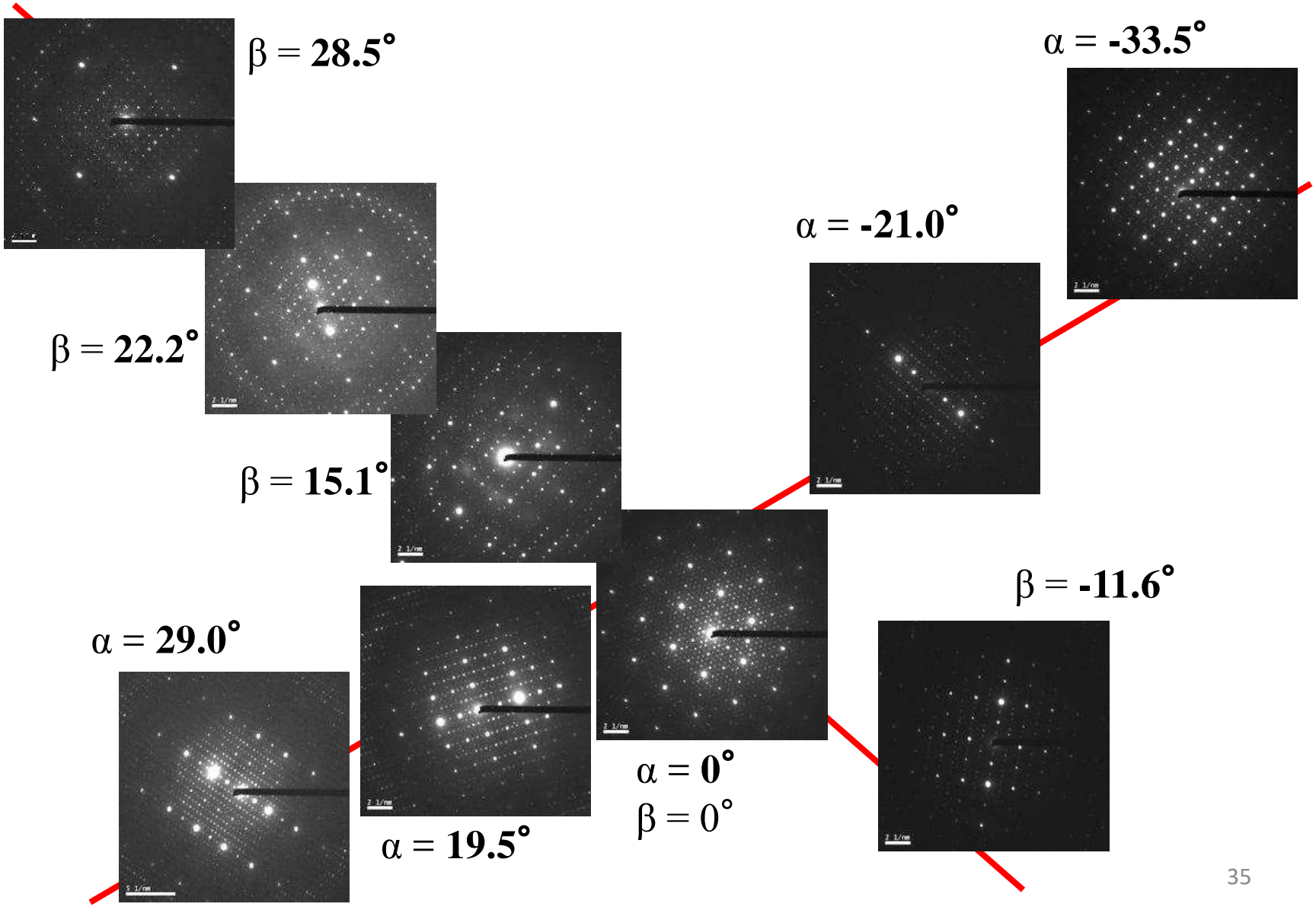

In-zone electron diffraction

Conventional in-zone ED acquisition

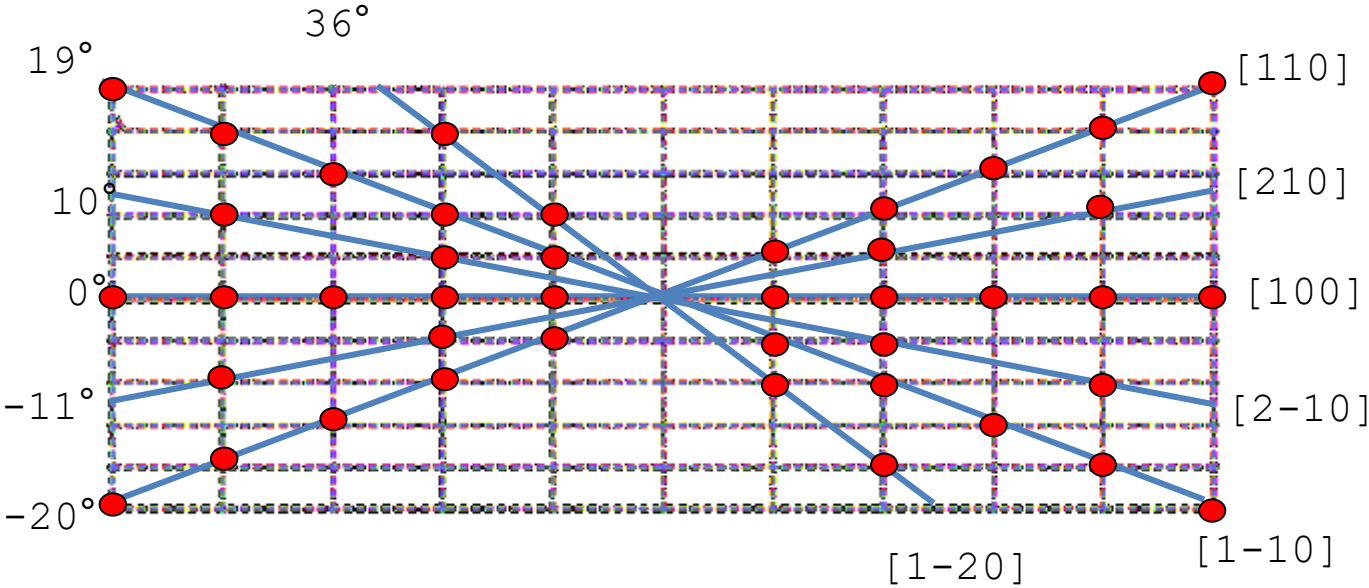

In-zone electron diffraction

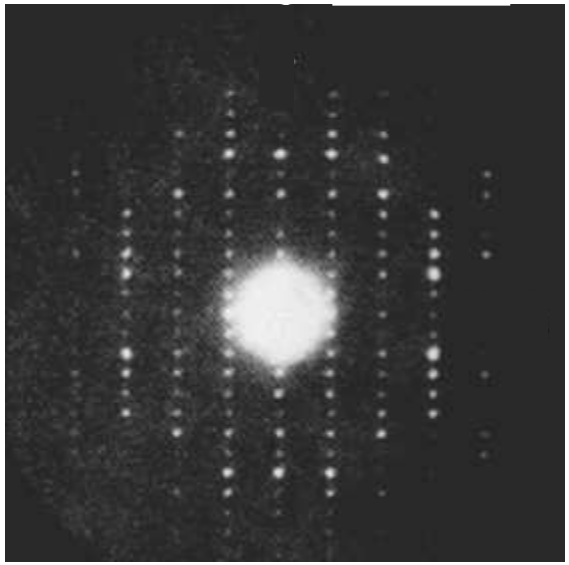

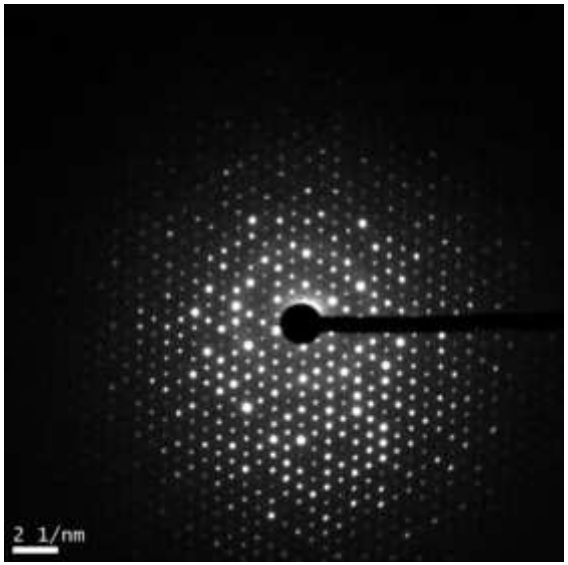

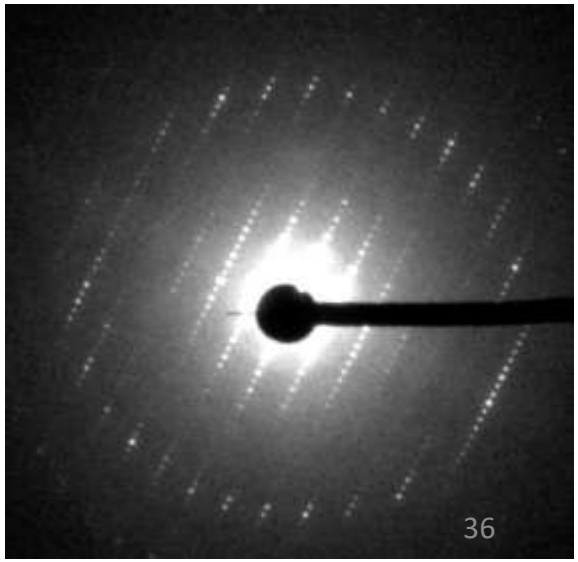

Cell parameter determination

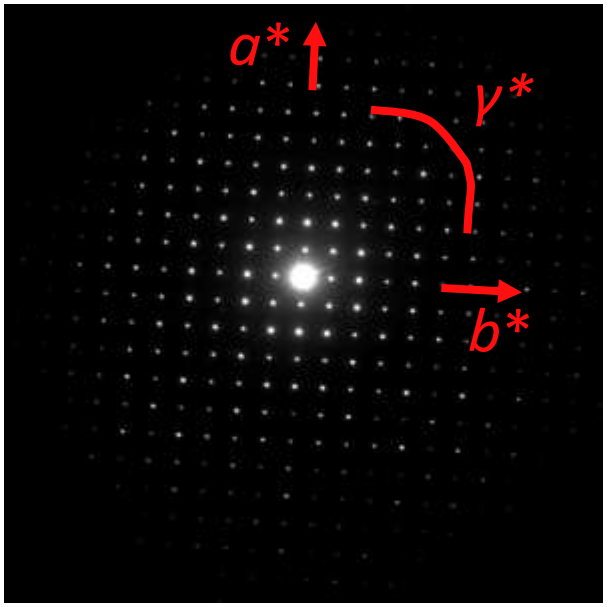

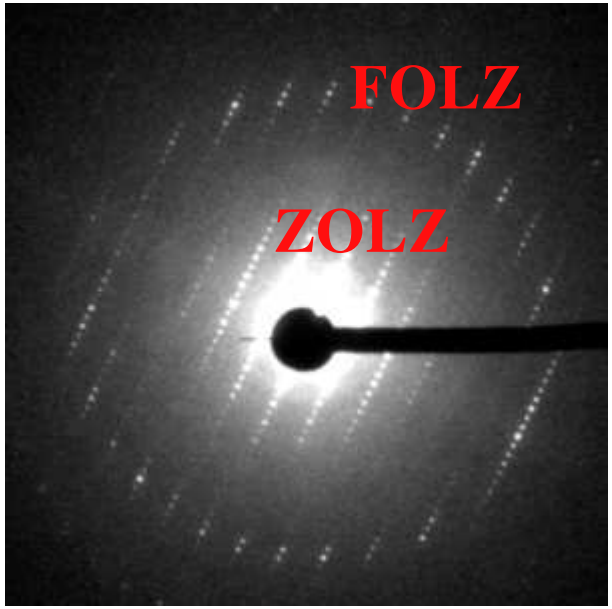

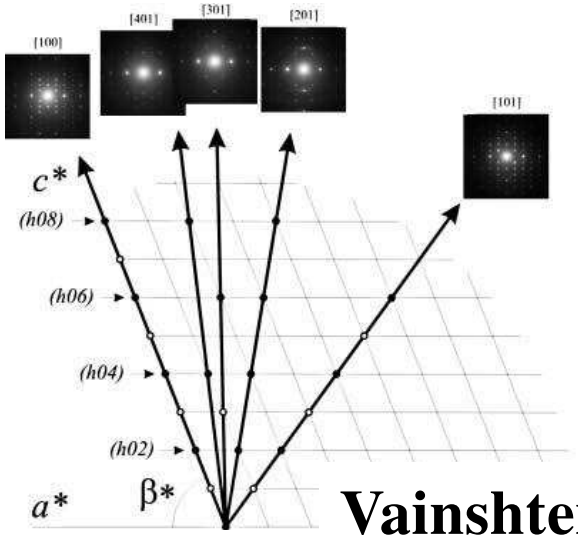

Vainshtein plot

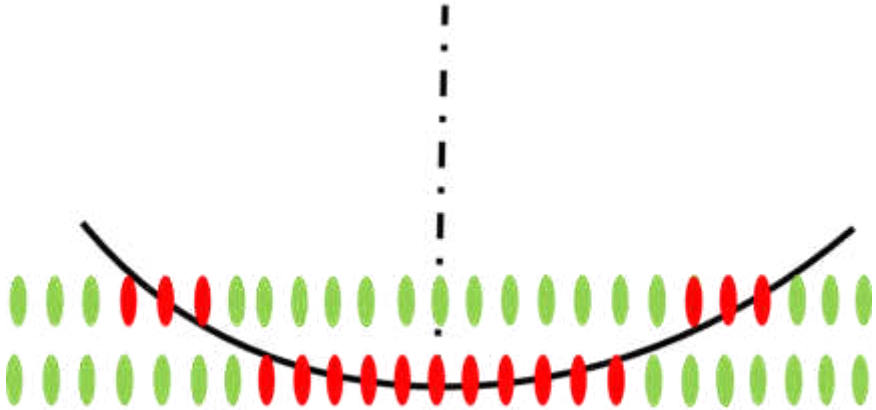

In-zone electron diffraction

Conventional in-zone ED acquisition

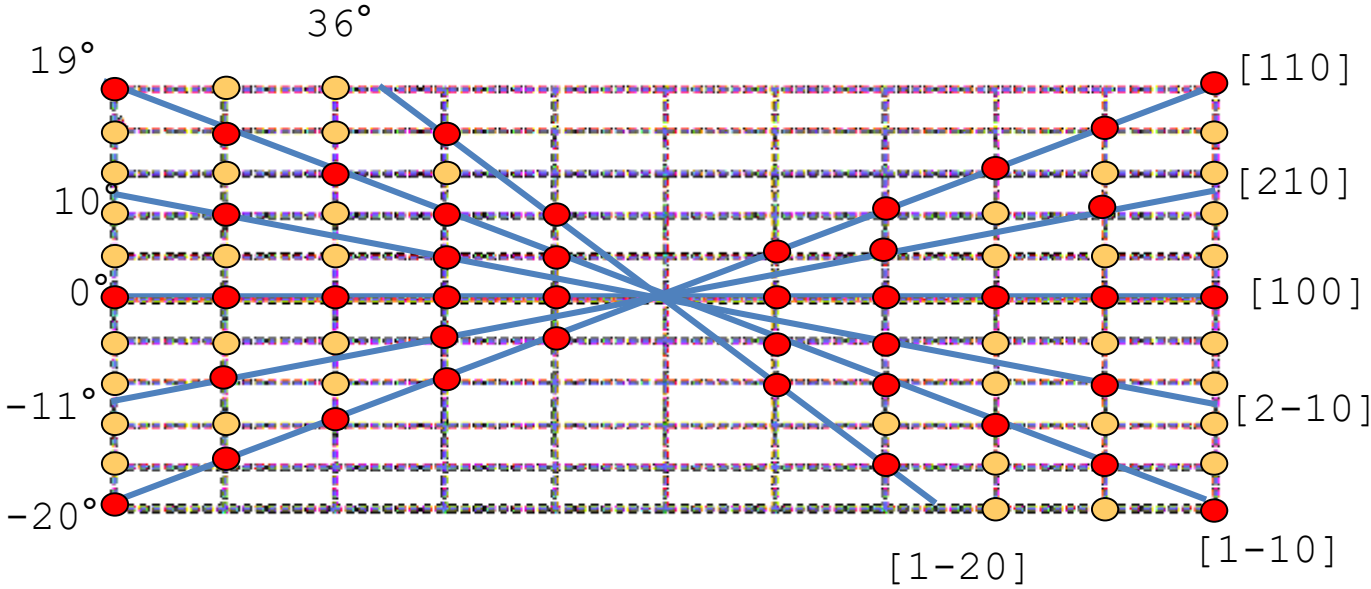

- **crystal orientation:** expertise, beam damage during orientation
- **limited number of zones:** few reflections, data from different crystals
- **most of high index reflections are missing**
- **in-zone patterns:** maximum dynamical effects, difficult to merge

Dynamic effects

Weak interaction

Strong interaction

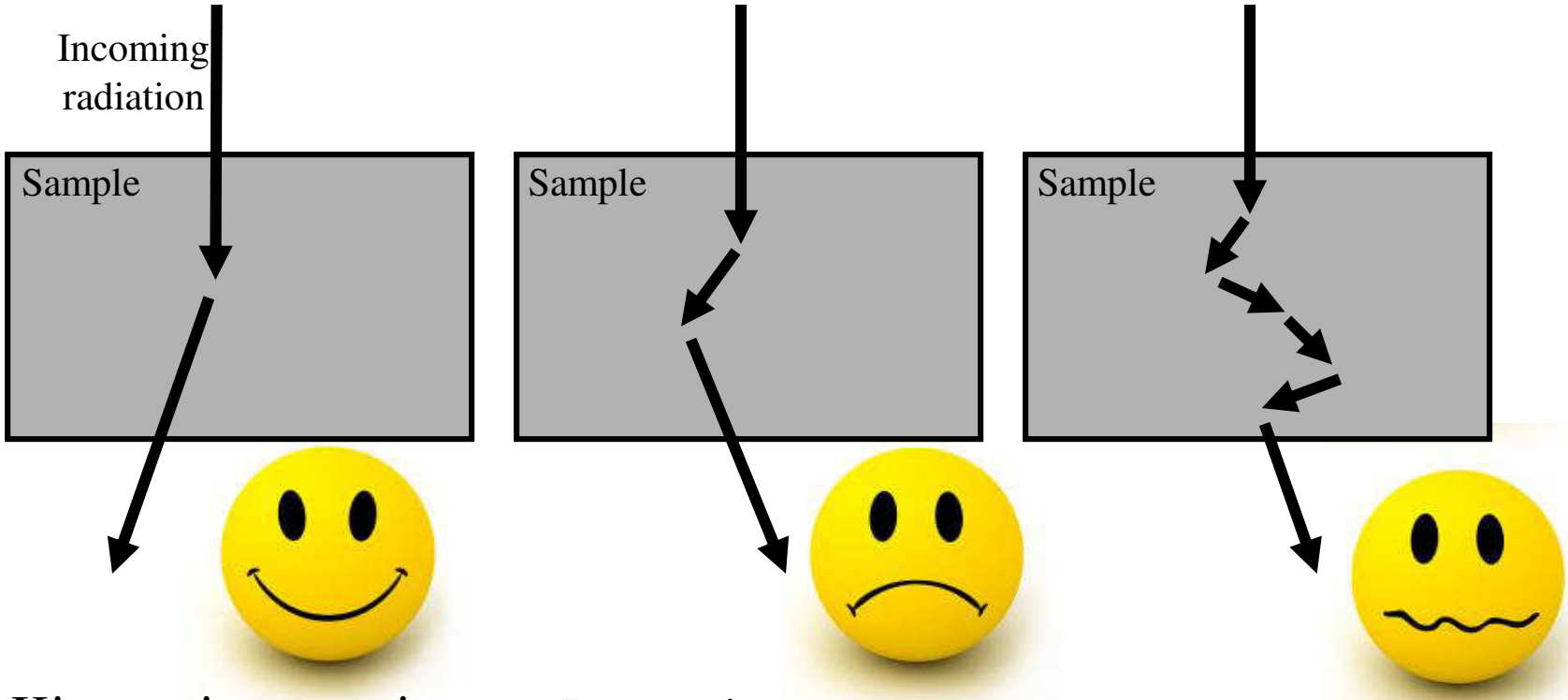

Kinematic scattering
Single scattering
$I_{hkl} \sim (F_{hkl})^2$
Always the case for X-rays

Dynamic scattering
2-beam scattering
Blackman formula
$I_{hkl} \sim F_{hkl}$

Dynamic scattering
Multi-beam
?

In-zone electron diffraction

Kinematic scattering

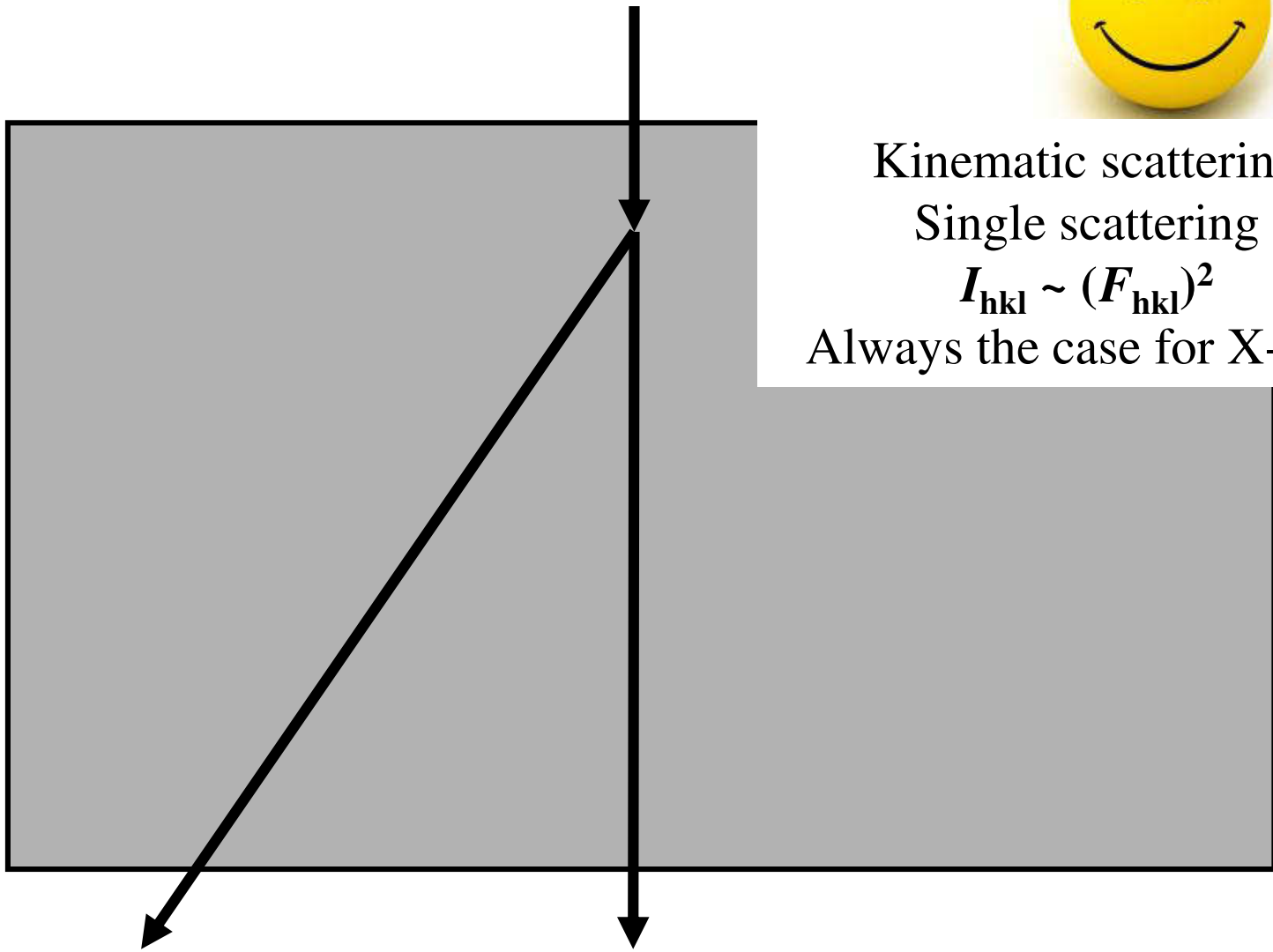

Kinematic scattering
Single scattering
$I_{hkl} \sim (F_{hkl})^2$
Always the case for X-rays

In-zone electron diffraction

Dynamic scattering

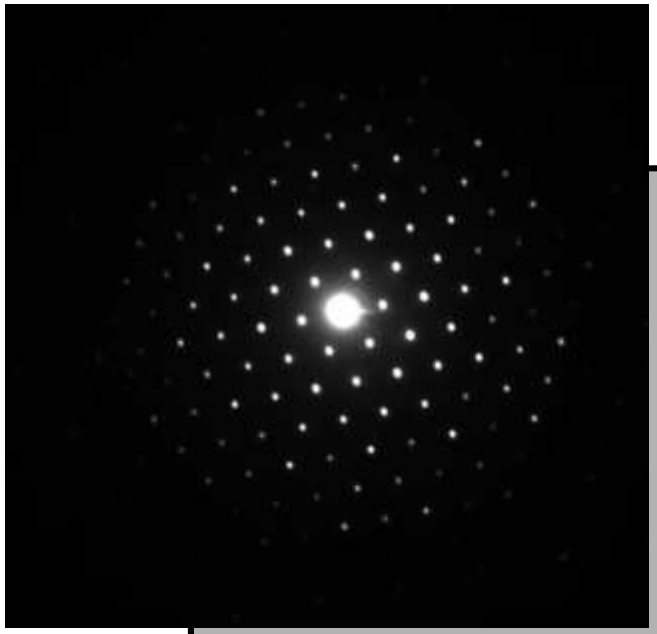

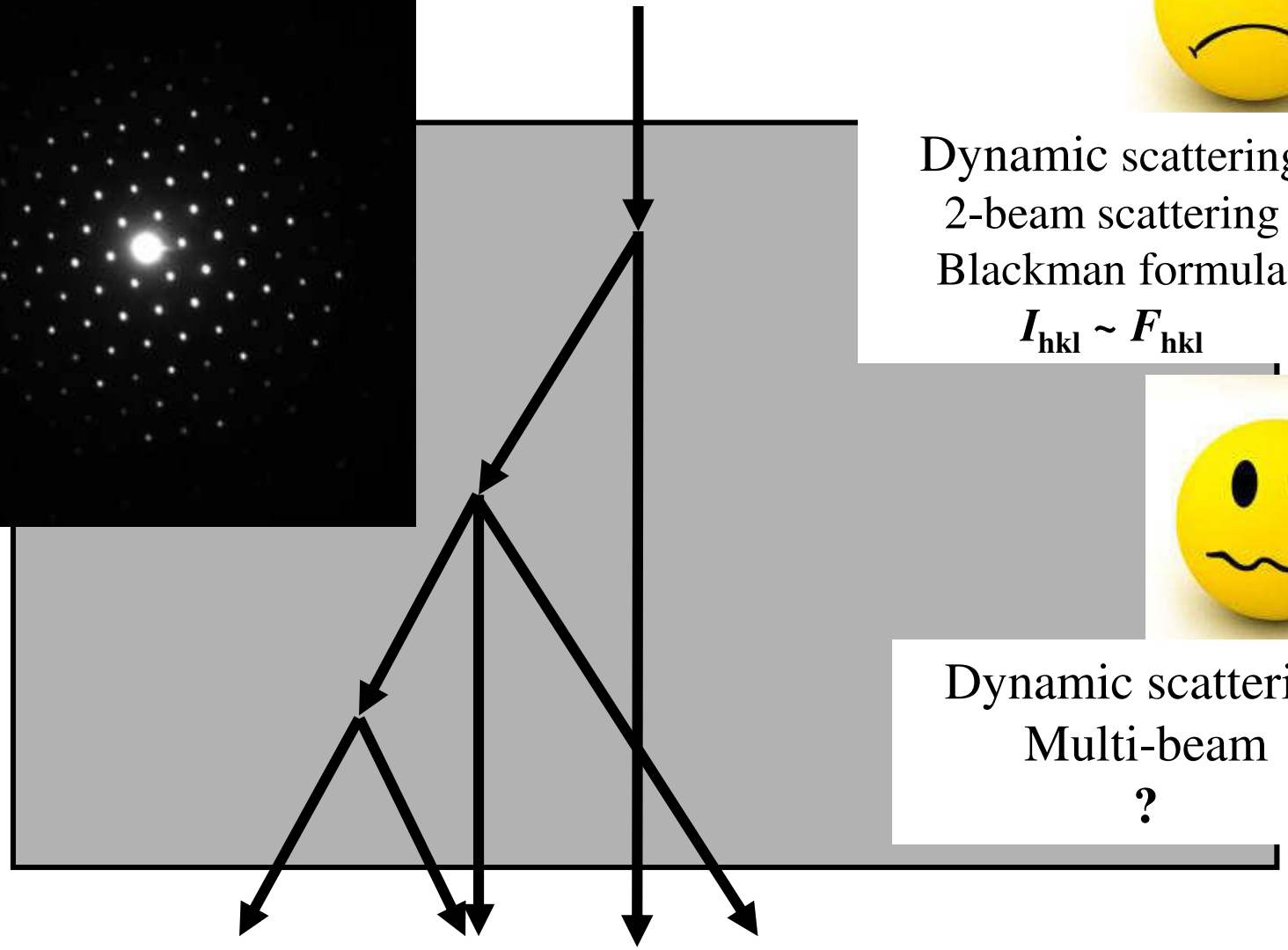

Dynamic scattering
2-beam scattering
Blackman formula
$I_{hkl} \sim F_{hkl}$

Dynamic scattering
Multi-beam
?

In-zone electron diffraction

Precession electron diffraction

Courtesy of Northwestern University, USA
(C.S. Own, L. Marks)

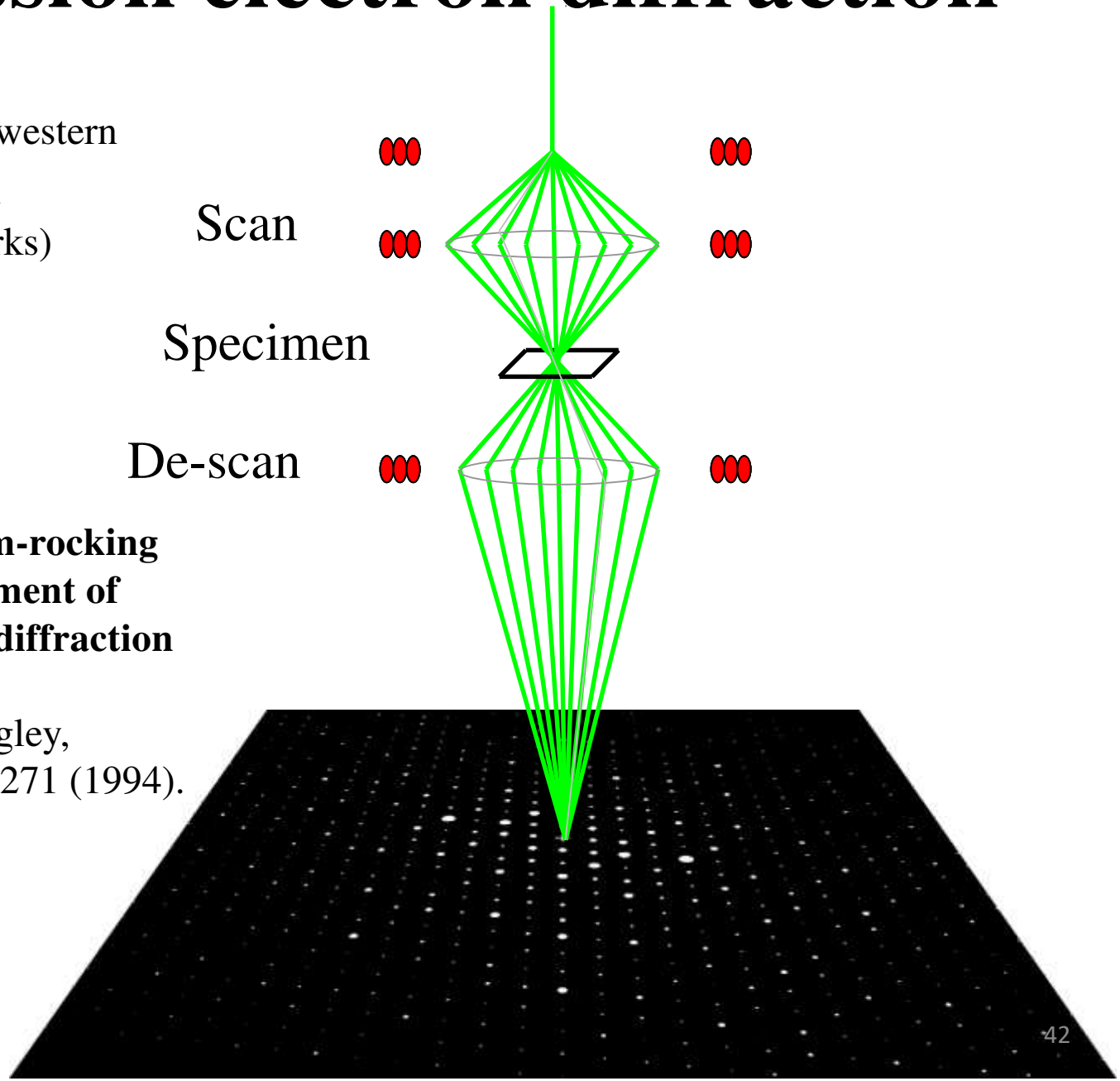

Double conical beam-rocking system for measurement of integrated electron diffraction intensities.
R. Vincent, P.A. Midgley, *Ultramicroscopy* 53, 271 (1994).

Precession Electron Diffraction

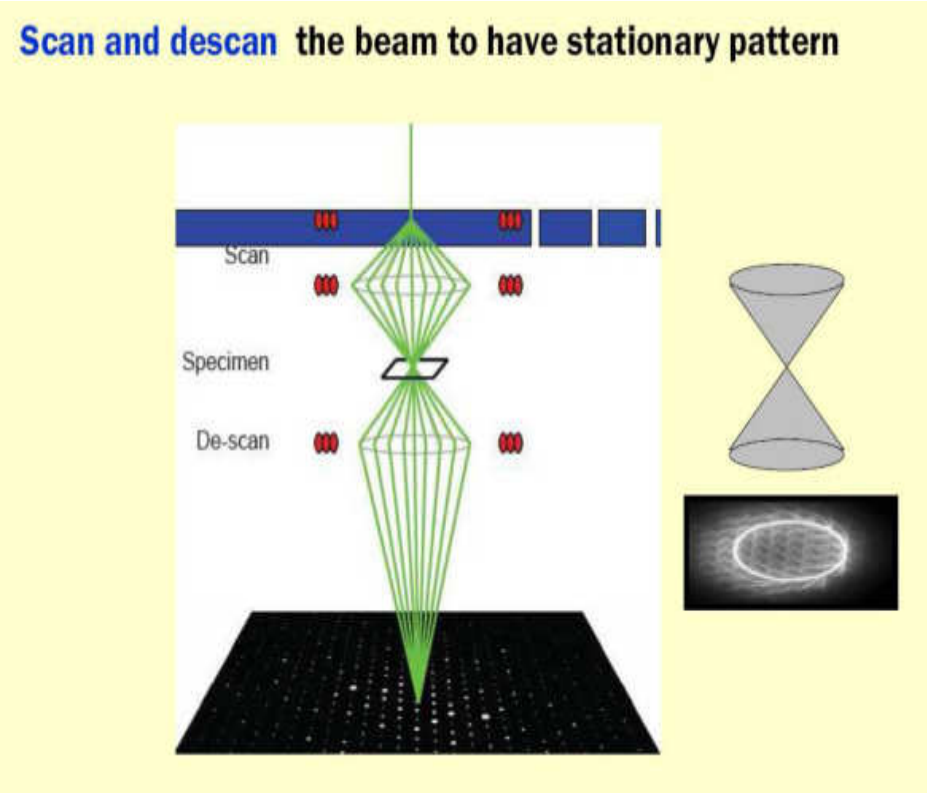

DigiStar by NanoMEGAS

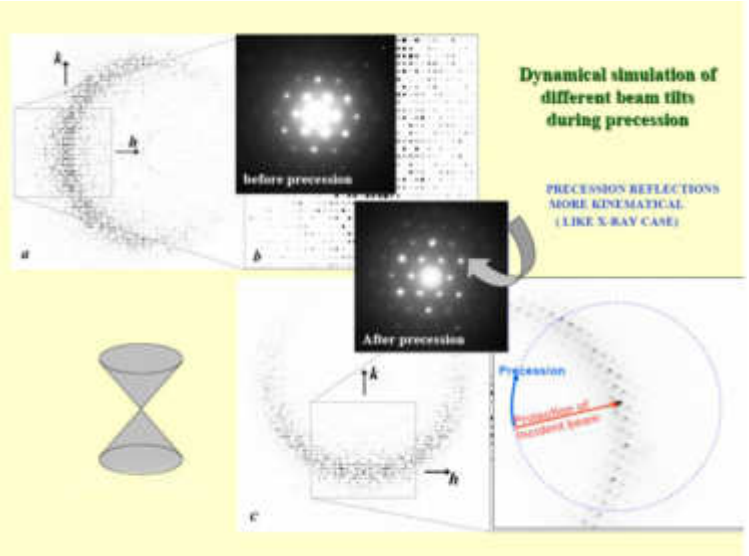

Beam is rotating very fast avoiding full orientation of the zone

Double conical beam-rocking system for measurement of integrated electron diffraction intensities. R. Vincent, P.A. Midgley, *Ultramicroscopy* **53**, 271 (1994).

Precession Electron Diffraction

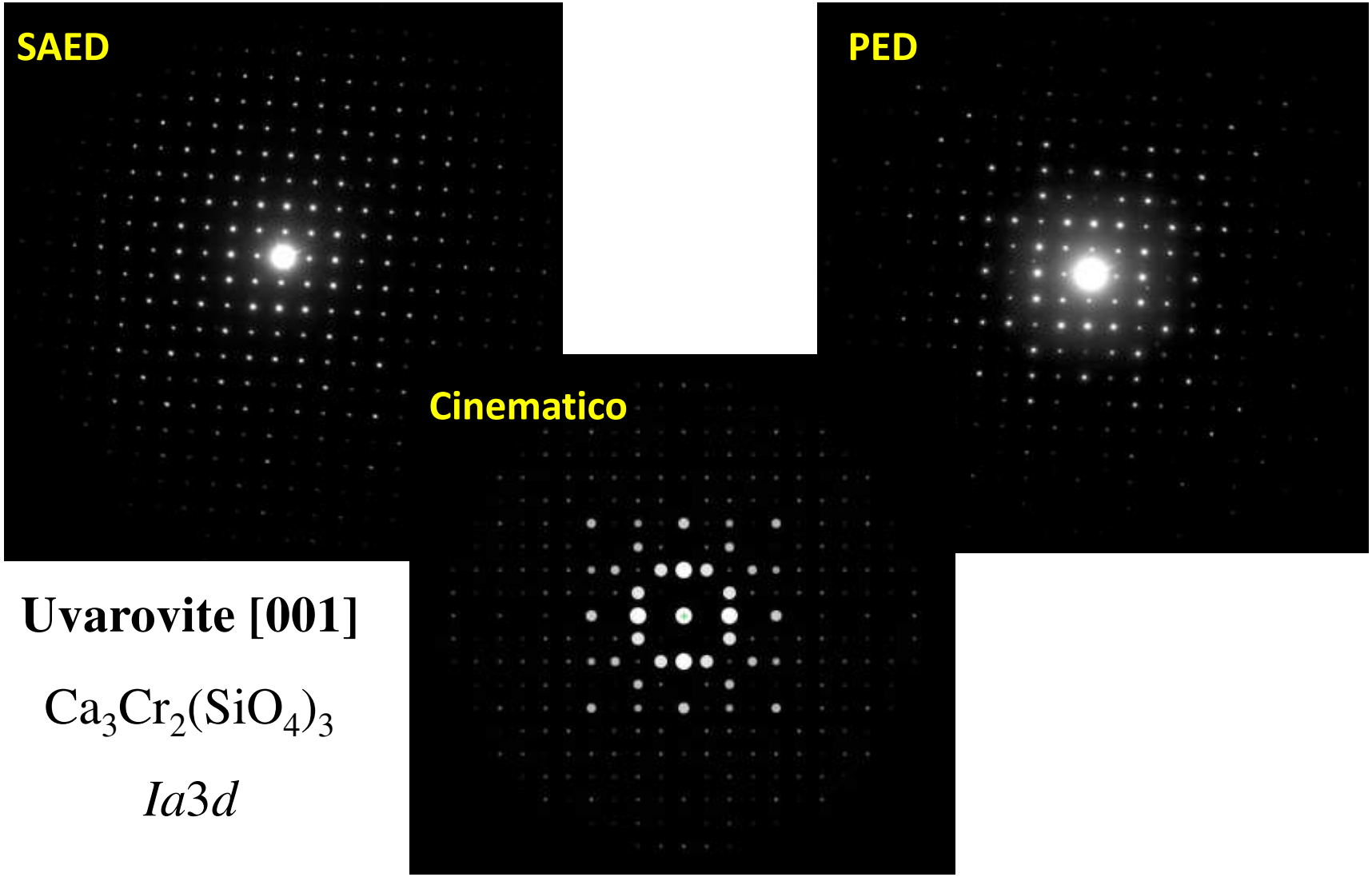

Uvarovite [001]

$Ca_3Cr_2(SiO_4)_3$

Ia3d

In-zone electron diffraction

Structure solution with three-dimensional sets of precessed electron diffraction intensities. M. Gemmi, S. Nicolopoulos, *Ultramicroscopy* **107**, 483 (2007).

Structure solution by in-zone ED

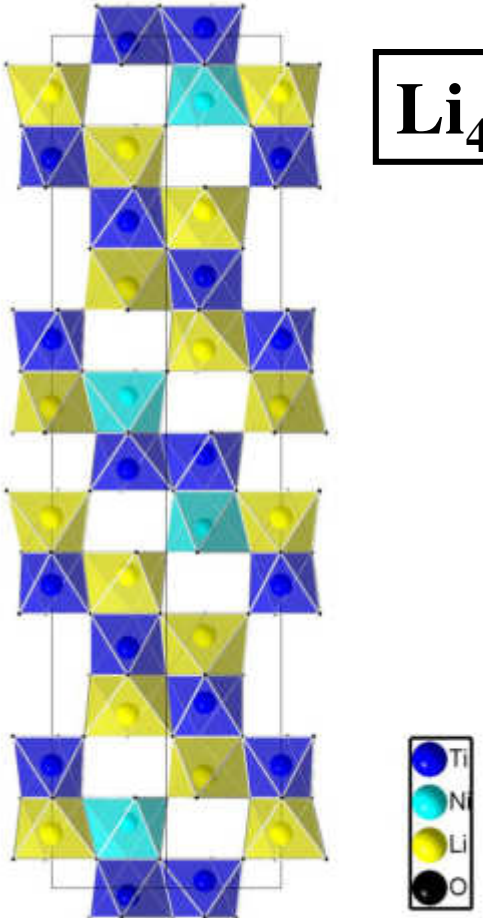

$Li_4Ti_8Ni_3O_{21}$

$LiBH_4$

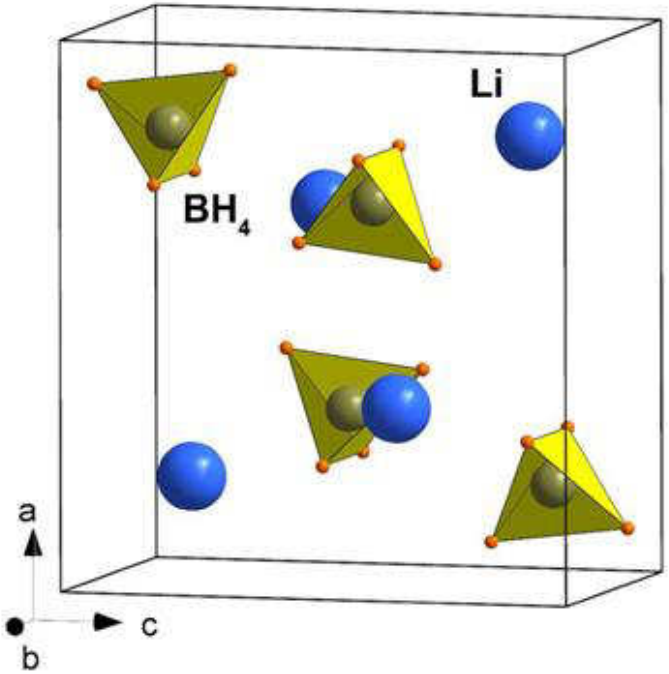

Structure solution of the new titanate $Li_4Ti_8Ni_3O_{21}$ using precession electron diffraction. M. Gemmi, H. Klein, A. Rageau, P. Strobelb, F. Le Cras, *Acta Crystallogr B* **66**, 60 (2010).

Crystal Structure of a Lightweight Borohydride from Submicrometer Crystallites by Precession Electron Diffraction. J. Hadermann, A. Abakumov, S. Van Rompaey, T. Perkisas, Y. Filinchuk, G. Van Tendeloo, *Chem Mater* **24**, 3401 (2012).

Structure solution by in-zone ED

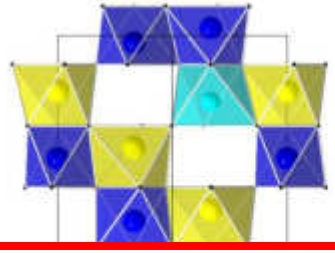

$Li_4Ti_8Ni_3O_{21}$

$LiBH_4$

$I_{hkl} \neq c\ F_{hkl}^2$

Negative thermal factor

Missing light atoms

Difficulties in sorting the correct solution

Direct elctron crystallographic determination of zeolite zonal structures. D.L. Dorset, C.J. Gilmore, J.L. Jorda, S. Nicolopoulos, *Ultramicroscopy* 107, 462 (2007).

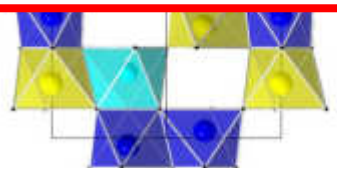

Structure solution of the new titanate $Li_4Ti_8Ni_3O_{21}$ using precession electron diffraction. M. Gemmi, H. Klein, A. Rageau, P. Strobelb, F. Le Cras, *Acta Crystallogr B* **66**, 60 (2010).

Crystal Structure of a Lightweight Borohydride from Submicrometer Crystallites by Precession Electron Diffraction. J. Hadermann, A. Abakumov, S. Van Rompaey, T. Perkisas, Y. Filinchuk, G. Van Tendeloo, *Chem Mater* **24**, 3401 (2012).

Can we use the TEM as a (primitive) single-crystal diffractometer?

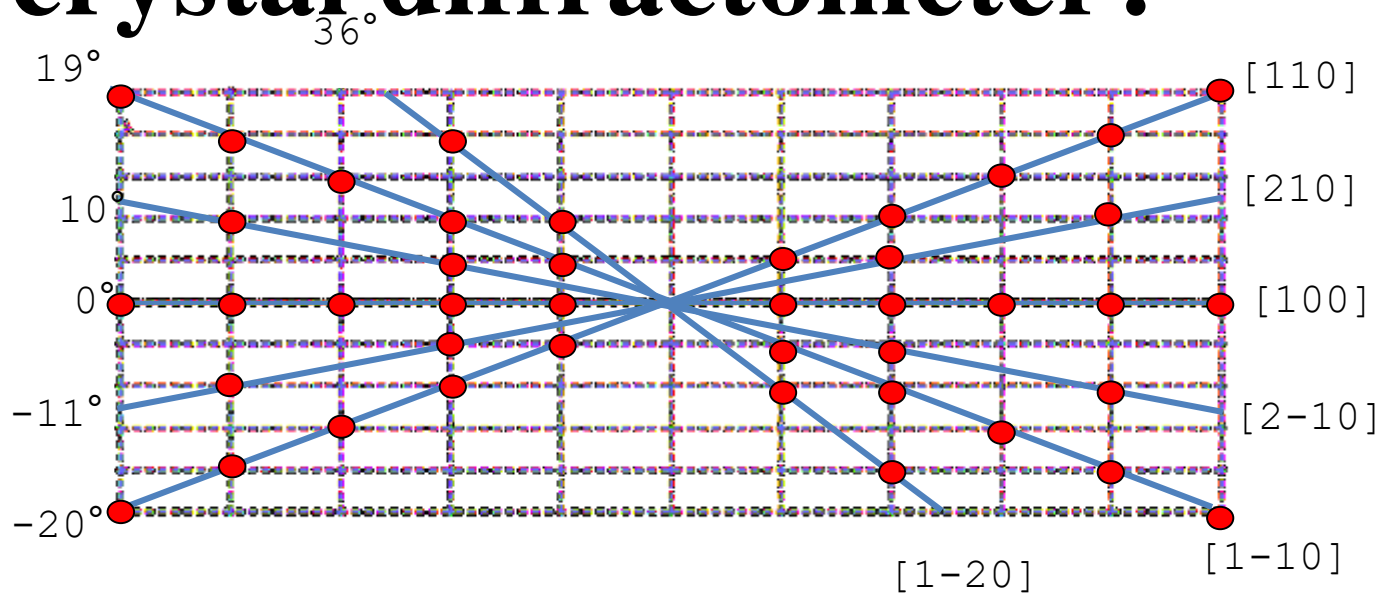

In-zone electron diffraction

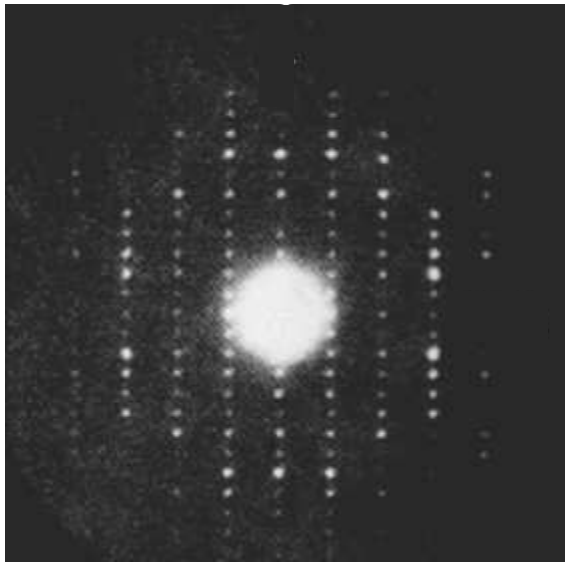

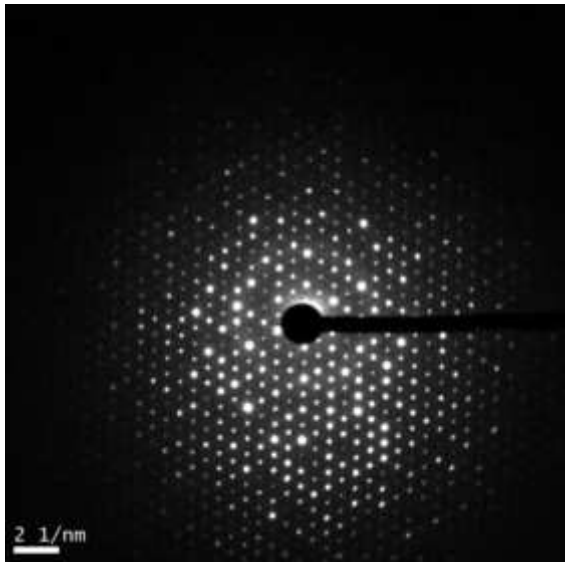

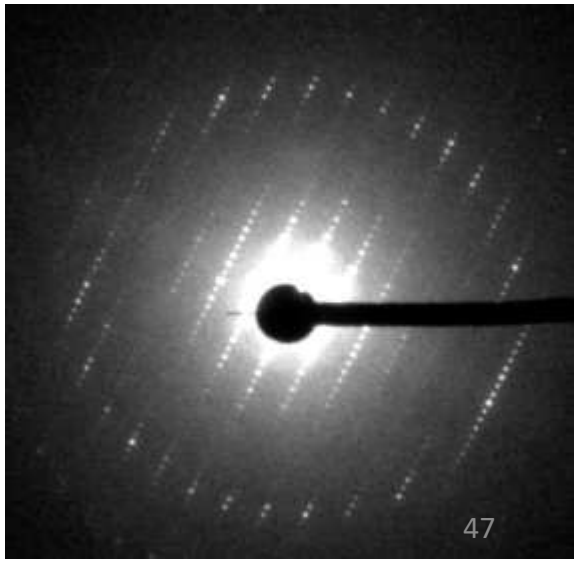

Tomographic acquisition strategy

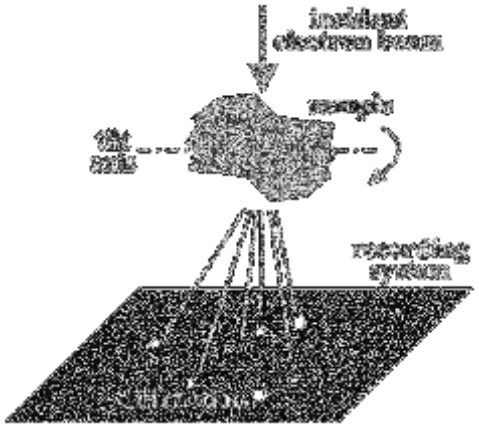

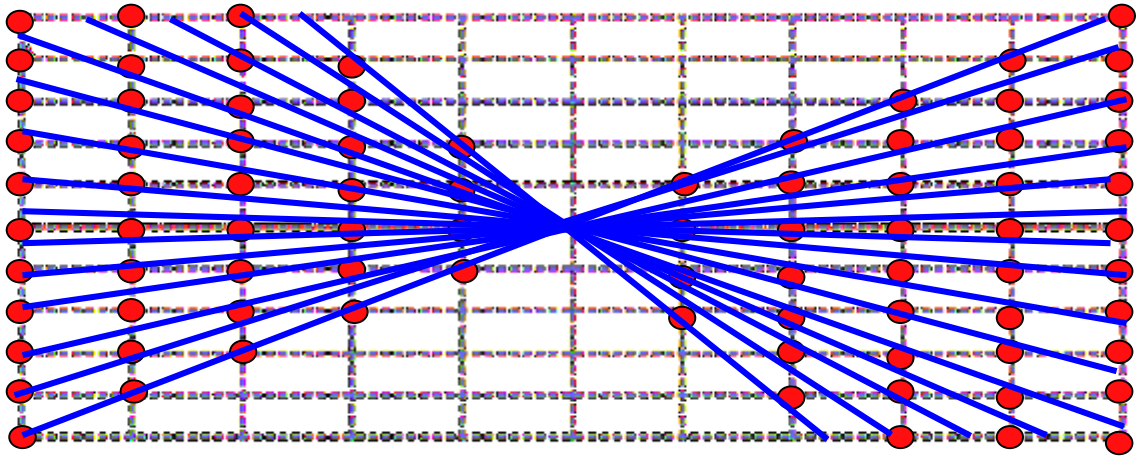

Automated electron Diffraction Tomography (ADT or EDT):

acquisition of not oriented diffraction patterns in fixed steps of 1°

- **no need for crystal orientation:** fast and easy acquisition
- **off-zone patterns:** reduction of dynamical effects
- **use of the full tilt range of the microscope:** improved completeness and collection of high index reflections

EDT

Towards automated diffraction tomography. Part I - Data Acquisition.
U. Kolb, T. Gorelik, C. Kübel, M.T. Otten, D. Hubert, *Ultramicroscopy* 107, 507 (2007).

Tomographic acquisition strategy

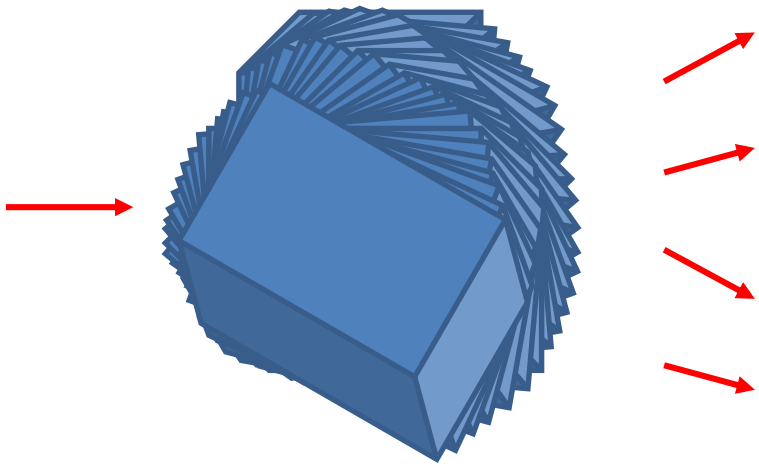

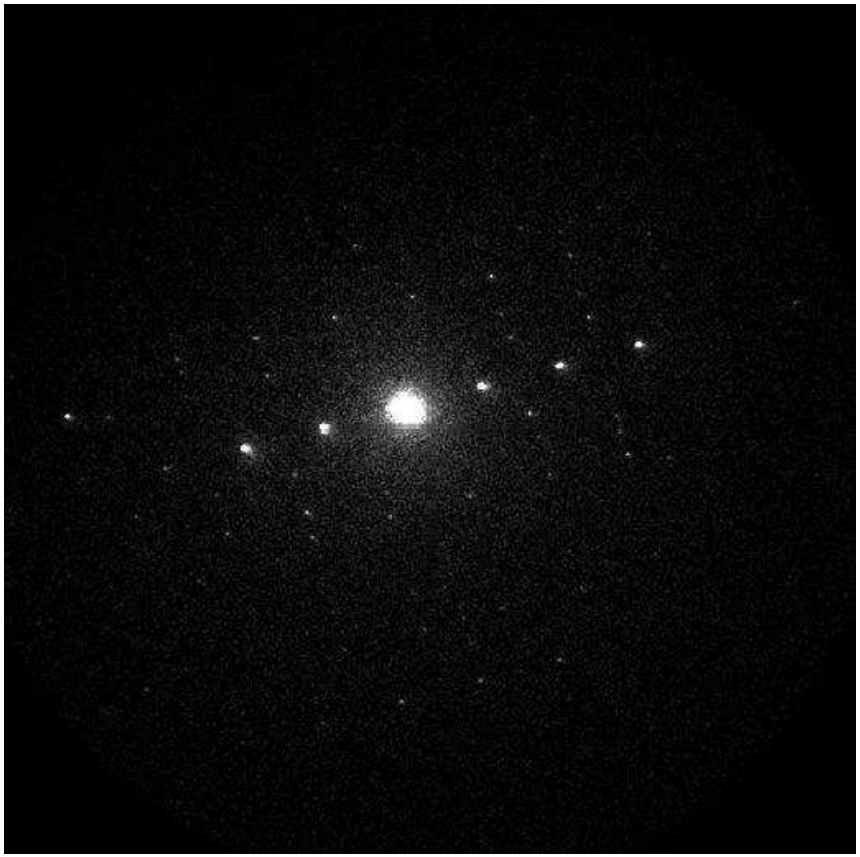

ADT is easy, fast and highly reproducible

EDT

Towards automated diffraction tomography. Part I - Data Acquisition.
U. Kolb, T. Gorelik, C. Kübel, M.T. Otten, D. Hubert, *Ultramicroscopy* 107, 507 (2007).

Zonal vs. Tomographic ED acquisition

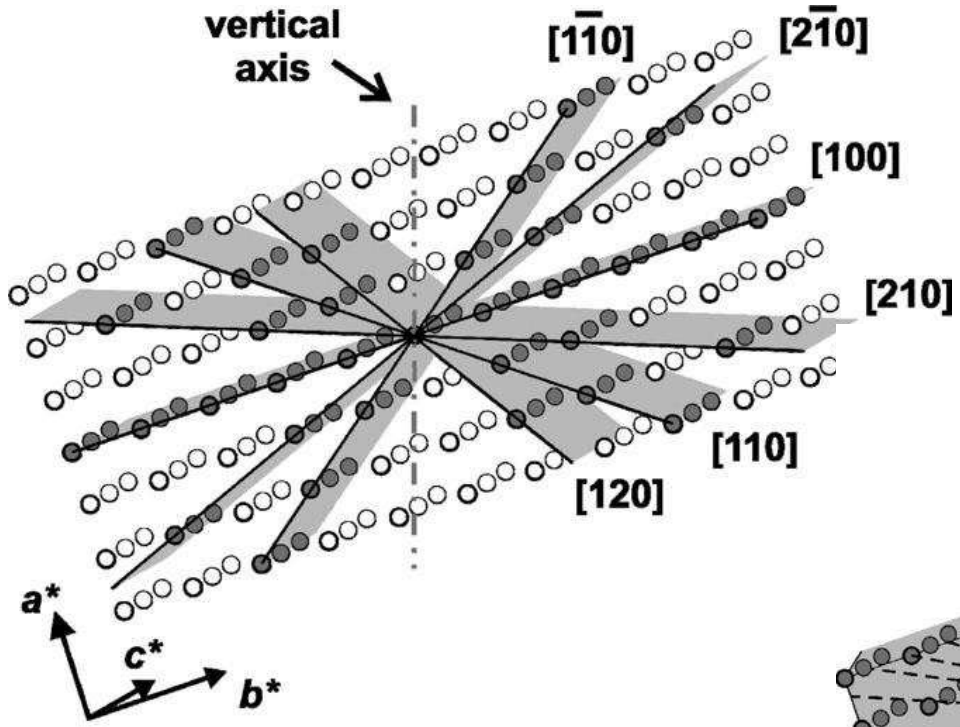

Conventional ED acquisition:
collection of **oriented crystallographic zones**

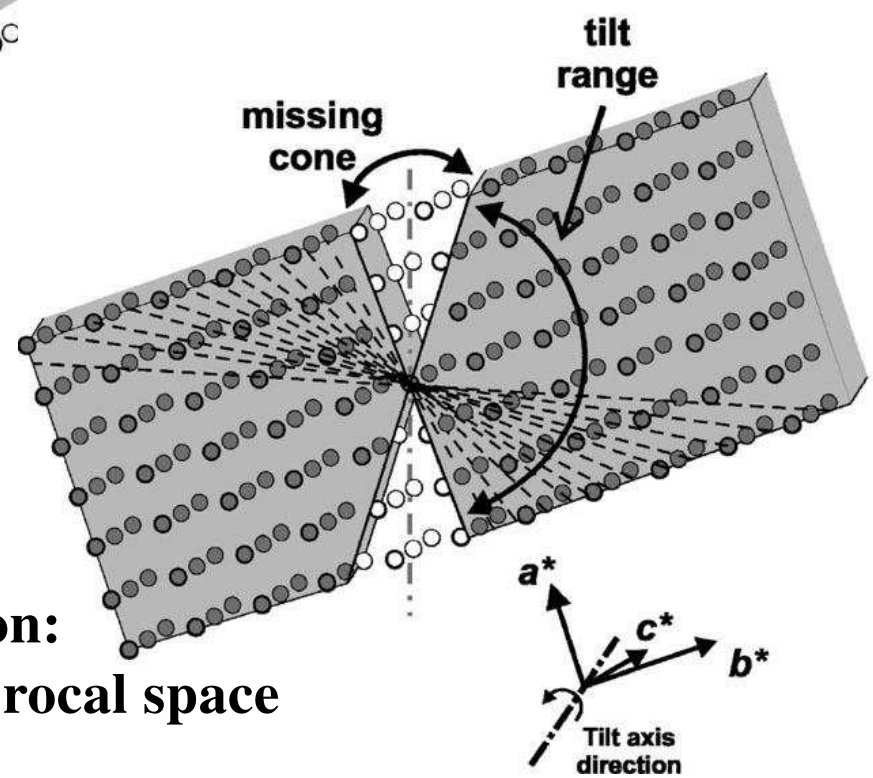

Tomographic acquisition:
sampling the **full accessible reciprocal space**
in **steady steps**
around an **arbitrary (non-crystallographic) axis**

EDT

ADT data analysis

ADT data are less dynamical

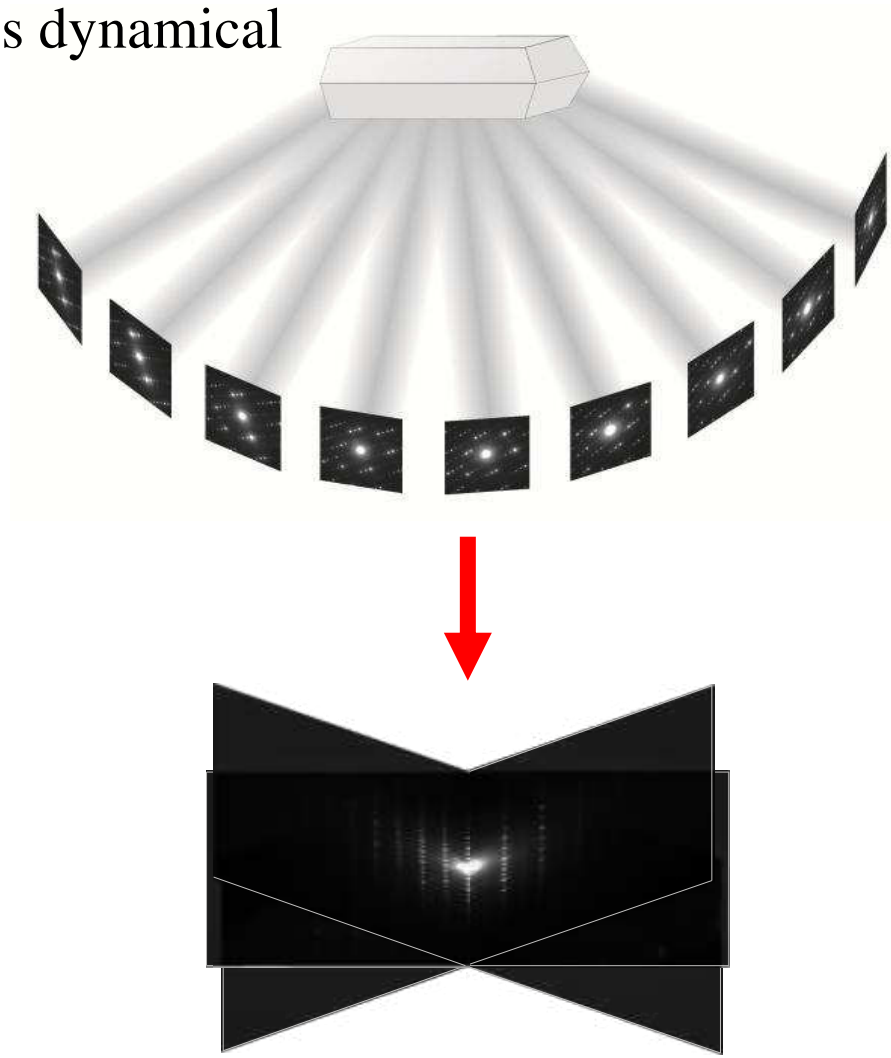

EDT

Towards automated diffraction tomography. Part II – Cell parameter determination.
U. Kolb, T. Gorelik and M.T. Otten, *Ultramicroscopy*, **108**, 763-772 (2008).

3D reconstructed diffraction volume visualization

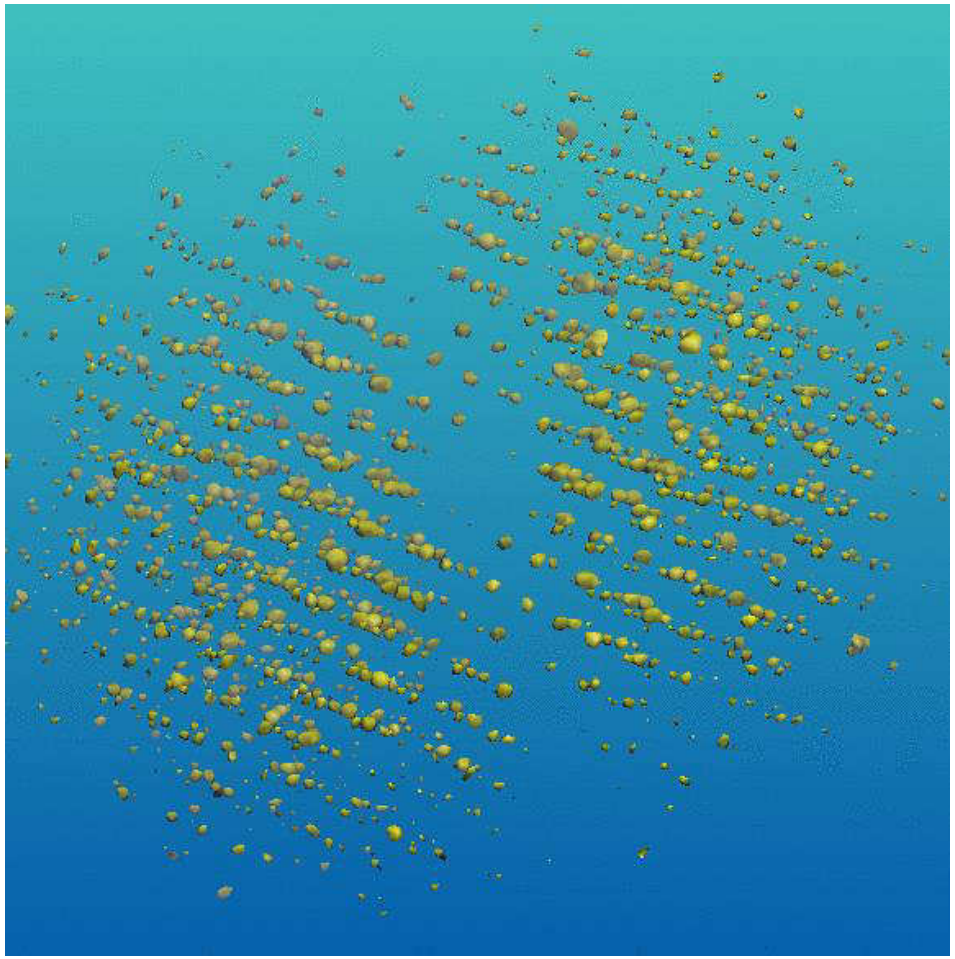

EDT

Cell parameters & Orientation

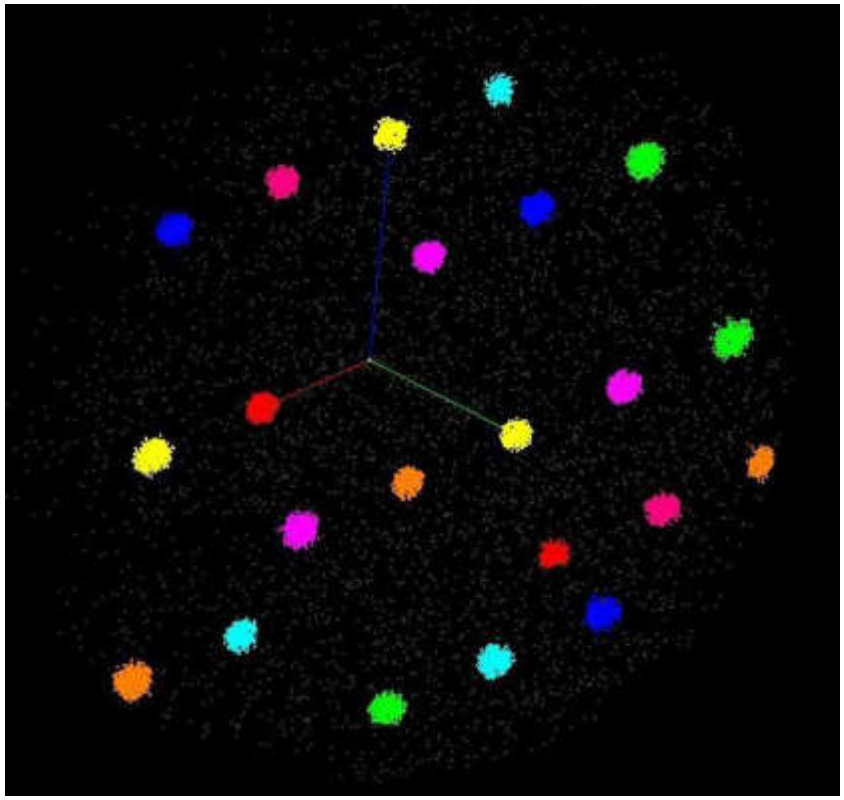

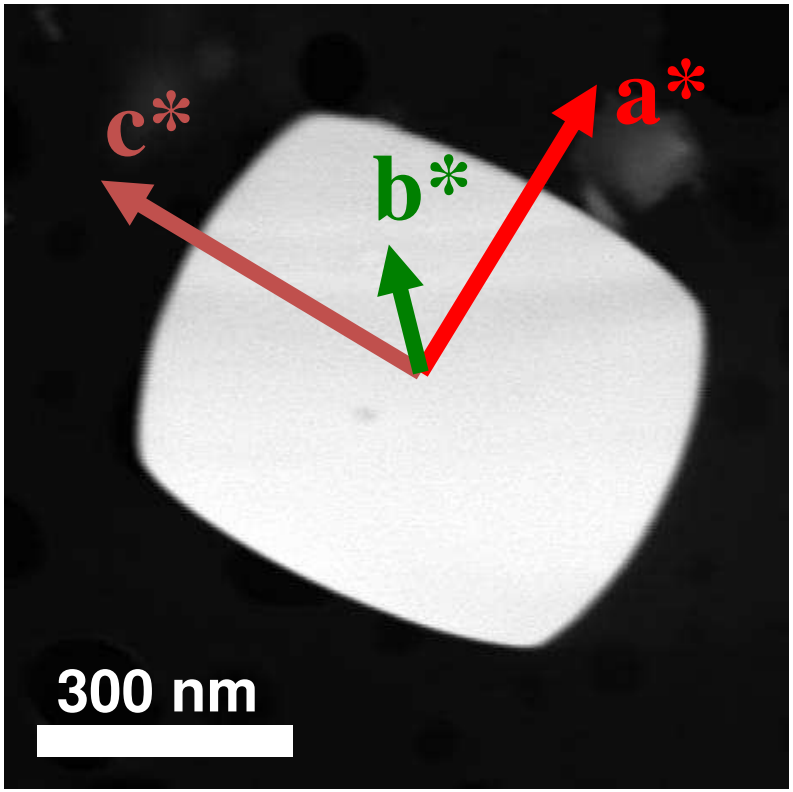

Cell parameters

manual selection or clustering in difference vector space

Orientation matrix

correlation with crystal shape for determination of direction of growth and facets

EDT

Disorder & Symmetry

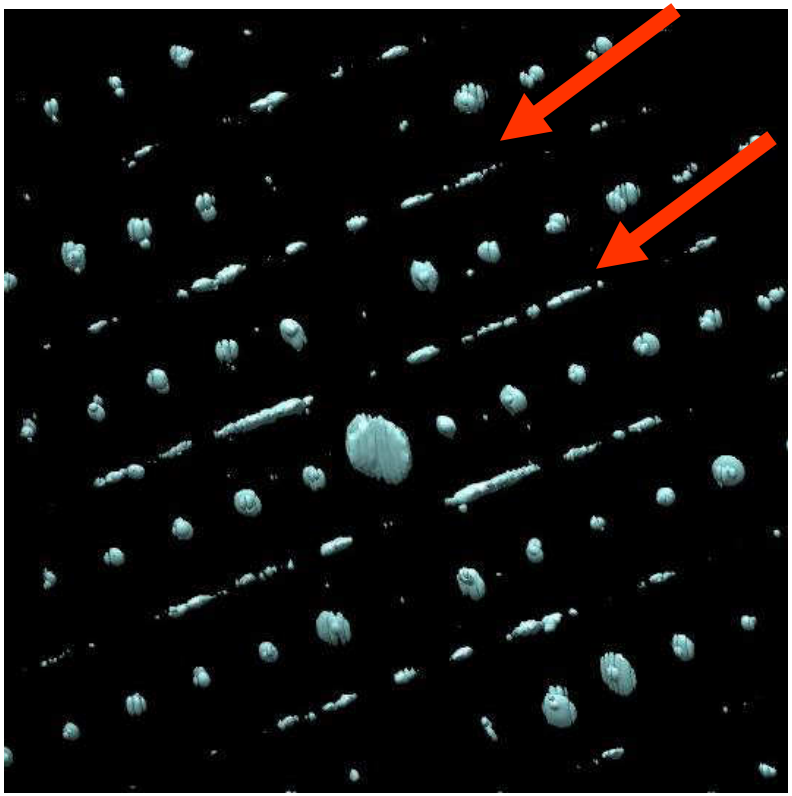

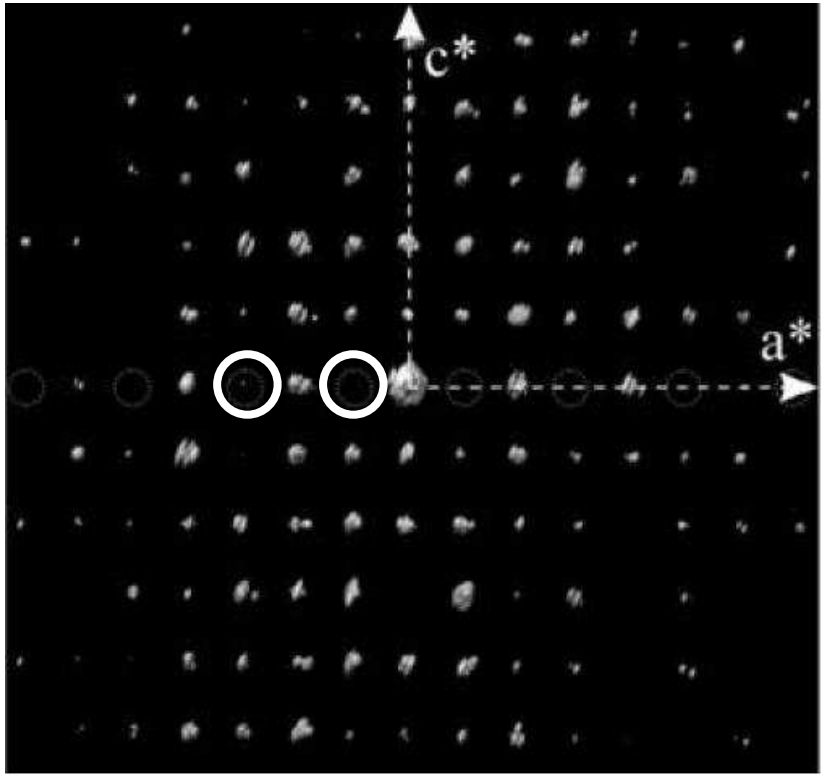

Disorder

$0kl : k = 2n+1$

Extinctions

$hk0 : h = 2n$

EDT

Intensity integration

Determination of the reflection position

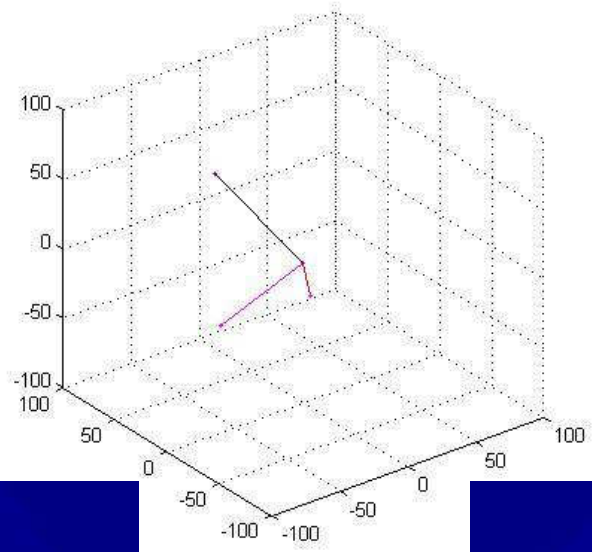

Set an appropriate integration area

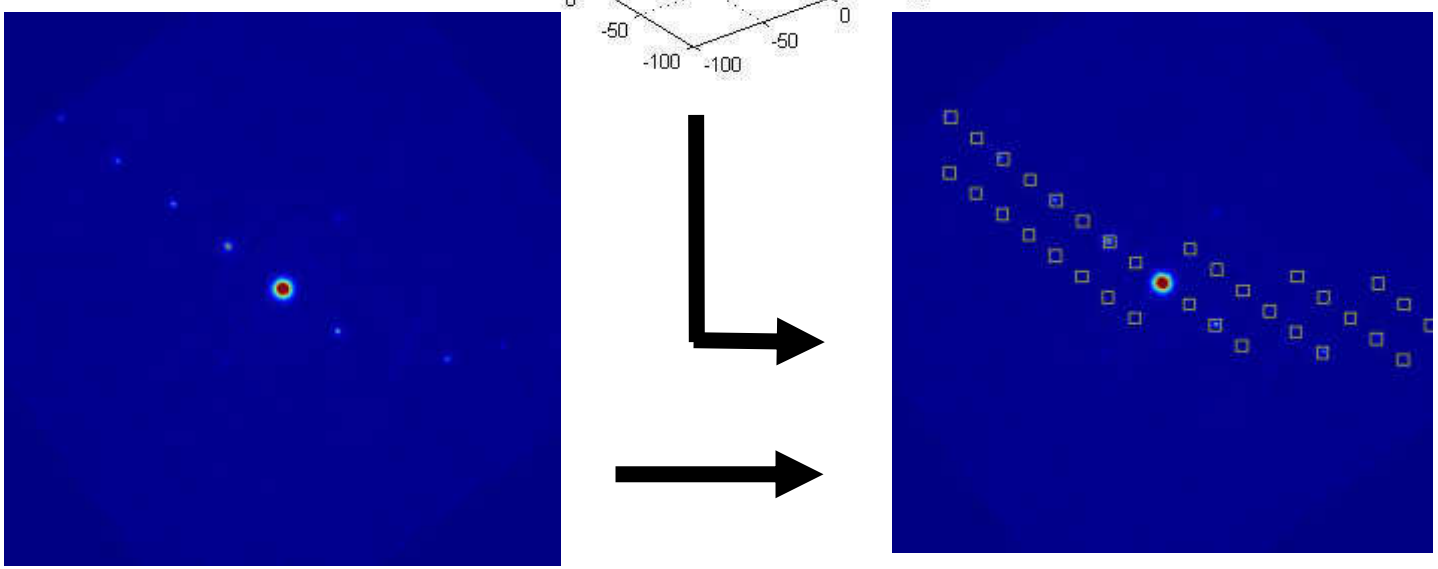

"Ab initio" structure solution from electron diffraction data obtained by a combination of automated diffraction tomography and precession technique.
E. Mugnaioli, T. Gorelik, U. Kolb, *Ultramicroscopy* **109**, 758 (2009).

EDT

Intensity integration

Determination of the reflection position

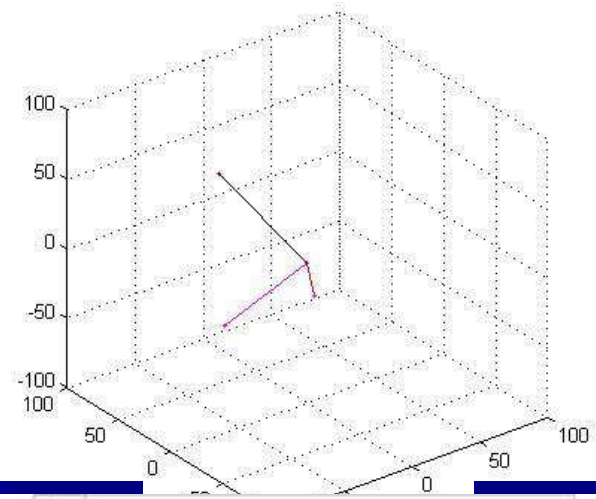

Set an appropriate integration area

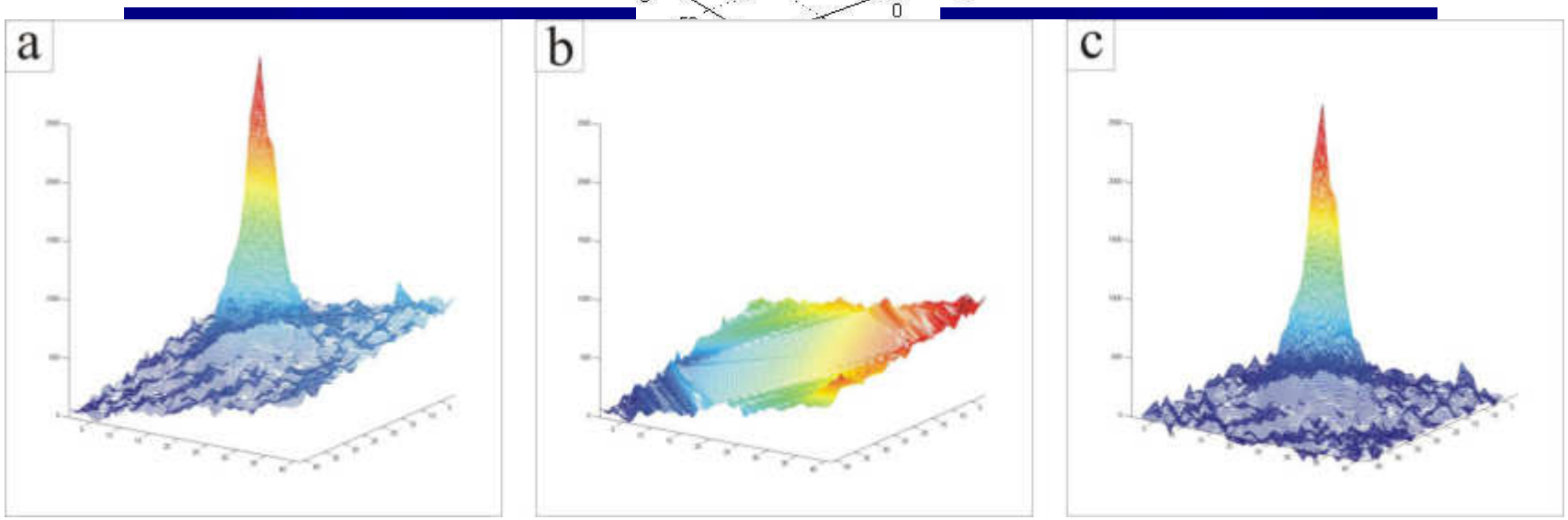

"Ab initio" structure solution from electron diffraction data obtained by a combination of automated diffraction tomography and precession technique.
E. Mugnaioli, T. Gorelik, U. Kolb, *Ultramicroscopy* **109**, 758 (2009).

EDT

Excitation error

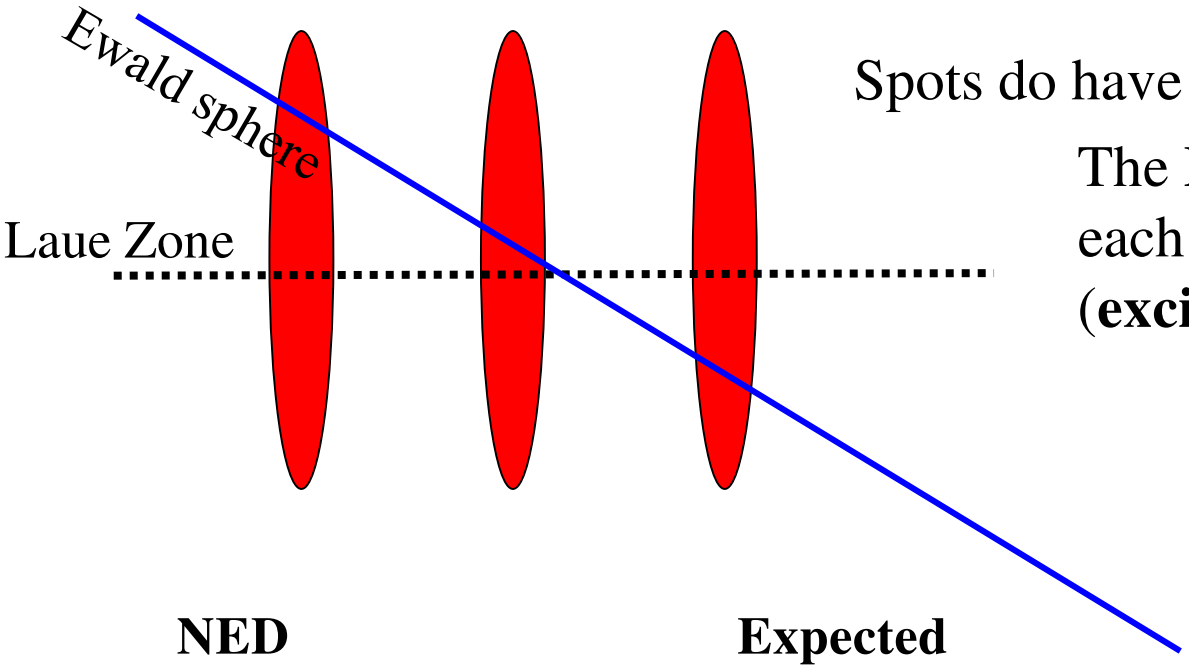

Spots do have a volume (**spike**)

The **Ewald sphere** cuts each spot in a different way (**excitation error**)

NED

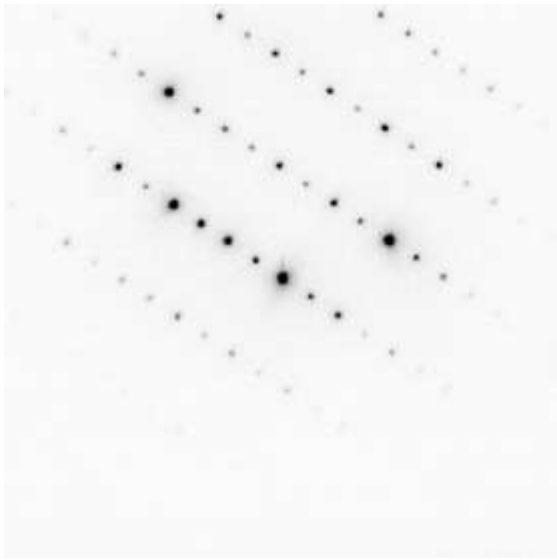

Expected

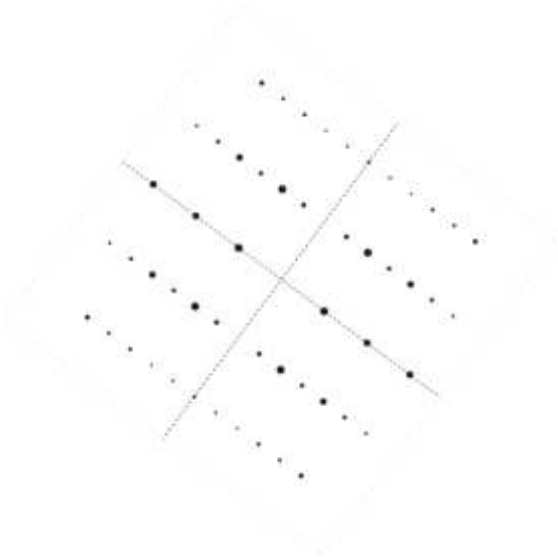

Precession Electron Diffraction

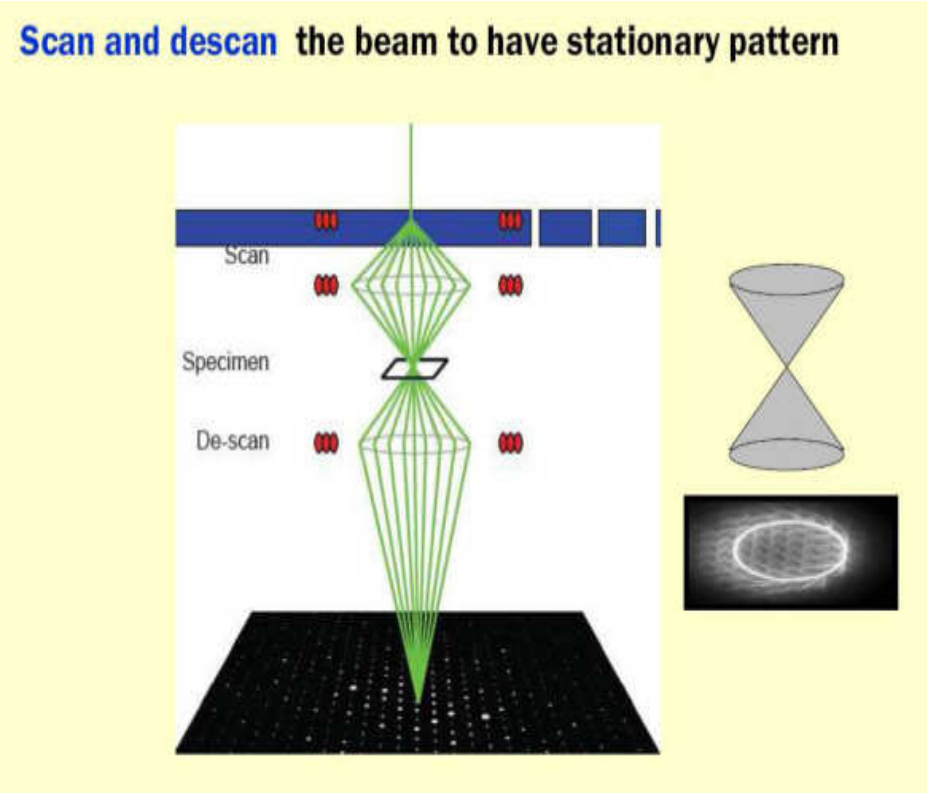

DigiStar by NanoMEGAS

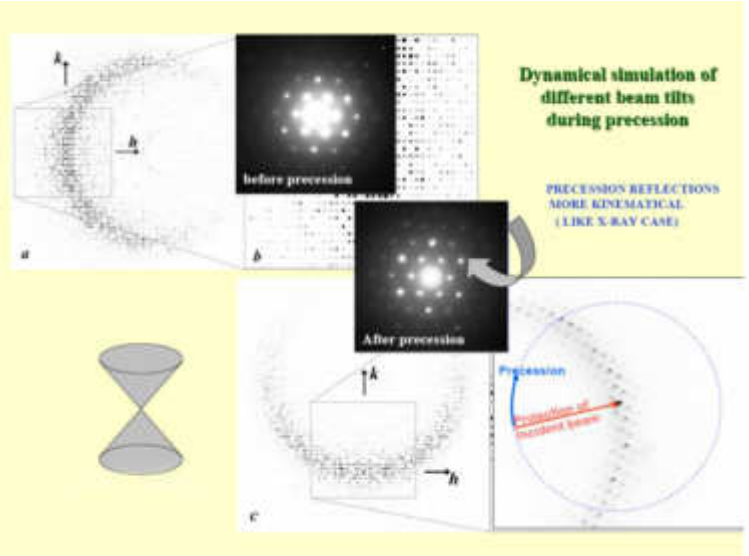

Beam is rotating very fast avoiding full orientation of the zone

Double conical beam-rocking system for measurement of integrated electron diffraction intensities. R. Vincent, P.A. Midgley, *Ultramicroscopy* **53**, 271 (1994).

In-zone electron diffraction

ADT + Precession

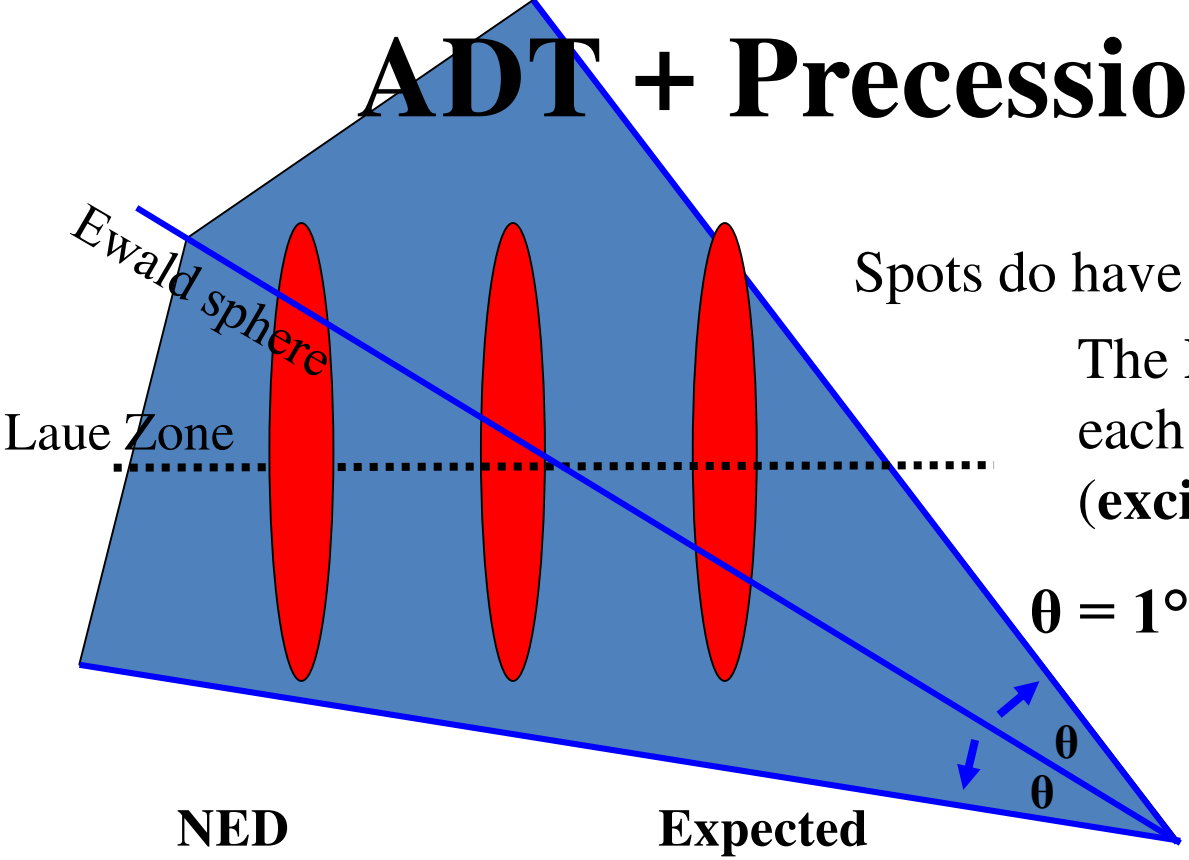

Spots do have a volume (**spike**)

The **Ewald sphere** cuts each spot in a different way (**excitation error**)

θ = 1° **PED** makes Ewald sphere to integrate **reflection volume**

NED

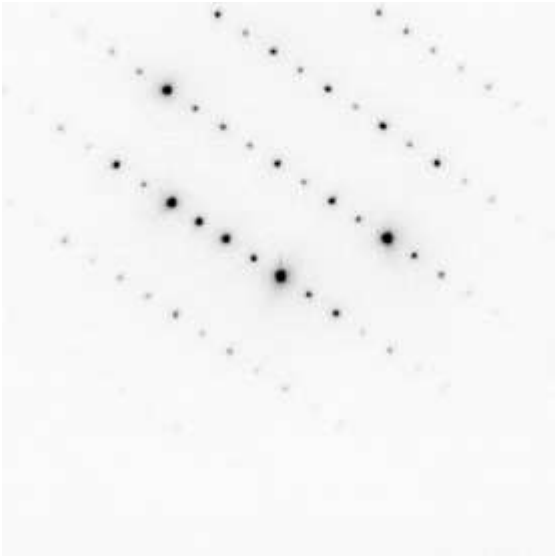

Expected

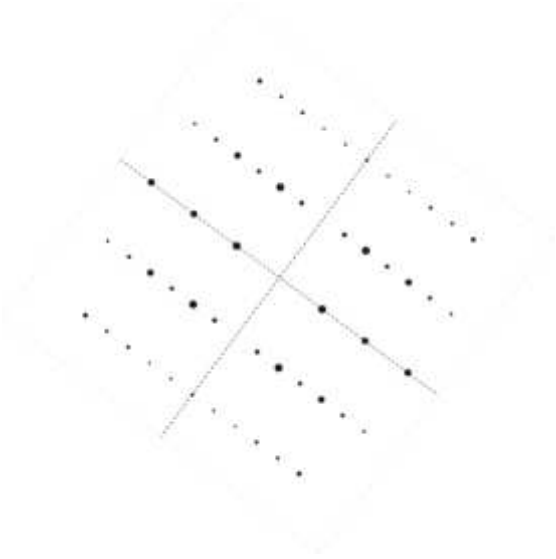

PED

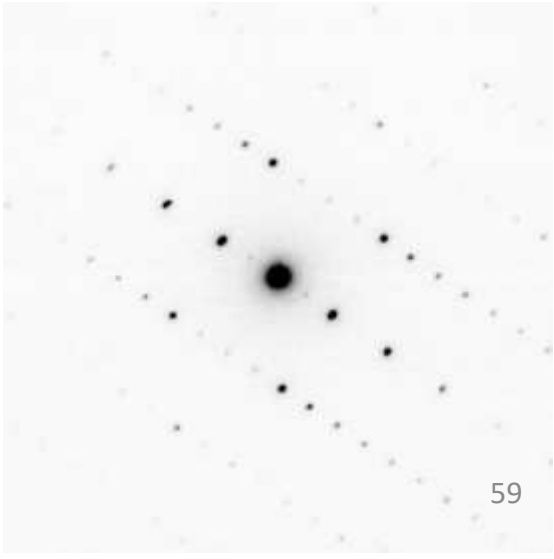

Test structures

	Space group	N° indep. reflections	N° indep. atoms	Volume (Å³)	Resolution (Å)	Completeness
Inorganic materials						
Calcite $CaCO_3$	R-3c	106	3	120	0.8	97%
Semiconductor 6H-SiC	P6mm	52	6	130	0.9	100%
$Na_2W_4O_{13}$	P-1	738	10	262	0.8	69%
Barite $BaSO_4$	Pnma	355	5	350	0.8	82%
ZnSb	[illegible]	[illegible]	[illegible]	[illegible]	[illegible]	70%
Layered $Na_2Ti_6O_{13}$						72%
$Li_{26}Ti_8Ni_4O_{21}$						91%
$Na_2W_2O_7$						91%
Zeolites						
Natrolite	Fdd2	719	10	2250	0.8	92%
ZSM-5	Pnma	2288	39	5490	1.0	79%
IM-5	Cmcm	2170	71	16380	1.2	68%
Organics and Hybrids						
10-CNBA $C_{29}NH_{17}$	$P2_1/c$	1871	30	2000	1.0	90%
Basolite $C_6H_4CuO_5$	Fm-3m	384	7	18640	1.2	99%

$$I_{hkl} \sim F_{hkl}^2$$

kinematical (1-scatter) approximation

…like in X-ray

EDT

~ 200 structures solved by ADT in 6 years

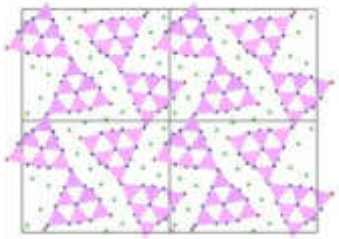

Phosphates
Mugnaioli E et al (2012)
Eur J Inorg Chem, 121

Organics
Kolb U et al (2010)
Polym Rev 50, 385

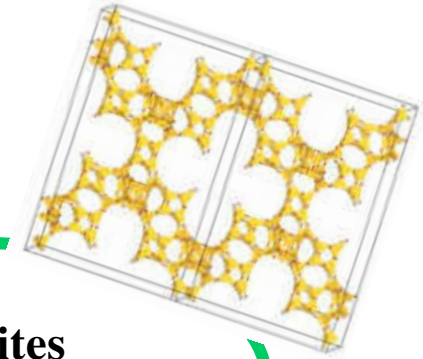

Zeolites
Jiang J et al (2011)
Science 333,1131

Hybrids calcium-silicates
Bellussi G et al (2012)
Angew Chem Int Ed 51, 666

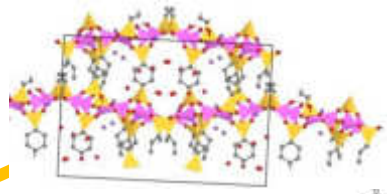

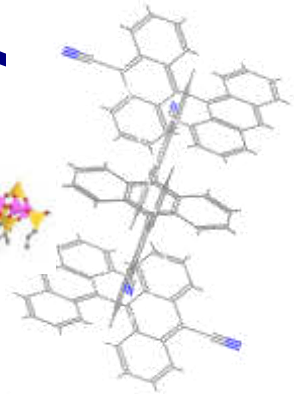

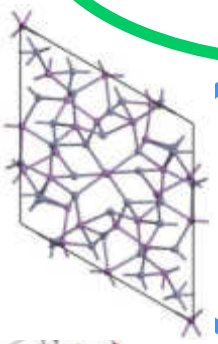

Intermetallic phases
Birkel CS et al (2010)
J Am Chem Soc 132, 9881

Layered titanates
Andrusenko I et al (2011)
Acta Crystallogr B 67, 218

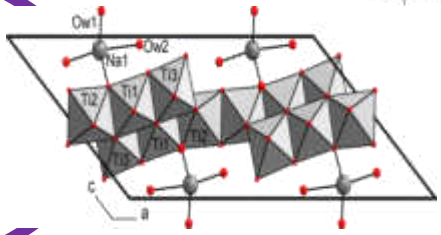

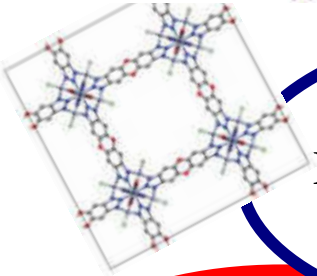

Metal Organic Frameworks (MOF)
Denysenko D et al (2011)
Chem-Eur J 17, 1837

Ca-compounds
Mugnaioli E et al (2012)
Angew Chem Int Ed 51, 7041

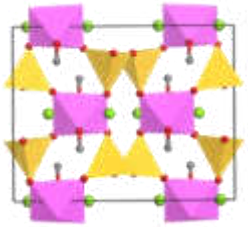

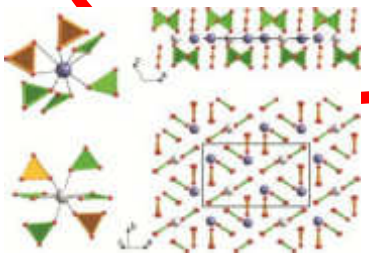

High pressure phases
Gemmi M et al (2011)
Earth Planet Sc Lett 310, 422

Minerals
Rozhdestvenskaya I et al (2011) *Mineral Mag* 75, 2833

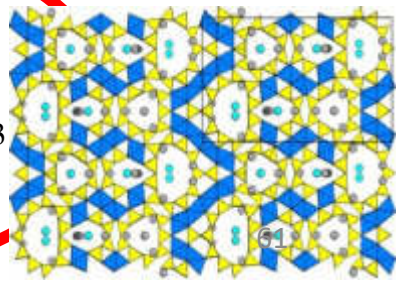

Tomographic acquisition strategy

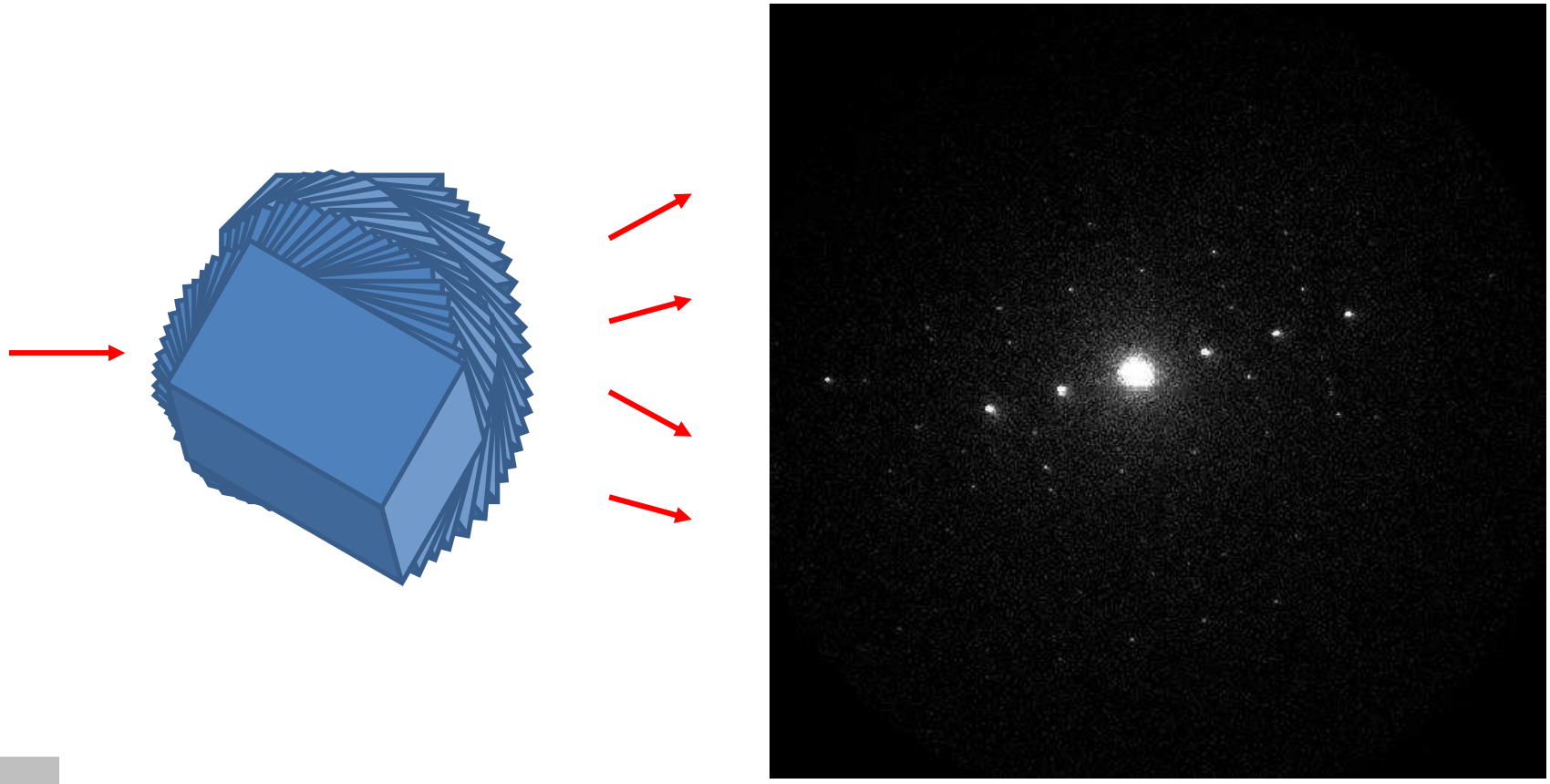

Towards automated diffraction tomography. Part I - Data Acquisition.
U. Kolb, T. Gorelik, C. Kübel, M.T. Otten, D. Hubert, *Ultramicroscopy* 107, 507 (2007).

Data analysis

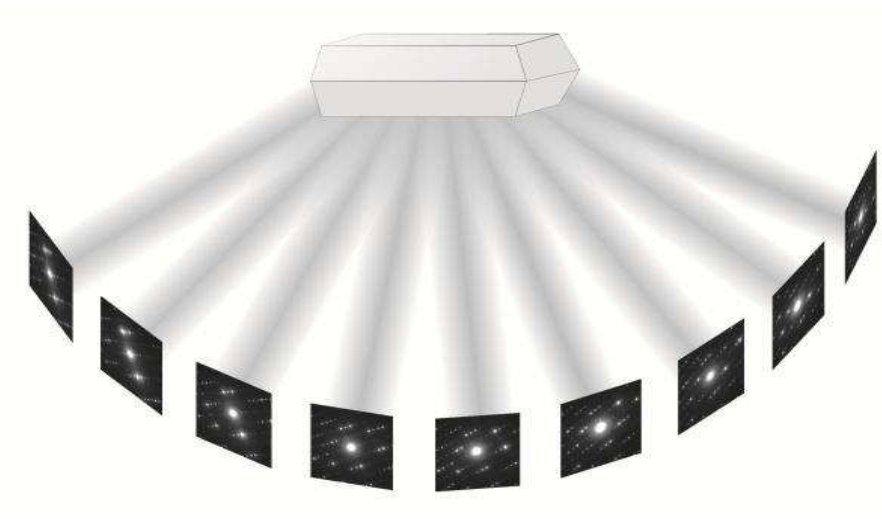

Reconstruction of 3D diffraction space

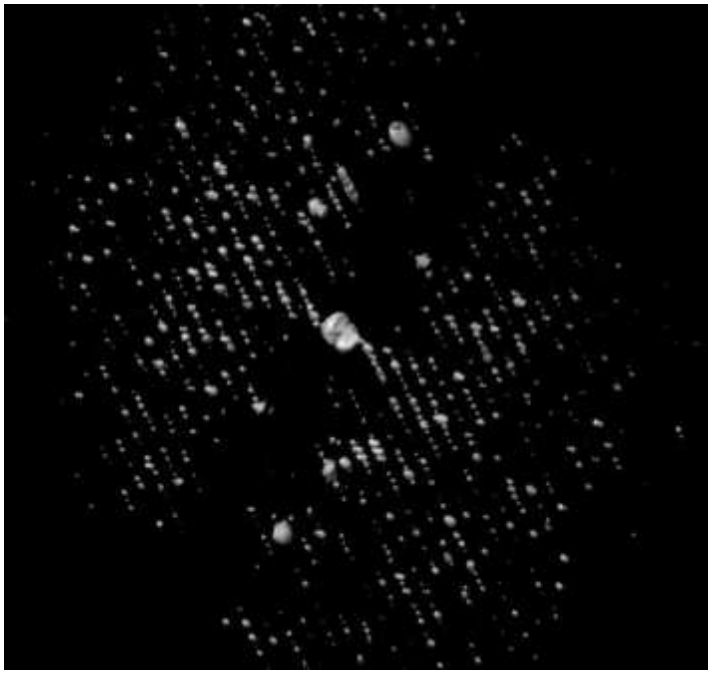

We need:
- accurate centring
- accurate tilt axis determination

EDT analysis

Towards automated diffraction tomography. Part II – Cell parameter determination.
U. Kolb, T. Gorelik and M.T. Otten, *Ultramicroscopy* **108**, 763 (2008).

Accurate diffraction centering

Centre of the central beam or Friedel pair

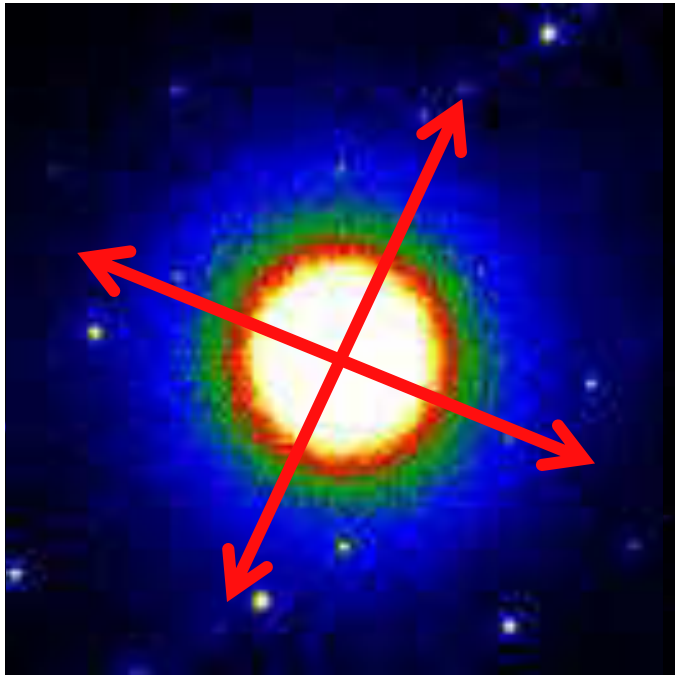

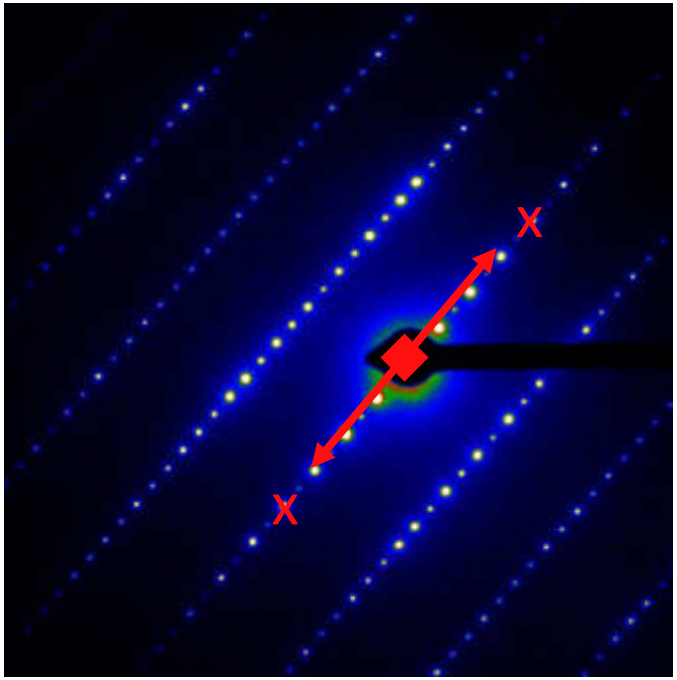

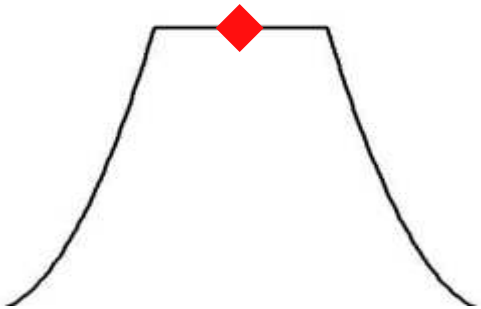

Tilt axis azimuth

The tilt axis azimuth changes for different camera lengths and for different diffraction focus

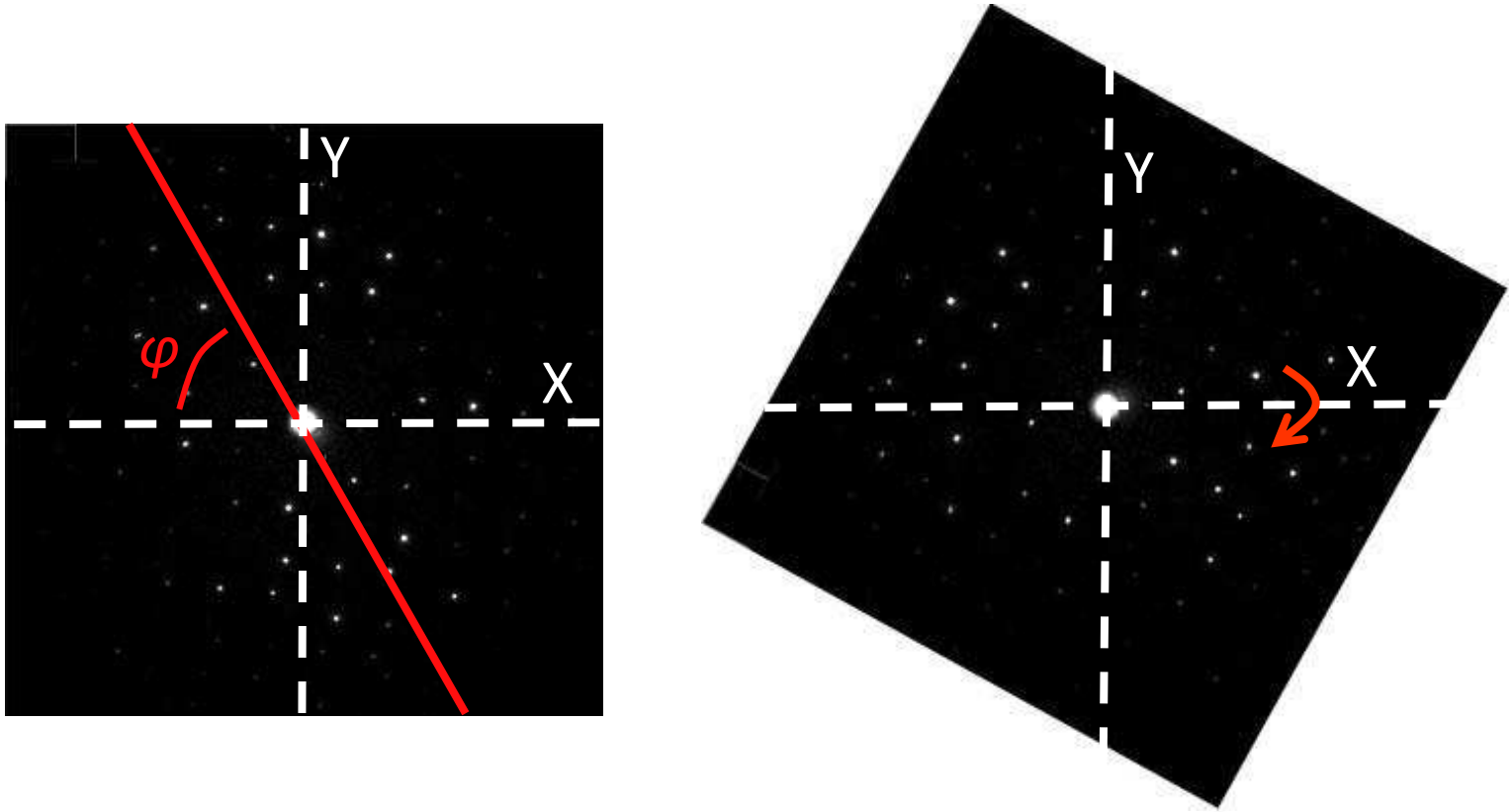

Tilt axis determination

Correct tilt axis

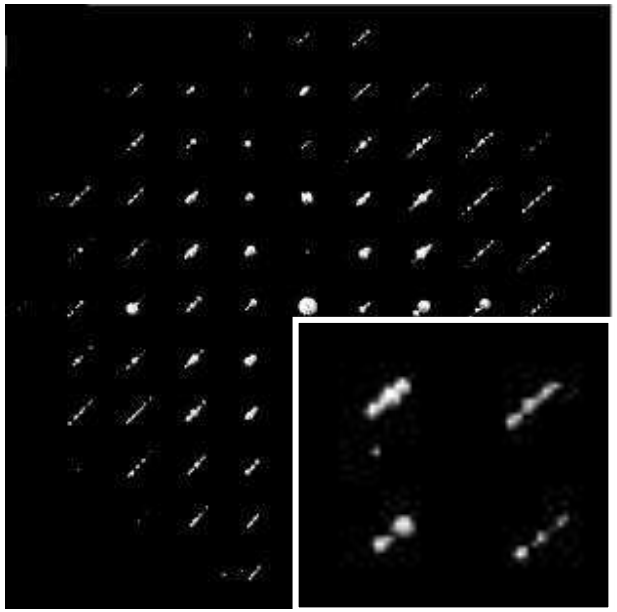

Incorrect tilt axis

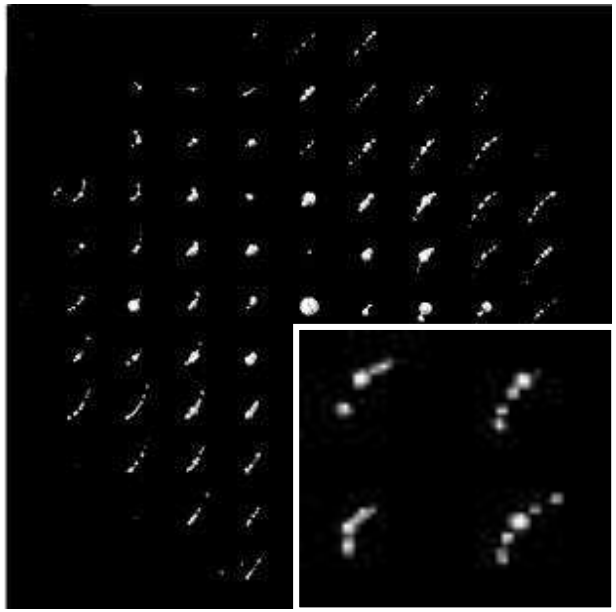

If the tilt axis is wrong, in the reconstructed volume reflection rows are “bananas”

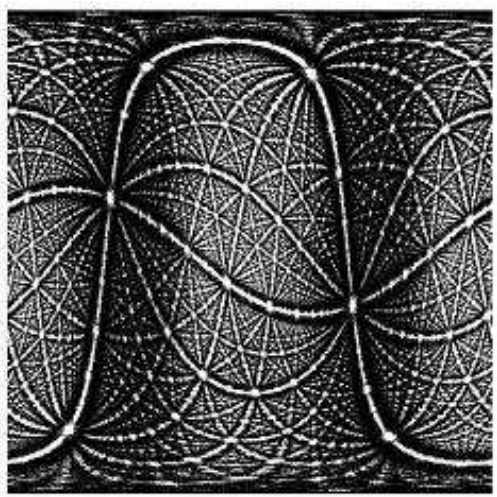

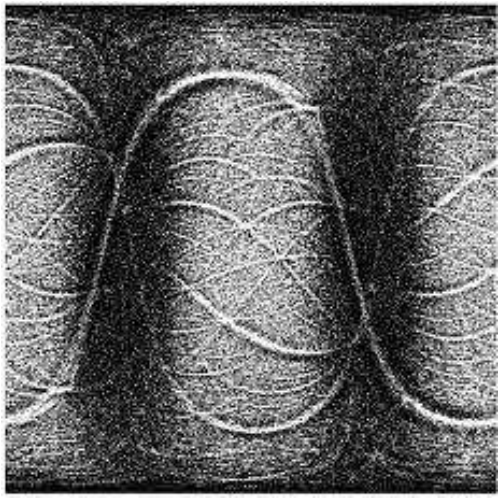

Stereographic projection of difference vectors

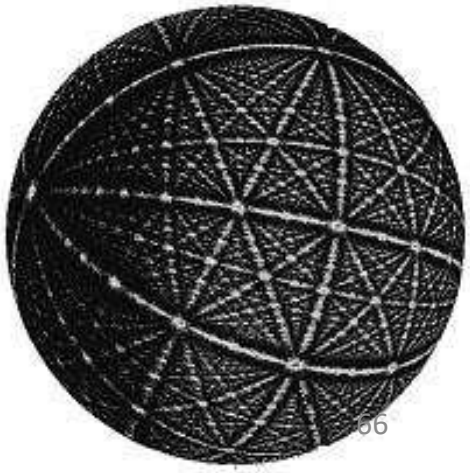

EDT analysis

Diffraction volume reconstruction

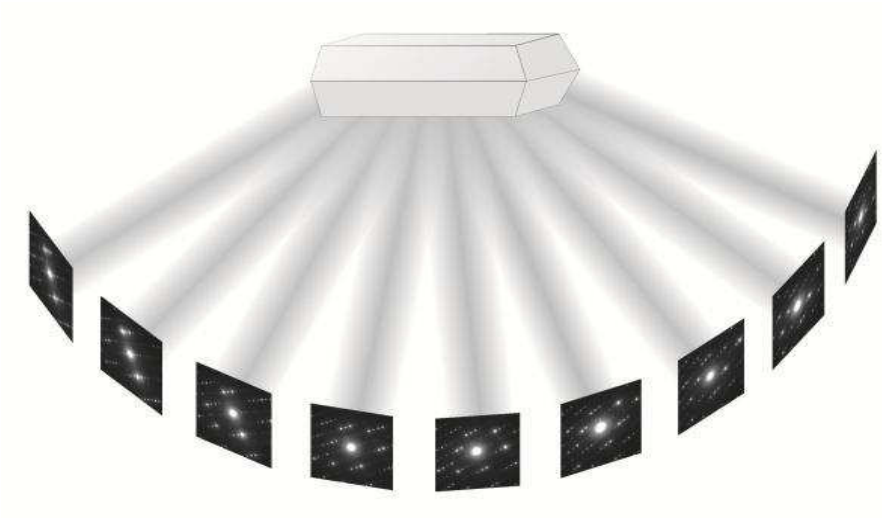

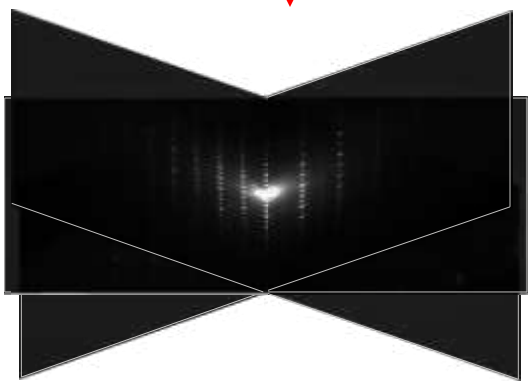

reconstruction of
3D diffraction space

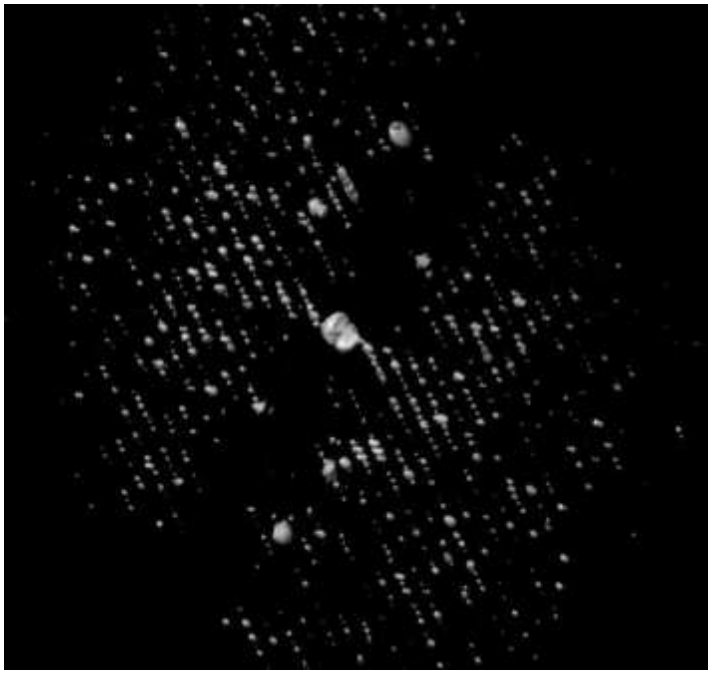

3D reconstructed diffraction volume visualization

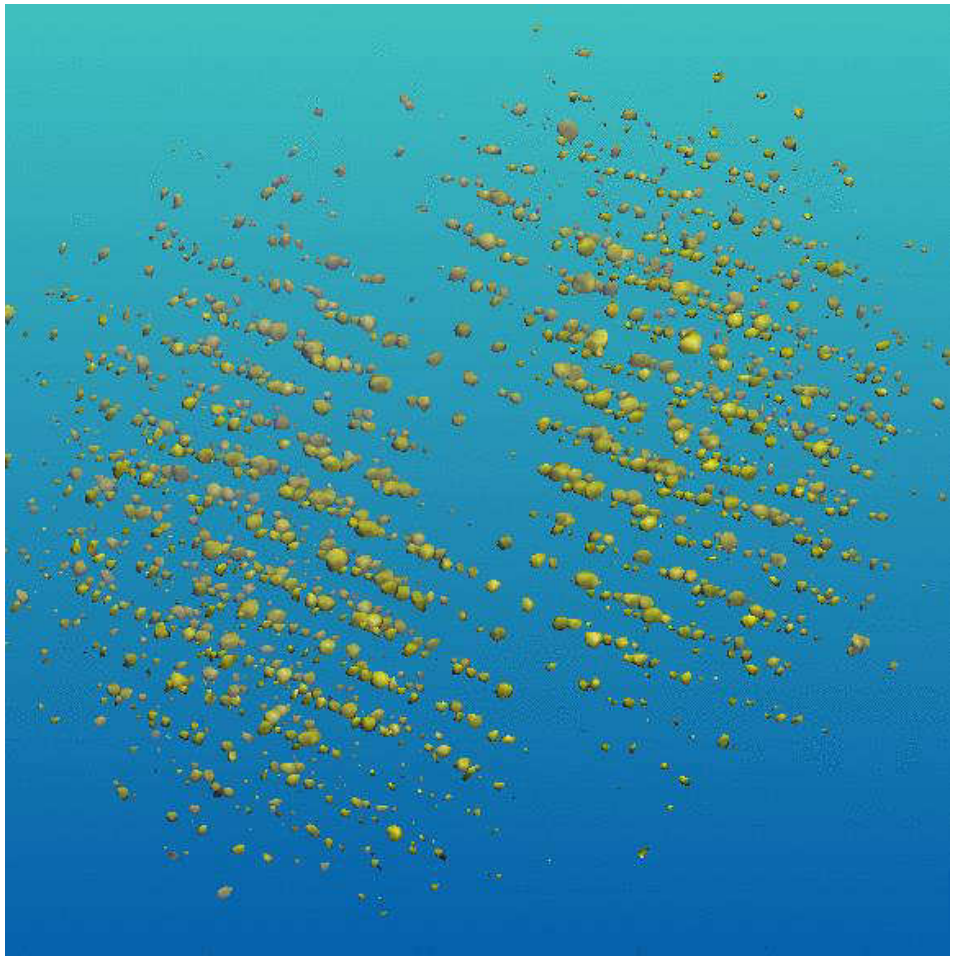

Cell determination – clustering

Hand cell picking

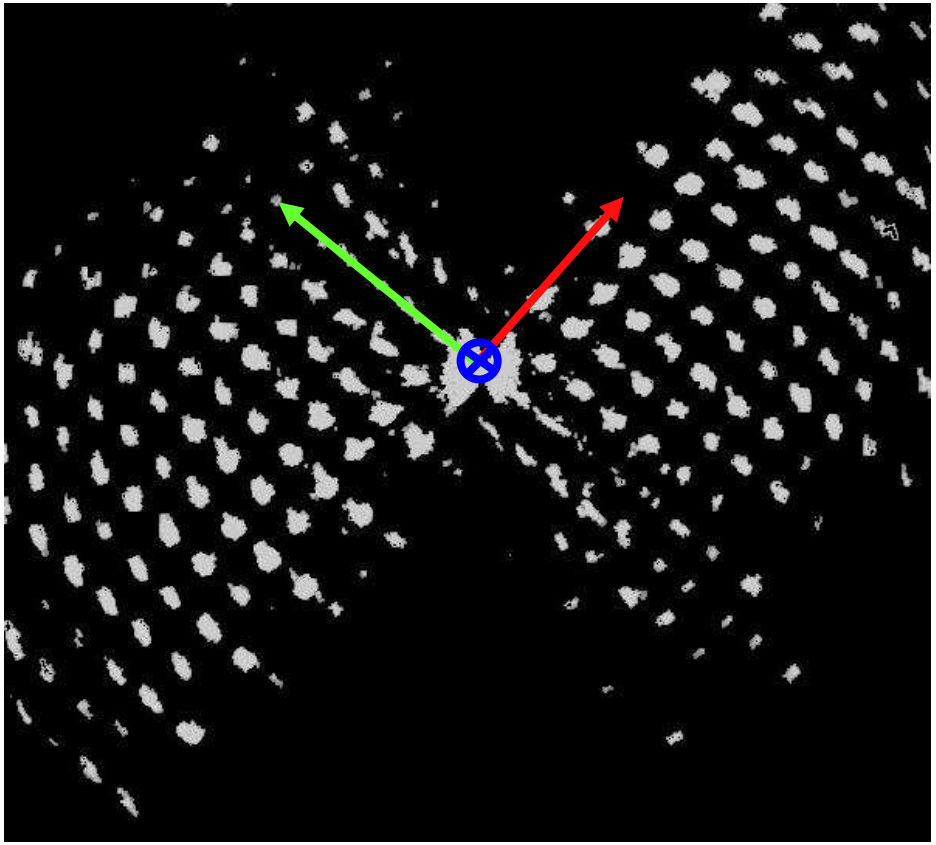

Automatic clustering

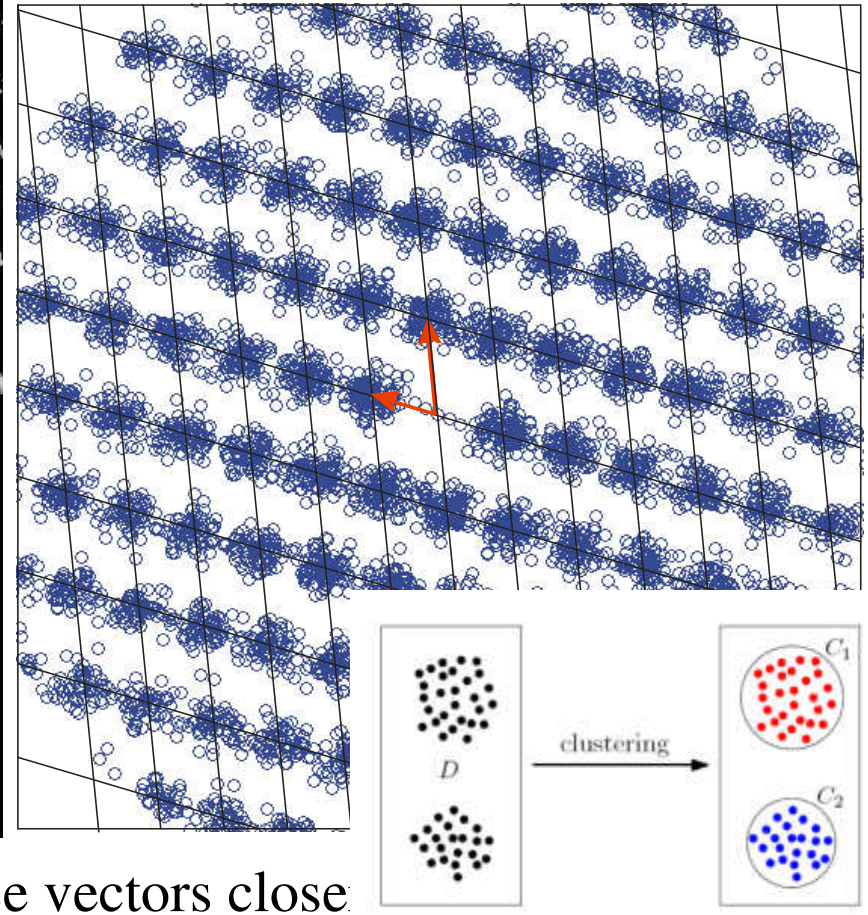

The three not-coplanar difference vectors close to the centre define the primitive cell (Niggli cell)

Reflection indexing

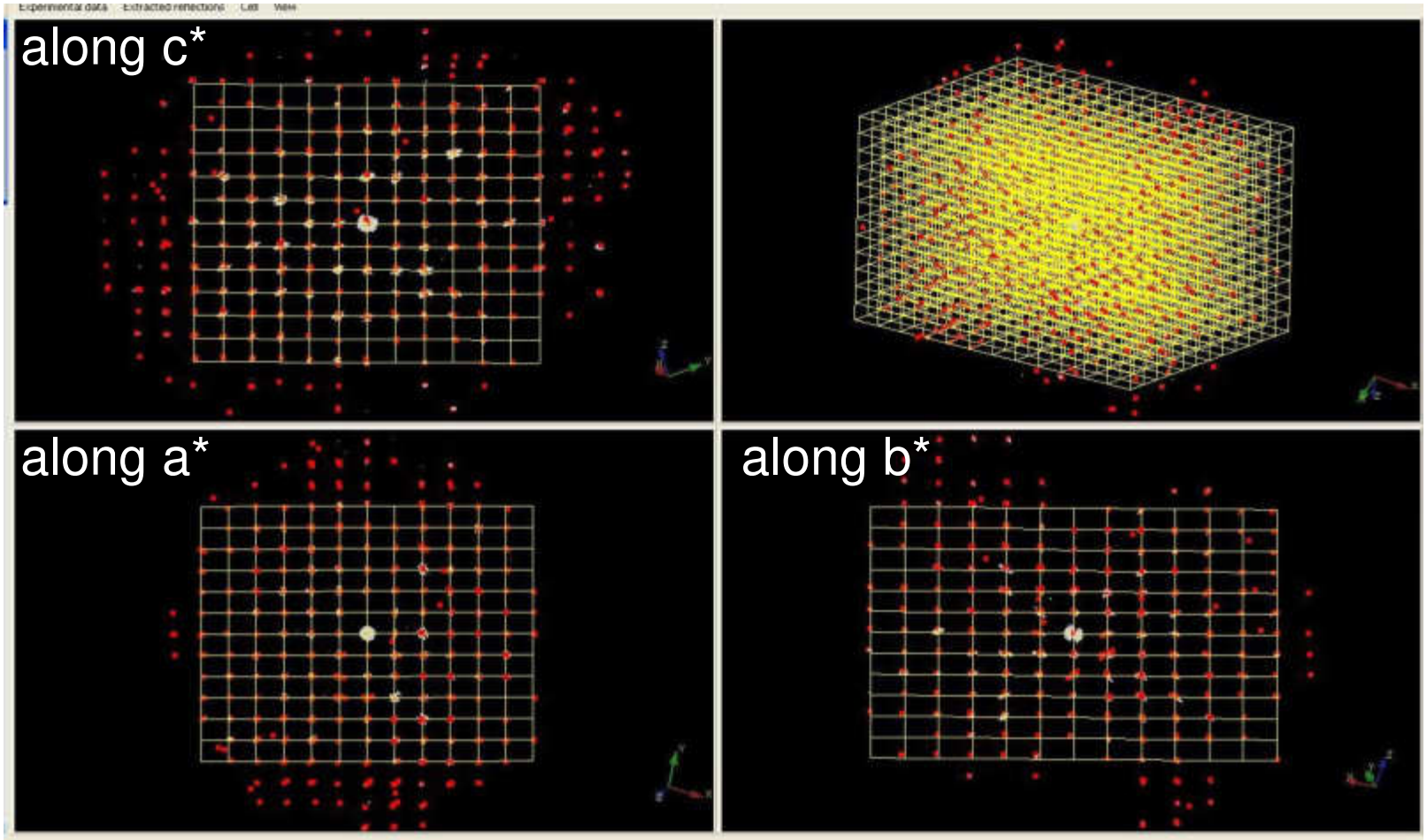

Reflection indexing

cell superimposed to the 3D reconstructed diffraction volume

Extinctions & Space group

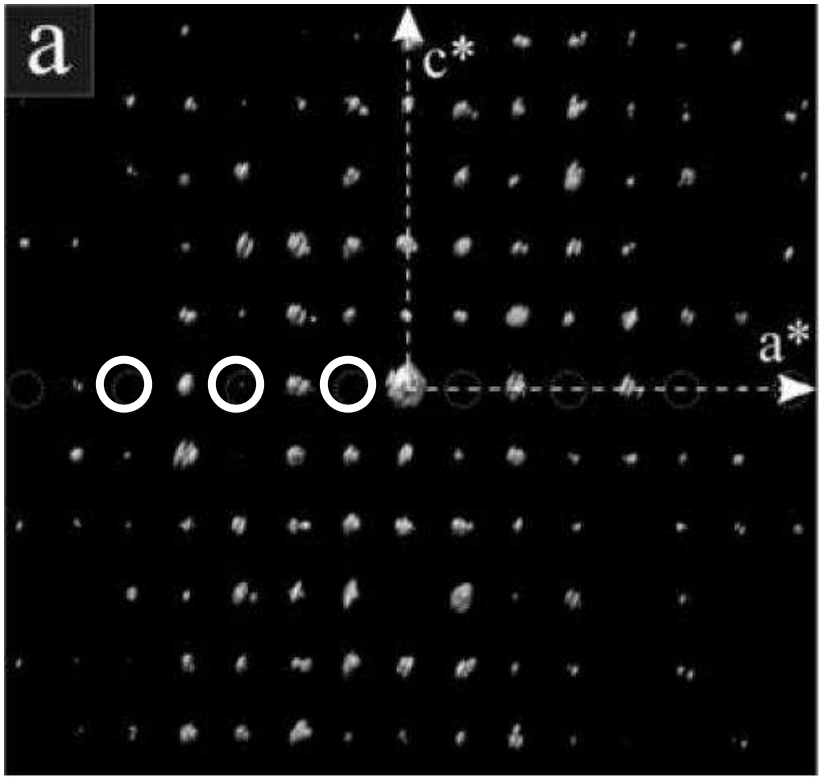

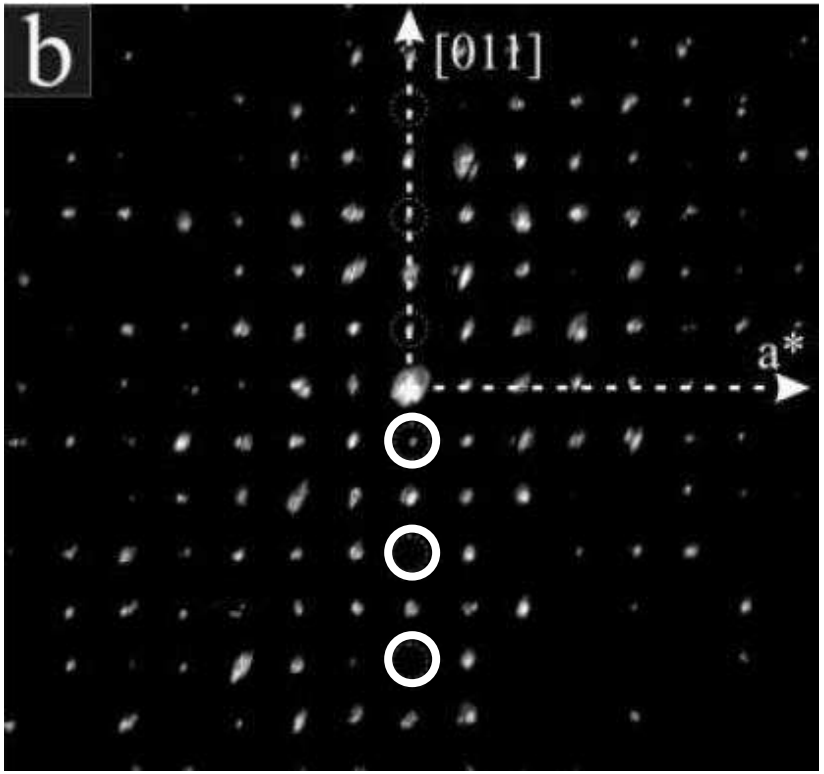

Extinctions

$$\left.\begin{array}{l} hk0 : h = 2\mathrm{N} \\ 0kl : k+l = 2\mathrm{N} \end{array}\right\} \quad Pn\text{-}a$$

Space group determination

3. SPACE-GROUP DETERMINATION AND DIFFRACTION SYMBOLS

Table 3.2 (*cont.*)

MONOCLINIC, Laue class $2/m$

Unique axis b			Extinction symbol	Laue class $1\,2/m\,1$		
Reflection conditions				Point group		
hkl $0kl$ $hk0$	$h0l$ $h00$ $00l$	$0k0$		2	m	$2/m$
			$P1-1$	**$P121$** (3)	**$P1m1$** (6)	**$P1\,2/m\,1$** (10)
		k	$P12_11$	**$P12_11$** (4)		**$P1\,2_1/m\,1$** (11)
	h		$P1a1$		$P1a1$ (7)	$P1\,2/a\,1$ (13)
	h	k	$P1\,2_1/a\,1$			$P1\,2_1/a\,1$ (14)
	l		$P1c1$		**$P1c1$** (7)	**$P1\,2/c\,1$** (13)
	l	k	$P1\,2_1/c\,1$			**$P1\,2_1/c\,1$** (14)
	$h+l$		$P1n1$		$P1n1$ (7)	$P1\,2/n\,1$ (13)
	$h+l$	k	$P1\,2_1/n\,1$			$P1\,2_1/n\,1$ (14)
$h+k$	h	k	$C1-1$	**$C121$** (5)	**$C1m1$** (8)	**$C1\,2/m\,1$** (12)
$h+k$	h,l	k	$C1c1$		**$C1c1$** (9)	**$C1\,2/c\,1$** (15)
$k+l$	l	k	$A1-1$	$A121$ (5)	$A1m1$ (8)	$A1\,2/m\,1$ (12)
$k+l$	h,l	k	$A1n1$		$A1n1$ (9)	$A1\,2/n\,1$ (15)
$h+k+l$	$h+l$	k	$I1-1$	$I121$ (5)	$I1m1$ (8)	$I1\,2/m\,1$ (12)
$h+k+l$	h,l	k	$I1a1$		$I1a1$ (9)	$I1\,2/a\,1$ (15)

Unique axis c			Extinction symbol	Laue class $1\,1\,2/m$		
Reflection conditions				Point group		
hkl $0kl$ $h0l$	$hk0$ $h00$ $0k0$	$00l$		2	m	$2/m$

EDT analysis

Intensity integration

Determination of the reflection position

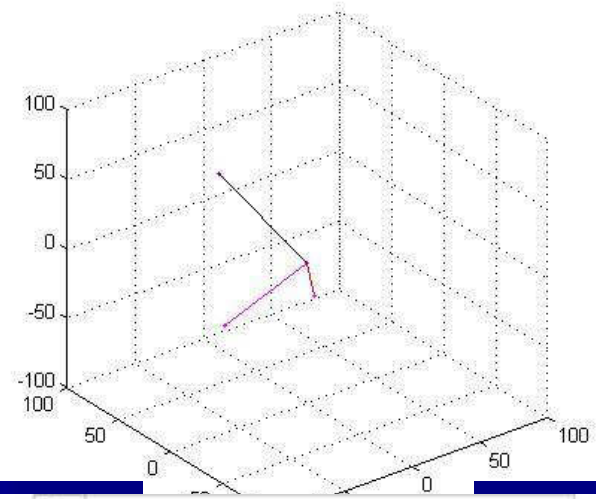

Set an appropriate integration area

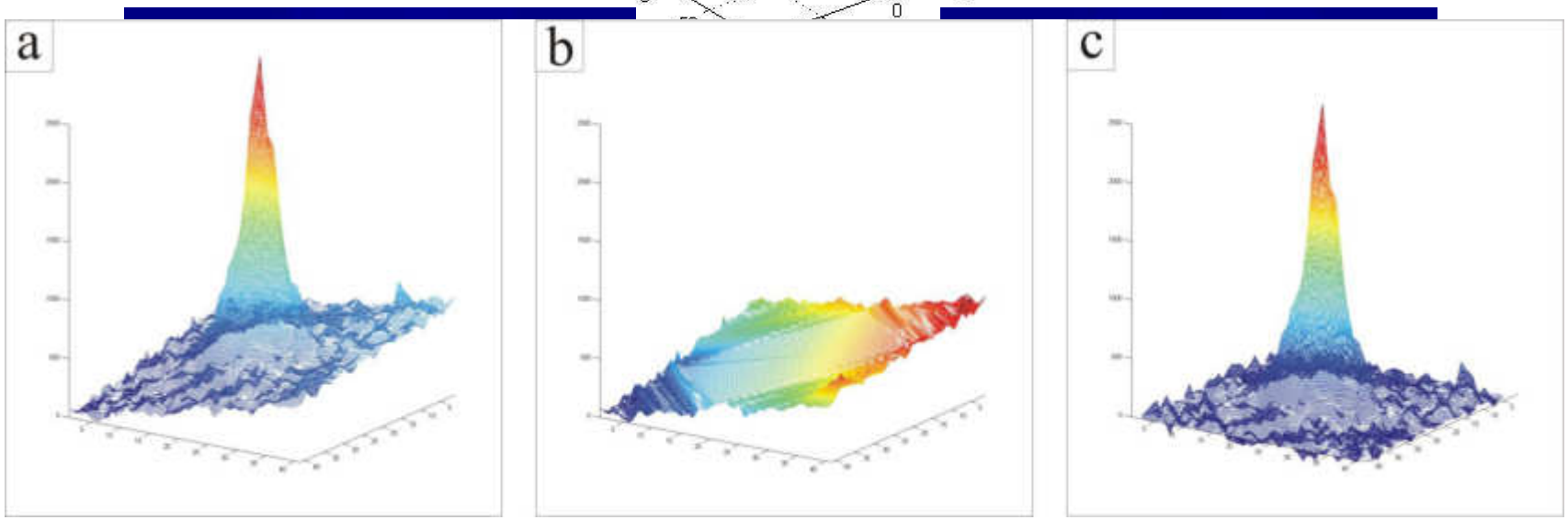

"Ab initio" structure solution from electron diffraction data obtained by a combination of automated diffraction tomography and precession technique.
E. Mugnaioli, T. Gorelik, U. Kolb, *Ultramicroscopy* **109**, 758 (2009).

Software for data analysis

ADT3D

In-house made Matlab routines

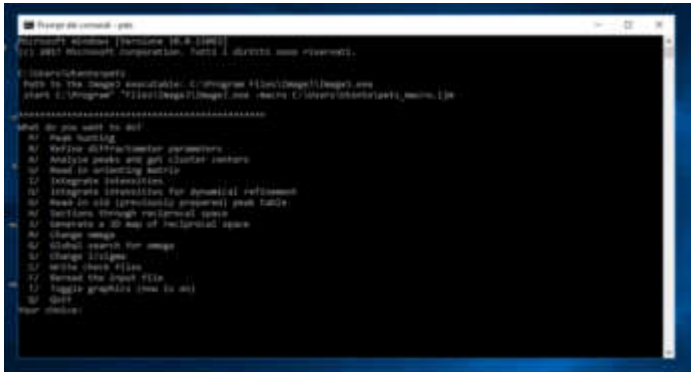

PETS – ***by Lukas Palatinus***

*.hkl file

h	*k*	*l*	*I*	*σ(I)*	
-26	0	-2	2.19	1.48	1
-26	1	-2	0.41	0.64	1
-26	1	0	2.86	1.69	1
-26	1	2	0.82	0.91	1
-26	2	0	14.93	3.86	1
-26	3	-2	1.15	1.07	1
-26	3	0	9.01	3.00	1
-26	4	0	3.07	1.75	1
-25	-2	-4	1.76	1.33	1
-25	-1	-2	1.91	1.38	1
-25	0	4	27.11	5.21	1
-25	1	-4	0.09	0.30	1
-25	1	0	3.25	1.80	1
-25	1	2	0.45	0.67	1
-25	2	-4	3.13	1.77	1
-25	2	-2	2.79	1.67	1
-25	2	0	3.57	1.89	1
-25	2	2	0.36	0.60	1
-25	3	-2	6.02	2.45	1
-25	3	0	4.52	2.13	1
-25	3	2	7.56	2.75	1
-25	4	-2	4.49	2.12	1
-25	4	0	15.28	3.91	1
-25	5	-2	1.44	1.20	1

Software for structure analysis

SIR
direct methods and simulated annealing

SHELX suite
direct methods & refinement

JANA
charge flipping & dynamical refinement

SIR input

natro.sir - Blocco note

File Modifica Formato Visualizza ?

```
%Job natrolite
%Window
%Structure natrolite
%Initialize
%Data
   Cell    6.586  18.293  18.64    90.0000  90.00   90.0000
   Spacegroup F d d 2
   Content  Si 24   Al 16  Na 16   O 96
   Reflections C:\wingfile\natrolite\adt3d\natro.hkl
   Format(3i4, 2f8.2)
   Nosigma
 ! Electrons
   Wavelength 0.019700
   Fosq
   ResM 1
%Phase
   Tangent 200 100
%End
```

you can omit

or 'Fobs'

1) Wilson Statistic
2) Phase Search (Direct Methods)
3) Interpretation of the Potential Map

The result: a Potential Map

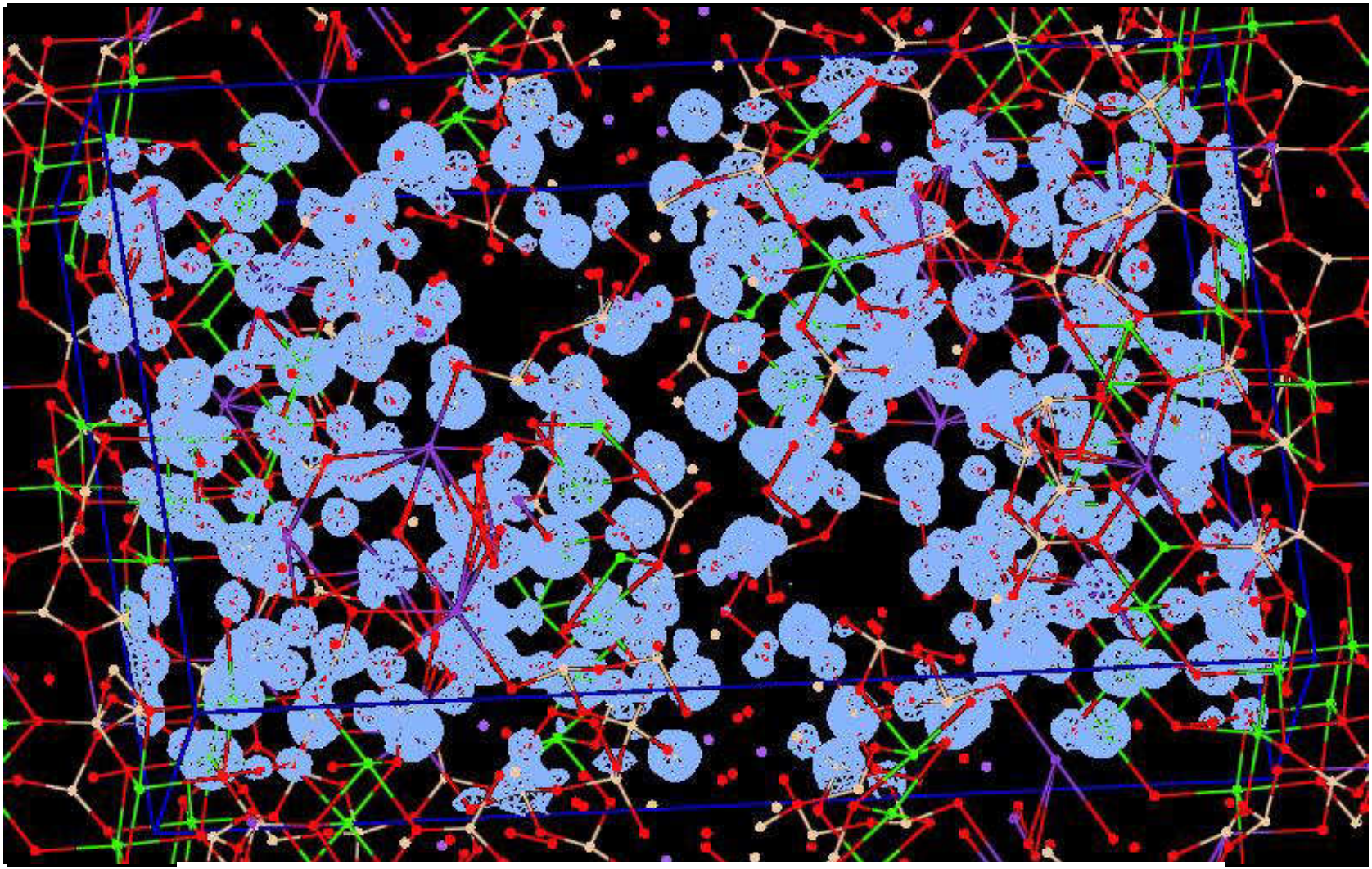

The Potential Map is automatically interpreted in terms of atom positions

Atom positions and final model

natro_new_good.out - Blocco note

File Modifica Formato Visualizza ?

```
Recovered the best trial (157) in terms of residual value.
Final residual value =  19.92%

*** warning *** freely floating origin along   z
```

The atom position list has to be interpreted

Serial	Atom	Label	Height*10	x	y
1)	Al	Al1	23	0.402	-0.038
2)	Si	Si1	22	0.250	0.250
3)	Si	Si2	22	0.211	0.152
4)	O	O1	17	0.405	0.042
5)	Na	Na1	17	0.282	0.032
6)	O	O2	17	0.182	0.067
7)	O	O3	15	0.289	0.155
8)	O	O4	15	0.227	0.181
9)	O	O5	14	0.431	-0.023
10)	O	O6	12	0.311	-0.060
11)	O	O7	5	0.173	0.031
12)	O	O8	5	0.118	0.031
13)	O	O9	5	0.420	0.087
14)	Q	Q2	4	0.341	0.171
15)	Q	Q3	3	0.174	0.052

O

Na

H_2O

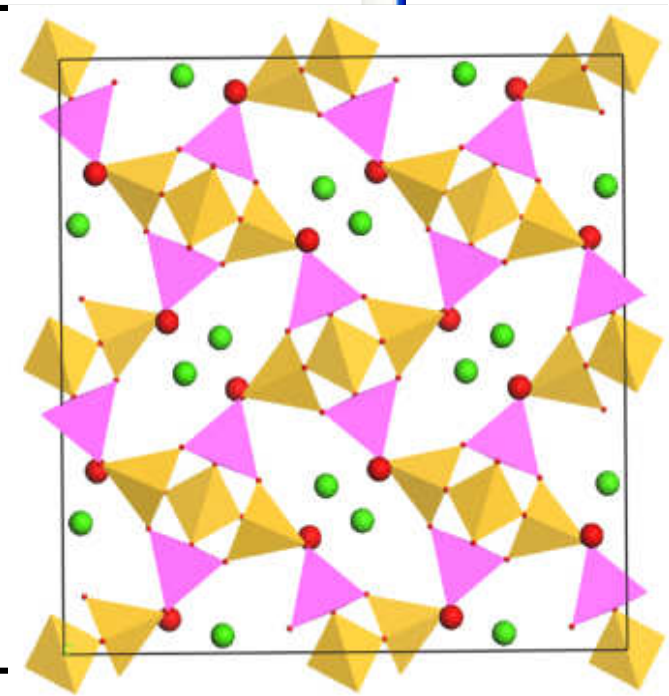

Helps: Composition, interatomic distances and coordination

Structure solved!!

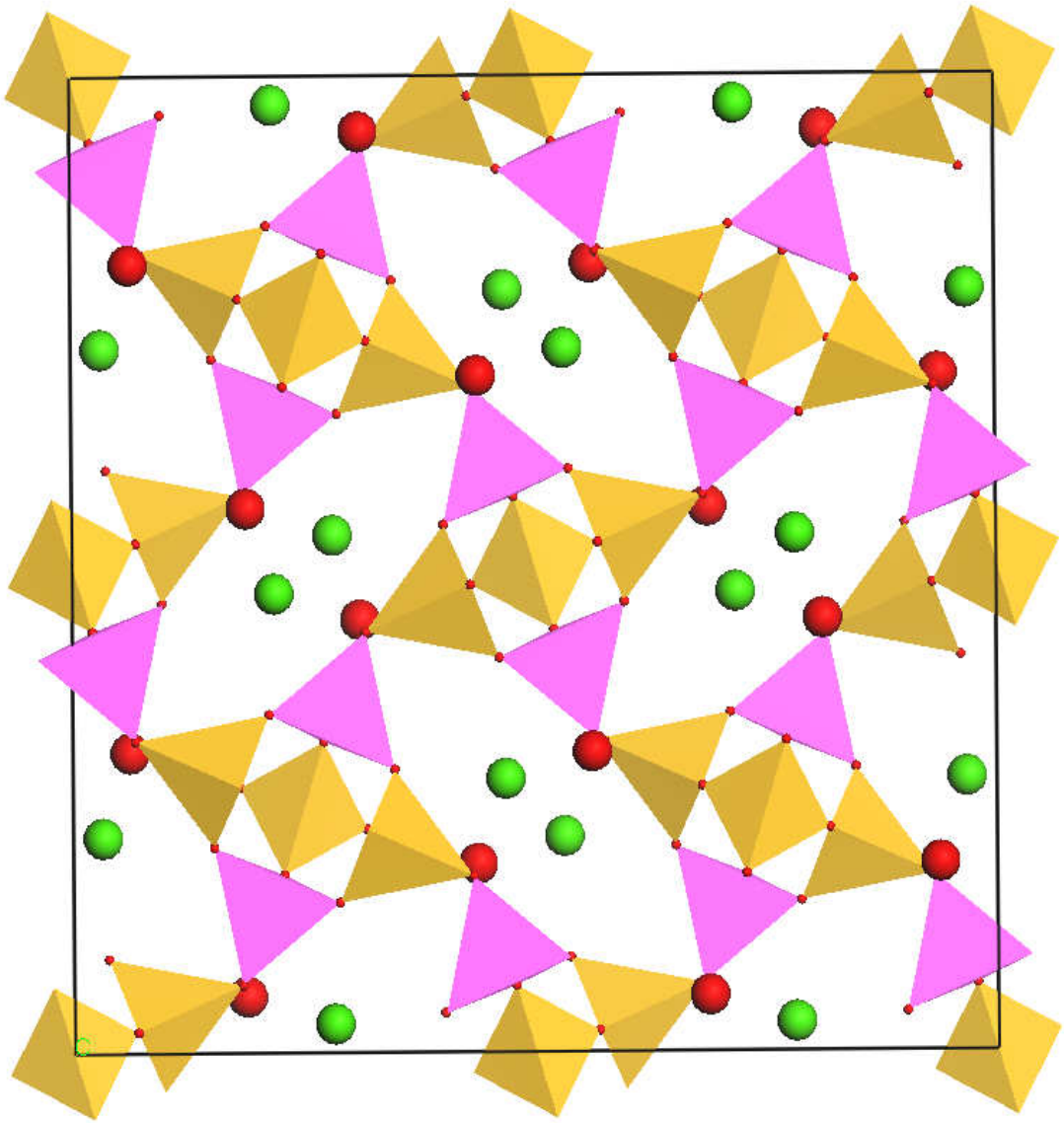

EDT analysis

Polyphasic samples: HAPy

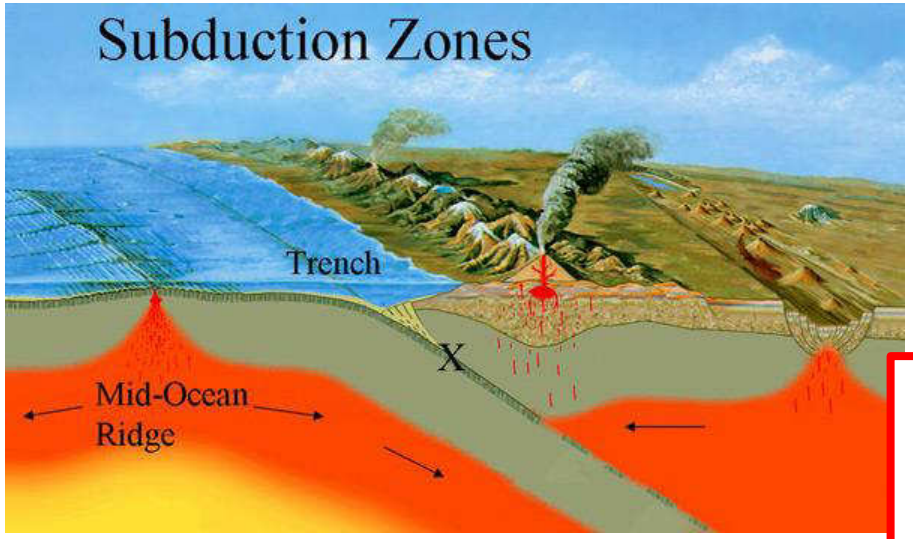

A new phase was detected at 5.2 Gpa, 700ºC,

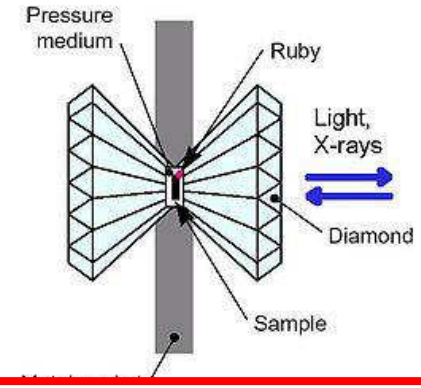

Conventional ED:
C-centred monoclinic cell
a=9.9Å, b=11.8 Å, c=5.1Å, β=110°

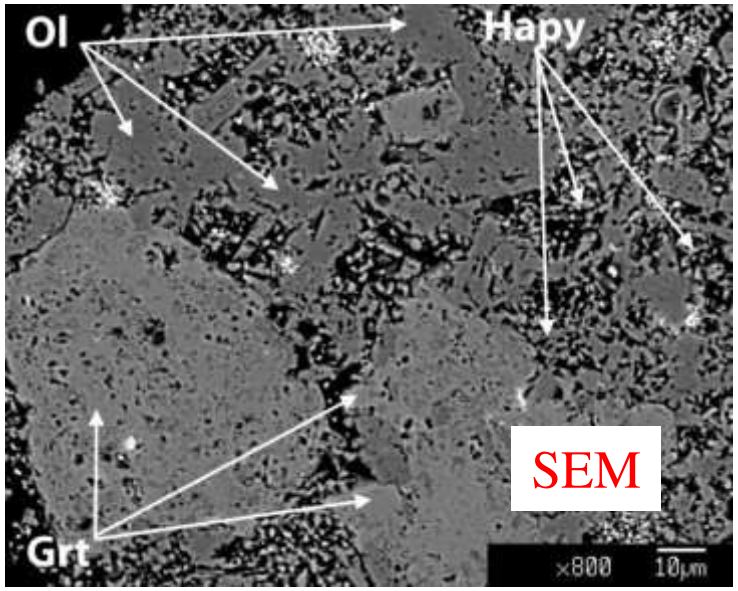

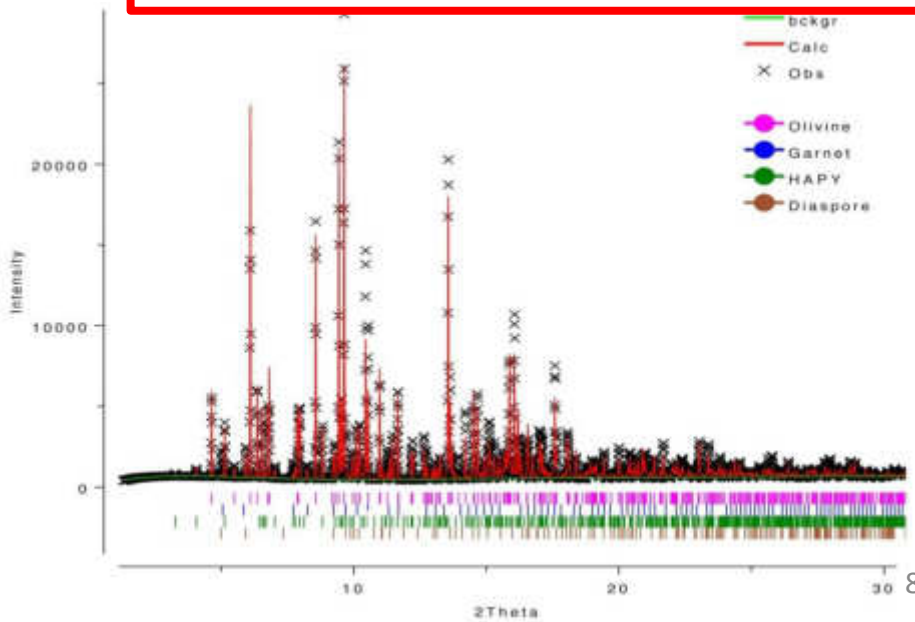

EDT Examples

Polyphasic samples: HAPy

86% completeness, 1.0 Å resolution

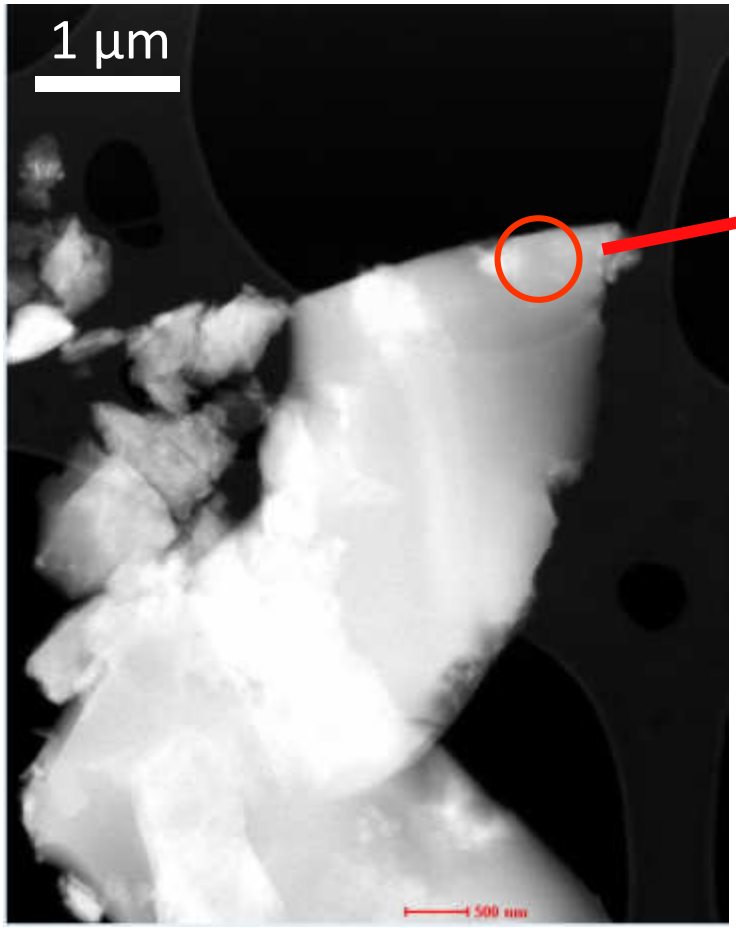

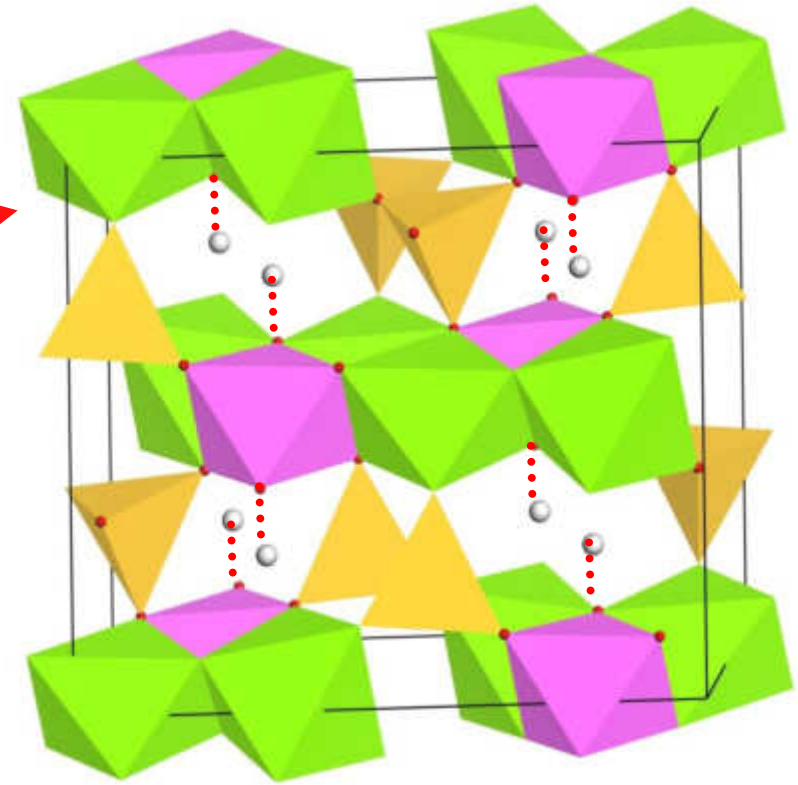

Hydrous Al-bearing Pyroxene (HAPy)

$Mg_2Al(OH)_2AlSiO_6$

A new hydrous Al-bearing pyroxene as a water carrier in subduction zones.
M. Gemmi, J. Fischer, M. Merlini, S. Poli, P. Fumagalli, E. Mugnaioli, U. Kolb, *Earth Planet Sc Lett* **310**, 422 (2011).

Charoite

EDT Examples

Charoite

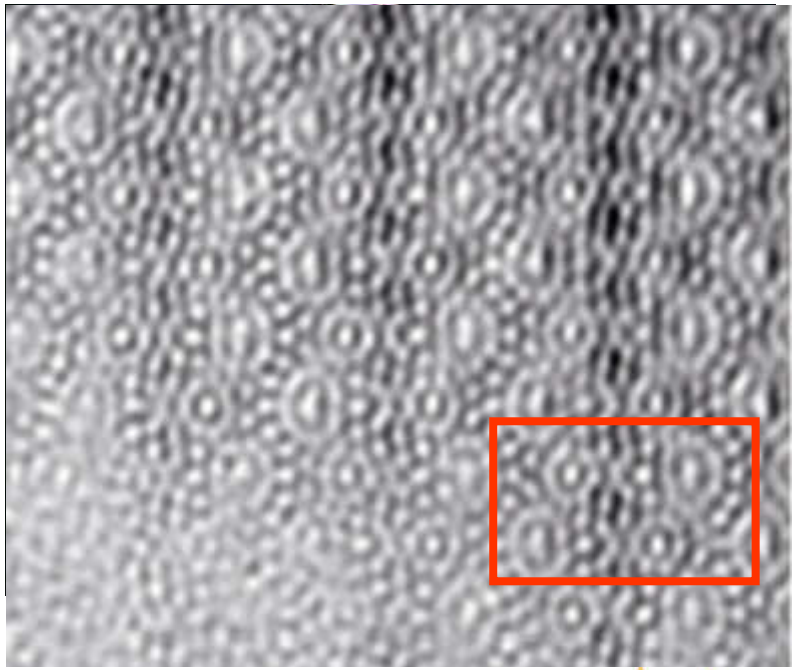

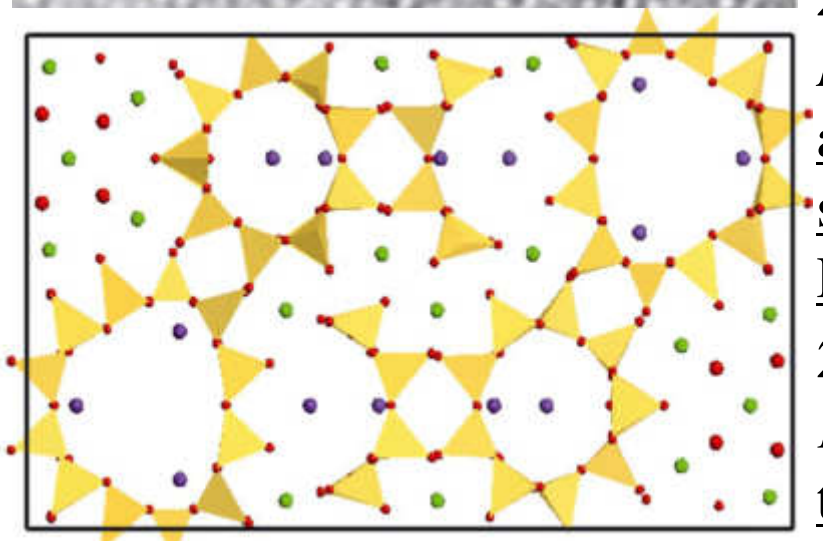

1978. Rogova et al., *Zapiski Vsesoyuznogo Mineralogischeskogo Obshchetva*: charoite is recognized as a new mineral

1985. Nikishova et al., *Crystal Chemistry and Strucutre of Minerals*: on the basis of XRPD charoite is assigned to spacegroup P2/m (β = 94.3°)

2009. Rozhdestvenskaya et al., *Mineral. Mag.*: on the basis of XRPD and HRTEM a tentative charoite strucutre is proposed in spacegroup $P2_1/m$ (β = 96.3°)

2009. Rozhdestvenskaya et al., *Z. Kristallogr.*: SAED and HRTEM reveal the presence of different polytypes

EDT Examples

Charoite

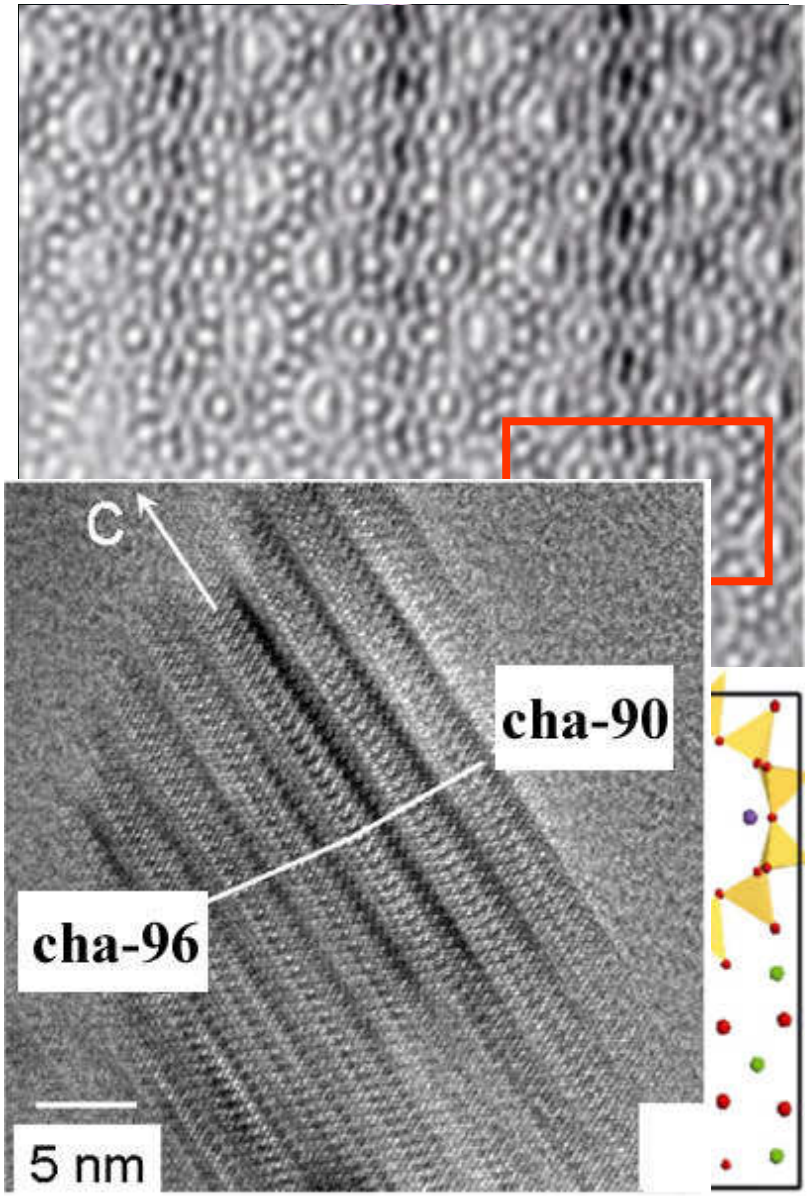

[010]

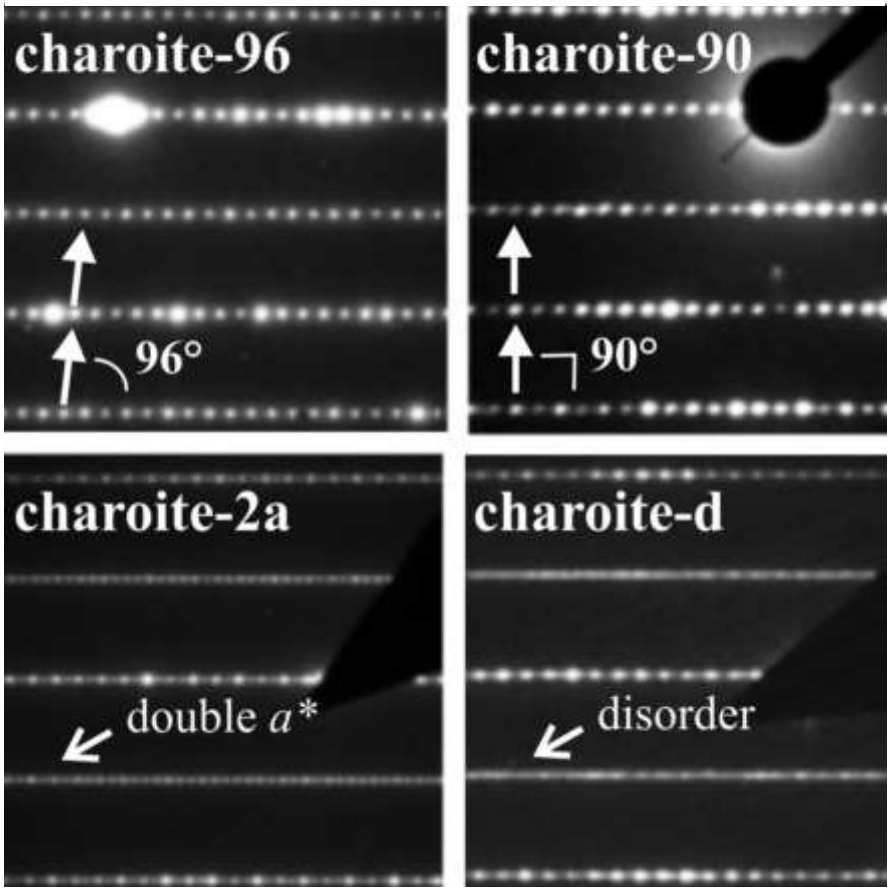

EDT Examples

Charoite

EDT confirms **two ordered polytypes** and allows to measure their **cell parameters** (in **3D**)

Charoite-90: a=31.96Å, b=19.64Å, c= 7.09Å, α=90.0°, $\boldsymbol{\beta}$**=90.0°**, γ=90.0°

Charoite-96: a=32.11Å, b=19.77Å, c= 7.23Å, α=90.0°, $\boldsymbol{\beta}$**=95.9°**, γ=90.0°

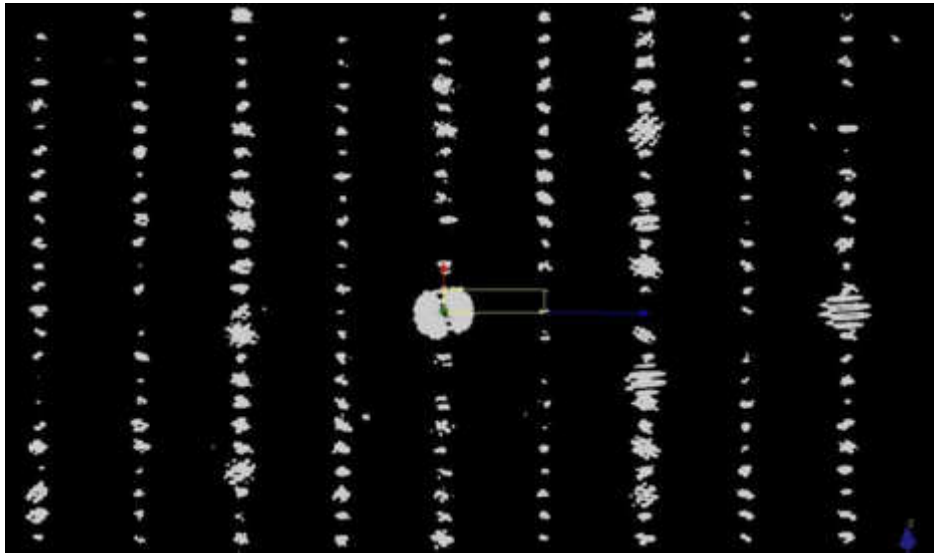

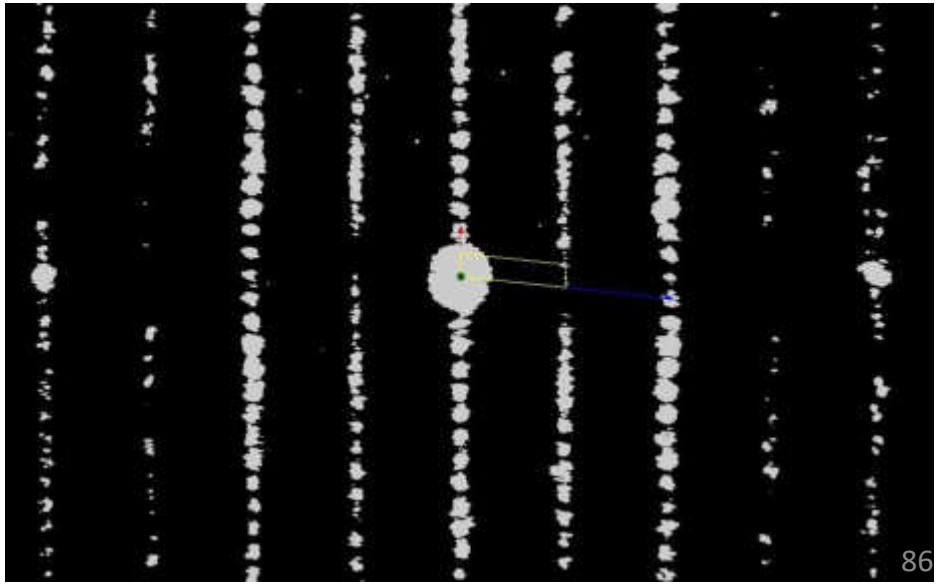

Charoite

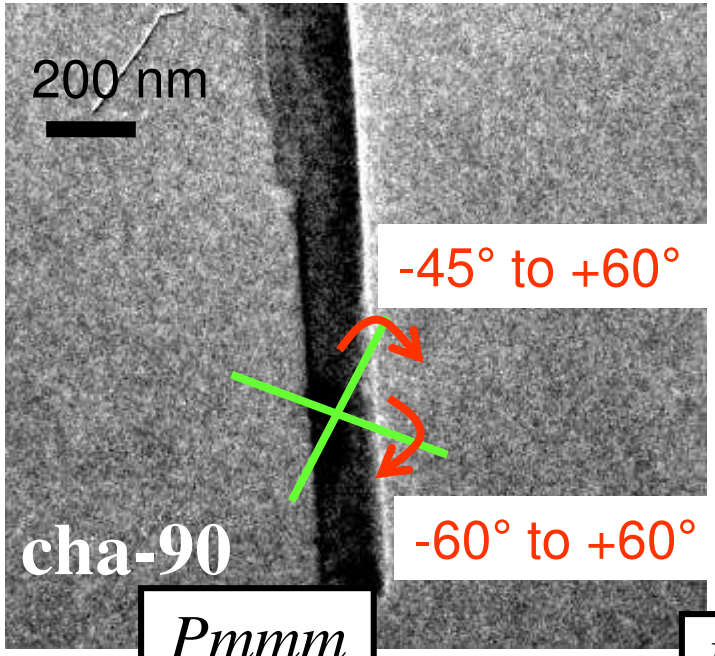

Pmmm

P2/m

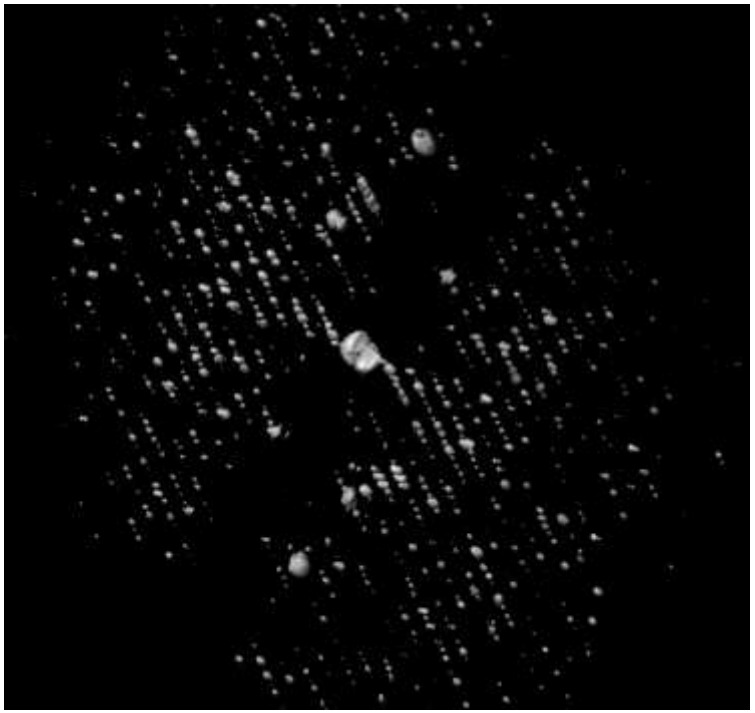

Angstrom	Number	Rint
up to 10.0	3	2.27%
10.0 - 8.0	4	2.89%
8.0 - 6.0	13	16.02%
6.0 - 5.0	12	15.00%
5.0 - 4.0	[illegible]	[illegible]
4.0 - 3.0	[illegible]	[illegible]
3.0 - 2.5	[illegible]	[illegible]
2.5 - 2.0	[illegible]	[illegible]
2.0 - 1.8	123	23.30%
1.8 - 1.6	203	25.05%
1.6 - 1.4	320	21.73%
1.4 - 1.3	247	23.60%
1.3 - 1.2	311	24.23%
1.2 - 1.1	66	[illegible]
All	1653	21.73%

Angstrom	Number	Rsym
up to 10.0	3	2.27%
10.0 - 8.0	4	2.89%
8.0 - 6.0	16	3.70%
6.0 - 5.0	9	6.99%
5.0 - 4.0	4	10.95%
4.0 - 3.0	1	10.22%
3.0 - 2.5	0	10.65%
2.5 - 2.0	306	12.50%
2.0 - 1.8	209	13.22%
1.8 - 1.6	350	15.11%
1.6 - 1.4	557	14.84%
1.4 - 1.3	431	14.66%
1.3 - 1.2	539	16.17%
1.2 - 1.1	94	20.31%
All	2793	13.32%

Space group: $P2_1/m$

8495 total reflections
2878 independent ones
97% completeness
1.18 Å resolution

EDT Examples

Charoite

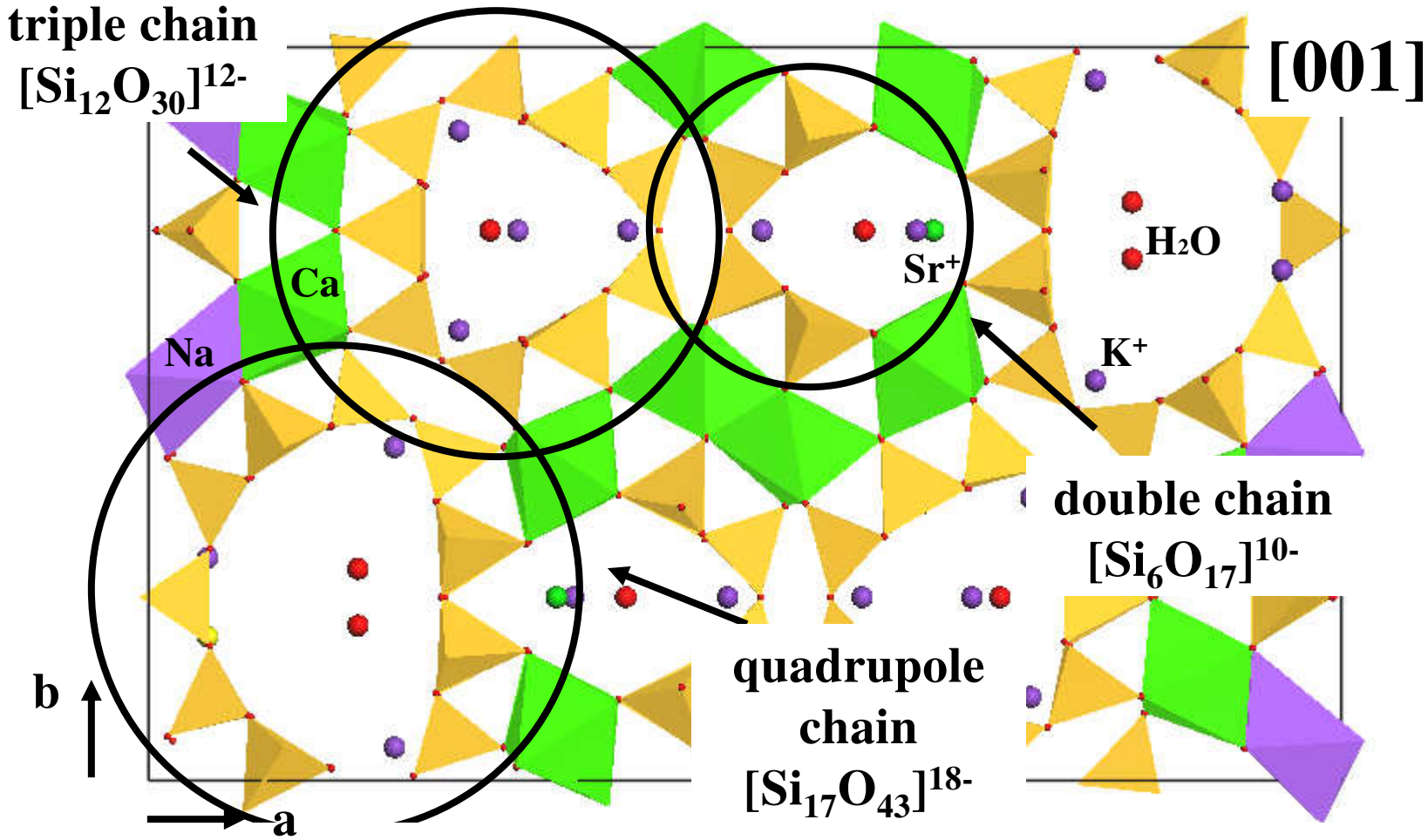

The structure of charoite, $(K,Sr,Ba,Mn)_{15\text{-}16}(Ca,Na)_{32}[(Si_{70}(O,OH)_{180})](OH,F)4.0 * nH_2O$, solved by conventional and automated electron diffraction.

I. Rozhdestvenskaya, E. Mugnaioli, M. Czank, W. Depmeier, U. Kolb, A. Reinholdt, T. Weirich, *Mineral Mag* **74**, 159 (2010).

Charoite

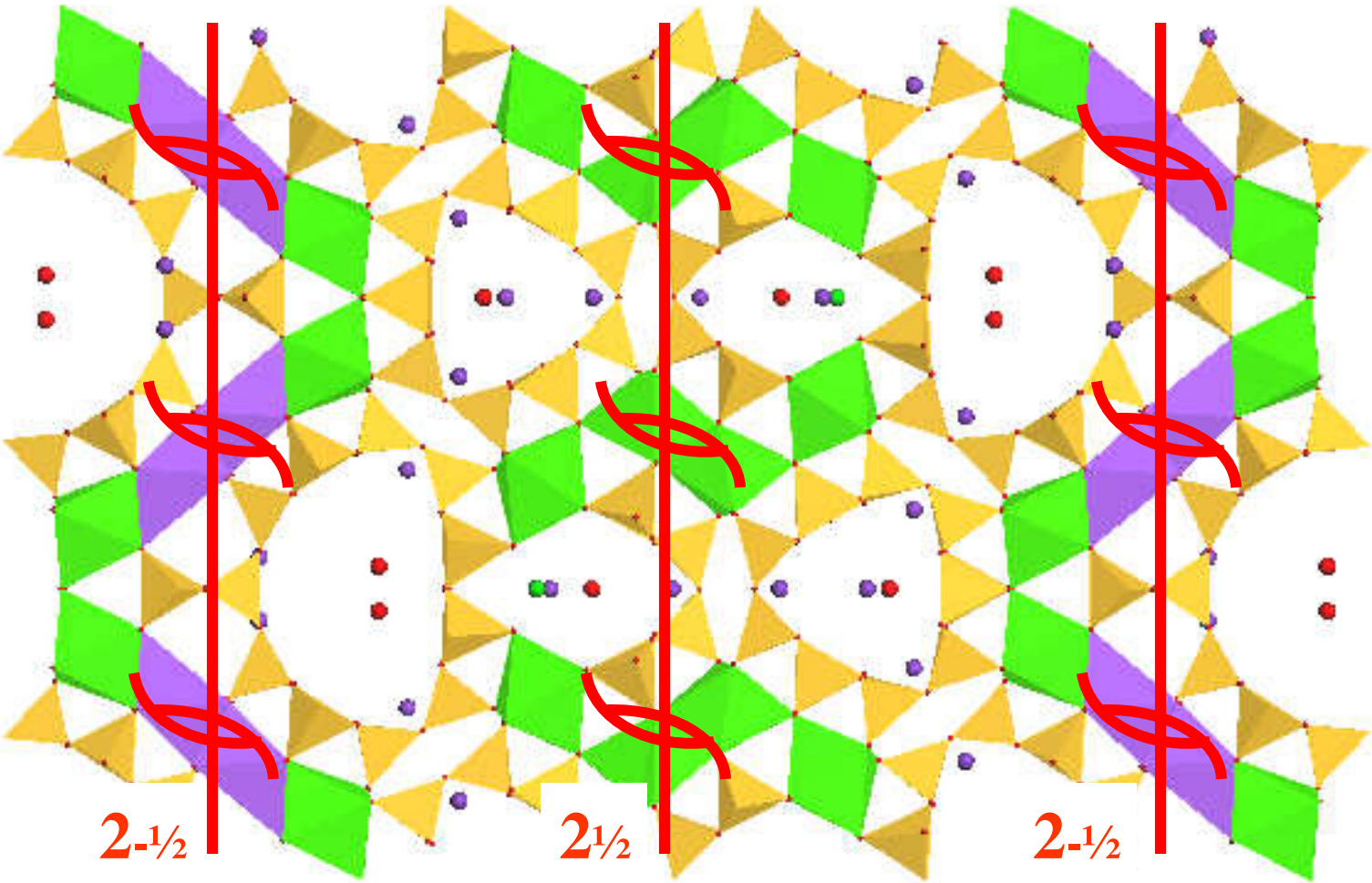

Charoite as **OD layers** shifted by ¼ c or -¼ c

Possible sequences with the maximum degree of order (MDO):

MDO1 (cha-90): ¼,-¼,¼,-¼… & **MDO2** (cha-96): -¼,-¼,-¼,-¼…

Charoite

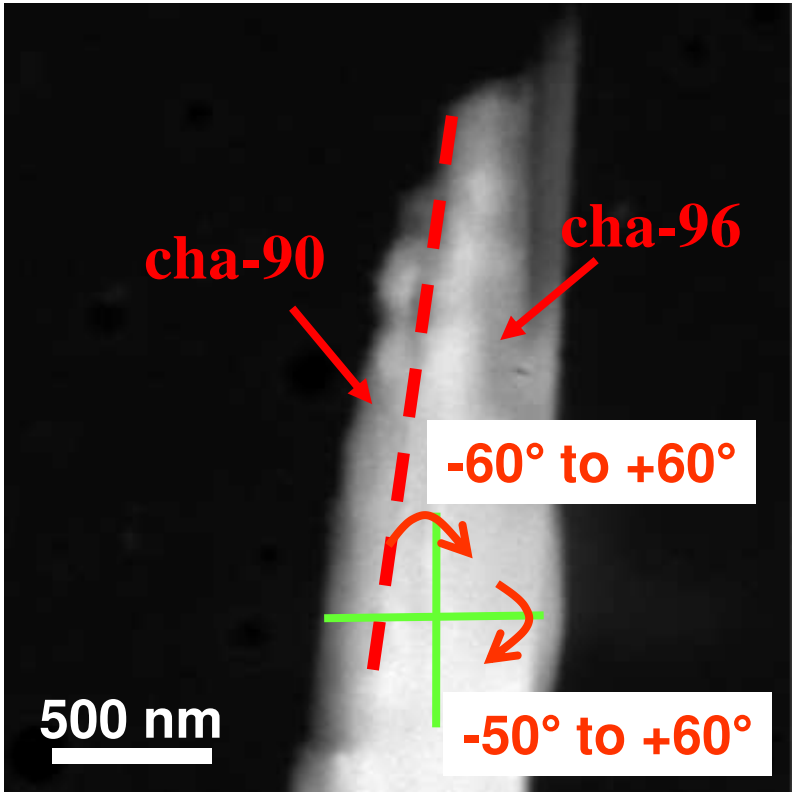

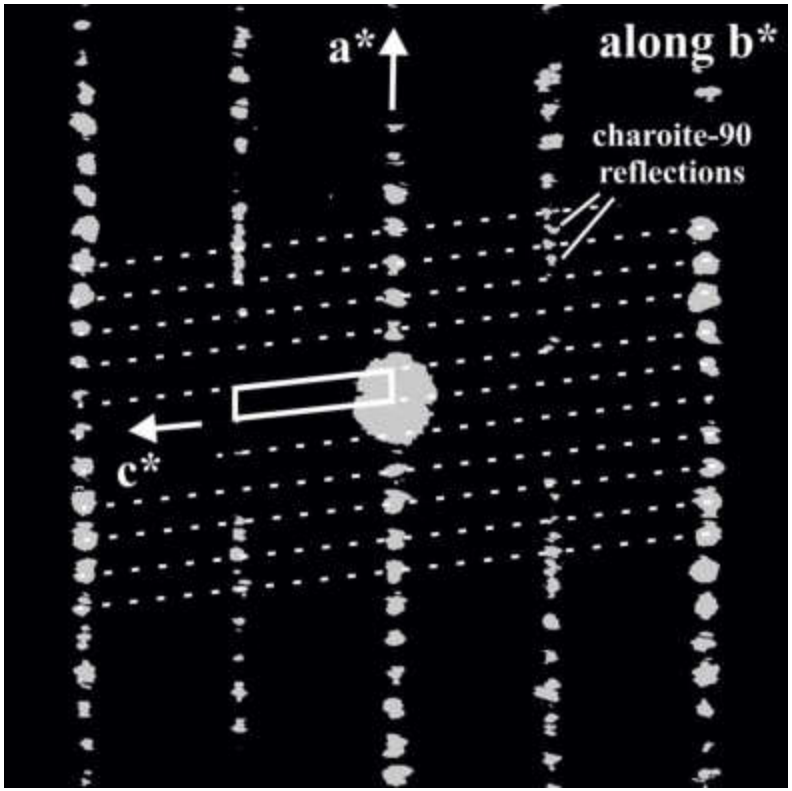

10271 total reflections
3353 independent reflections
97% completeness
1.15 Å resolution

R_{sym} = 22%

Space group:
$P2_1/m$

EDT Examples

Charoite

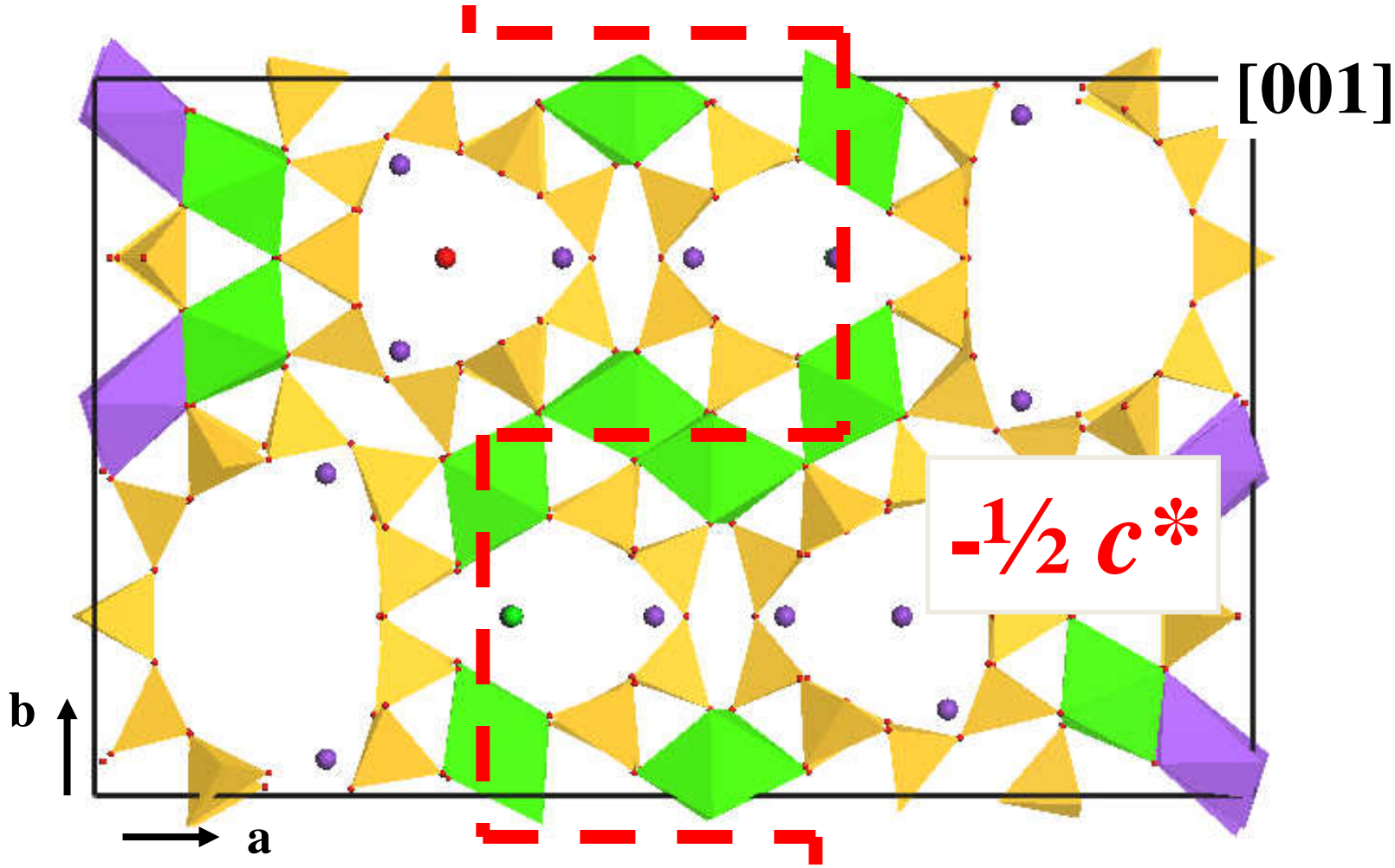

Essential features of the polytypic charoite-96 structure compared to charoite-90.
I. Rozhdestvenskaya, E. Mugnaioli, M. Czank, W. Depmeier, U. Kolb, S. Merlino, *Mineral Mag* **75**, 2833 (2011).

Charoite

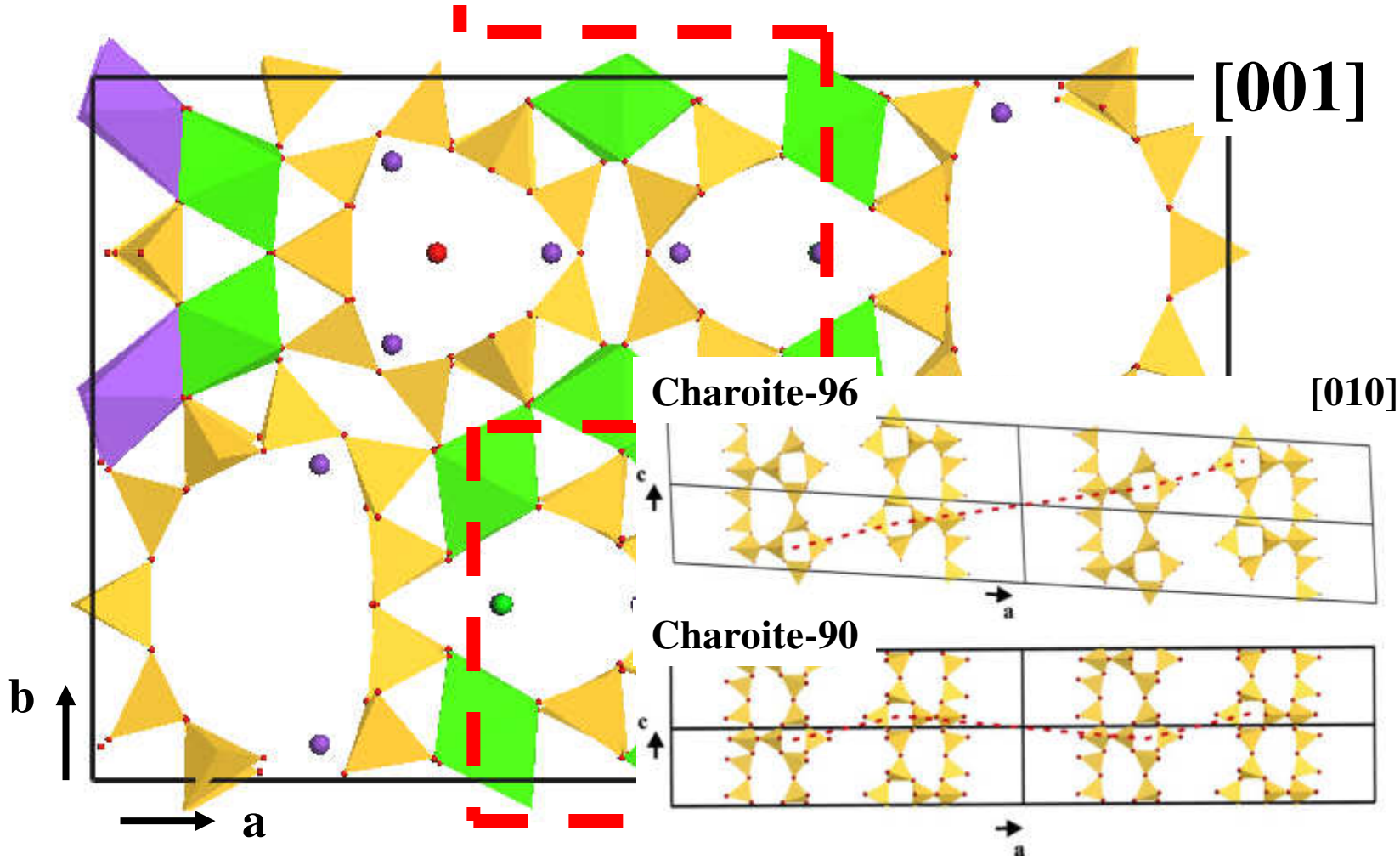

Essential features of the polytypic charoite-96 structure compared to charoite-90.
I. Rozhdestvenskaya, E. Mugnaioli, M. Czank, W. Depmeier, U. Kolb, S. Merlino, *Mineral Mag* **75**, 2833 (2011).

Garnet Codera dike pegmatite

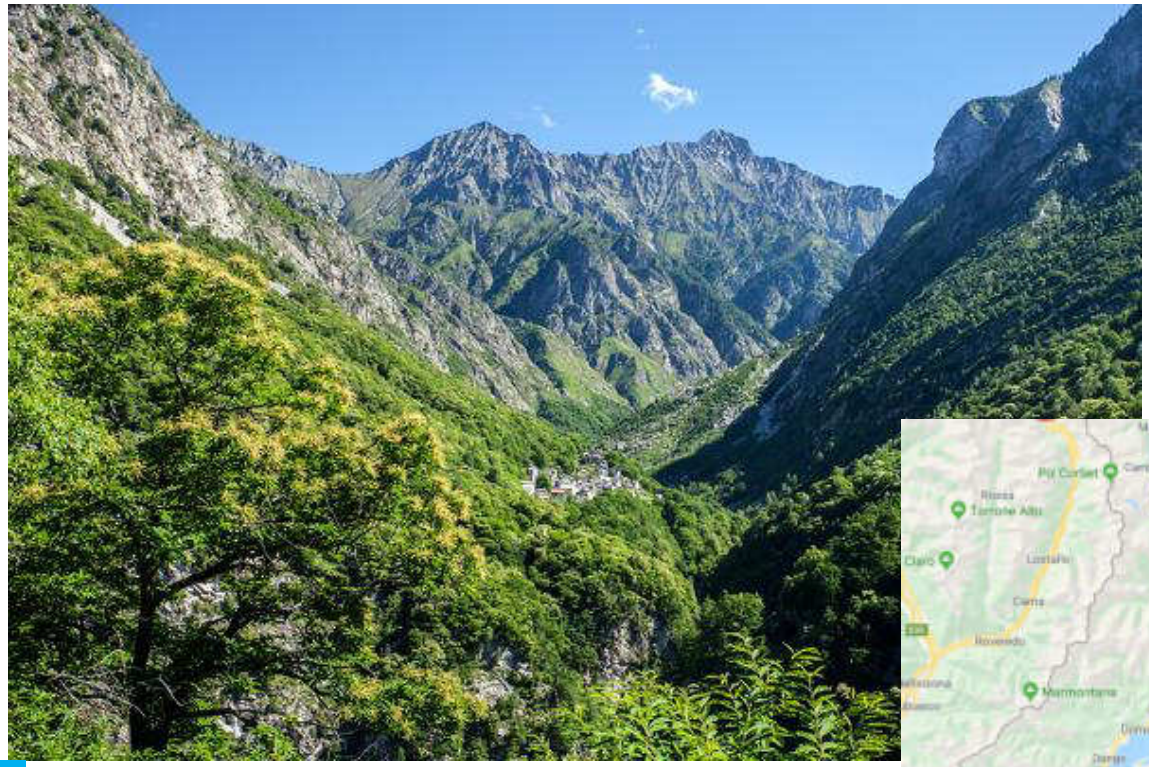

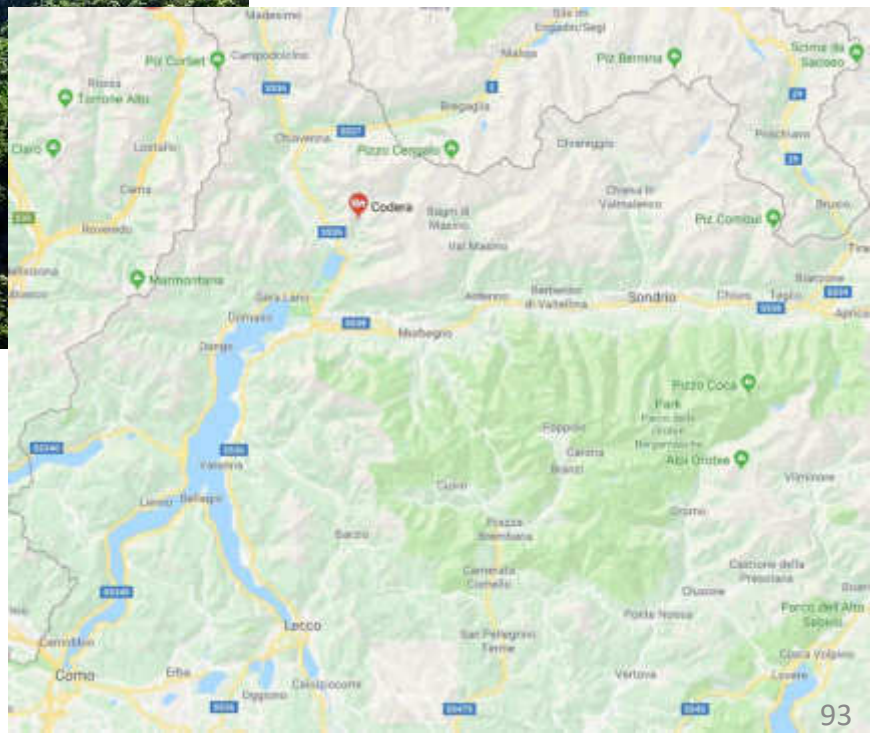

EDT Examples

Metamict minerals

Matamict phase from Garnet Codera dike pegmatite (Central-Western Italian Alps)

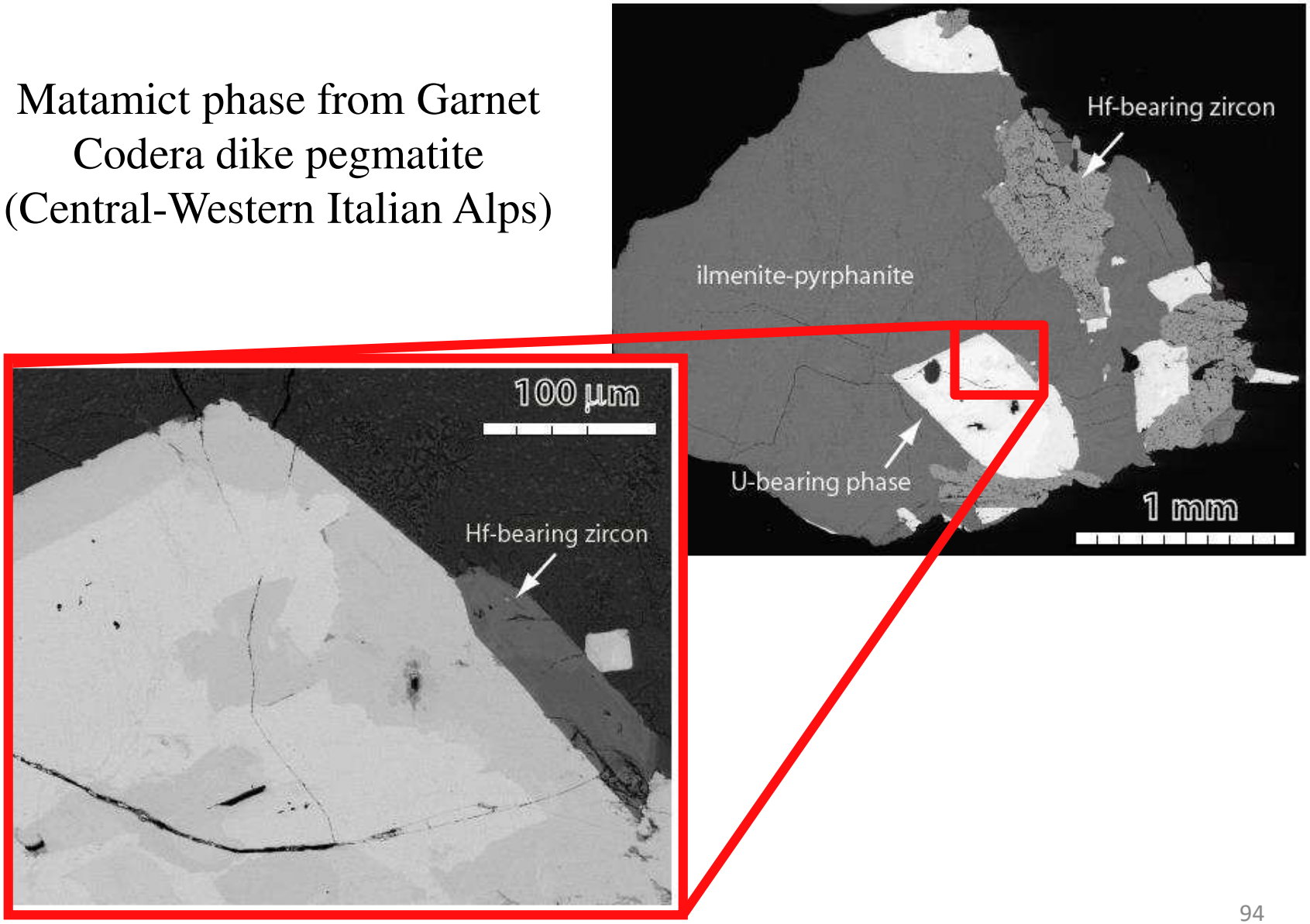

EDT Examples

Metamict minerals

Metamict process
the structure of minerals containing radioactive elements is progressively destroyed by radiations produced by radioactive decay

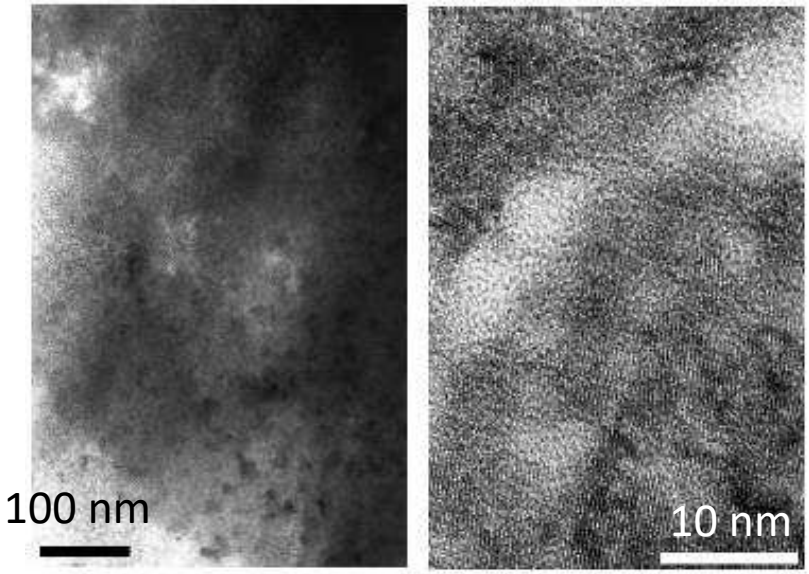

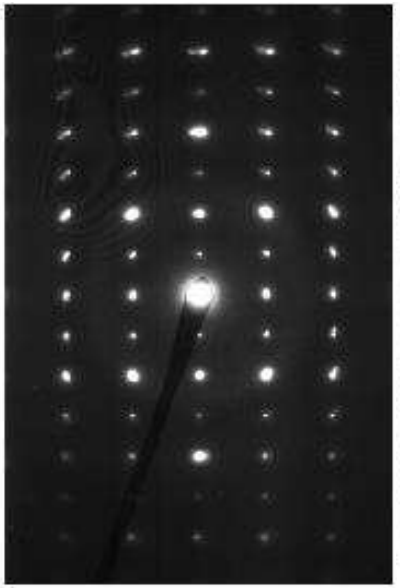

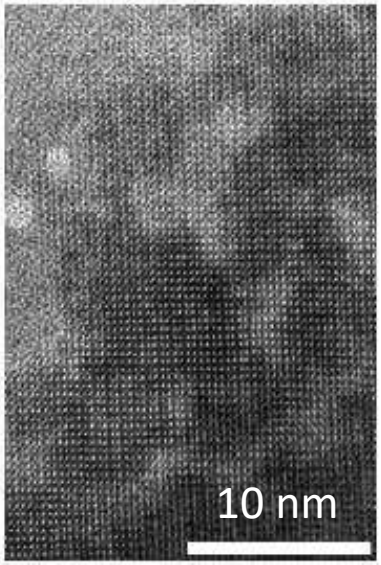

Sometimes, **iso-oriented more crystalline areas of few tens of nanometers** are preserved in the mostly amorphous matrix

EDT Examples

Samarskite-(Y)

WDS:

Nb_2O_5	36%
Ta_2O_5	15%
UO_2	14%
YO_3	9%
FeO	5%
Fe_2O_3	4%
TiO_2	4%

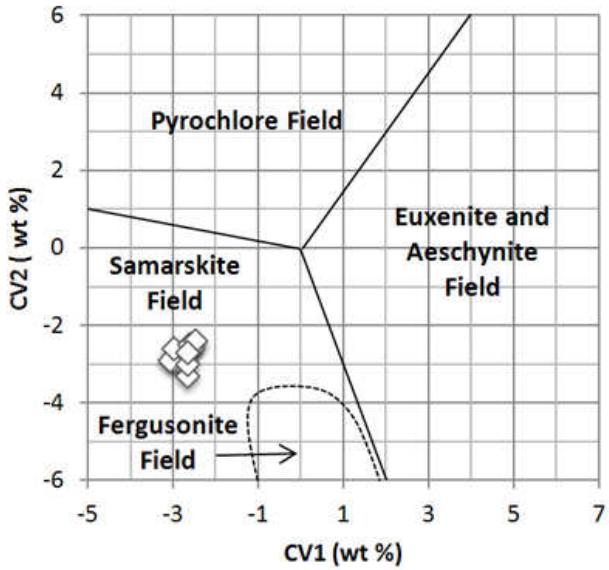

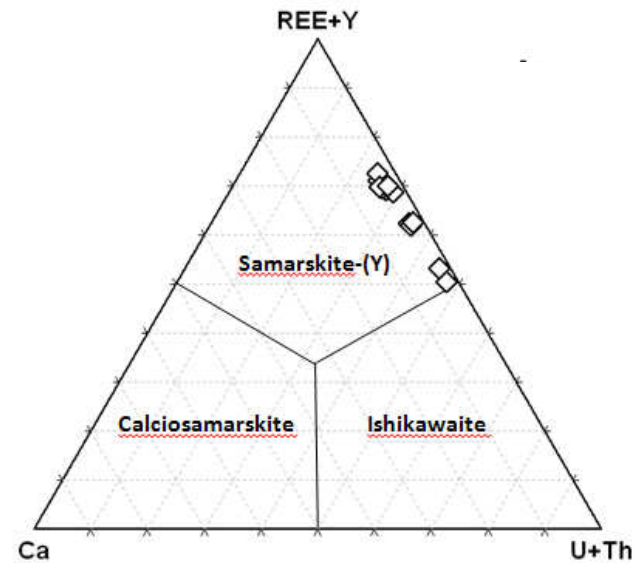

Samarskite is normally associated with formula:

$(Y,REE,Fe,U,Th,Ca)_4(Nb,Ta,Ti)_4O_{16}$

$(Y,REE,Fe,U,Th,Ca)_3(Nb,Ta,Ti)_5O_{16}$

EDT Examples

Samarskite-(Y)

For X-ray diffraction, sample **annealing** and **recrystallization** are necessary

When samarskite is recrystallized **in atmosphere**, **several compounds** form

When samarskite is recrystallized **in reducing conditions (H_2)**, an **ixiolite** or **columbite** structure is obtained

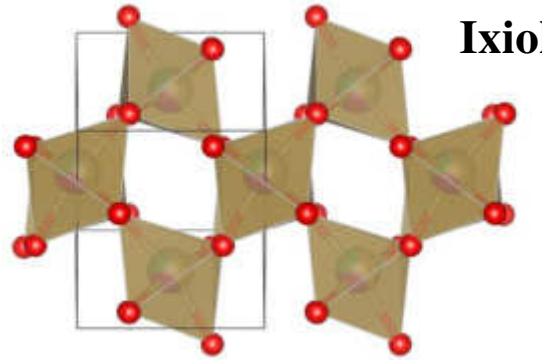

Ixiolite

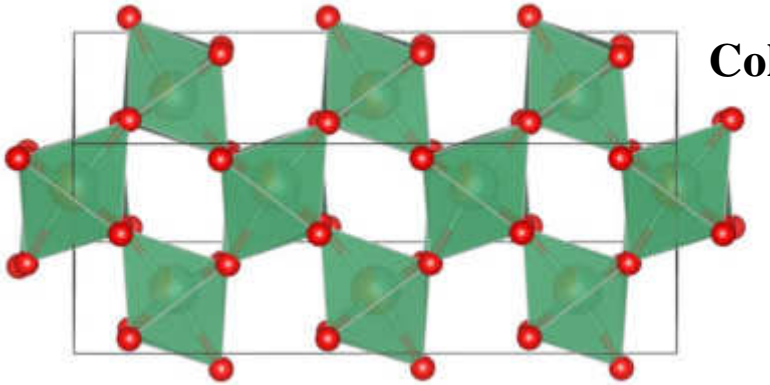

Columbite

EDT Examples

Polymorphism of samarskite and its relationship to other structural related Nb-Ta oxides with α-PbO_2 structure. Y. Sugitani, Y. Suzuki, K. Nagashima, *Am. Mineral.* 70, 856 (1985).

Preservation of the samarskite structure in a metamict ABO4 mineral: a key to crystal structure identification. N. Tomašić, A. Gajović, M.R. Linarić, D. Su, R. Škoda, *Eur. J. Mineral.* 22, 435 (2010).

EDT on samarskite-(Y) crystalline relicts

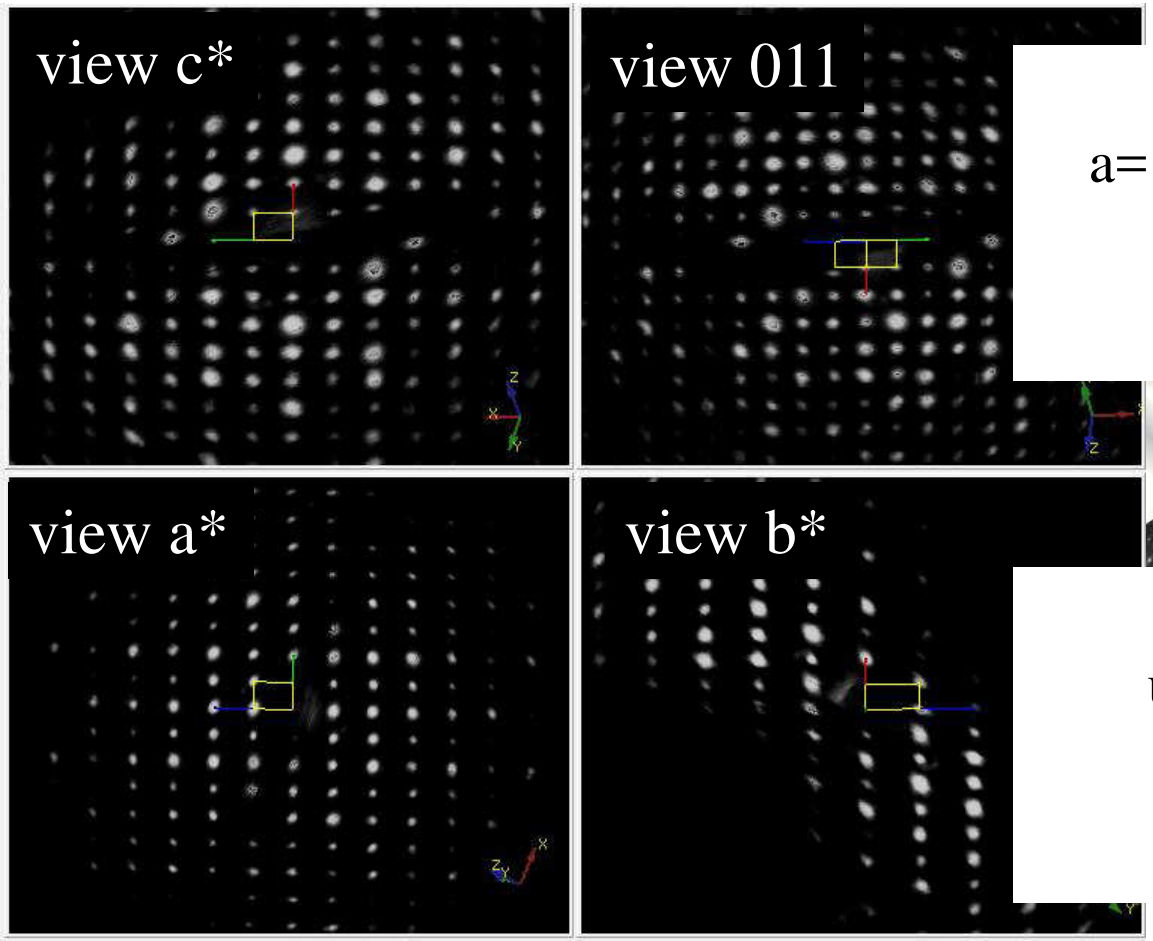

Cell parameters:
a=10.9Å, b=7.5Å, c=5.1Å

Extinction symbol:
Pn–a

1661 reflections
up to 0.8Å resolution
(86% completeness)

R_{sym} = 21.3%

EDT Examples

EDT on samarskite-(Y) crystalline relicts

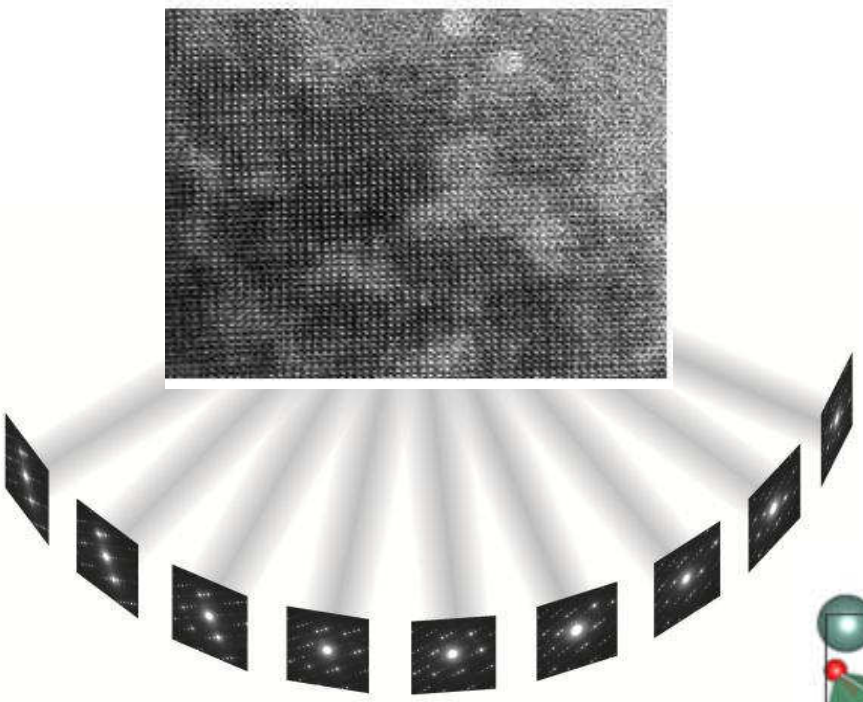

Ab-initio determination by direct methods:

Nioboaeschynite-(Y)

$(Y,REE,Fe,U,Th,Ca)_3(Nb,Ta,Ti)_5O_{16}$

$(Y,U,Fe^{2+})_2(Nb,Ta,Ti,Fe^{3+},Fe^{2+})_4O_{12}$

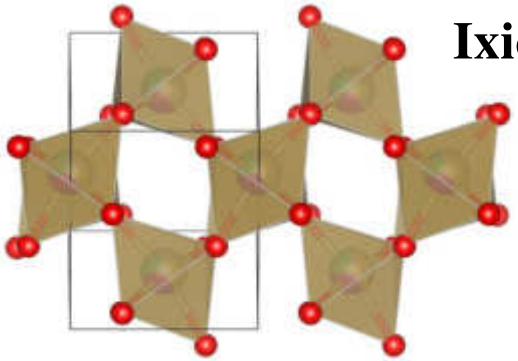

Ixiolite

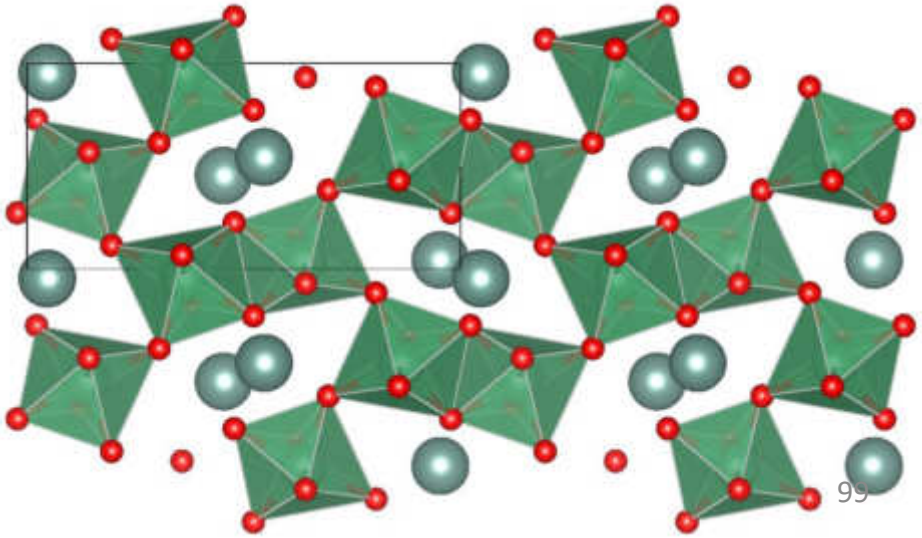

How small?

$Cu_{2-x}Te$

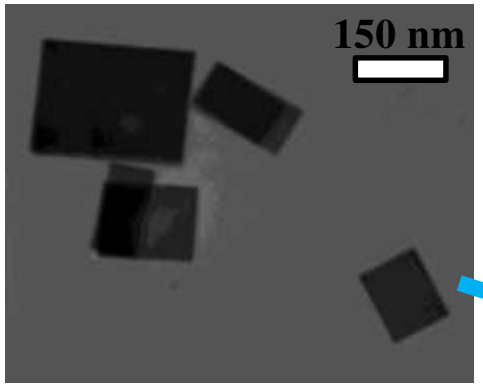

Space group: $P222_1$
a=7.5Å, b=22.8ÅÅ, c=29.6Å
58 independent atoms

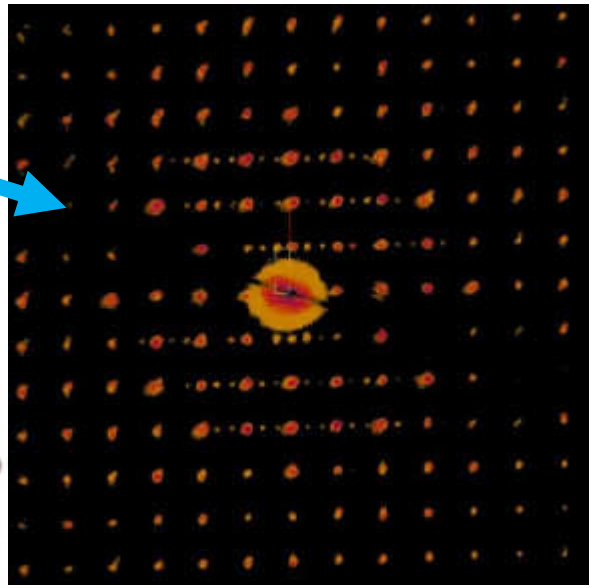

$Zn_{1+x}Sb_7$

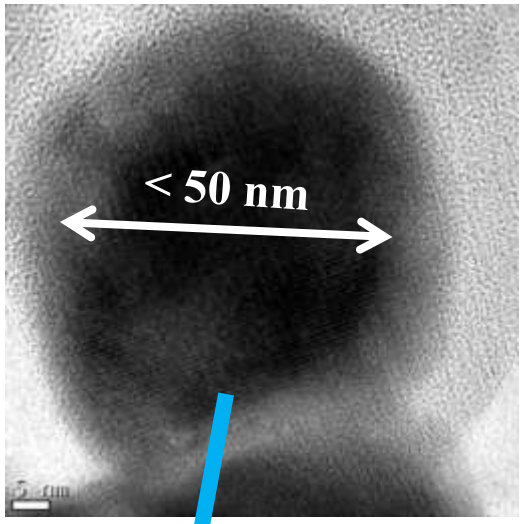

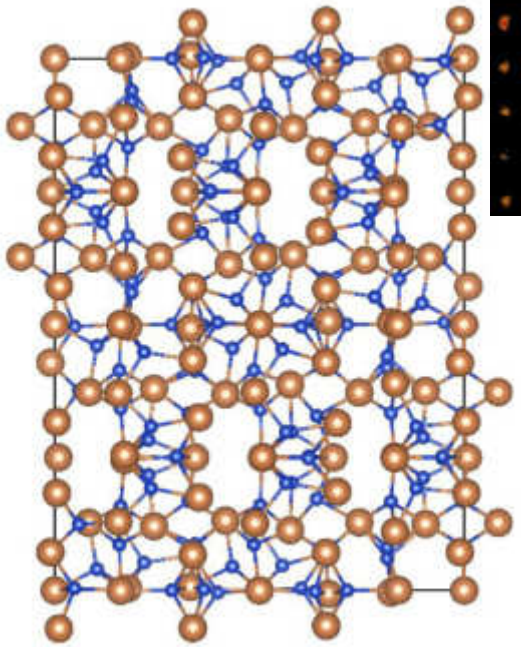

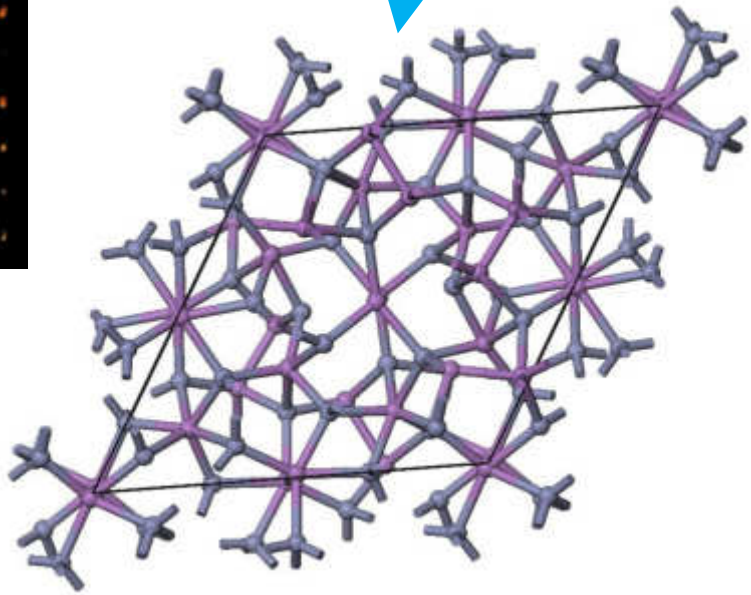

Space group: *P*-1
a~b=15Å, c=7.8Å
30 independent atoms
Birkel *et al.*, *JACS* **132**, 9881 (2010)

EDT: limits and strengths

Intergrown phases

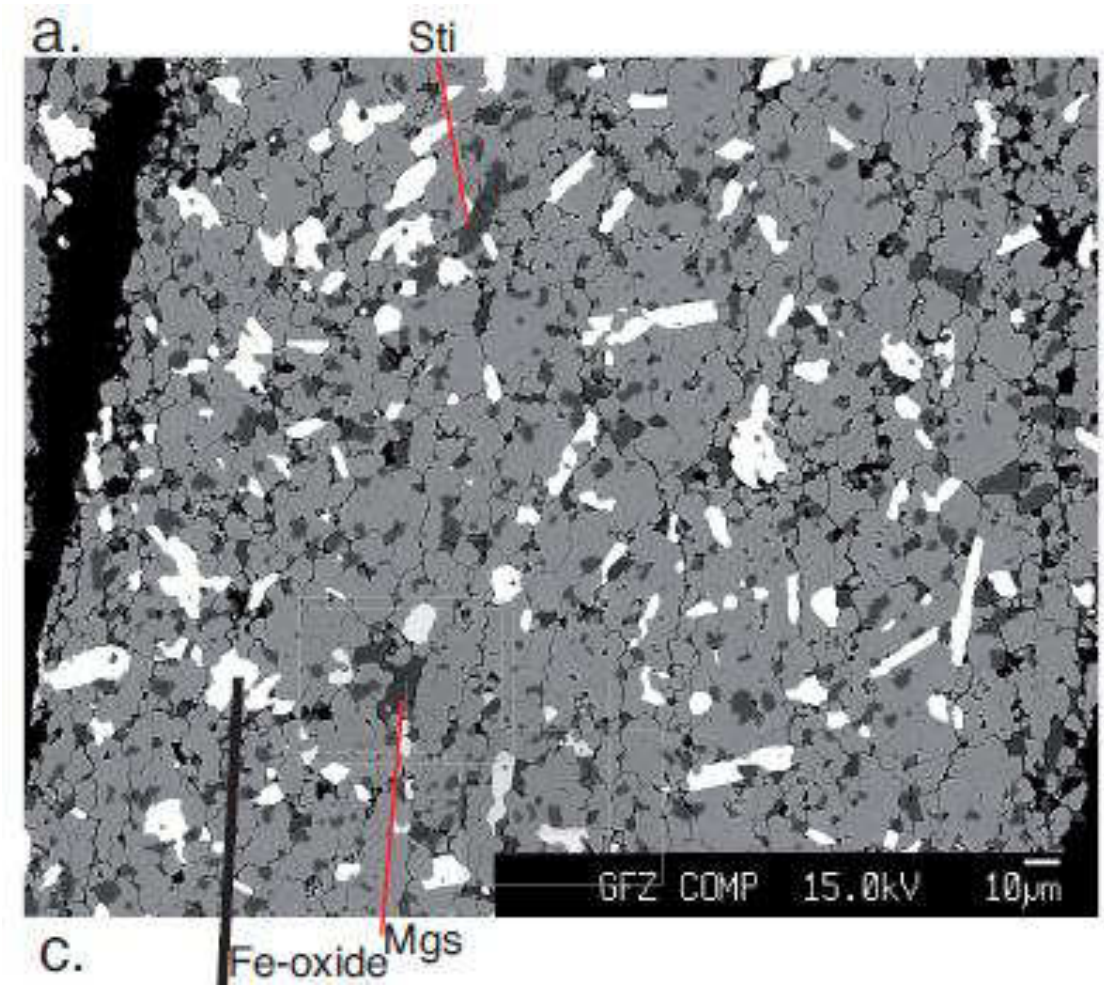

Synthesis and structural characterization of Cr-bearing magnesian h-magnetite recoverable to ambient conditions. M. Koch-Müller, E. Mugnaioli, D. Rhede, S. Speziale, U. Kolb, R. Wirth, *Am Mineral* **99**, 2405 (2014).

Intergrown phases

HP Magnetite – Fe_3O_4

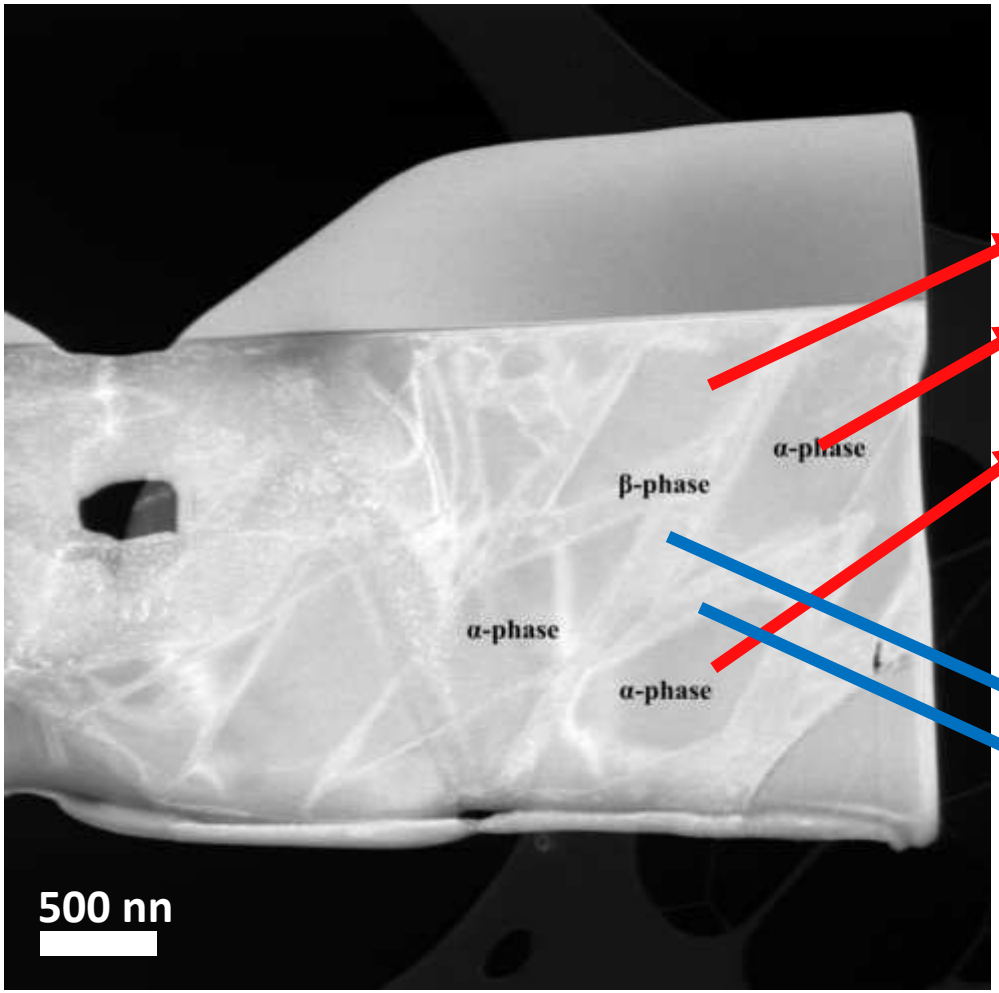

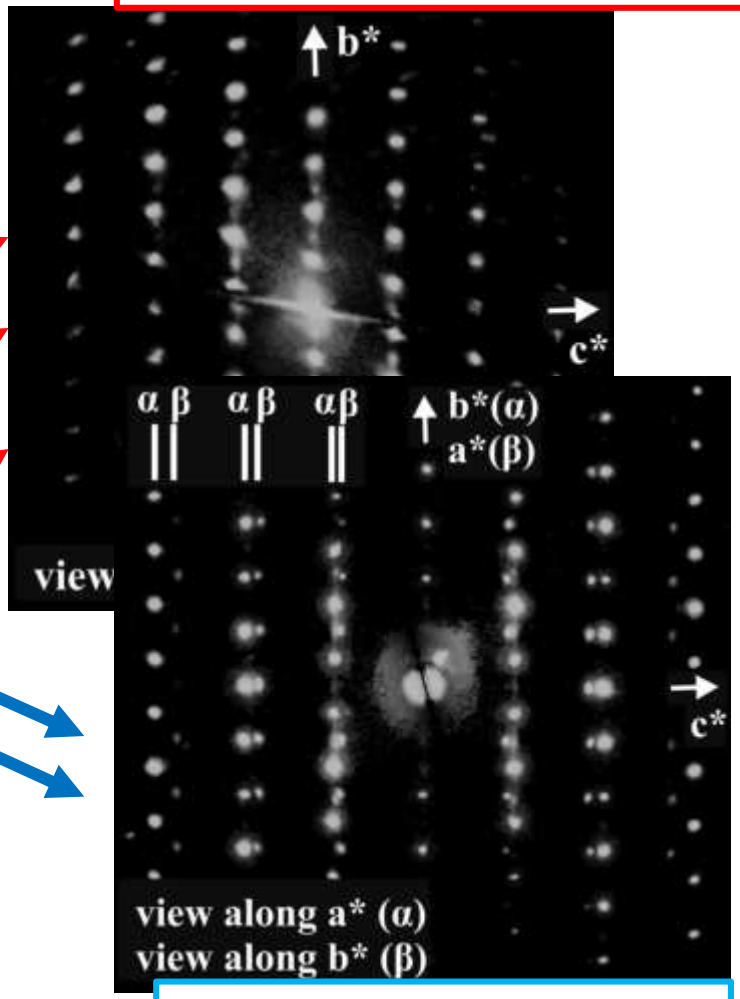

Goethite – FeO(OH)

Synthesis and structural characterization of Cr-bearing ma
recoverable to ambient conditions. M. Koch-Müller, E. Mugnaioli, D. Rhede, S. Speziale, U. Kolb, R. Wirth, *Am Mineral* **99**, 2405 (2014).

EDT: limits and strengths

How complex?

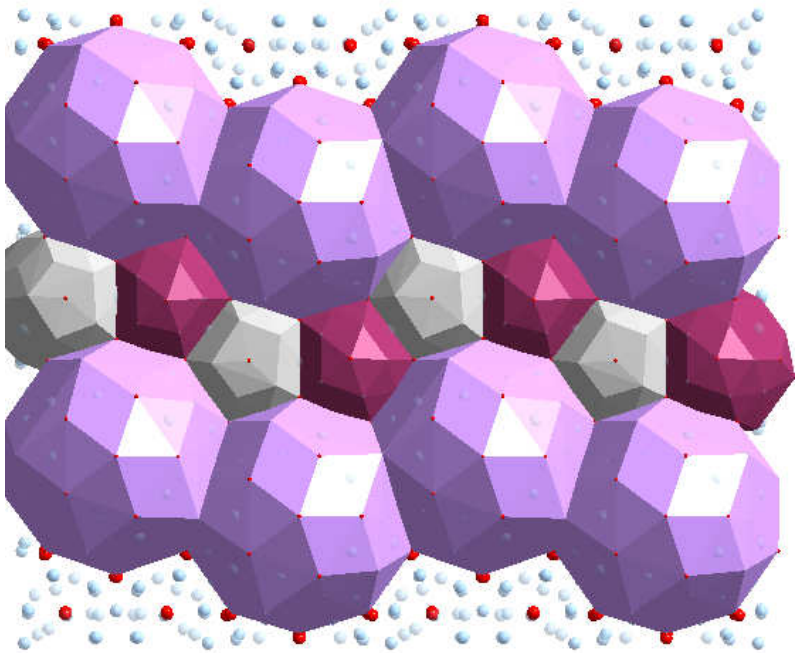

Quasicrystal approximant $Al_{77}Rh_{15}Ru_8$
Space group: *Pbma*
a=23.4Å, b=16.2Å, c=20.0Å
19 independent Rh/Ru, 59 independent Al
Samuha *et al.*, *Acta Cryst B* **70**, 999 (2014)

Charoite-90
Space group: $P2_1/m$
a=32.0Å, b=19.6Å, c=7.1Å, β=90.0°
36 independent Si/Ca/Na/K/Sr
54 independent O
Rozhdestvenskaya *et al.*,
Mineral Mag **74**, 159 (2010)

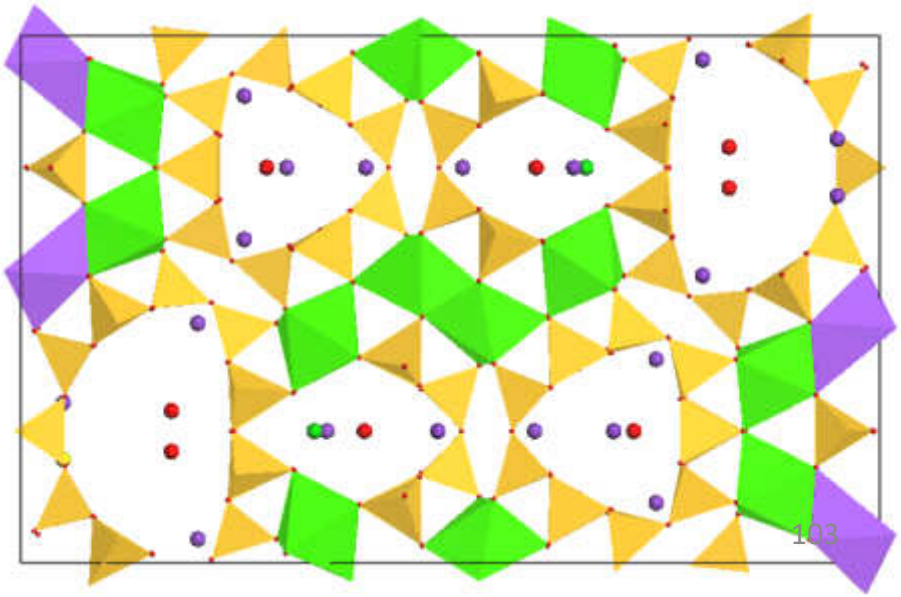

Inorganic zeolites

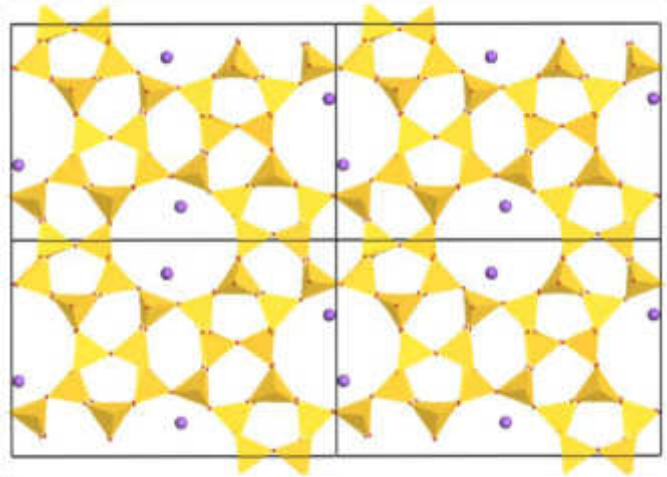

ZSM-5
Space group: *Pnma*
a=20.1Å, b=19.9Å, c=13.4Å
12 independent Si/Al, 27 independent O
Mugnaioli & Kolb, *Microp Mesop Mat* **166**, 93 (2013)

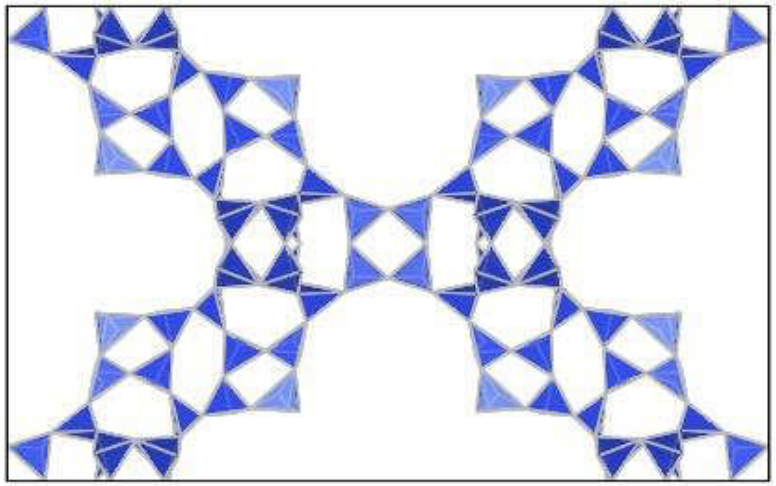

ITQ-43
Space group: *Cmmm*
a=26.1Å, b=41.9Å, c=12.8Å
11 independent Si/Ge, 28 independent O
Jiang *et al.*, *Science* **333**, 1131 (2011)

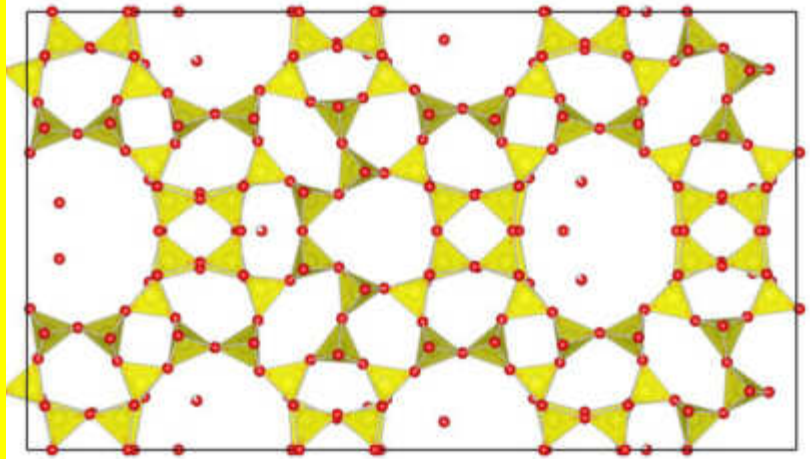

IM-17
Space group: *Amm*2
a=12.7Å, b=22.2Å, c=39.1Å
24 independent Si, 60 independent O
Lorgouilloux *et al.*, *RSC Adv* **4**, 19440 (2014)

Inorganic zeolites

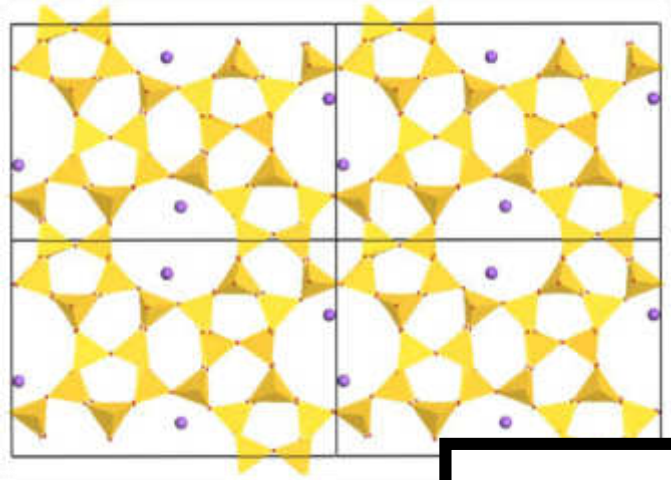

ZSM-5
Space group: *Pnma*
a=20.1Å, b=19.9Å, c=13.4Å
12 independent Si/Al, 27 independent O
Mugnaioli & Kolb, *Microp Mesop Mat* **166**, 93 (2013)

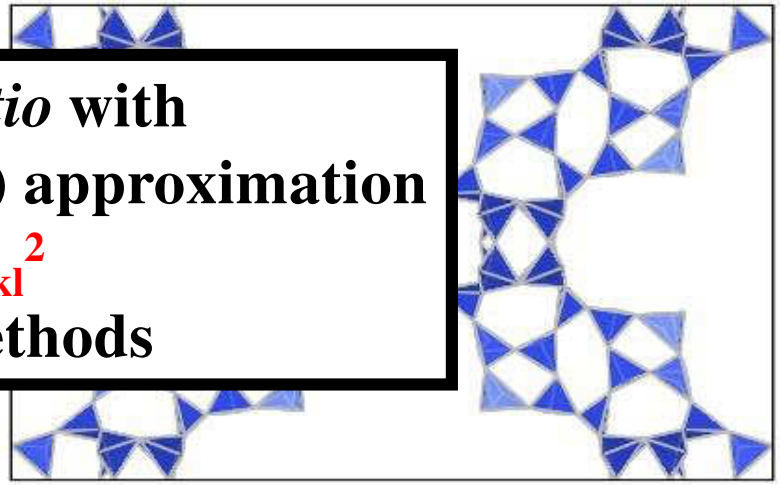

Solved *ab-initio* with kinematical (1-scatter) approximation
$I_{hkl} \sim F_{hkl}^2$
by direct methods

11 indepen
Jiang *et*

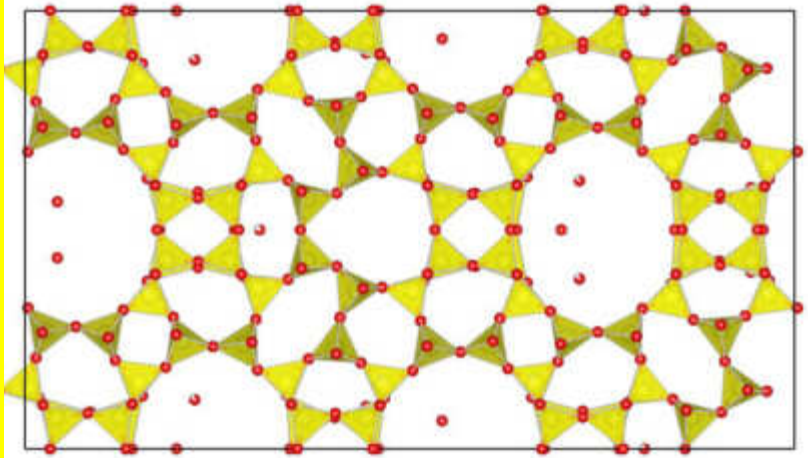

IM-17
Space group: *Amm*2
a=12.7Å, b=22.2Å, c=39.1Å
24 independent Si, 60 independent O
Lorgouilloux *et al.*, *RSC Adv* **4**, 19440 (2014)

EDT: limits and strengths

How accurate?

$(Na,\square)_5[MnO_2]_{13}$

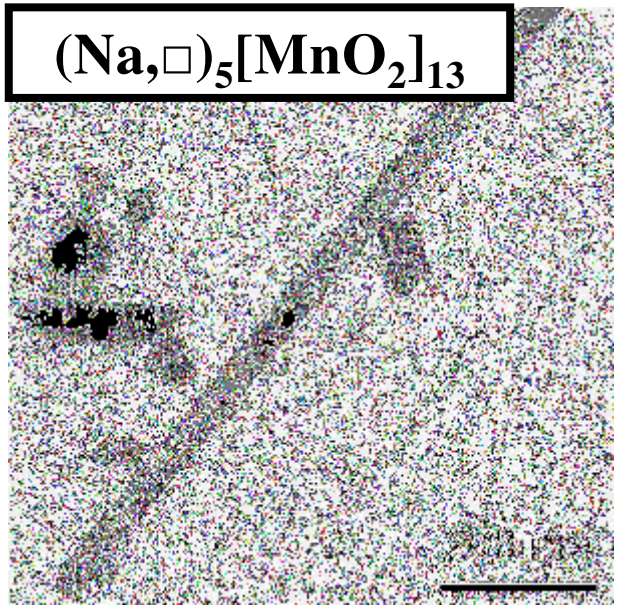

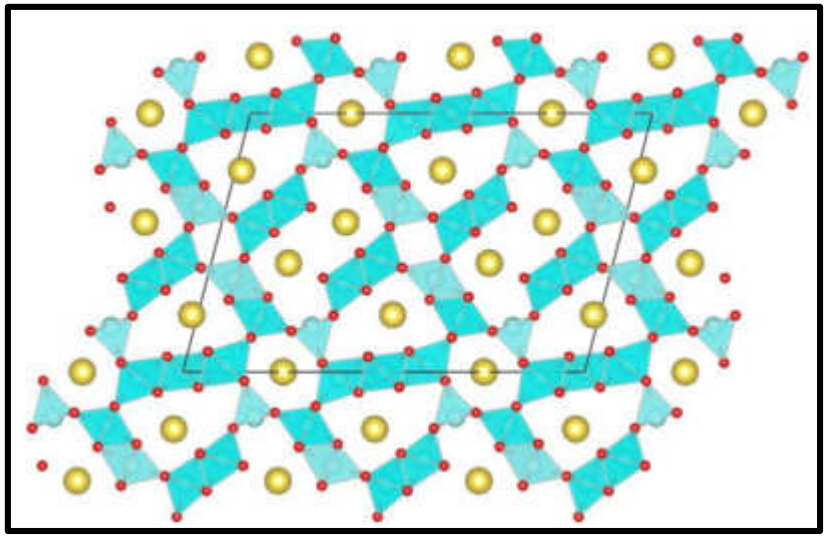

Space group: *C*2/*m*
Completeness (0.8Å): 74%
R_{sym}(I): 13.5%

R_1: 17.1%

	S-XRPD Rietveld	EDT Kinematical
<Mn1-O>	191	185
<Mn2-O>	194	196
<Mn3-O>	191	190
<Mn4-O>	201	193
<Mn5-O>	192	189
<Mn6-O>	188	191
<Mn7-O>	195	195

Structure refinement from precession electron diffraction data. L. Palatinus, D. Jacob, P. Cuvillier, M. Klementová, W. Sinkler, L.D. Marks, *Acta Crystallogr A* **69**, 171 (2013).

Dynamical refinement

R(obs) = 0.0698	wR(obs) = 0.0767
R(all) = 0.2411	wR(all) = 0.0899
GOF(obs) = 2.23	GOF(all) = 1.56

Mn2–		Mn4–		Mn7–	
O2	200	O6	208	O3	218
O4	197	O8	197		
O1 x2	194	O7 x2	193	O5 x2	192
O3 x2	188	O9 x2	187	O12 x2	193

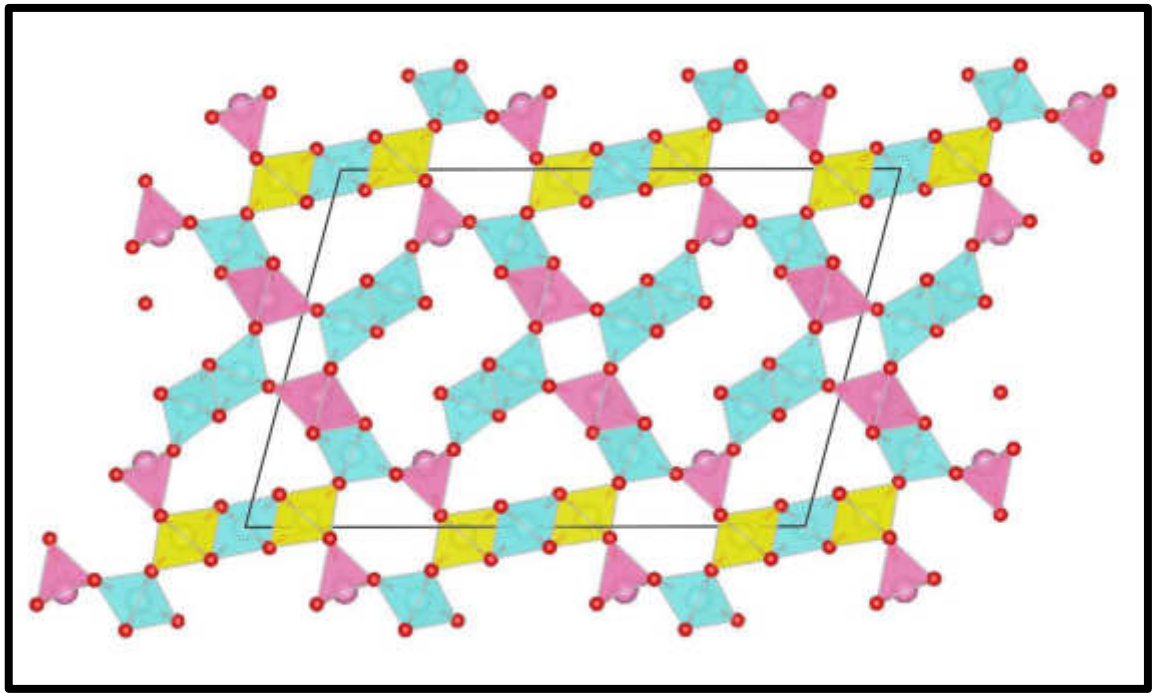

$(Na,\square)_5[MnO_2]_{13}$ nanorods: a new tunnel structure for electrode materials determined *ab initio* and refined through a combination of electron and synchrotron diffraction data.
E. Mugnaioli, M. Gemmi, M. Merlini, M. Gregorkiewitz, *Acta Crystallogr B* **72**, 893 (2016).

Dynamical refinement

Paracetamol

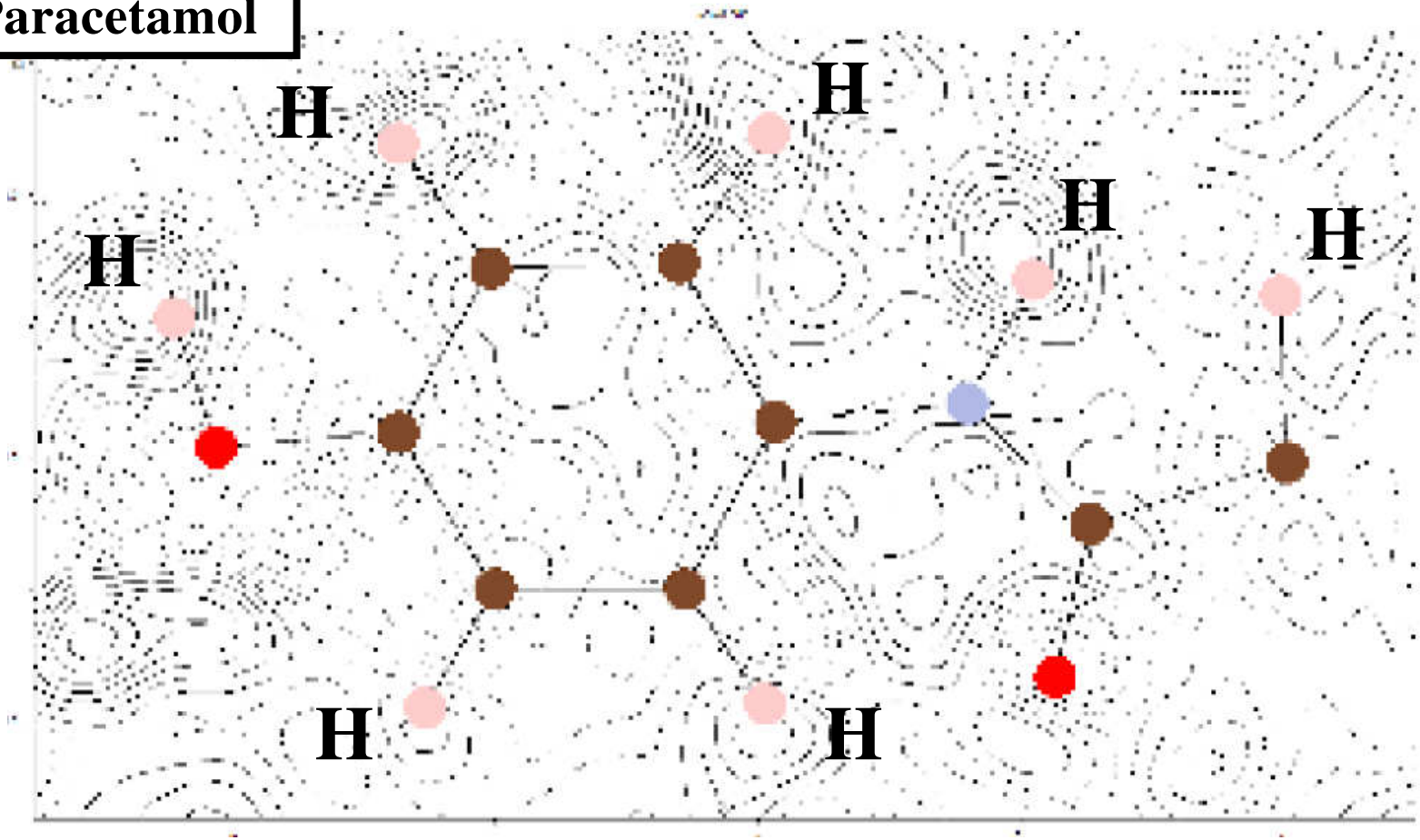

Hydrogen positions in single nanocrystals revealed by electron diffraction. L. Palatinus, P. Brázda, P. Boullay, O. Perez, M. Klementová, S. Petit, V. Eigner, M. Zaarour, S. Mintova, *Science* **355**, 166 (2017).

Dynamical refinement

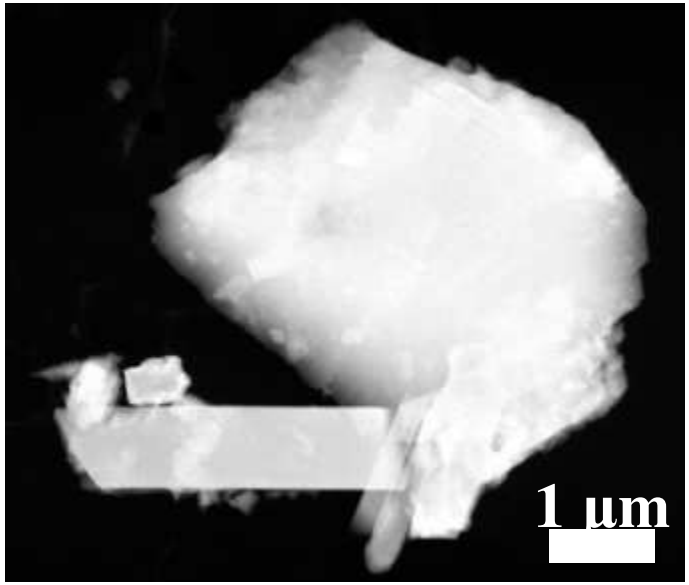

Natrolite

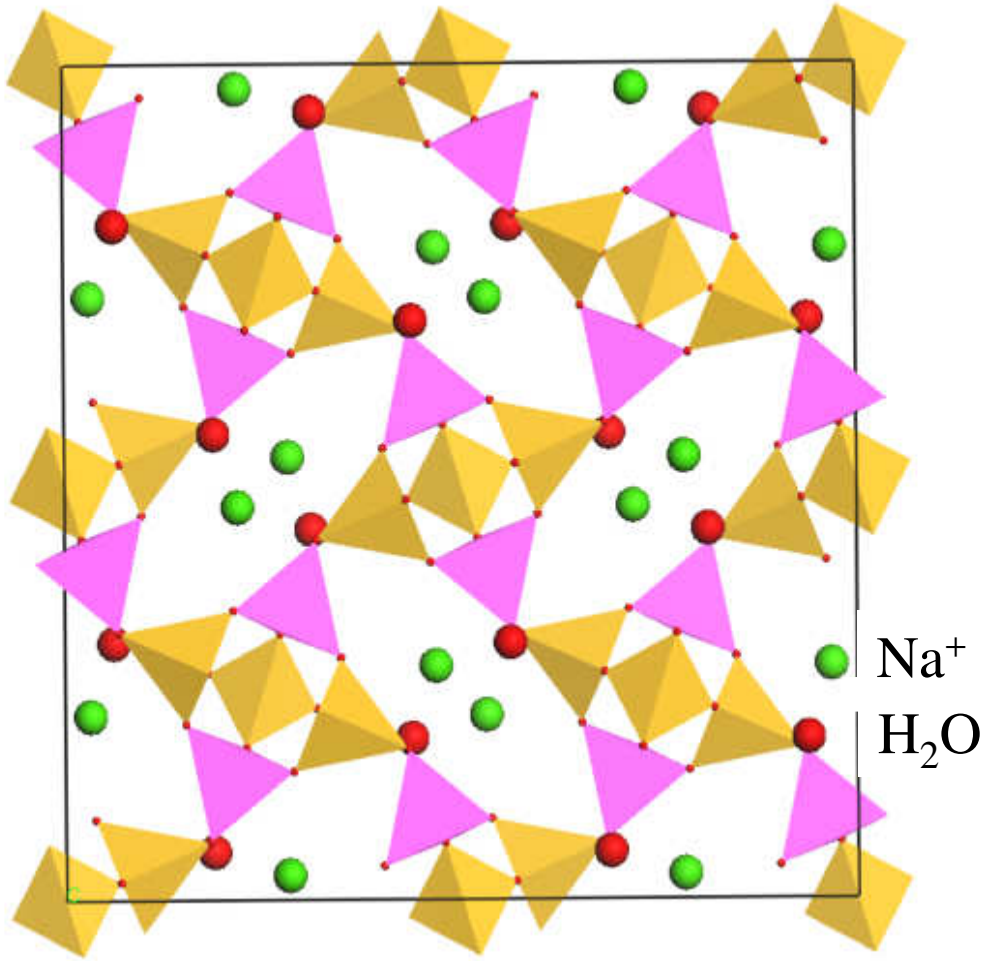

Space group: *Fdd*2

a=18.3Å, b=18.6Å, c=6.6Å

10 independent atoms

V = 2250 Å^3

Complete solution *ab-initio*
by charge flipping,
O_{water} and Na^+ included

EDT: limits and strengths

Dynamical refinement

Detection of hydrogen atoms of H_2O molecule trapped into natrolite channel

Maxima in the difference Fourier map after dynamical refinement

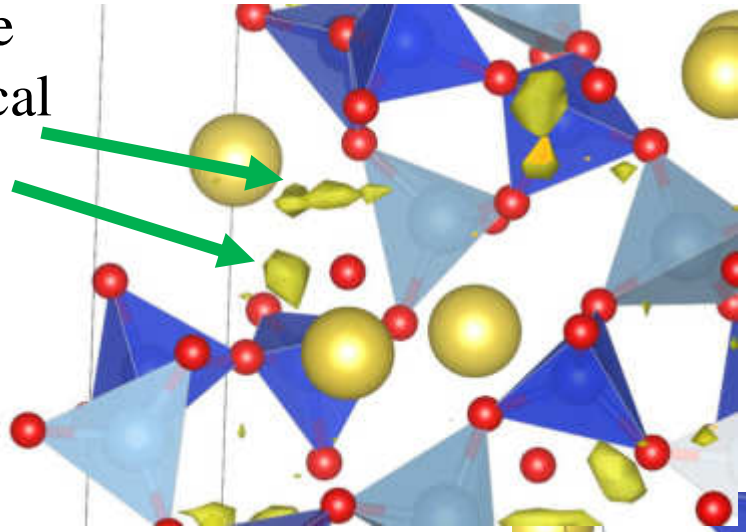

***R*(obs) =** 15.05%

O-H distances: 1.1-1.3 Å

The water molecule plane is orthogonal to the Na-Na axis

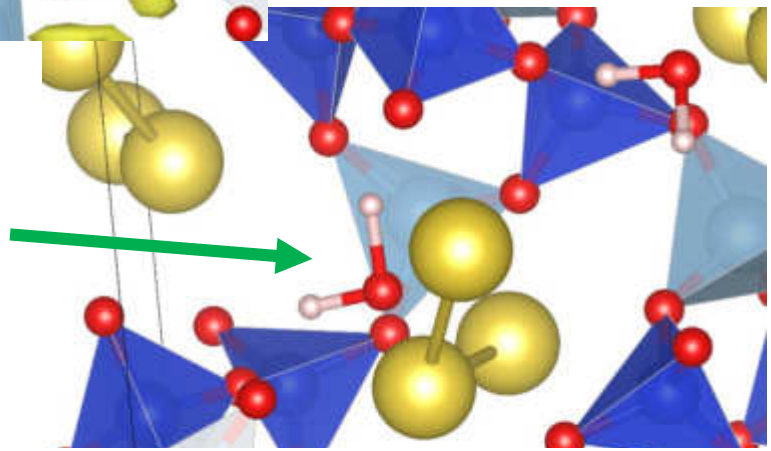

Single-crystal analysis of nanodomains by electron diffraction tomography: mineralogy at the order-disorder borderline. E. Mugnaioli, M. Gemmi, *Z Kristallogr*, doi: 10.1515/zkri-2014-1805.

Structure intrinsically disordered

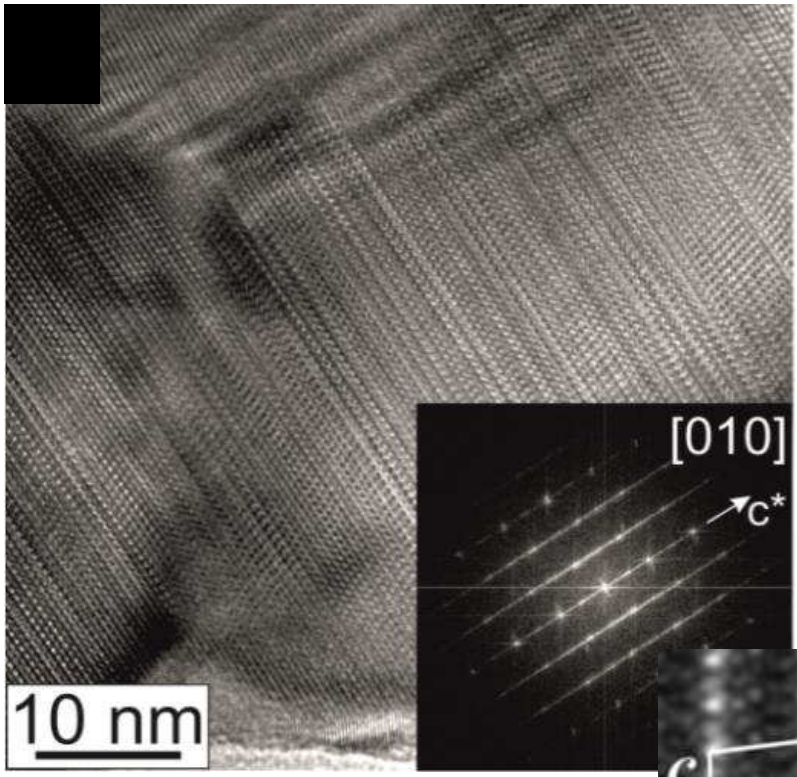

R_1: 37.6%

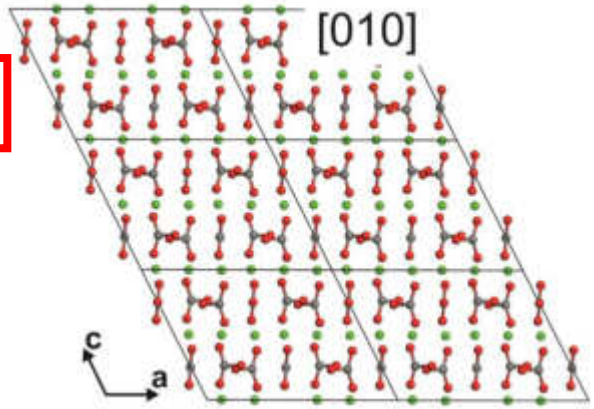

Vaterite

Mugnaioli *et al.*, *Angew Chem Int Ed* **51**, 7041 (2012)

Denisovite

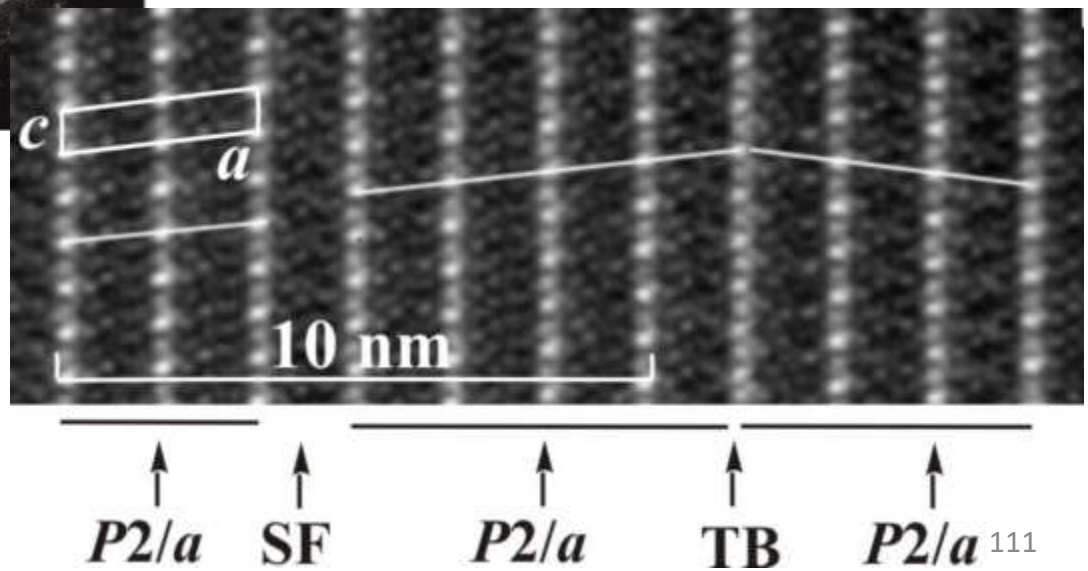

R_1: 31.7%

Rozhdestvenskaya *et al.*, *IUCrJ* **4**, 223 (2017)

EDT: limits and strengths

The real limit: Beam sensitivity

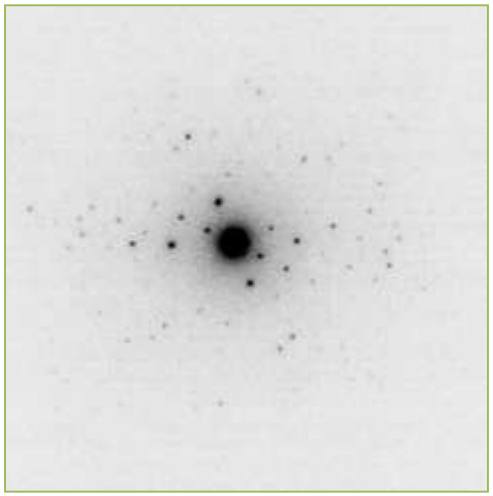

Low resolution data

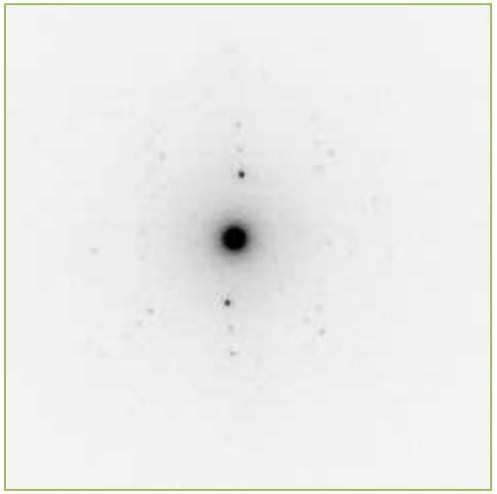

Non-homogeneous intensity degradation during the acquisition

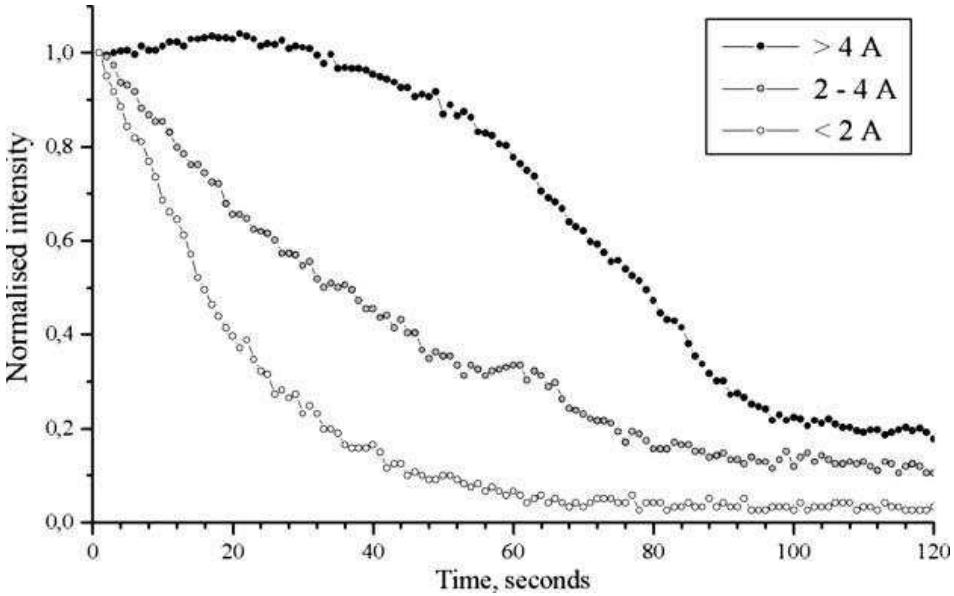

Structural Characterization of Organics Using Manual and Automated Electron Diffraction. U. Kolb, T.E. Gorelik, E. Mugnaioli, A. Stewart, *Polym Rev* **50**, 385 (2010).

Beam sensible samples

Organics and ED

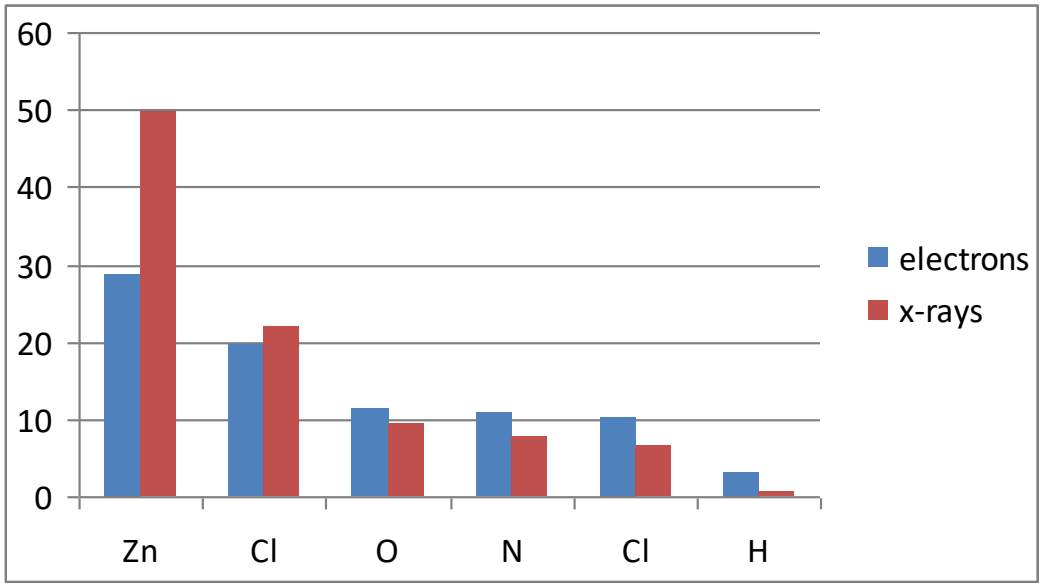

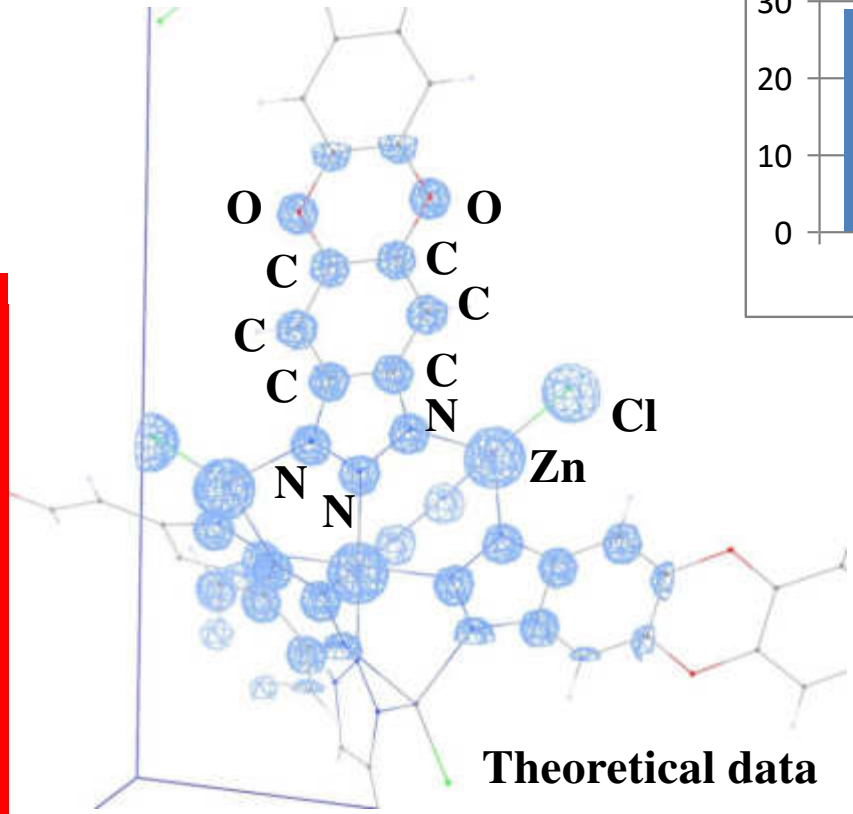

Theoretical data

Due to the Coulomb interaction, **in theory** electrons can detect more easily **light atoms**, down to H^+

Beam sensible samples

Beam damage reduction

Beam sensible samples

Automatic routine for crystal tracking in STEM

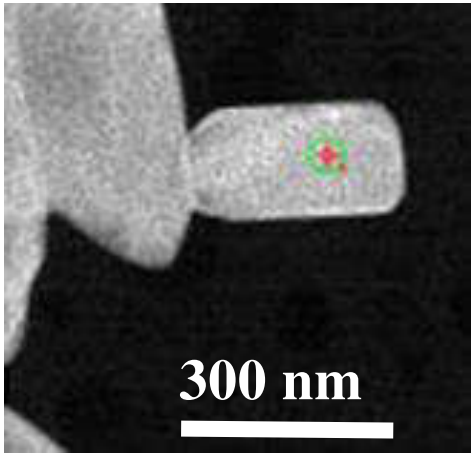

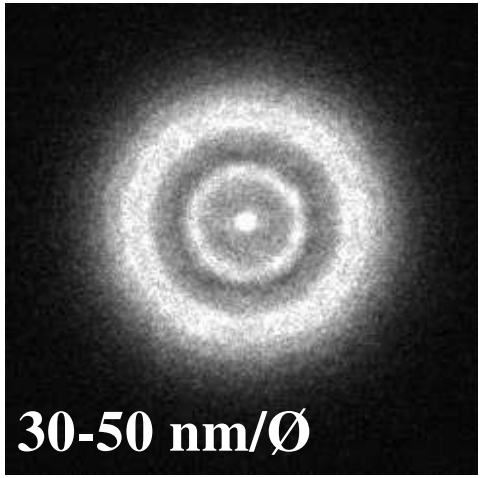

Nanodiffraction

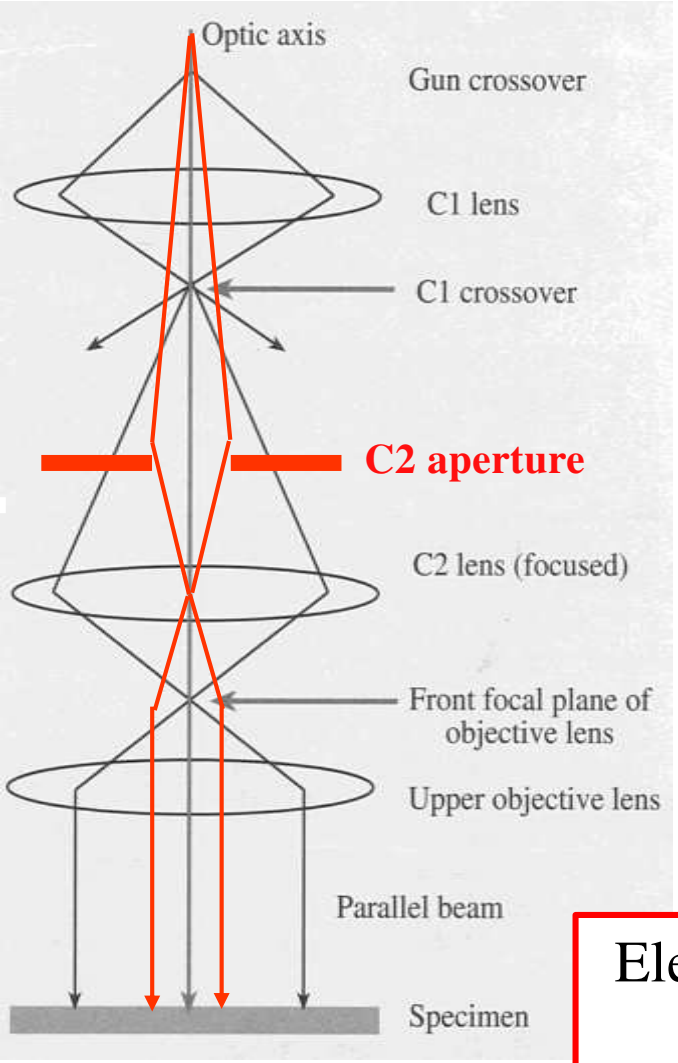

Acquisition area shift

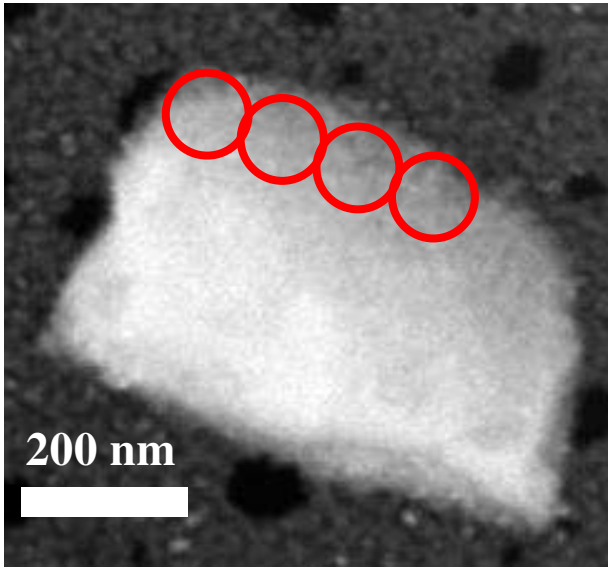

Liquid N_2 temperature

Electron dose rate
~ 15 e/Å^{2}s

Single electron detector (MEDIPIX)

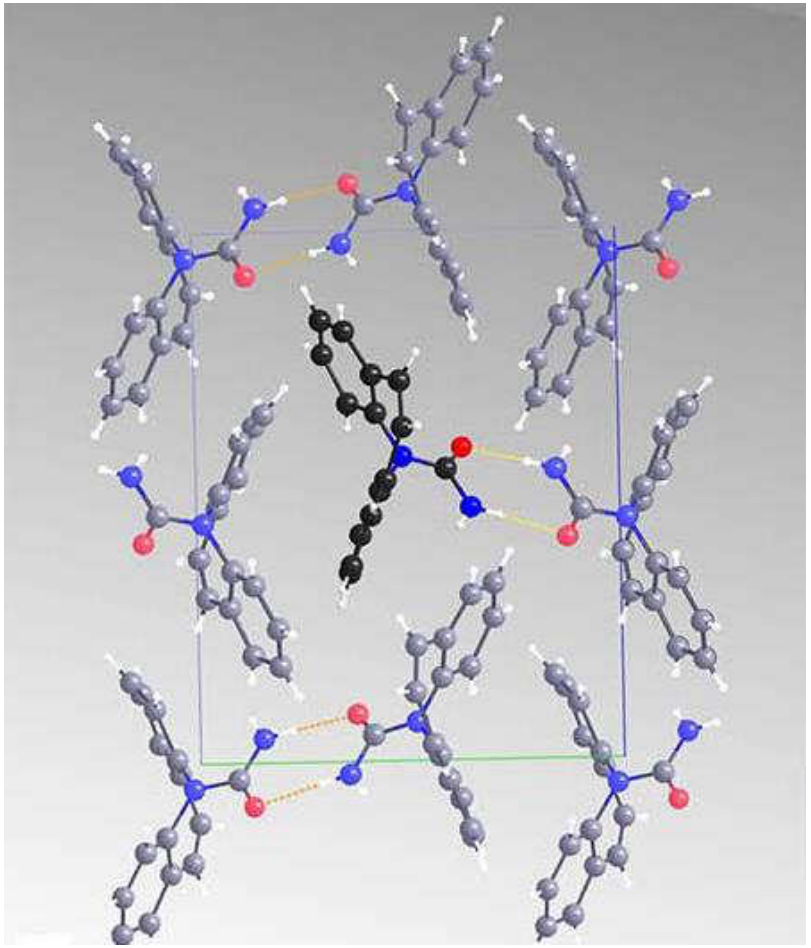

***Ab initio* structure determination of nanocrystals of organic pharmaceutical compounds by electron diffraction at room temperature using a Timepix quantum area direct electron detector.** E. van Genderen, M.T.B. Clabbers, P.P. Das, A. Stewart, I. Nederlof, K.C. Barentsen, Q. Portillo, N.S. Pannu, S. Nicolopoulos, T. Gruene, J.P. Abrahams, *Acta Crystallogr A* **72**, 236 (2016).

Beam sensible samples

Continuous (fast) acquisition

Standard CCD camera binning 4 (512x512 px)

Exposure: 0.5 s

$\mathbf{Dh_{exp}} = 0.14°$

$\mathbf{Dh_{dead}} = 0.29°$

$\mathbf{Dh_{tot}} = 0.43°$

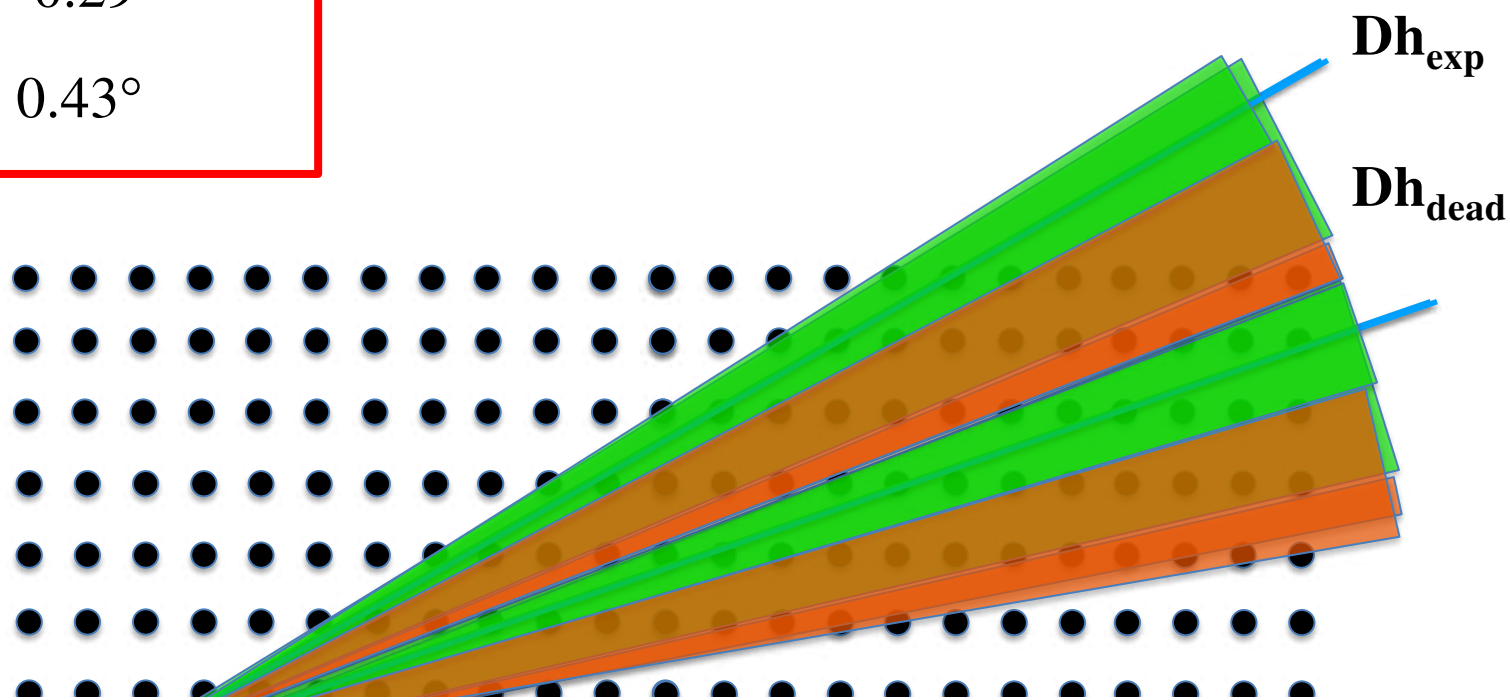

Beam sensible samples

Fast electron diffraction tomography. M. Gemmi, M.G.I. La Placa, A.S. Galanis, E.F. Rauch, S. Nicolopoulos, *J Appl Crystallogr* **48**, 718 (2015).

Continuous (fast) acquisition

Standard CCD camera binning 4 (512x512 px)	Timepix detector 512x512 px
Exposure: 0.5 s	**Exposure: 0.45 s**
$Dh_{exp} = 0.14°$	$Dh_{exp} = 0.83°$
$Dh_{dead} = 0.29°$	$Dh_{dead} = 0.08°$
$Dh_{tot} = 0.43°$	$Dh_{tot} = 0.91°$

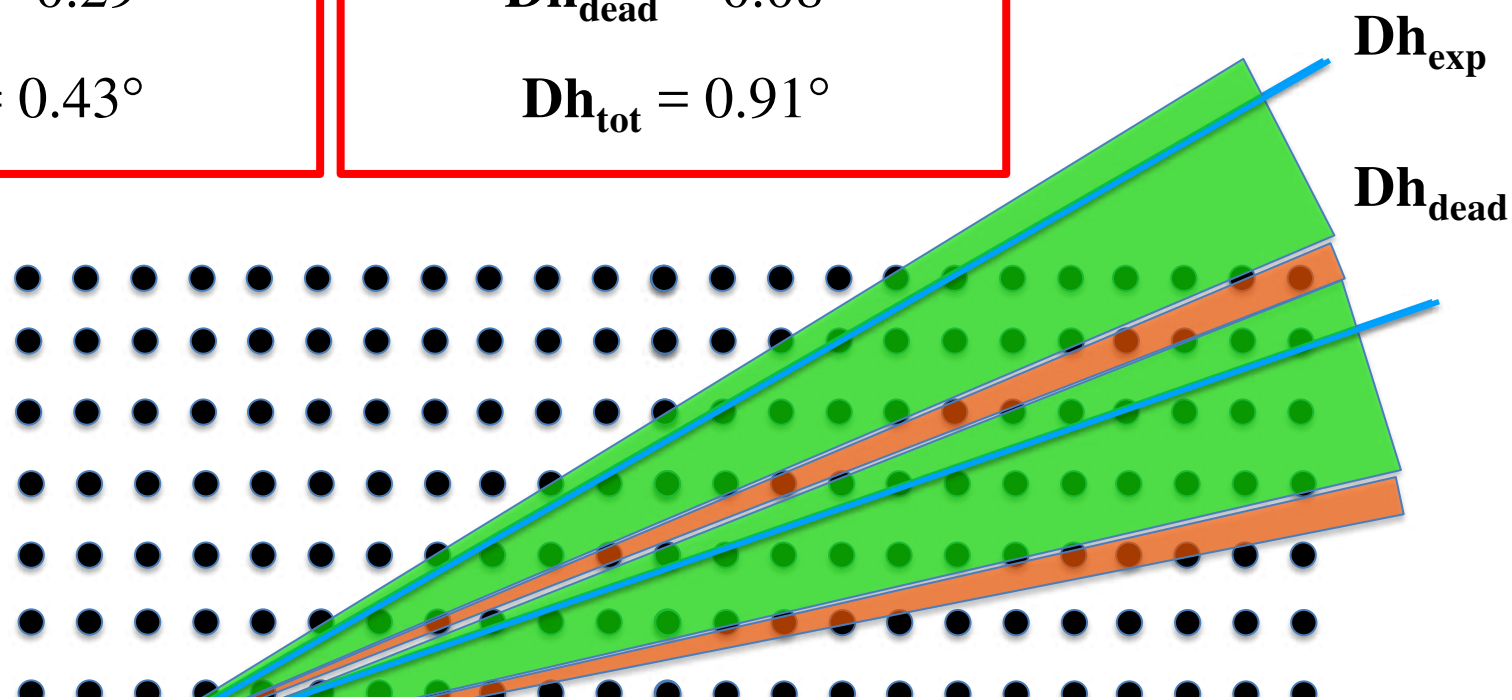

Beam sensible samples

Fast electron diffraction tomography. M. Gemmi, M.G.I. La Placa, A.S. Galanis, E.F. Rauch, S. Nicolopoulos, *J Appl Crystallogr* **48**, 718 (2015).

TEM at CNI@NEST – Pisa

DigiSTAR for precession electron diffraction *and* **ASTAR** for orientation mapping

Liquid N_2
cryo-transfer sample holder

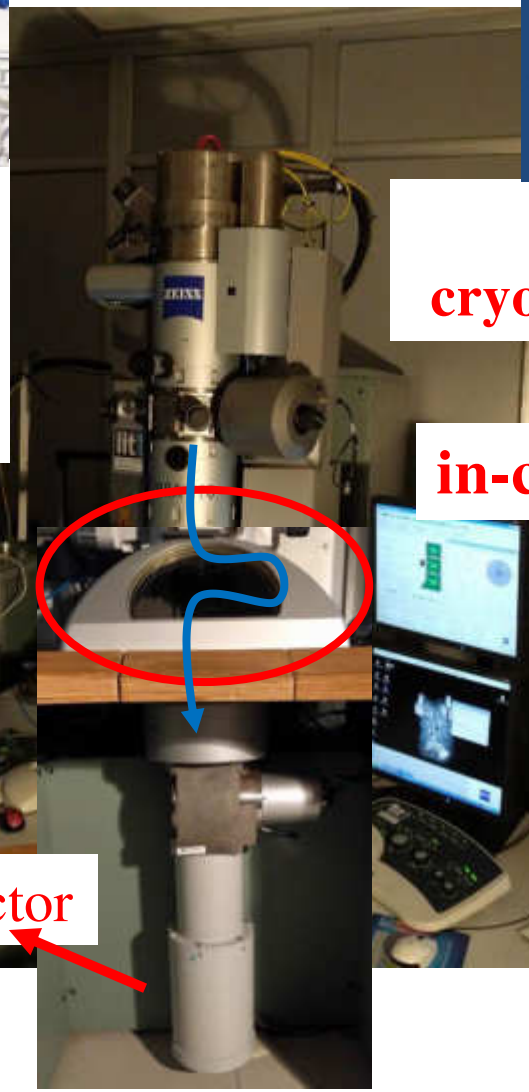

in-column Ω energy filter

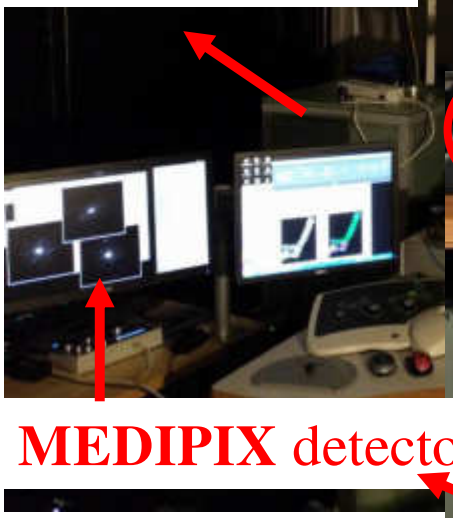

MEDIPIX detector

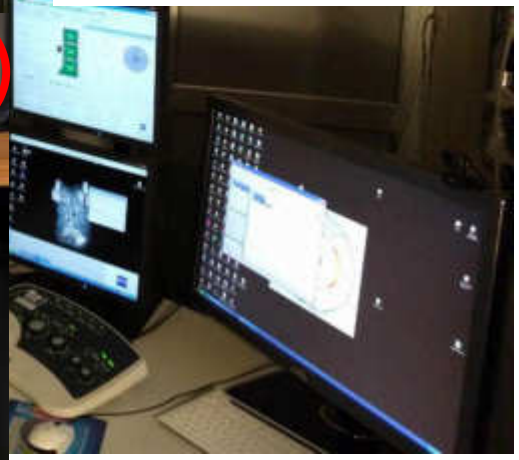

Beam sensible samples

Very beam sensitive porous materials

Zeolite – ITQ-57

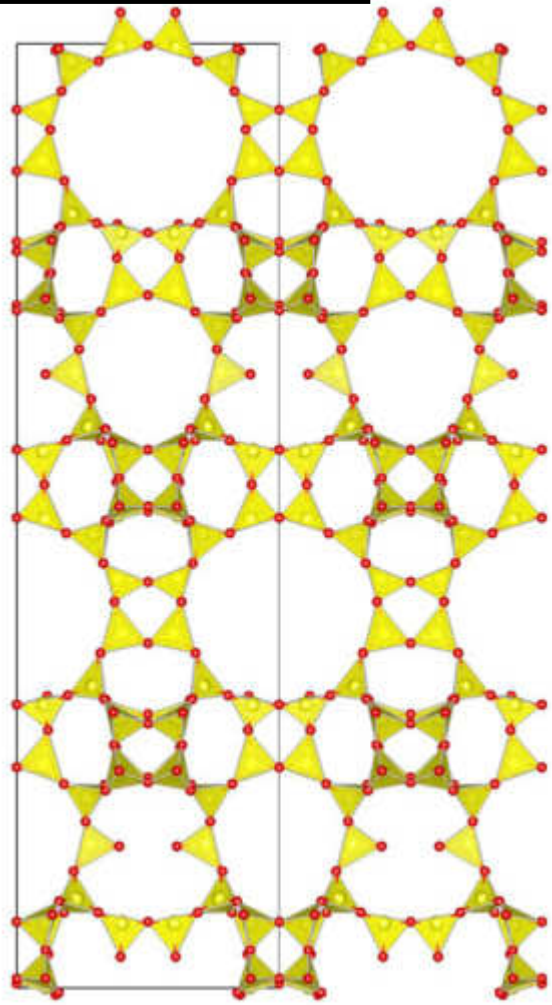

MOF – NP164

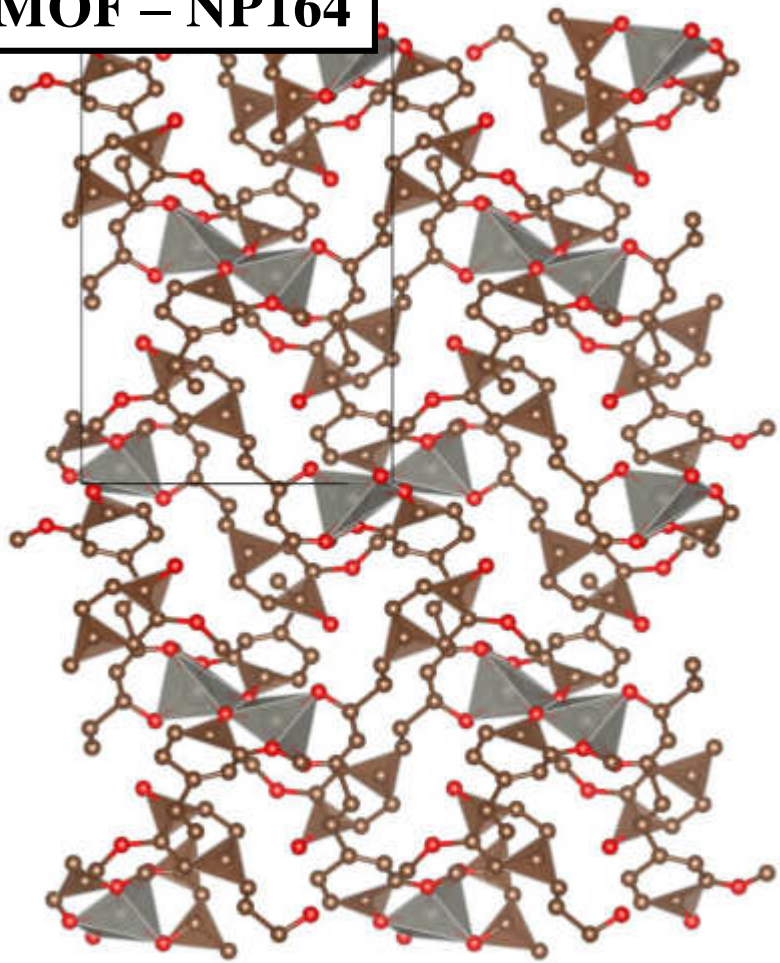

Beam sensible samples

Pharmaceutics

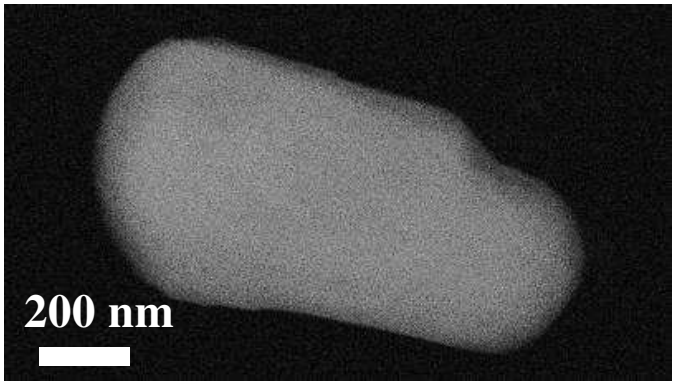

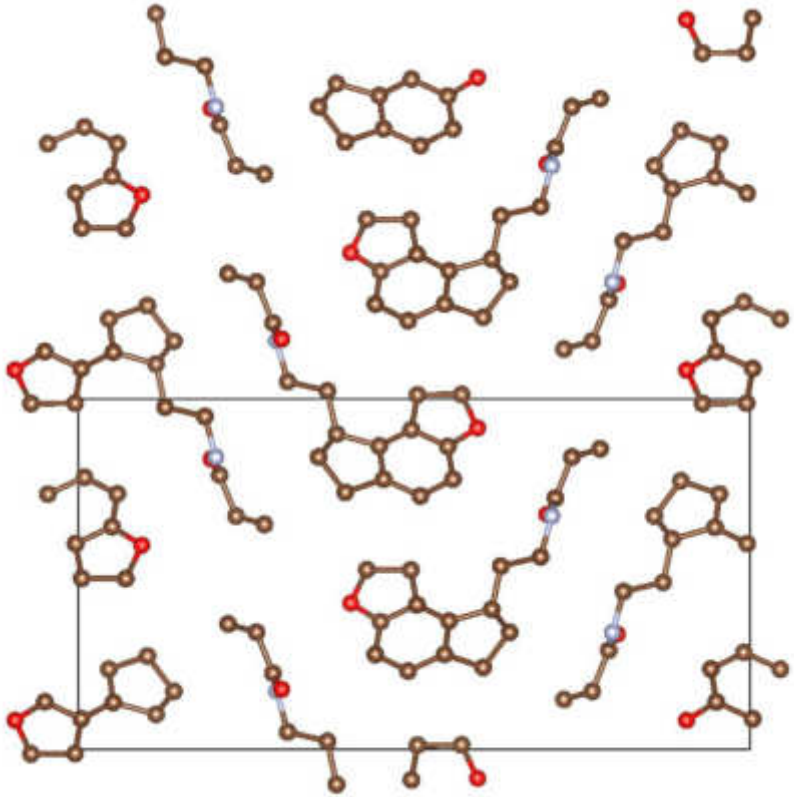

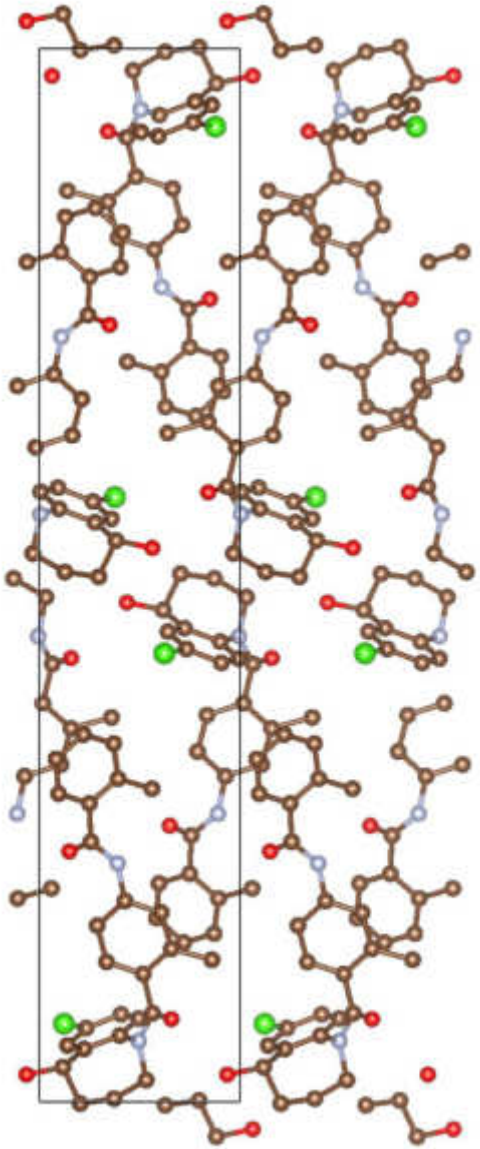

Beam sensible samples

Proteins

Lysozyme

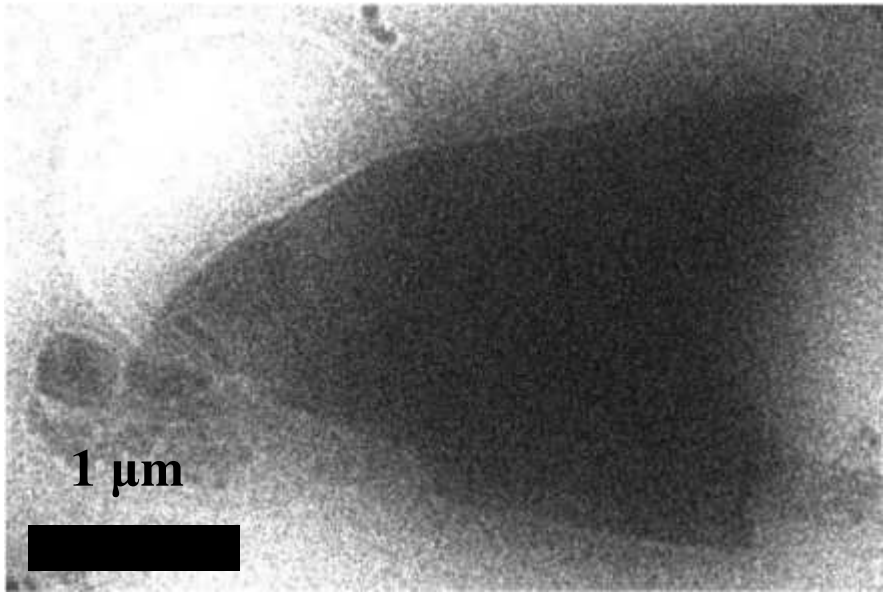

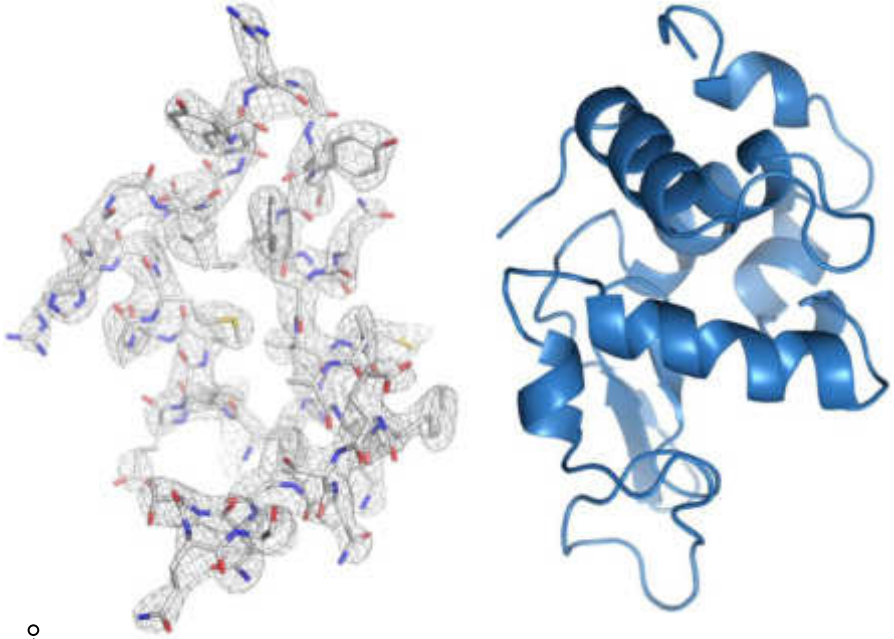

Resolution 2.0 Å

Three-dimensional electron crystallography of protein microcrystals.
D. Shi, B.L. Nannenga, M. G Iadanza, T. Gonen, *eLife* **2**, e01345 (2013).

Electron crystallography of ultrathin 3D protein crystals: Atomic model with charges.
K. Yonekura, K. Kato, M. Ogasawara, M. Tomita, C. Toyoshima, *PNAS* **112**, 3368 (2015).

Proteins

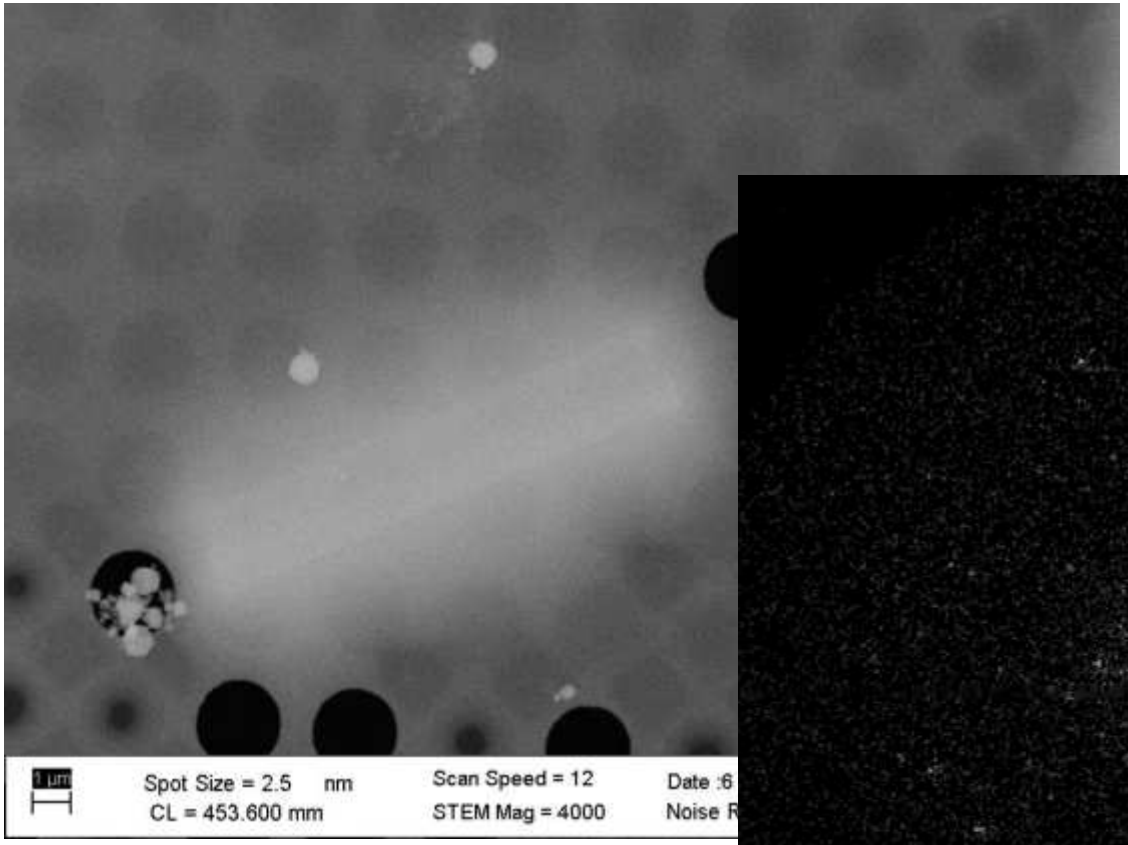

✓ Sample preparation

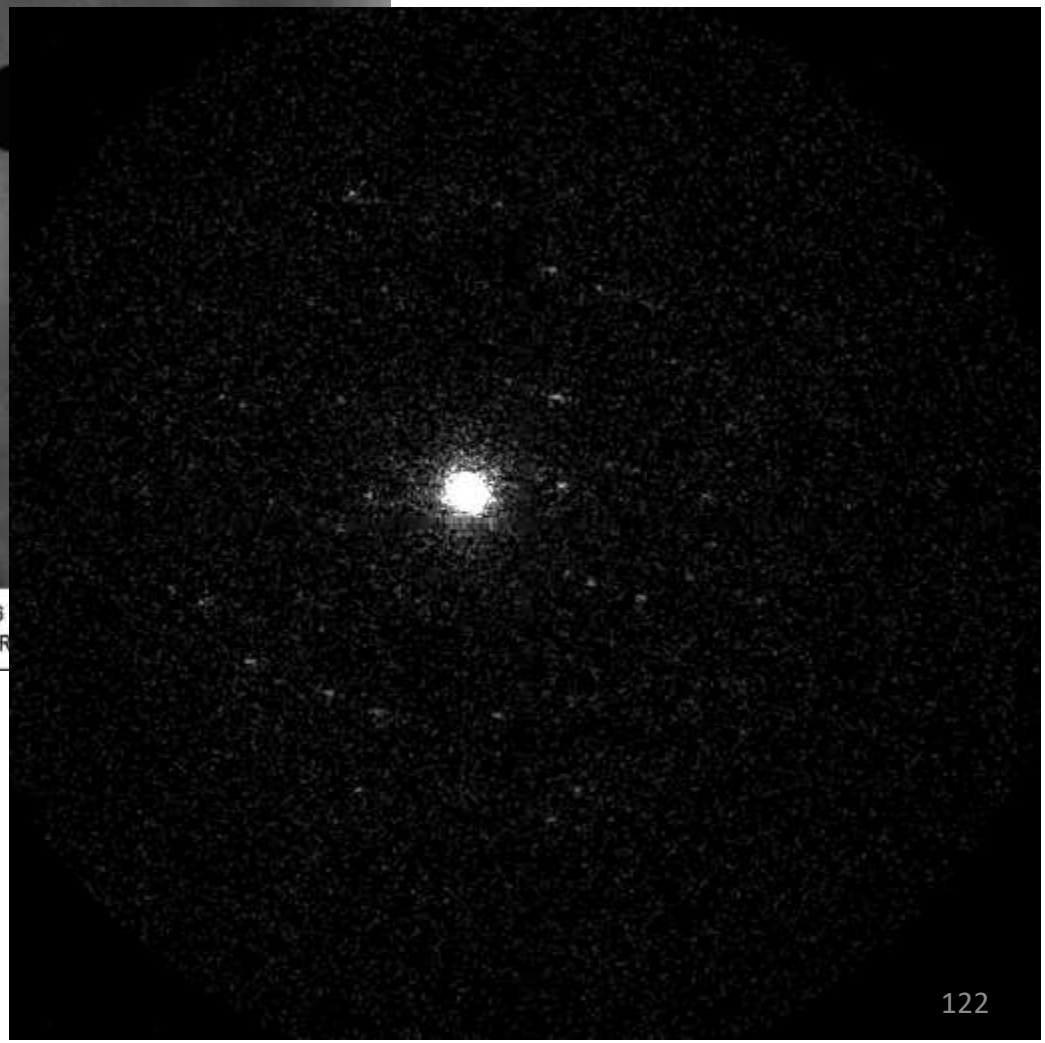

✓ Data acquisition

- SAED continuous
- NB continuous
- Step + precession

Beam sensible samples

Proteins

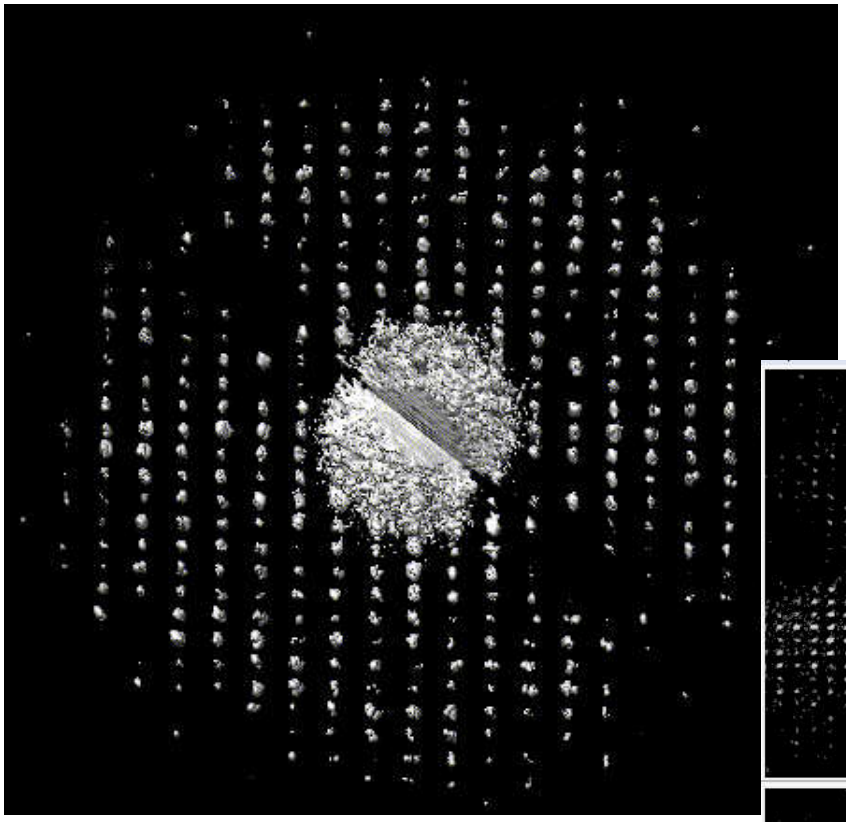

✓ Cell parameters

✓ Space group

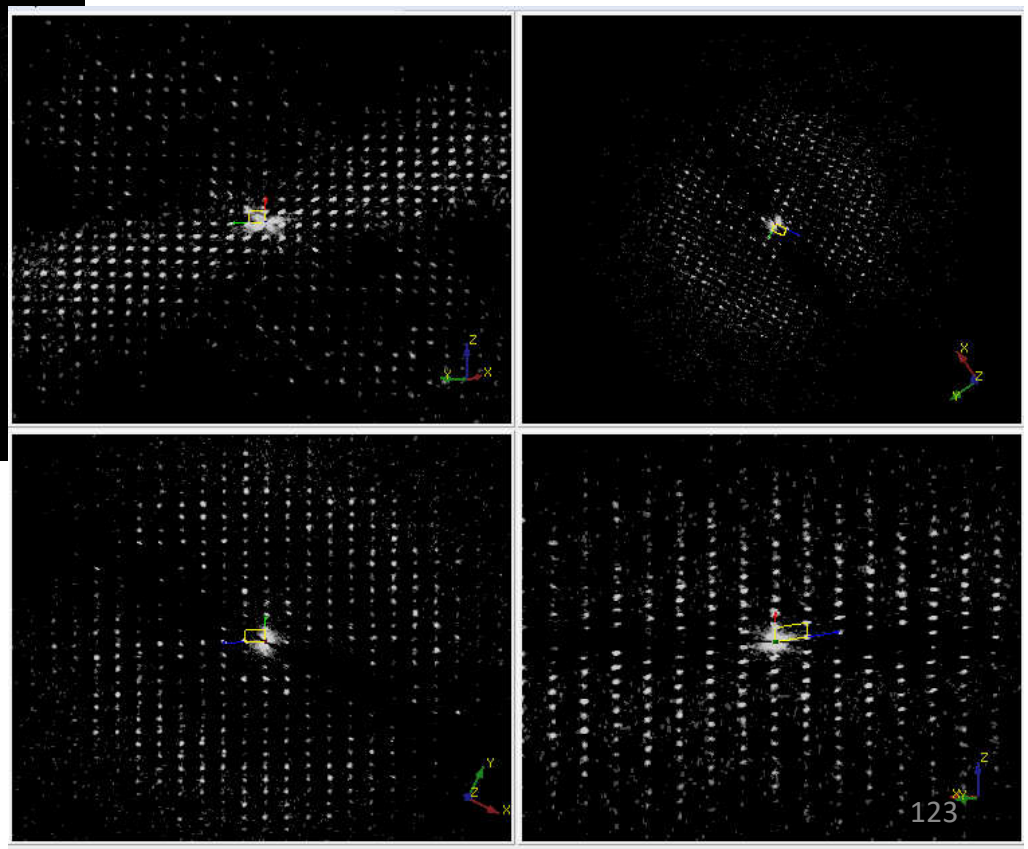

Intensity integration

✗ Phasing

Beam sensible samples

Concluding remarks

- **Electron crystallography** (both **imaging** and **diffraction**) deliver valuable support for the characterization of **nanocrystalline materials**
- … and sometimes, it is **the only option!**
- Imaging deliver information on the **'local structure'** of the material and on **grain boundary** relations and **disorder features**
- **Electron diffraction (tomography)** delivers more complete and higher resolution **3D structural data** and often allows to determine the atomic structure of the phases present in the sample
- The current challenge is the possibility to work with more and more **beam sensitive materials**: porous materials, very hydrated materials, organics, macromolecules
- A **TEM**, an expensive machine, but that can be afforded by a **single University**, or actually by a **single Research Institute**

Acknowledgements

Ute Kolb, Tatiana Gorelik – Johannes Gutenberg University of Mainz

Mauro Gemmi, Arianna Lanza, Valentina Capello – Istituto Italiano di Tecnologia@NEST Pisa

Stavros Nicolopoulos – NanoMEGAS

Regione Toscana

Thank you for your attention!